

McGill University

RECENT CARBONATE REEF SEDIMENTATION
OFF THE EAST COAST OF CARRIACOU,
WEST INDIES

By

W. J. F. Clack

A thesis submitted to the faculty of Graduate Studies
and Research in partial fulfillment of the requirements
for the degree of Doctor of Philosophy in
the Department of Geological Sciences

Montreal, Québec

August, 1976

W.J.F. CLACK

1977

ABSTRACT

Previously unstudied, two back-reef bays east of Carriacou, W. I. have different patterns of reef sediment transport and deposition.

In Grand Bay, four log normal grain size populations and the patterns of their mixing and occurrence are consistent with the transport competence of observed waves and represent lag, rolling, saltating and suspended sediment populations. They are deposited as bimodal fine grained lagoonal sand and as an overlying, shoreward prograding body of bimodal medium grained sand.

In Watering Bay, bottom sediment is in equilibrium with the strongest tidal currents and is transported into deeper water at the northern, open end of the bay. Current velocities can be closely estimated, using bottom sediment grain size distributions, transport competence curves, and the von Karman-Prandtl equation for flow over a hydrodynamically rough surface.

The Watering Bay pattern of back-reef sedimentation is developed after the Grand Bay pattern has led to restriction of tidal flow and the development of strong tidal currents.

Auteur: W. J. F. Clack
Titre: SÉDIMENTATION DANS LE COMPLEXE CARBONATÉ RÉCENT AU LARGE
DE LA CÔTE EST DE CARRIACOU, ÎLES DU VENT.
Département: Sciences Géologiques
Degré: Docteur de Philosophie

RESUMÉ

Deux baies formées derrière un récif à l'est de Carriacou, Îles du Vent, jamais étudiées auparavant, exhibent des mécanismes de transport et de déposition différents.

À Grand Bay, quatre populations à grosseur de grains en distribution logarithmique normale ainsi que leurs styles de mélange et d'occurrence demeurent consistants avec l'abilité des vagues observées, à transporter le sable. Les populations représentent les dépôts stationnaires ainsi que les résultats de roulement, sautellement et suspension des grains composant ce dépôt. Elles sont déposées en ensemble bi-modal à grains fins dans un environnement de sables lagunaires et constituent en même temps une progression vers la plage, d'un autre ensemble bi-modal à grains moyens, recouvrant le dépôt lagunaire.

À Watering Bay, les dépôts de fonds existent en équilibre avec les plus intenses courants de marée et subissent un transport vers les eaux profondes à l'extrémité ouverte, nord, de cette baie. Les distributions de grosseur des grains, les courbes d'intensité de transport ainsi que l'équation von Karman-Prandtl pour un courant liquide continu sur une surface hydrodynamiquement irrégulière, permettent une approximation de la vitesse des ces courants.

Le mode de sédimentation en arrière-récif à Watering Bay a pris forme à la suite de la restriction des courants de marée due au mode de déposition de Grand Bay.

CONTENTS

	<u>Page</u>
LIST OF FIGURES	iv
LIST OF TABLES	vii
LIST OF PLATES	viii
1 INTRODUCTION	1
REGIONAL SETTING	2
Geography	2
Geology	5
Climate	5
Winds and Waves	6
Hydrology	8
METHODS OF STUDY	9
ACKNOWLEDGEMENTS	12
2 ENVIRONMENTS	14
COASTAL ENVIRONMENTS	15
FRINGING REEFS	17
MARINE GRASS BEDS	20
Fringing Reef Flat	20
Shoreward Watering Bay	21
Central Watering Bay	21
Shoreward Jew and Grand Bays	22
Central Grand Bay	24
PATCH REEFS	26
CORAL GRAVEL BANKS	27
STABLE SAND	28
UNSTABLE SAND	29
GRAVEL-FLOORED CHANNELS	30
REEF CREST	31
REEF SLOPE	33
FORE REEF	34
SUMMARY AND DISCUSSION	35
3 SEDIMENTS	37
SOURCES	37
Barrier Reefs	37
Patch Reefs	38
Marine Grass Beds	39
Fauna of Sand Environments	40
Tertiary Outcrops	40
SEAFLOOR SURFACE FEATURES	41
GRAIN SIZE CLASSES	42
AREAL VARIATION OF TEXTURAL PARAMETERS	44
SCATTER PLOTS OF GRAIN SIZE DISTRIBUTION	
STATISTICAL PARAMETERS	50
Jew and Grand Bays	52
Watering Bay	55
CONSTITUENT GRAIN COMPOSITION	57
Molluscs	59
Corals	61
Coralline Algae	61
Halimeda	62

	SUMMARY	64
4	HYDRODYNAMICS OF SEDIMENT TRANSPORT	67
	PREVIOUS WORK	67
	APPLICATION OF SAND TRANSPORT EXPERIMENTS AND THEORY TO SKELETAL CARBONATE GRAINS IN SEA WATER	70
	Unidirectional Flow	73
	Oscillatory Flow	79
5	SEDIMENT TRANSPORT AND DEPOSITION IN GRAND BAY	83
	GRAIN SIZE COMPONENT POPULATIONS	83
	VARIATION IN GRAIN SIZE COMPONENT POPULATIONS FROM REEF CREST TO SHORE	86
	INTERPRETATION	93
	DISCUSSION	96
	SUMMARY AND MODEL OF REEF SEDIMENT TRANSPORT AND DEPOSITION IN GRAND BAY	100
6	SEDIMENT TRANSPORT AND DEPOSITION IN WATERING BAY	108
	HYDROLOGY	108
	Waves	109
	Tides and Currents	110
	Nature of Current Flow in Watering Bay	115
	SEDIMENT TRAPS	116
	Location 35	117
	Current Measurements	117
	Current Velocity Profiles and Roughness Length ..	118
	Shear Velocities	119
	Theoretical Competence and Grain Size Distributions	121
	Location 75	125
	Current Velocity Profiles and Roughness Length ..	126
	Shear Velocities	127
	Theoretical Competence and Grain Size Distributions	127
	Location 24	132
	Winds and Waves	132
	Current Measurements	135
	Current Velocity Profiles and Roughness Length ..	136
	Shear Velocities	137
	Theoretical Competence and Grain Size Distributions	138
	Rates of Sediment Trapping	143
	Summary and Discussion of Sediment Trap Results ...	147
	BED MATERIAL GRAIN SIZE DISTRIBUTIONS AND SEDIMENT TRANSPORT IN WATERING BAY	152
	SUMMARY AND MODEL OF SEDIMENT TRANSPORT AND DEPOSITION IN WATERING BAY	162
7	SUMMARY AND GENERAL MODEL OF REEF SEDIMENT TRANSPORT AND DEPOSITION	168
	GENERAL MODEL	176
	CONCLUSIONS	188
	REFERENCES	191

APPENDICES

1. GRAIN SIZE ANALYSIS	206
2. CONSTITUENT GRAIN COMPOSITION ANALYSIS	212
3. WATERING BAY - CURRENT VELOCITIES AT FIVE FEET (1.52M).	216

LIST OF FIGURES

	<u>Page</u>
1. Location and regional bathymetry map	3
2. Regional winds and waves	7
3. Map of traverses, sampling stations and echo sounding lines	10
4. Bathymetry map	16
5. Map of submarine environments east of Carriacou	18
6. Bathymetry and environments, traverse 5, Watering Bay	23
7. Bathymetry and environments, traverse 16, Grand Bay	25
8. Textural classes of sediment	43
9(A) Map of seabed features	45
9(B) Map of sediment textures	45
10(A) Map of sediment mean grain size	47
10(B) Map of dispersion (standard deviation) of sediment grain size distribution	47
11(A) Map of sediment grain size distribution skewness .	48
11(B) Map of sediment grain size distribution kurtosis .	48
12. Cross plots of grain size distribution statistical parameters, Jew and Grand Bays	53
13. Cross plots of grain size distribution statistical parameters, Watering Bay	56
14. Constituent grain compositions and grain size distributions of three representative samples from Grand Bay	60
15. Settling velocities related to grain size for skeletal carbonate grains in sea water	71
16. Relation of grain size to settling velocity and to threshold shear velocity and roughness velocity in unidirectional flow	76
17. Relation of grain size to threshold orbital velocity in oscillatory flow	81

18.	Grain size component populations of sample 138R (ripple trough), Grand Bay	85
19.	Grain size component populations on traverse 16, Grand Bay	87
20.	Comparison of grain size component populations, traverses 15 to 18, Grand Bay	92
21.	Comparison of sediment transport curves for oscillatory flow with grain size component populations of traverse 16	98
22.	Model of sediment transport and deposition in Grand Bay	104
23.	Variations of grain size distributions in prograding back-reef sand body, Grand Bay model	106
24.	Neap and spring tides and tidal currents at location 35, Watering Bay	111
25.	Tidal current velocities at four stations in northern Watering Bay and one station outside the reef	112
26.	Tidal current paths followed by drift bottles releas- ed during northward flow, Watering Bay	114
27.	First approximations of roughness length from current profiles at location 35, Watering Bay	120
28.	Shear velocities at location 35, Watering Bay	122
29.	Results of sediment trap at location 35 compared to transport competence of measured shear velocities at same location	124
30.	First approximations of roughness length from current profiles at location 75, Watering Bay	128
31.	Results of sediment trap at location 75 compared to transport competence of calculated shear velocities ..	130
32.	Wind, wave, sand ripple and tidal current observations at location 24, Watering Bay	134
33.	Results of sediment trap 24-1 compared to transport competence of calculated shear velocities	139
34.	Results of sediment trap 24-2 compared to transport competence of calculated shear velocities	141
35.	Results of sediment trap 24-3 compared to transport competence of calculated shear velocities	142

36.	Sediment trap and surface sample grain size distributions for all traps, Watering Bay	153
37(A)	Index map, Watering Bay	158
37(B)	64th percentiles of bed sample grain size distributions	158
37(C)	Interpreted maximum shear velocities using 64th percentiles and transport competence curves	158
37(D)	Calculated maximum current speeds at 5 feet (1.52 m) depth in Watering Bay	158
38.	General models of back-reef sedimentation with constant sea level	178
39.	General models of back-reef sedimentation	
	A&B: rate of sea level rise subequal to rate of sediment supply	
	C: rate of sea level rise much greater than rate of sediment supply	180
40.	Sequence of back-reef sedimentation for a given sea level rise curve	183

LIST OF TABLES

	<u>Page</u>
A. Weights in grams of sample collected by sediment trap - in half phi grain size intervals and in total sample	145
B. Rates of sediment trapping	148

LIST OF PLATES

	<u>Page</u>
1. Aerial photograph - eastern coast and northern Carriacou	197
2. Aerial photograph - Watering Bay	198
3. Aerial photograph - southwest Grand Bay	199
4. Reef slope and fore-reef environments, Watering Bay traverse six	200
5. Upper reef slope and reef crest environments, Watering Bay barrier reef	201
6. Back edge of reef crest	202
7. Watering Bay lagoon environments	203
8. Watering Bay lagoon and patch reef environments	204
9. Grand Bay lagoon environments	205

CHAPTER 1 - INTRODUCTION

Studies of modern carbonate environments and sedimentation have been carried out in many parts of the world, but in most of these investigations mechanical analyses of the sediment grain size populations have been used in a mainly descriptive manner. Correlation of grain size distributions with processes of sediment production, transportation, and deposition usually has been in very general terms. To understand these relations better the processes responsible for the observed grain size distributions must be studied.

The barrier reefs and associated sediment east of Carriacou W.I. have not been investigated previously. The back-reef area is divided into two main bays (Fig. 1). Sediment in the larger, southern bay is affected and transported by waves moving shoreward from the reef. Sediment in the northern bay is affected and transported mainly by strong tidal currents parallel to shore.

The proximity of two relatively small and uncomplicated areas with different hydrologic and sediment transport regimes offers an opportunity to test the significance of grain size distributions of back-reef skeletal sands in terms of the processes which affect them.

The purposes of this study have been to:

- (1) Map the bathymetry, major environments and sediment distribution in the submarine ^{area} east of Carriacou for the first time.
- (2) Investigate and interpret the differences in grain size distributions in contiguous areas under the influence of

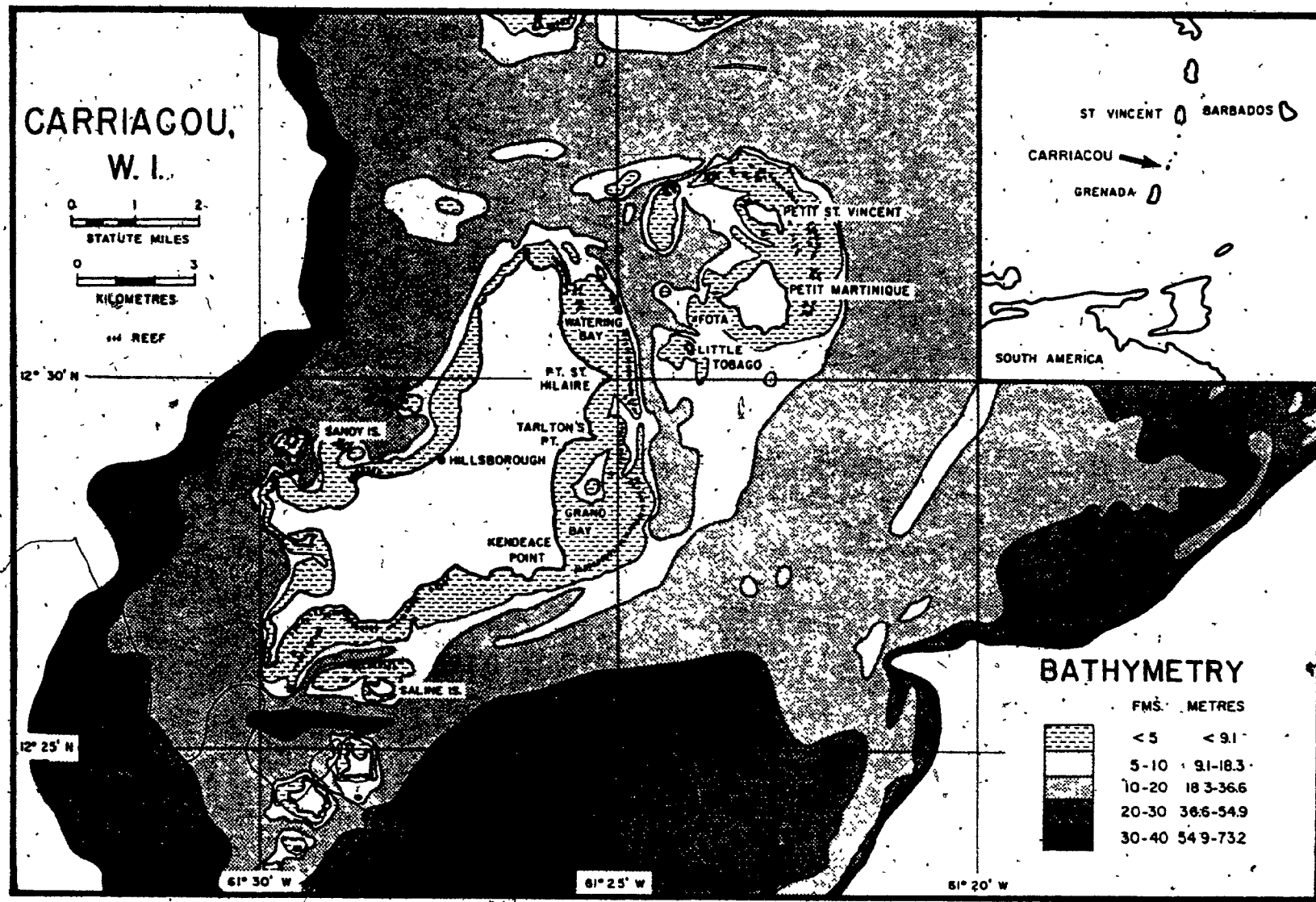
- different hydrologic regimes.
- (3) Investigate the grain size distributions of sediments in transport along and near the sea floor, and to compare these with the grain size distributions of sea floor sands, and with theoretically transportable grain sizes determined from water current measurements.
 - (4) Investigate the amount of control exerted by skeletal structure on the grain size distributions of carbonate skeletal sands.
 - (5) Develop a model of reef sediment production, transportation and deposition on the basis of the above and other considerations, such as time and sea level changes.

REGIONAL SETTING

Geography

Carriacou (Lat. 12°30'N.: Long. 61°26'W.), one of the Grenadine Islands in the Windward Group, is approximately 21 miles (33.8 km) north of Grenada and 48 miles (77.28 km) south of St. Vincent (Fig. 1). It rises from a water depth of 12 to 20 fathoms (22 to 37 m) on the western side of the Lesser Antilles ridge. It is a mountainous island approximately 13 square miles (33.7 square km) in area. Mt. D'Or and Chapeau Carre reach elevations of 817 and 954 feet (249 and 291 m) respectively, near the southern end of the island. A central ridge of 600 to 800 feet (183 to 244 m) elevation joints Mt. D'Or to High North (975 feet - 297 m) at the northern end of the island.

FIG. 1 Location and regional bathymetry map
 Modified from British Admiralty Chart 2872.



Carriacou is administered as a district of Grenada. It may be reached by motorized mail schooner, sailing for 5 hours between St. Georges, Grenada and Hillsborough, capital of Carriacou. LIAT now stops at a small airfield south of Hillsborough on its service between Grenada and St. Vincent. On the island taxis and buses provide service to all parts on an extensive system of roads.

The population of the island numbers approximately 7,000 and is engaged mainly in agriculture, boat building and seafaring. Agriculture provides the main exports of Marie Galante: cotton and lime oil. According to Kay (1966) 50 of 58 cargo sailing vessels registered in Grenada in 1959 were built on Carriacou or on the small nearby island of Petit Martinique.

A small telephone exchange and cable office is situated in Hillsborough which is the only area with electricity and running water. Water is often a major problem. Wells have been sunk; but the water is of limited quantity and quality. Roof catchments serve the needs of the population, and a dry year causes hardship for everyone.

With the exception of beautifully zoned reefs around Sandy Island (Fig. 1) coral reef development to the west of Carriacou is poor. Small fringing reefs are present only around Jack a Dan Island and off small points of land along the southern half of the coast. Reefs along the southern coast, north of Saline Island and in Manchioneal Bay, were not examined.

In the study area along the east coast a well developed barrier reef is present at one-quarter to one mile (0.4 to 1.6 km) offshore. The lagoon is divided into three bays. Watering (Windward) Bay occupies the northern third of the coast. Jew Bay, between Point St. Hilaire and Tarlton's Point halfway along the coast, is smaller. Tarlton's and Kendeace Points bound Grand Bay along the southern half of the coast.

Geology

Carriacou is on a volcanic arc which has been the site of eruptions in historic times on the islands of St. Vincent and Martinique. It is the only island of the Windward Group south of Guadelupe which is not predominantly of direct volcanic origin and which has considerable limestone. The general geology and paleontology have been described by Trechmann (1935) and Martin-Kaye (1958). The stratigraphy consists of Upper Eocene to Upper Oligocene Lower Tuffs, the Lower Miocene Carriacou Limestone Series, and the Upper Miocene and/or Pliocene Upper Tuffs. The units are bounded by and include possible unconformities. Generally the strata have a gentle to moderate dip to the southeast.

Climate

Carriacou has a relatively dry climate and no permanent streams. The uplands are wooded for the most part reflecting a more abundant rainfall than occurs on the eastern and southern coasts; where the vegetation consists mainly of short

grasses, scrub and cacti.

The average annual temperature is approximately 81°F (27.2°C) (Anon., 1948). The average monthly air temperatures range from 78 to 82°F (25.6 to 28.3°C). The average monthly sea water temperatures never differ by more than one degree from the average monthly air temperatures.

Carriacou is south of the area of high hurricane probability. The last one to seriously effect the island was on September 22, 1955 (Kay, 1966).

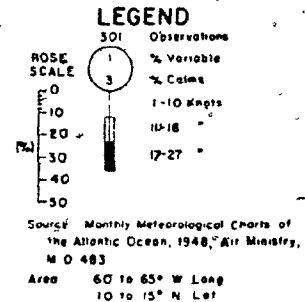
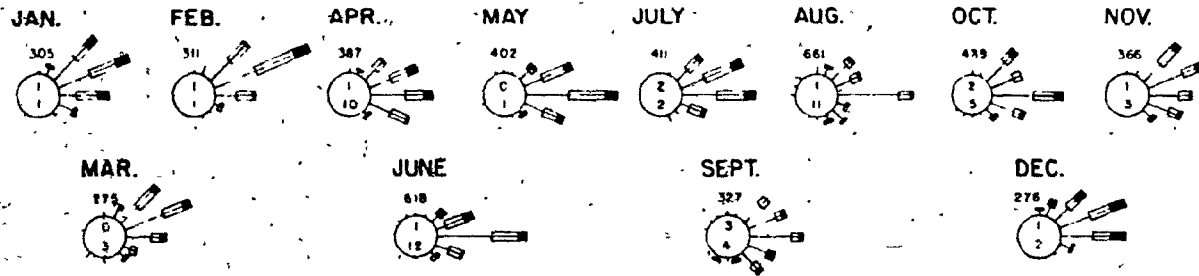
Winds and Waves

Carriacou lies within the belt of the constant Northeast Trade Winds. Generally the winds of late autumn and winter are strong and mainly northeasterly, while those of spring, summer and early autumn are weaker and more easterly (Fig. 2). Monthly mean wind speeds at Pearls Airport on the east coast of Grenada, from 1963 to 1967 inclusive, varied from 5 to 12 knots (9.3 to 22.2 km/hr). For those five years the average monthly mean wind speeds for the windiest months, December and January, were 10 knots (18.5 km/hr), and for the calmest months, August and September, were 8 and 7 knots (14.8 and 13.0 km/hr) respectively (written communication, Mr. W. Ogilvie).

The seasonal variations in wave directions reflect those of winds, winter being the only season when there is a strong, northeasterly component (Fig. 2). Variations in intensity, as indicated by wave period and height, also reflect those of the winds. Throughout the year the dominant wave period is between 5 and 7 seconds, and the modal wave height of these waves is

SEASONAL VARIATIONS IN WINDS AND WAVES

WINDS



WAVES

WINTER

SPRING

SUMMER

AUTUMN

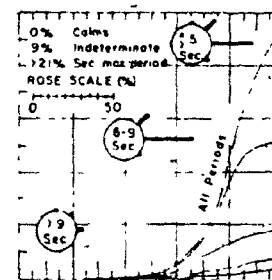
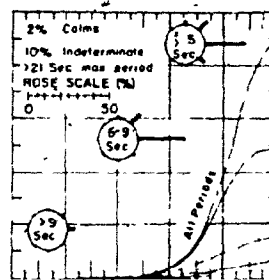
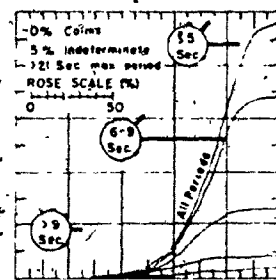
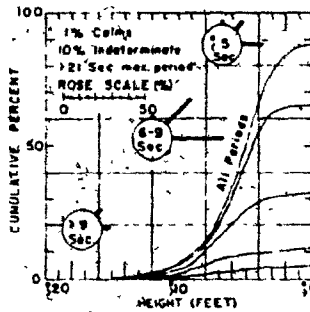
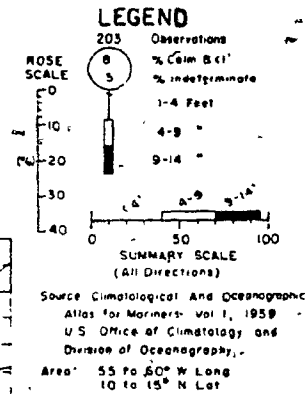
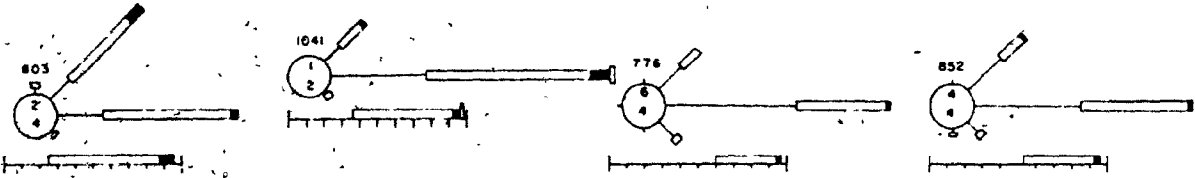


Fig. 2. Regional Winds and Waves

between 4 and 5 feet (1.2 and 1.5 m). The median heights of all waves are 5, 4.75, 3.3 and 3.8 feet (1.52, 1.45, 1.01, and 1.16 m) for winter, spring, summer and autumn respectively (anon. 1959).

Hydrology

Tides in the vicinity of Carriacou are of the mixed type. The harmonic constants listed in the Admiralty Tide Tables (1967) indicate that diurnal components are dominant in Hillsborough Bay on the west coast and that semi-diurnal components are dominant in the Tobago Cays approximately 9 miles (14.5 km) to the north. The tidal ranges are small, the differences between mean high high water and mean low low water at the springs near the solstices being 1.7 and 2.0 feet (0.5 and 0.6 m) in Hillsborough Bay and the Tobago Cays respectively.

West and northwest flowing regional currents ranging from 0.3 to 1.5 knots (15.4 to 77.2 cm/sec) throughout the year (Anon., 1948) probably represent local wind driven currents plus the Equatorial Current as it passes from the Atlantic into the Caribbean.

Reversing tidal streams run in front of and between the islands in the area. The regional current has the effect of hindering the south and east flowing streams and adding to the north and west flow. The times of change and the rates of the tidal streams are greatly affected by the strength of the current.

No currents were observed in the southern two bays behind the barrier reef east of Carriacou. In Watering Bay to the

north however, there is a reversing current similar to that outside the reef. The predominance of the north-flowing current here is not a result of regional currents but of water being driven over the reef by the winds and waves and flowing out the open northern end of the bay.

METHODS OF STUDY

Field work was carried out during an eight day reconnaissance visit in December, 1966, from mid-June to mid-September, 1967, and from late March to late May, 1968.

As no detailed bathymetry maps of the study area were available, it was necessary to construct one during the course of the study. Over 55 miles (88.6 km) of echo sounding profiles were run¹ (Fig. 3). A Kelvin Hughes Inshore recording echo sounder, powered by a twelve volt battery, was used.

The basic sampling pattern consisted of a rectangular grid with a north-south sample spacing of 1500 feet (457 m) and an east-west spacing of 750 feet (229 m). The east-west sampling lines were given traverse numbers (Fig. 3) to facilitate location and discussion in the text.

Air photographs (see Plates 1, 2 and 3) were used to locate sampling stations in the shallow water, lagoonal environments. Outside of the reefs the sampling system broke down because of the difficulties in recovering samples and in locating them accurately in the field. Sextant sightings measuring the angles between at least three known points on shore were used to locate unknown sampling stations later.

1. At the time of the study English units (feet) were used and the echo sounder was graduated in feet. Metric equivalents have been calculated.

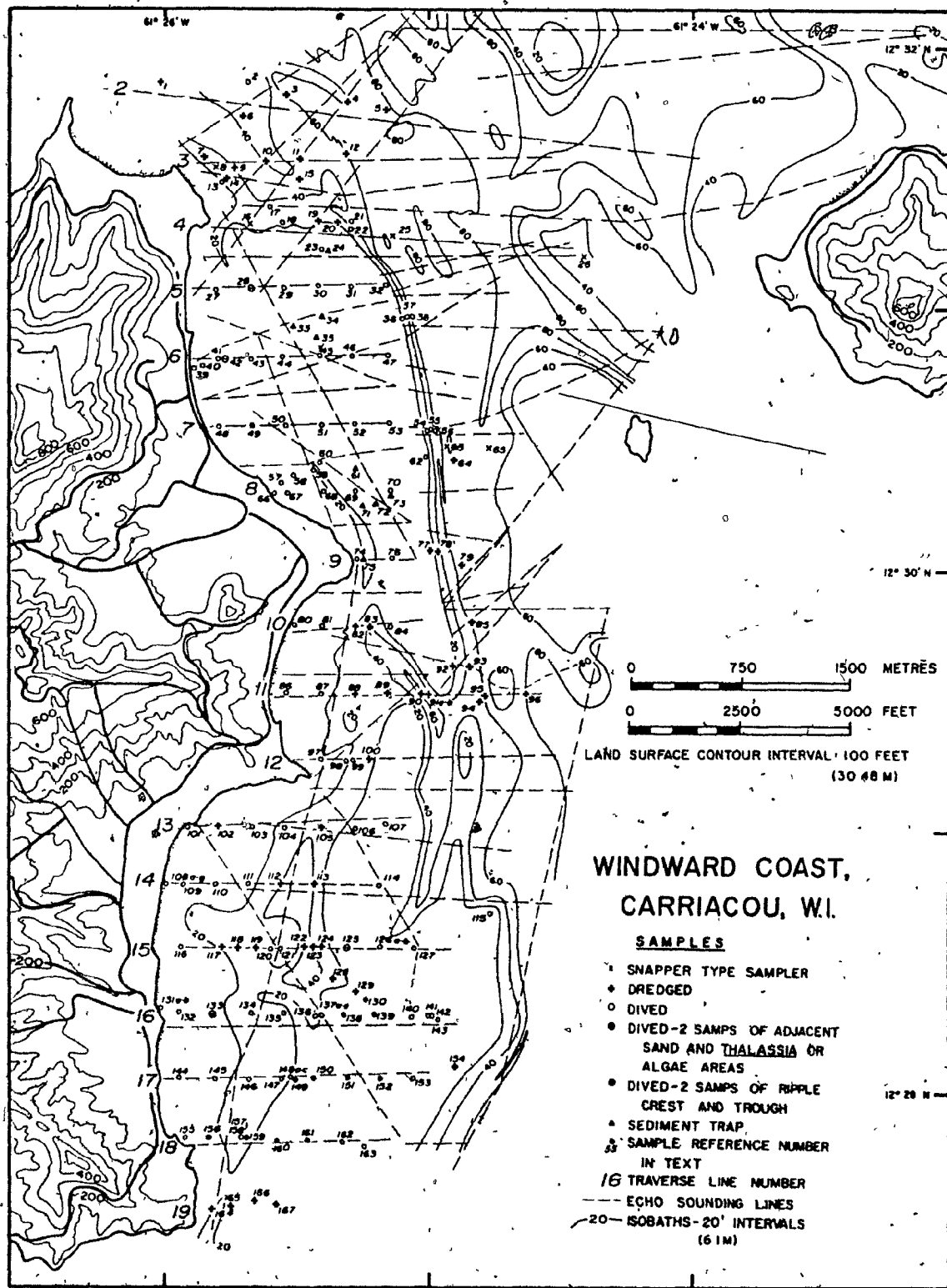


Fig. 3 Map of traverses, sampling stations, and echo sounding lines.

Most samples were collected by scooping the upper few centimeters of sediment in a 5 ounce (142 ml) bottle while skin diving. Samples were also collected during two SCUBA dives on the reef front of Watering Bay on traverses 6 and 7. In deep or very turbid water samples were collected with a small dredge or with a spring-loaded snapper type sampler. Two cores, each approximately one foot long, were collected on traverse 16 by pounding a plastic core barrel liner into the sediment.

In order to better understand the relationships between the grain size distributions of surface samples and those of sediment transported by tidal currents in Watering Bay, material in transport was collected in traps on and above the sea floor (Plate 7C). An Ott current meter (Type V, Sonas-Rion) was used during the 1968 season to obtain current velocities while some of the sediment traps were in place. This allowed comparisons to be made between theoretically transportable grain sizes and grain size distributions of the surface sediment and of the sediment in transport.

A total of 234 sediment samples were mechanically analyzed by standard wet and dry sieving techniques. These included 196 surface samples from 167 locations, 30 sediment trap samples and 8 core samples.

Abrasion of organic skeletons with variable durabilities and definite structure may tend to produce preferred grain size distributions. This effect was partially evaluated by component analyses of individual size fractions of three selected

representative samples from Grand Bay. Coarse fractions were examined in reflected light. Fine fractions were mounted and thin sectioned for examination in transmitted light under a microscope.

ACKNOWLEDGEMENTS

Field and other expenses arising from this study were met by funds from National Research Council of Canada Grant No. A2128 and an Imperial Oil grant to E. W. Mountjoy. The support of a National Research Council Scholarship from 1967 to 1969 is also gratefully acknowledged.

The author is indebted to his thesis supervisor, Dr. E. W. Mountjoy, for introducing him to the study and for his financial support, encouragement, critical reading and patience throughout this study. Many thanks are also due Dr. B. F. D'Anglejan for his advice and discussions concerning the study.

Of the many wonderful and kind people that the author met on Carriacou, he has only good memories and a desire to meet them again. Mr. Linton J. Rigg of Hillsborough arranged accommodation and provided an introduction to the island.

Mr. Zephrim McLaren and his family of Windward Village provided immeasurable help, hospitality and friendship. Mr. McLaren, Mr. Immanuel "Co-Coy" Bethel and Mr. Mervin Enoe at various times during the field seasons assisted the author with handling the boat and accompanied him while diving.

Dr. D. G. Patriquin during a week's visit in the field kindly identified many of the floral and faunal elements of the Thalassia beds.

Mr. G. B. Pendlebury accompanied the author during most of the 1967 field season and was of great assistance in all phases of the operation.

Some of the sample preparation and size analyses were done by Dr. Mountjoy's laboratory assistants, Mr. K. Egbuma and Mr. S. Moussadji.

Mr. W. Oglivie at Pearls Airport, Grenada kindly provided monthly wind speed and direction data for the years 1963 to 1967 inclusive.

The author wishes to express his gratitude and love to his wife, Jillian, for her encouragement and understanding, for her direct assistance in sample preparation and rough draft typing, and for matters not directly involved with the study.

The co-operation and understanding of Mrs. Anne Bafes during final typing and compilation are gratefully acknowledged.

CHAPTER 2 - ENVIRONMENTS

Since the properties of the biological communities and of the sediments are interdependent, and since both are controlled to a large degree by the physical-chemical conditions, the environments considered here are both biological and sedimentary. The study, however, has been made mainly from a sedimentological viewpoint, and the compositions and associations of the biological communities were not studied in detail.

The floral and faunal communities and zonation of coral reefs and lagoons in the Caribbean, Gulf of Mexico, Bahamas and Florida have been described in numerous textbooks, papers and guidebooks (excellent summary and bibliography in Bathurst, 1971 and Milliman, 1974). Reefs east of Carriacou are not basically different, differences being mainly of degree and related to differences in bathymetry and wave intensity. The most notable divergence is the apparent paucity of living Acropora cervicornis in the area, although this species was observed in abundance around Sandy Island on the west coast of Carriacou and around the islet of Mopion 2 miles (3.2 km) to the northeast. The only living A. cervicornis observed immediately east of Carriacou was a single bushy growth approximately 8 inches (20.3 cm) across immediately behind the barrier reef between traverses 7 and 8. Abundant dead and disarticulated branches of a coarser growth form were observed between 25 and 35 feet (7.6 and 10.7 m) depth on the reef slope around traverse 5, so there may be thickets of A. cervicornis on the reef slope in areas that were not observed (particularly in front of Grand Bay).

Previous to this study only a small scale general bathymetry map (Admiralty Chart 2872) was available. Profiles along more than 55 miles of echo sounding traverses (Fig. 3) were used to construct a detailed bathymetry map (Fig. 4).

The main environments are mapped on Figure 5. In Figures 6 and 7 details of the bathymetry and environments are presented for traverses 5 and 16, selected to represent Watering and Grand Bays respectively.

COASTAL ENVIRONMENTS

Sea cliffs bound the main points of land (St. Hilaire, Tarlton's and Kendeace) as well as the small points in Grand Bay. A gastropod fauna, dominated by Nerita and Purpura populates the rocks in the spray zone.

Well developed white carbonate sand beaches are present only in Jew and Grand Bays where vigorous surf conditions prevail. The coast line in Watering Bay is sheltered by numerous patch reefs and shoreward shoals. Also, because of the banks and islands to the east of Watering Bay, waves striking the reef front are smaller than those on the reef front in Grand Bay and give rise to smaller secondary waves in the back-reef. As a result mangroves grow along some of the more protected stretches of the shore in Watering Bay near traverse 8 and behind the fringing reef and reef flat between traverses 3 and 4. Beaches in Watering Bay are poorly developed and less than 10 feet (3 m) wide. They are built mainly of terrestrial black sand brought to the shore by ephemeral streams and sheetwash.

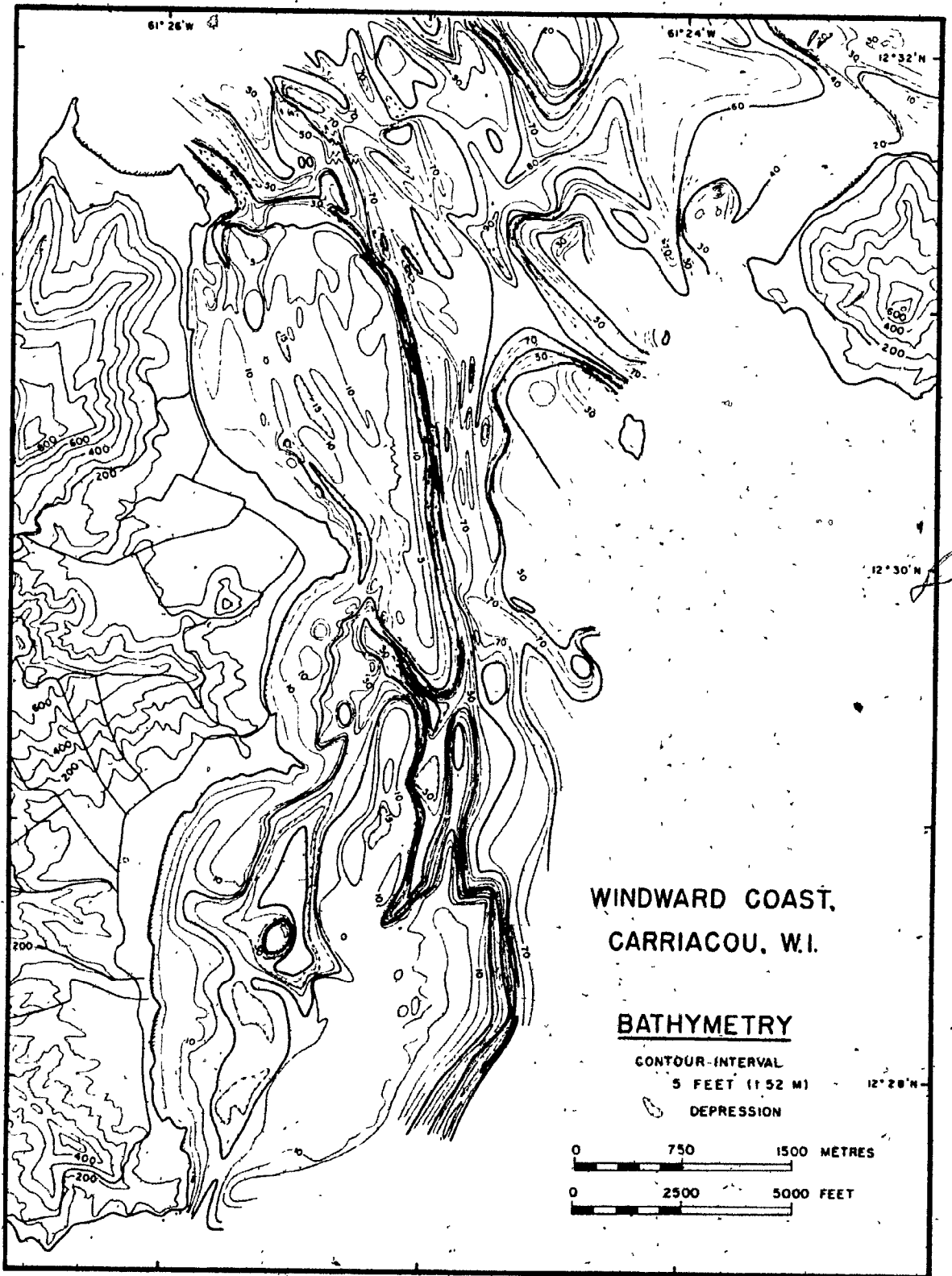


Fig. 4 Bathymetry map.

rather than of carbonate grains transported shorewards by waves.

FRINGING REEFS

Fringing reefs are present in front of the mangrove swamp at the northeast corner of Carriacou, along the northern quarter of Watering Bay, along the northern shore of Point St. Hilaire and along the southern shore of Tarlton's Point (Fig. 5). The latter three areas will be discussed first. Marine grass (Thalassia testudinum), non calcareous and coralline algae, and Porites divaricata grow on the top of the reefs a few inches below water level. Small gastropods and crabs are abundant. The substrate consists of coral gravel formed from interlocking dead branches of P. divaricata. At the seaward margins where the bottom surface drops abruptly as much as 7 feet (2.1 m) to marine grass beds, the flora and fauna is slightly more diverse with P. porites var. furcata, P. astreoides and the calcareous green algae Halimeda opuntia.

The fringing reef in front of the mangrove swamp is much better developed than the above reefs because it adjoins deeper water and is exposed to larger waves. The reef crest is separated from the mangrove swamp by a 125 to 375 foot (38 to 144 m) wide, shallow (1 foot, 0.3 m) reef flat of Halimeda sand and Thalassia beds.

Between the flat and the reef edge and parallel to the reef edge are two 20 to 30 feet (6.1 to 9.1) wide ridges with their tops at low water level. The inner ridge consists mainly of red algae encrusted Porites debris. Porites divaricata and

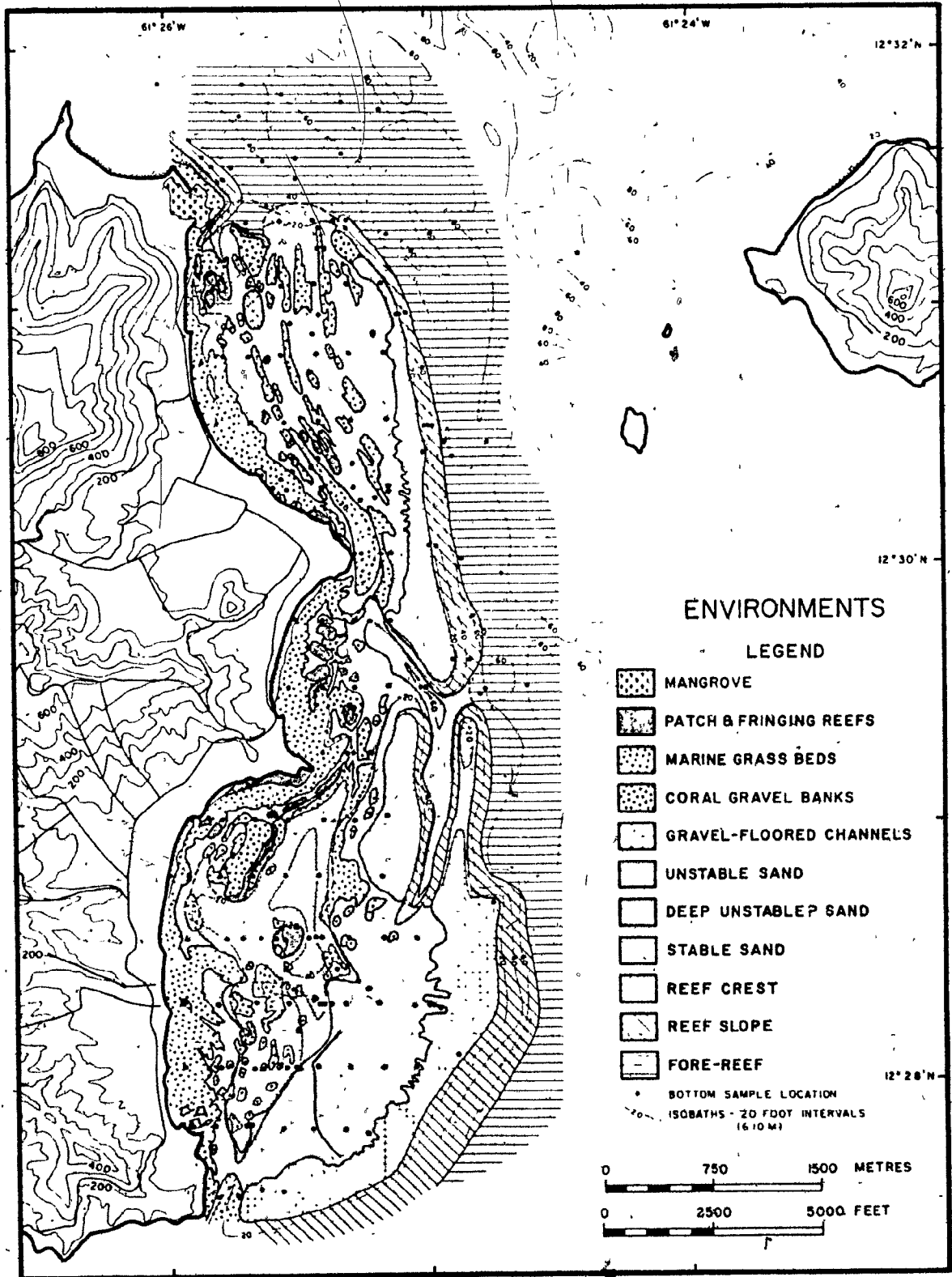


Fig. 5 Map of submarine environments east of Carriacou.

P. porites grow in shallow depressions amongst the rubble. Halimeda opuntia is abundant as is the long-spined black sea urchin Diadema antillarum and a brittle star-gastropod infauna.

The outer ridge consists of red algae encrusted Acropora palmata debris averaging one foot (0.3 m) across. Large blocks up to 3 feet (1 m) in diameter of A. palmata branches bound together by red algae rest on this ridge and are completely exposed at low low water in the spring months.

The outer reef crest is narrow and has an abrupt drop off at the seaward margin. The substrate is cavernous, coral and algal rock, with very little loose sediment. Acropora palmata is the dominant framework coral in this zone to the northwest and Montastrea annularis is dominant to the southeast. Species of Diploria and Siderastrea, and Favia fragum are present as secondary corals. Agaricia agaricites, bryozoa and red encrusting foraminifera, Homotrema rubrum, are common beneath overhanging surfaces.

On the reef slope between 8 and 17 feet (2.4 and 5.2 m) depth Porites porites, P. astræoides and the calcareous hydrozoan Millepora are most common. The slope is more gentle below 17 feet (5.2 m) and is covered with dead P. porites rubble and interstitial sand. At 35 feet (10.7 m) there is a level sand bottom with scattered gorgonians, Diploria and Siderastrea. On echo sounding profiles a 5-foot (1.5 m) high ridge and outer slope to a depth of 50 feet (15.2 m) was observed beyond the level sand area. The ridge and outer slope were not investigated by diving and could not be seen from the surface.

MARINE GRASS BEDS

Marine grass beds east of Carriacou display a wide variation in development and associated flora and fauna, dependent mainly upon water depth and the nature and degree of water agitation.

Fringing Reef Flat

The beds on the reef flat adjacent to the mangrove swamp at the north end of Watering Bay are the shallowest observed. This is an area of generally high and variable water temperatures, strong sunlight and small waves. The grass is Thalassia testudinum, much of which is killed during March, April and May when the beds are exposed at low low water during spring tides. Dead leaves drift shoreward and accumulate on the beach or contribute to the knee-deep hydrogen sulphide-rich organic mud around the southern end of the swamp behind the fringing reef to the south.

Halimeda opuntia and the red algae Amphiroa, Goniolithon and Galaxaura are most abundant in the northeastern beds in front of the swamp and behind the fringing reef crest. Blue-green algae is abundant especially in the southernmost beds.

The substrate consists mainly of Halimeda segments with Porites gravel to the northeast and more muddy, organic-rich sediments to the south. Mounds of coarse sand in the latter region appear to be the work of burrowing crabs.

Shoreward Watering Bay

In Watering Bay Thalassia beds extend from within 10 feet (3 m) offshore to a depth of around 7 feet (2.1 m) in an area from 50 to 200 feet (15.2 to 60 m) wide. Although waves passing over the beds are usually no higher than around 6 inches (15.2 cm) the bottom is affected and the water is usually turbid. No strong water currents affect the beds except at the outer margin in a few places.

The beds are relatively simple and there is not an extensive associated flora and fauna. Small sponges, brittle stars, the white sea urchin Tripneustes esculentus, the coral Manicina areolata and Halimeda opuntia are found throughout the beds. Towards the south colonies of Porites porites var furcata are fairly common (Plate 8D)

The coarse fraction of the muddy substrate consists mainly of Halimeda segments. In the shoreward half of the beds terrigenous grains form up to 50 percent of the sediment. Seaward this component decreases rapidly in abundance, as it is trapped amongst the grass and masked by autochthonous skeletal material.

Central Watering Bay

Grass beds associated with macroscopic, non-calcareous green algae (mainly Caulerpa and Dichtyota) form north-south orientated bands in Watering Bay (Plates 1 and 2). The orientation is a result of the strong north and south flowing tidal currents in the bay.



The beds have a maximum relief of about one foot (0.3 m) above the adjacent sand. Eroded crescentic "blowouts" and stabilized sand waves (approximately 10 feet (3 m) long and 5 inches (12.7 cm) high) are common within the beds at the northern end of Watering Bay in water depths between 15 and 20 feet (4.6 and 6.1 m).

The beds are extremely simple (Plate 7D). Thalassia is the dominant grass with minor Cymodocea. Calcareous algae are rare. Starfish and the large gastropods Strombus gigas and Cassis tuberosa were occasionally observed around and within the beds.

The proportion of macroscopic, non-calcareous green algae in the beds increases with the amount of gravel suitable to act as holdfasts in the dominantly coarse sand substrate. The gravel is red algae-coated coral debris (usually of Porites porites). The proportion of gravel and therefore of non-calcareous algae increases southwards.

Shoreward Jew and Grand Bays

The shallow, shoreward grass beds in the two southern bays are subjected to stronger wave action than those in Watering Bay and are, therefore, more complex. The grasses are Thalassia, Cymodocea and Diplanthera; Thalassia being the dominant form. Calcareous algae (both red and green), sponges, corals and gorgonians are all abundant within these beds. The identified forms are listed in Figure 7.

Except for Porites divaricata and P. porites, which live throughout the environment, the corals and gorgonians are most

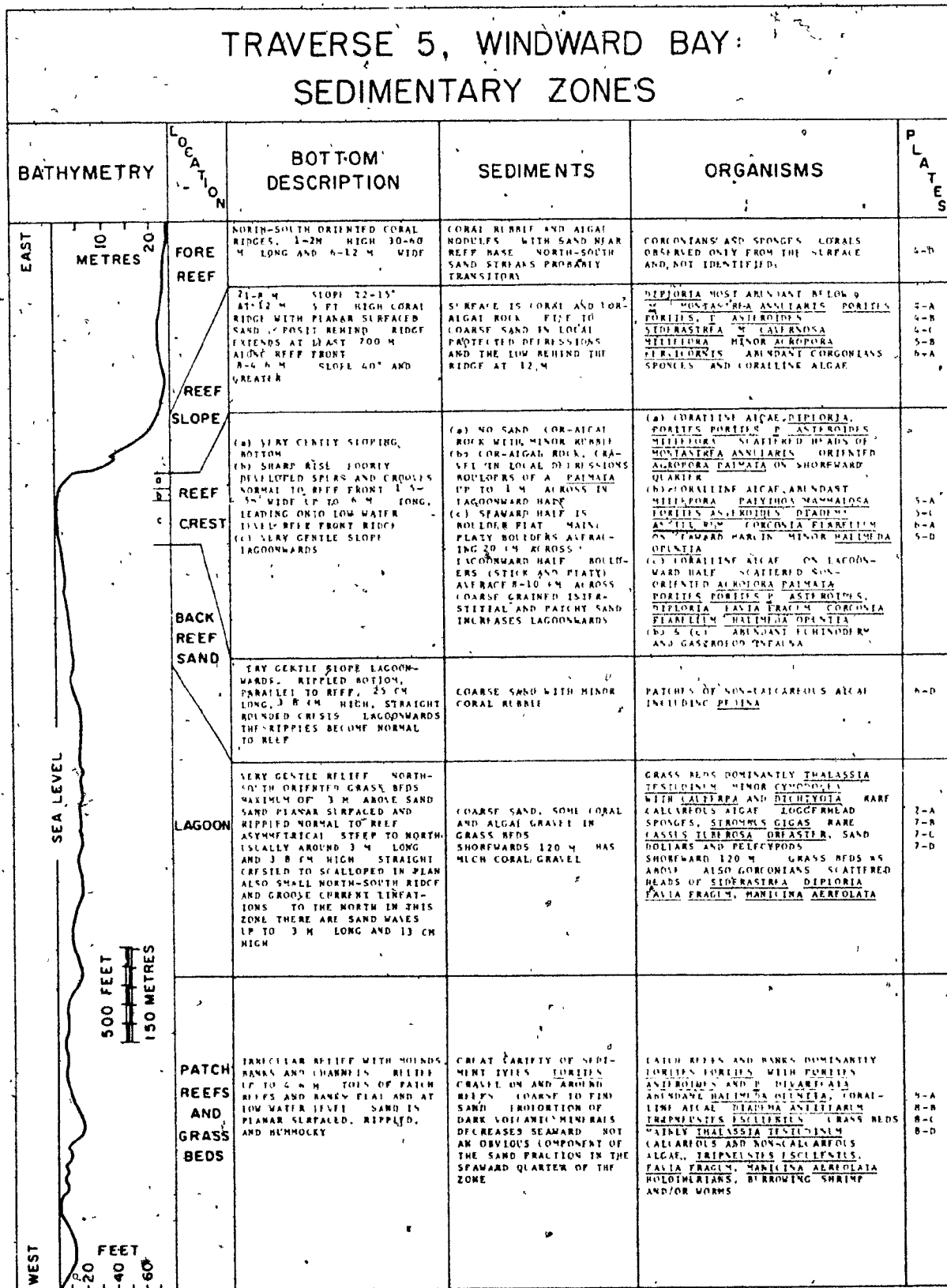


Fig. 6 Bathymetry and environments, traverse 5, Watering Bay.

abundant seaward in depths between 5 and 10 feet (1.5 and 3 m) where scattered small reef knobs are developed.

Circular and crescentic shaped "blowouts" are eroded by waves in water depths of less than 5 feet (1.5 m). These pits are up to 15 feet (6.1 m) across and have a relief of one foot (0.3 m). The substrate, consisting of Porites porites and P. divaricata rubble with interstitial coarse sand, is exposed at the edges of the pits.

Central Grand Bay

Below 15 feet (4.6 m) depth in Grand Bay the grass beds change character whether they are extensions of the shoreward beds or are separate beds. The proportion of Thalassia is reduced, and Diplanthera and Cymodocea are the dominant grasses. The calcareous algae are mainly green algae (Fig. 7, Plates 9D and 9C).

There is a gentle, almost indistinguishable relief between the higher interior of the grass beds and the adjacent sand. The substrate, both within and adjacent to the grass beds, is fine sand.

Patches of macroscopic non-calcareous algae, mainly Dictyota and Sargassum, are also developed in the deeper parts of Grand Bay. The deepest beds observed, either of grass or algae, were at 25 feet (7.6 m) on traverse 16. At greater depths in Grand Bay samples were dredged, and the bottom could not be seen because of turbid water.

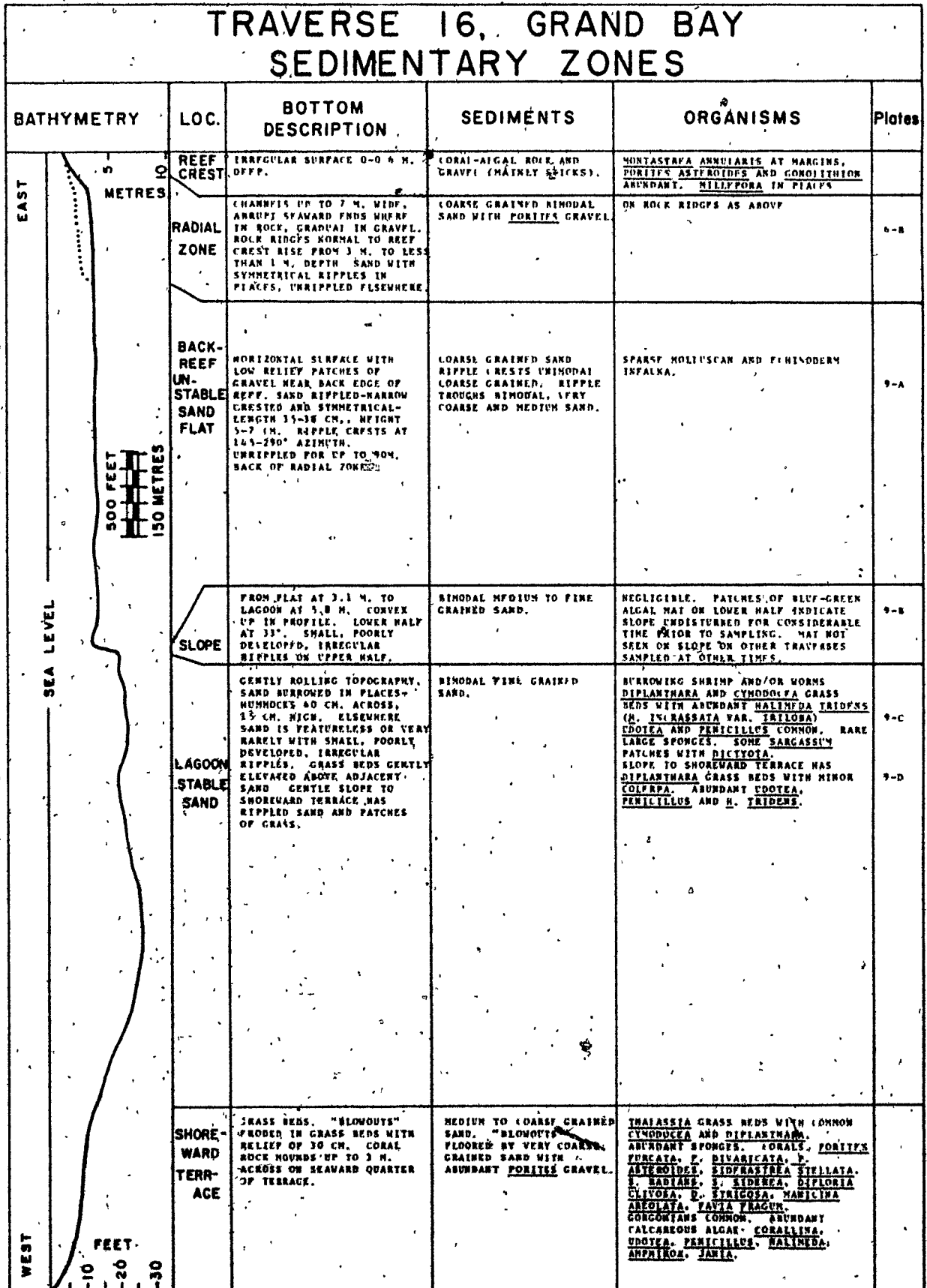


Fig. 7 Bathymetry and environments, traverse 16, Grand Bay.

Post Box

PATCH REEFS

Patch reefs in Watering Bay range in size from small Porites clumps 10 feet (3 m) across to Grand Cay which is an elliptical reef approximately 900 feet (274 m) long and 480 feet (146 m) wide (Plate 2). Maximum relief of the reefs above the floor of Watering Bay is 15 feet (4.6 m).

The reefs are poor in terms of numbers of species. The dominant species is Porites porites with lesser amounts of P. divaricata and P. astreoides (Plates 8A and 8B). The latter two species are common only near the top of the reef faces and on the reef flats near low water level. Other coral species are present only at the north end of Grand Cay which is affected by larger waves entering Watering Bay from the northeast. Monastrea annularis, Acropora palmata, Siderastrea and Millepora are all common at that locality. Calcareous algae, especially Halimeda opuntia, are major sediment producers on the patch reefs. Skeletal fragments of the molluscan fauna and the abundant echinoids, Diadema antillarum and Tripneustes esculentus form another fraction of the sediment.

Waves affecting the shoreward patch reefs of Jew and Grand Bays are larger than those in Watering Bay. As a result the sand sized sediment is removed from the tops of the Jew and Grand Bay reefs leaving mainly coral and red algal rock and gravel surfaces. The dominant corals are massive Diploria and Siderastrea. Millepora and gorgonians are also common on the more open, seaward reefs. On the most shoreward reefs Porites porites and P. astreoides occur.

The 700-foot (213 m) wide, subcircular patch reef near the centre of Grand Bay rises from a depth of 43 feet (13 m) to a depth of 10 feet (3 m). The slopes and top are coral and red algal gravel and coarse sand. The proportion of sand increases down the slopes and toward the landward edge. There is a fairly heavy cover of macroscopic non-calcareous green algae over most of the gravel. Scattered growths of Diploria, Siderastrea, Porites porites, P. divaricata, P. astreoides and Favia fragum populate the top of the reef. Halimeda opuntia is common over most of the reef but is most abundant towards the landward edge. A raised rim at the northeast corner is mainly coral and red algal rock with minor Diploria, Siderastrea, Acropora palmata, Millepora and gorgonians.

CORAL GRAVEL BANKS

Three areas east of Carriacou have a shallow substrate of coarse coral gravel populated by scattered corals and abundant gorgonians. These areas could be classed as reefs but are sufficiently different to be discussed separately. The differences include a lack of a rigid framework, either of red algal encrusted corals or of interlocking growing corals, and a lack of abrupt relief above adjacent sands. Similarly, where there is abundant marine grass, corals and gorgonians are more abundant than in those areas discussed as marine grass beds above.

The three areas (Fig. 5) are: north of Grand Cay (5 feet (1.5 m) deep) at the north end of the barrier reef in Watering Bay (10 to 15 feet (3 to 4.6 m) deep) and south of Tarlton's Point in Grand Bay (7 to 10 feet (2.1 to 3 m) deep). Corals include small clumps of

Montastrea annularis and scattered heads of Diplora, Siderastrea, Porites astreoides, P. porites and Favia fragum. Millepora is present as bladed growths and as crusts on gravel and gorgonians. The area in Grand Bay differs from the other two in that there is abundant Thalassia testudinum and Cymodocea amongst the coral and gravel. Halimeda opuntia grows in all areas.

STABLE SAND

"Stable" is a relative term. For example, very coarse sand may be stable in a given environment while medium sand and finer grain sizes are readily moved. In the stable sand environment east of Carriacou the substrate is fine sand with very little gravel or mud.

Several areas east of Carriacou are protected from the strong influence of waves and currents. The lack of mechanical agitation is reflected by the lack of current or wave-induced sediment-surface features, by the preservation of shrimp and/or worm burrow hummocks (Plate 8C), and by a grey cast to the color of the sediment. The grey cast is presumed to result from the presence and action of blue-green algae and/or bacteria and fungi. In an agitated environment soft organic films on sediment grains are rapidly abraded, and carbonate sand appears white.

The region between Grand Cay and the shore in Watering Bay is protected from waves by Grand Cay and adjacent banks and patch reefs. These and the configuration of the shoreline also nearly negate the action of tidal currents. In local areas such as to the north of raised grass beds tidal currents do not appear to

affect the bottom at all.

In Grand Bay below 20 feet (6.1 m) depth there is no evidence of strong wave or current action. As previously noted the grass beds in this environment are mainly Diplanthera and Cymodocea rather than Thalassia as in the shallower beds. The differences may be related to the depths of water and degree of light penetration, or also possibly to differences in turbulence. Diplanthera and Cymodocea appear to be more fragile and less solidly rooted than Thalassia, and it may be that they can become the dominant grasses only in a stable non-turbulent environment.

UNSTABLE SAND

Extensive areas of medium to coarse grained sand are present in the lagoons of Watering and Grand Bays. These areas are either shallow or unprotected so that the sediment surface comes under the influence of waves or tidal currents, and the sand is actively moved and transported. This is the most widespread and abundant environment in the area (Fig. 5). The small areas of unstable sand associated with the reefs or marine grass beds are not included here.

Most of Watering Bay is between 7 and 20 feet (2.1 and 6.1 m) deep and is affected by waves and by strong reversing tidal currents which disturb and transport the sand (Plate 7A and C). Linear north-trending marine grass and algae beds in this environment have been discussed above. Strombus gigas and Oreaster

are commonly observed. "Loggerhead" sponges (Plate 7B) occur near marine grass or macroscopic non-calcareous green algae beds. Abundant worms, small gastropods and pelecypods also inhabit the bottom. Features on the sediment surface vary from small current lineations to sand waves approximately 10 feet (3 m) long and 5 inches (12.7 cm) high.

In Grand Bay the unstable sand environment is present for approximately 2,000 feet (610 m) behind the barrier reef and on the shoaling slope between the shoreward marine grass beds and the stable sand environments. The area is at a nearly constant depth between 10 and 12 feet (3 and 3.6 m). Medium to coarse-grained sand on the surface is strongly rippled (Plate 9A) by secondary waves passing shorewards from the reef. The shoreward edge of this back-reef sand flat (Plate 3) is a slope of 25 to 30 degrees (Plate 9B and C) extending to a depth of 20 to 40 feet (6.1 to 12.2 m) in the stable sand environment.

GRAVEL-FLOORED CHANNELS

Two channels, one off Point St. Hilaire and the other off Kendeace Point (Fig. 5), are floored by coral and algal gravel with interstitial and patchy coarse sand. Both channels are 20 to 26 feet (6.1 to 7.9 m) deep.

Scattered Diploria and Siderastrea heads, Montastrea annularis, gorgonians, Millepora and Diadema antillarum are present in the channel off Point St. Hilaire. There are outcrops of the volcanic conglomerate exposed on Point St. Hilaire to a depth of 26 feet (7.9 m) on the seaward side of the channel.

This area is the site of some of the strongest tidal currents behind the barrier reef, often resulting in choppy water when the currents oppose the wave direction.

There are no large corals or gorgonians in the channel off Kendeace Point. No currents were observed there during the study. However, the presence of the channel and the texture of the sediment indicate that currents are active here, probably during strong easterly storms when waves transport considerable water over the reef into the lagoon.

REEF CREST

This environment, from the upper break in slope on the reef front to the edge of the back-reef sand, is the biologically most complex and variable submarine environment east of Carriacou. It is the site of maximum organic production and the obvious source area of most of the lagoonal sediment.

All the reef crests mapped (Fig. 5) are characterized by extensive encrusting growth of red algae, by abundant red encrusting foraminifera (Homotrema rubrum) and by the absence of sand except in small protected depressions.

Several sub-environments, any one of which may or may not be present along a given traverse across the reef, constitute the reef crest environment. From the seaward side the sub-environments are: the gently sloping outer reef terrace at 17 to 10 feet (5.2 to 3 m) depth, the spur and groove zone, the algal ridge, the boulder flat and the radial zone.

Watering Bay barrier reef crest is nearly 10,000 feet (3048 m) long and up to 1,200 feet (366 m) wide. It is generally

350 to 400 feet (107 to 122 m) wide. The reef crest on traverse 5 (Fig. 6) is representative of the northern half where the spur and groove and radial zone sub-environments are absent.

South of approximately traverse 6 a radial zone is developed, reaching its greatest development near traverse 8 (Plate 2). This zone consists of ridges and channels oriented normal to the reef crest landward of the algal ridge and boulder flat. Maximum relief is 10 feet (3 m). The channels are floored by coarse sand and coral and algal gravel. The ridges are extremely variable and may consist of red algal coated boulders, of coral and algal rock, of living Montastrea annularis or of living Acropora palmata (Plate 6C). Seaward the ridges merge with the boulder flat and the channels become shallower. Mounds composed mainly of Montastrea annularis and areas of scattered Acropora palmata growth were observed in this zone.

The best developed spur and groove features observed on the reef front occur near traverse 9. They are less than 100 feet (30.5 m) long with less than 10 feet (3 m) of relief. The grooves (surge channels) are 15 to 20 feet (4.6 to 6.1 m) wide and floored by coral and red algal rock.

On traverse 11 there is a major reef pass at a depth of 50 to 60 feet (15.2 to 18.3 m). Strong water currents were not observed in the pass which is floored by medium to coarse-grained sand. The coarsest sands in the pass occur near the bottom of the adjacent steep reef slopes.

South of the reef pass to approximately traverse 14 two reef ridges are separated by a 50 foot (15.2 m) deep channel running parallel to the reef front and opening onto the reef pass. Shallower parts of the inner ridge have abundant Acropora palmata and Millepora growth, but for the most part there is little coral or algal growth on the ridge crests.

The Grand Bay barrier reef crest is not as well known as that of Watering Bay. The few observations made on the reef front indicate that spur and groove structures are poorly developed or absent and that the reef front terrace is mainly coralline and algal rock with minor coral growth. Heavy surf conditions precluded examination of the algal ridge.

A wide radial zone is present on the lagoonward half of the reef crest and is extremely variable in composition and in development of the ridges. Acropora palmata is not as abundant as it is on the Watering Bay reef crest. Montastrea annularis and Diploria are the most abundant corals. Where the ridges are of coralline and algal rock and growing corals (Plate 6B) the relief is more abrupt than in Watering Bay.

REEF SLOPE

The barrier reef slope environment is outside the gently sloping front terrace of the reef crest and extends from about 15 feet (4 - 6 m) to 60 to 75 feet (18.3 to 25.9 m) water depth. The nature of the bottom, sediments and organisms of the Watering Bay barrier reef slope north of approximately traverse 6.5 is outlined in Figure 6.

To the south of traverse 6.5 the slope is gentler (6° slope overall) and has less coral growth, especially on the upper parts. Ridges of living coral parallel to the reef crest occur on the reef slope and have flat sand areas behind them. They occur progressively deeper on the reef slope towards the south (Fig. 4). The Grand Bay barrier reef slope is probably around 5 to 6 degrees. Ridges are developed at a depth of approximately 60 feet (18.3 m).

Coral growth is extremely active in this environment. Massive forms such as Diploria, Montastrea and Siderastrea are the dominant corals.

FORE REEF

This environment was observed only during dives near the base of the Watering Bay barrier reef slope, and on a few occasions when the water was unusually clear, through a glass-bottomed box from the surface between Little Tobago and Carriacou. North-south ridges and channels predominate. Some, and probably most, of the ridges are sites of active coral growth. Sand, coral rubble and algal nodules make up the rest of the bottom. Gorgonians and sponges probably are abundant, as attempts to sample the bottom with a snapper type sampler often brought up pieces of these organisms.

Kranck (1968) reported that, in this region of the southern Grenadines, sand bottom is present behind the reefs and islands, but that wherever currents are uninterrupted, as in the fore-reef and inter-island environments, the bottom consists of coral

growth and algal nodules. She interpreted thin patches and stringers of sand in the coral growth-algal nodule areas as being transitional, undergoing tidal and seasonal changes. This interpretation is probably correct on the basis of measured current strengths.

SUMMARY AND DISCUSSION

The submarine areas east of Carriacou are the sites of considerable carbonate sediment production, transportation and deposition. Three bays are enclosed by a well-developed barrier coral reef lying from one-quarter to one and a quarter mile (0.4 to 2.0 km) offshore. The flora and fauna and their associations in the various environments are not significantly different than those described in many Caribbean reef areas.

The two main bays (Watering and Grand) contain the same major reef and back reef environments (reef crest, unstable sand, stable sand, grass beds, patch reefs and beaches) but with differences in their development. The differences can be related to differences in exposure to waves, size, bathymetry and hydrology of the two bays.

Grand Bay is more exposed, larger and deeper than Watering Bay. Larger waves impinge on the reef front, and larger secondary and wind waves are developed behind the reef in Grand Bay than in Watering Bay, which is partially protected by banks and small islands to the east and northeast. However, the bottom of Watering Bay is scoured by reversing north-south tidal currents which were not observed in Grand Bay.

The above differences cause the following contrast in similar environments in the bays:

- (1) Beaches in Grand Bay are well developed and are composed of carbonate sand transported shoreward by the waves. Beaches in Watering Bay are poorly developed and are composed mainly of black, terrigenous sand transported to the shore by ephemeral streams and sheet wash during rain storms.
- (2) Shoreward Thalassia beds have a much more extensive and varied associated flora and fauna in Grand Bay than in Watering Bay.
- (3) The unstable sand substrate in Grand Bay is transported shoreward from the barrier reef into the deeper lagoon by secondary waves. That in Watering Bay is transported mainly laterally by strong tidal currents.
- (4) Nearly half of Grand Bay between the shoreward Thalassia beds and the barrier reef is deeper than 20 feet (6.1 m) and is floored by stable sand which is not moved by normal waves. Stable sand substrate is uncommon in Watering Bay and occurs mainly in small areas associated with the outer edge of the shoreward Thalassia beds behind Grand Cay.
- (5) A back-reef radial zone is well developed on the landward side of the barrier reef crest only in southern Watering Bay and in Grand Bay.

CHAPTER 3 - SEDIMENTS

SOURCES

In both Grand and Watering Bays sediment is mainly bioclastic carbonate with minor amounts of terrestrial material in the shoreward areas. No inorganically produced loose carbonate grains were observed. Therefore, the main sediment sources are those environments having a high productivity of organisms with carbonate skeletons.

Barrier Reefs

Barrier reefs are obvious sources of most of the sediment in the bays. Corals, coralline algae and Halimeda, the most common sediment contributors, are all abundant on the reef crests where they are exposed to vigorous wave action and to weakening and erosion by various boring and grazing organisms (see Goreau and Hartman, 1963; discussion in Swinchatt, 1965, Chapter 9, Milliman, 1974). Other sediment contributors on the reef crest include the echinoderm and gastropod infauna.

A wide range of grain sizes is produced on the barrier reefs—from 3 feet (0.9 m) diameter boulders of Acropora palmata to mud-sized grains. It is extremely difficult to estimate the grain size distribution of all sediment produced. There is no single place one could sample such a grain size distribution. The coarsest gravel sizes are produced and transported intermittently by storm waves, and are concentrated on the boulder flat of the reef crest or immediately behind the reef. Sand-

sized material is probably produced and transported in traction load nearly continually by the waves and currents washing over the reef. Very fine sand and mud-sized material is probably produced continually and transported in suspension load almost immediately. A long term, detailed sampling program of these materials would be required to estimate the rate and grain size distribution of sediment production.

Sediment produced on the reef crests is moved into the lagoons by waves and currents passing over the reef. Sediment lobes trending to the northwest in Watering Bay behind the barrier reef indicate the direction of net sediment transport under the influence of waves and the dominant north-flowing tidal currents (Plate 2).

Patch Reefs

The role of patch reefs as suppliers of sediment to the lagoon in Watering Bay is also clearly evident on Plate 2. North of most of the reefs there is a dark "tail" of green algae and grass beds. The plants use Porites porites rubble swept from the reefs by the north flowing tidal currents as holdfasts. Sand-sized material, derived from broken coral, Halimeda and coralline algae on the patch reefs is transported along the same trend.

The one large patch reef in Grand Bay does not appear to supply coarse sediment to the adjacent deeper environments except possibly for a small amount in a landward direction. The sediment on the lower slopes of the reef is as fine as the

sediment present in the adjacent stable sand environment.

Marine Grass Beds

The generally abundant calcareous flora and infauna of the marine grass beds produce considerable sediment. Within the beds skeletal breakdown is probably mainly the result of biological processes such as boring by algae, pelecypods, worms and sponges, and grazing by fish and gastropods (Swinchatt, 1965).

Wave action on the shoreward beds probably does not move much sand-sized detritus seaward. Most material of this size grade is trapped within the beds by the grass, or moves shoreward onto the beaches. Fine sediment moved seaward in suspension is quickly removed from the study area by currents.

Beds in a position to supply sediment to the unstable sand environment (elongate, north-south beds in Watering Bay) were described above as lacking a plentiful associated calcareous flora and fauna. Therefore, they are unlikely to be important sediment sources.

Deep beds in the stable sand environment of Grand Bay produce coarse (Gastropods and Halimeda) and fine (Penicillus, Melobesia, Udotea) sediment. It is doubtful that much sediment is moved from these beds except for some of the fines during severe storms.

In general marine grass beds do not supply much sediment to adjacent environments but do produce and accumulate sediment in place (Scoffin, 1970).

Fauna of Sand Environments

The skeletal parts of pelecypods and echinoids living in the sand environments form only a small part of the sediment. Cemented linings of burrows of shrimp and/or worms are often excavated by waves or currents and broken, supplying multi-granular grains to the sediment.

Tertiary Outcrops

Eocene to Pliocene outcrops on land supply mainly sand- and mud-sized material to some of the beaches and shoreward grass beds. Main source rocks are andesitic and basaltic variable agglomerates and tuffs. Plagioclase, pyroxene, olivine and magnetite are the main minerals, and the beaches are black where terrestrial supply dominates (mainly in Watering Bay).

During a rain storm samples were taken of material washing down the cliff on the southern side of Tarlton's Point, of the suspended material in sea water a few feet from shore and of the bottom sediment a few feet from shore. X-ray diffraction analyses of the less than two micron size fractions of the three samples exhibited only peaks characteristic of montmorillonitic and expandable clays.

Boulder deposits of volcanics and limestones are present near shore at the foot of cliffs on the three main points of land.

SEAFLOOR SURFACE FEATURES

Features such as ripple marks and current lineations are direct evidence of the action of waves and currents which transport bottom sediments and affect their textures. Orientations of these features and the paths followed by bottles half filled with water and released to drift with northerly flowing tidal currents in Watering Bay are mapped on Figure 9A.

In Watering Bay the dominance of northerly flowing tidal currents is borne out by the abundance of irregular asymmetrical ripple sets which are steep to the north. Asymmetrical ripples, steep to the south, were of short duration and were observed only at two stations that were occupied for a full day. Two types of grain movement on planar surfaces were observed (sites indicated by "P" on Fig. 9A): scattered rolling of individual grains at location 50, and saltation and rolling of coarse sand over the entire surface at location 45.

Regular, long-crested symmetrical ripples, indicative of wave action (Harms, 1969), are present only in three areas: immediately behind the reef, in the shoreward third of the bay, and at the northern end of the bay where waves are refracted around the reef and into the bay.

In Grand Bay very regular, long-crested symmetrical ripples are indicative of the dominance of wave action. Waves passing over the barrier reef are refracted and diffracted, crossing the back-reef sand flat in different directions from different segments of the reef to produce a complex pattern of ripple orientations (Fig. 9A).

GRAIN SIZE CLASSES

Percentages of gravel (sieve diameter coarser than -10 or 2 mm), sand (4 to -10 or 0.06 to 2 mm) and mud (finer than 40 or 0.06 mm) in each of 204 seafloor, beach and core samples were plotted on a ternary diagram (Fig. 8) which is divided according to the grain size classification of Folk (1968) and Folk et al. (1970). The classification is modified in that one percent rather than 0.01 percent gravel content is required before the prefix "slightly gravelly" is applied. This is an arbitrary division, used to separate the samples in the "sand" and "slightly gravelly sand" fields more evenly for mapping purposes.

A striking feature is the abundance of sand followed by gravel, with little mud-sized material. Only three samples contain less than 50 percent sand and they contain more than 50 percent gravel. Two of these samples (21, 38) were collected near the base of the reef front of Watering Bay and the other (137b) was from a linear deposit of molluscan and coral debris at the base of the slope from the back-reef sand flat in Grand Bay.

Of the seventeen samples containing more than 5 percent mud only five contain more than 10 percent mud. The most mud rich sample contained 17.06 percent mud and was from location 109 in a shoreward Thalassia bed on traverse 14 in Grand Bay. Other mud rich samples were also from shoreward Thalassia beds, from deep water in central Grand and Jew Bays and from depths greater than 20 feet (6.1 m) at the northern end of Watering Bay (Fig. 9B).

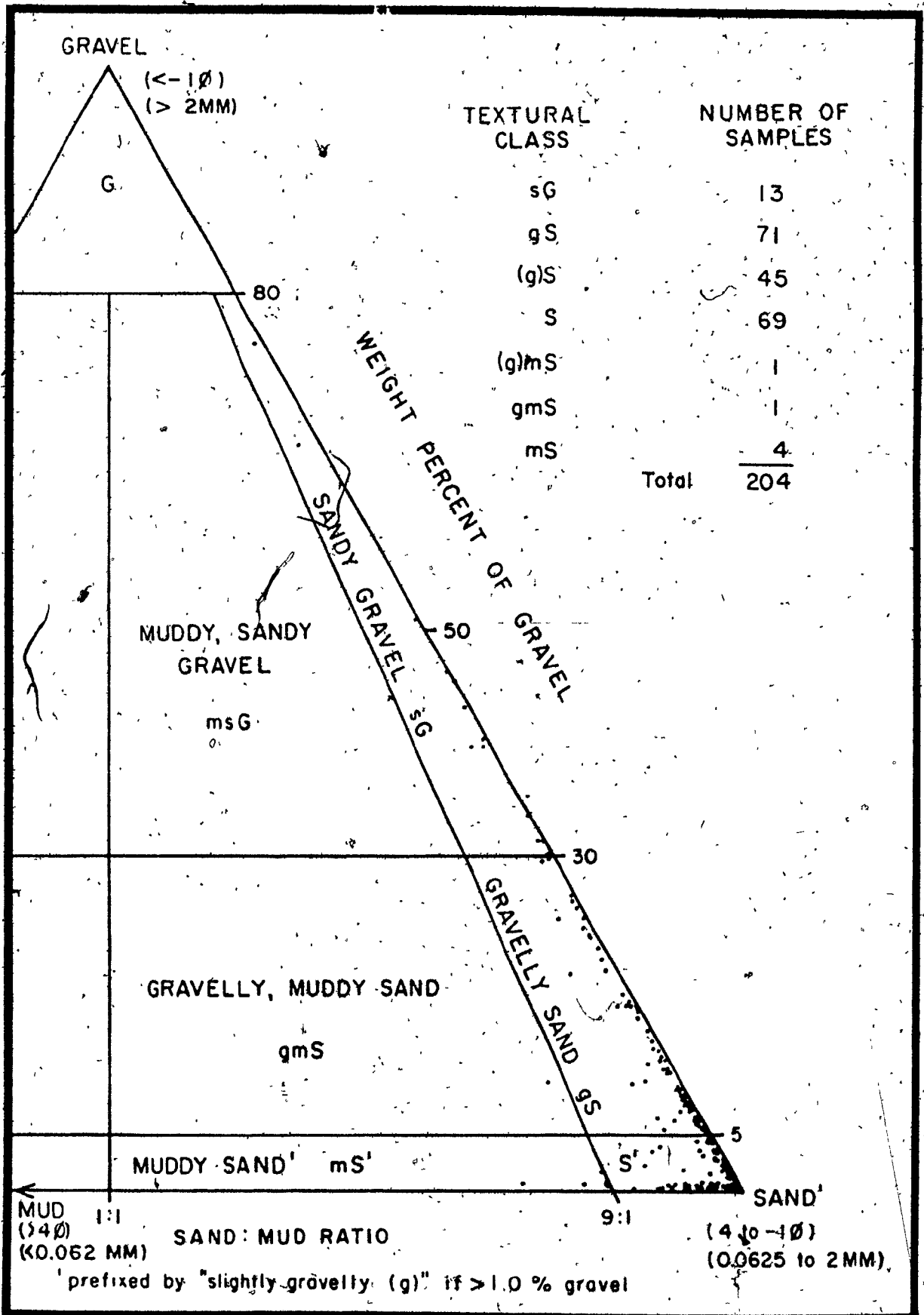


Fig. 8 Textural classes of sediment.

AREAL VARIATION OF TEXTURAL PARAMETERS

Maps of textural classes, mean grain size, grain size standard deviation, skewness and kurtosis are presented in Figs. 9B, 10A, 10B, 11A and 11B respectively. The statistical parameters are moment measures (see Appendix I) calculated by computer using 5.5 ϕ (0.0225 mm) as the mid point of the pan fraction which was finer than 4 ϕ (0.0625 mm).

In the forereef environment outside of Watering Bay gravelly to slightly gravelly, coarse to very coarse skewed, meso- to leptokurtic sand samples and unsampled gravel areas are attributable to proximity of source, in situ coral and coralline algae growth, and strong tidal currents.

On the reef slope from south of traverse 7 towards the north there is an increase in grain size from mainly coarse sand to very coarse sand. Textures change from sand, slightly gravelly sand and gravelly sand to sandy gravel. The northward increase in grain size probably reflects the development of stronger tidal currents to the north in the restriction between the reef and the banks around Fota and Little Tobago Islands (Figs. 1 and 3).

The sea floor on the reef crest is dominantly coral-algal rock, coral growth and gravel as large as boulder size (coarser than 25.6 cm). Analyzed sand samples were from small depressions in the rock and from amongst corals.

In the unstable sand environment of Watering Bay the grain size distribution of the dominant sediment type is moderately widely dispersed; meso- to leptokurtic and either positively or

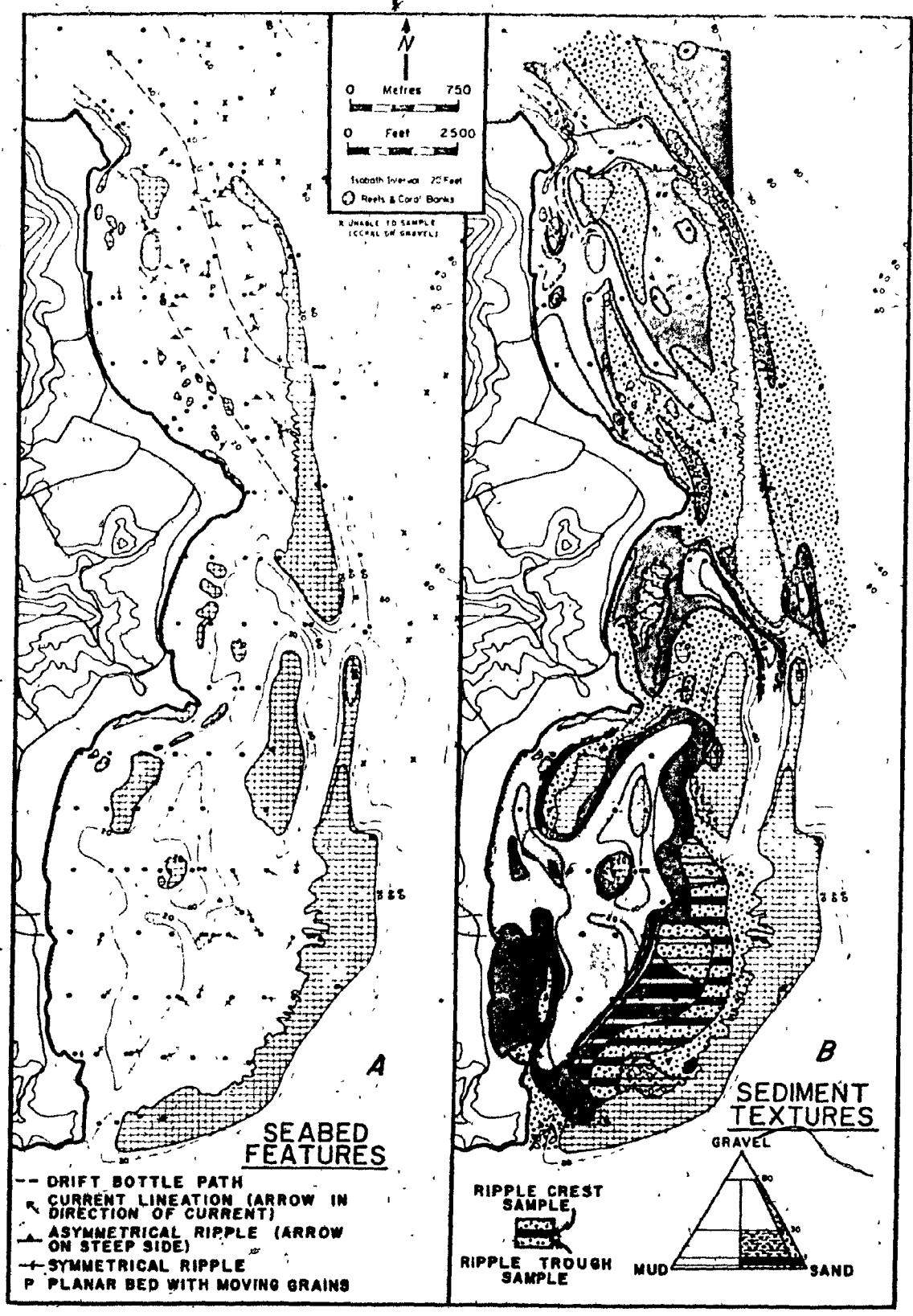


Fig. 9 (A) Map of seabed features.
(B) Map of sediment textures.

negatively skewed coarse sand. Waves have their greatest influence in the immediate back reef and at the open northern end of the bay. Oscillatory wave currents winnow and remove the finer grain sizes to produce the coarser and more negatively (coarse) skewed sediments in these areas.

Samples from deeper water immediately north of Watering Bay have less gravel and are finer (medium grained sand) than samples from the shallow back-reef area. They are also finer than samples from further north. This is probably a "shadow effect" to produce an area of deposition. The coarsest grains swept from the bay are deposited near the top of the slope, the intermediate sand grain sizes come to rest on the slope and the finer grains sizes are removed to the north. Further to the north, the currents sweeping around from outside the barrier reef affect the bottom and the sediments are coarser grained. Fine sands and mud are swept from the area and deposited in the lee of the island or in deeper water on the western side of the Antilles Ridge.

In Grand Bay, samples from both ripple troughs and ripple crests were taken at most locations on the unstable back-reef sand flat. The grain size distributions of ripple crest samples have single modes intermediate to the modes of corresponding bimodal ripple trough samples. Ripple trough samples always contain more gravel, do not differ greatly in mean grain size, are generally more widely dispersed and are more platykurtic compared to corresponding ripple crest samples.

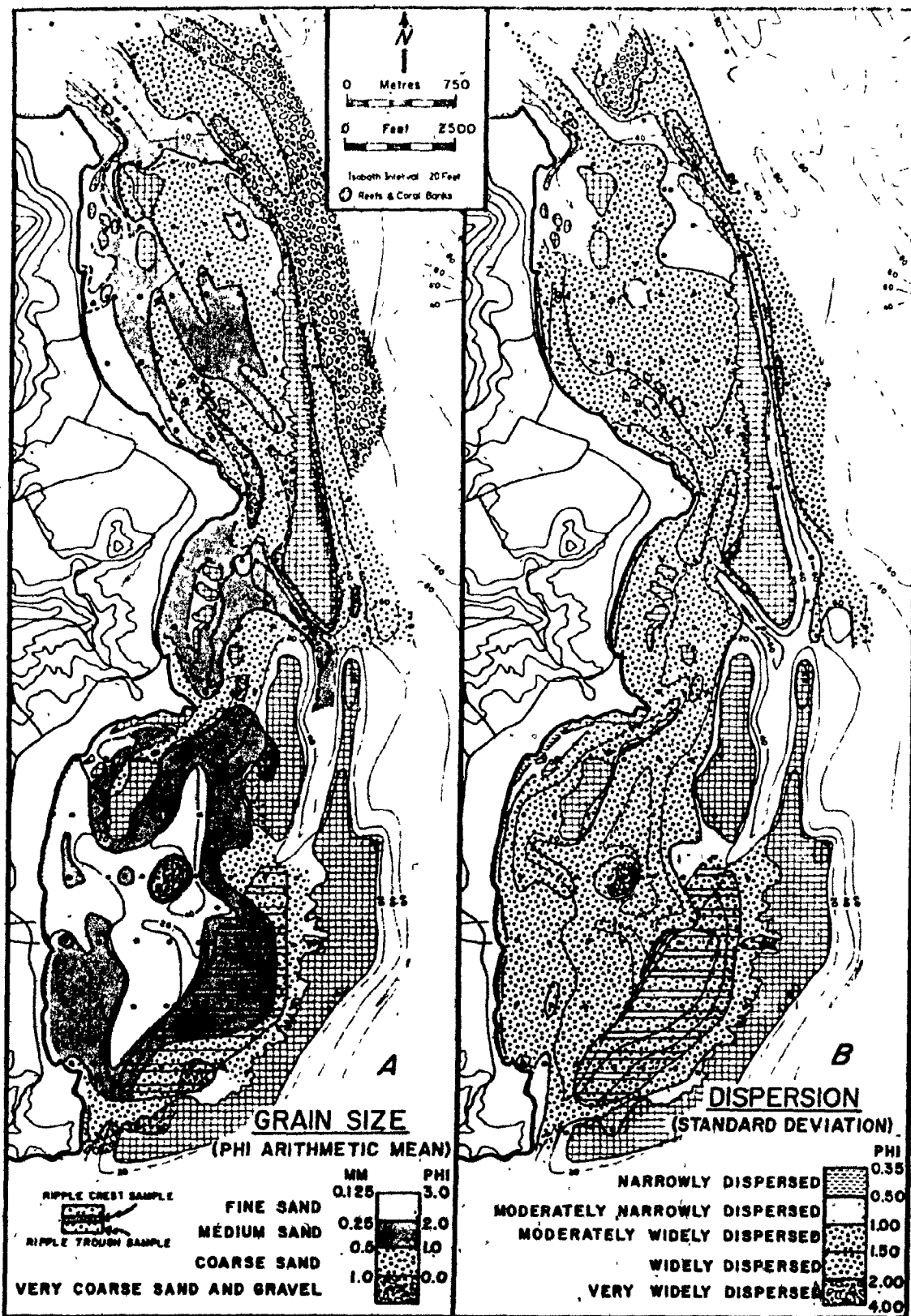


Fig. 10 (A) Map of sediment mean grain size.
(B) Map of dispersion (standard deviation) of sediment grain size distribution.

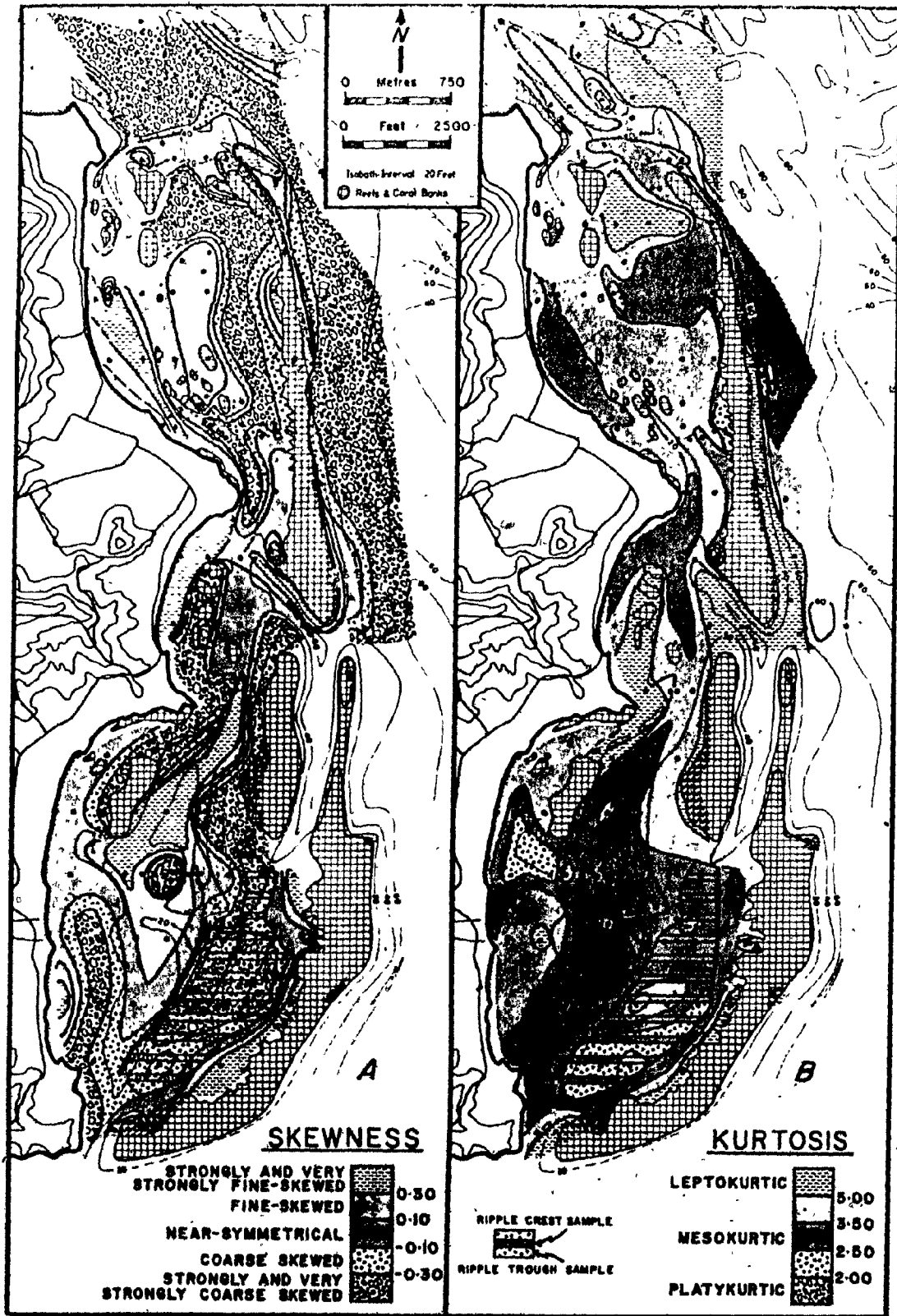


Fig. 11 (A) Map of sediment grain size distribution skewness.
(B) Map of sediment grain size distribution kurtosis.

In both ripple crest and ripple trough samples, the shoreward decrease in gravel weight percent, mean grain size, and standard deviation and the concomitant increase in negative (coarse) skewness is the result of shoreward transport and progressive selection and windowing of the reef produced grain size populations by wave action.

The finer grain sizes, winnowed from the back-reef unstable sand flat, come to rest in the deeper stable sand environment where they form bimodal fine grained, moderately widely dispersed, symmetrical to strongly fine skewed, mesokurtic sands.

The general relative fineness, wide dispersion and fine skewness of samples from shoreward Thalassia beds are the result of the baffling and trapping effects of the grass. These processes and effects have been discussed at length by Ginsburg and Lowenstam (1958), Swinchatt (1965) and Davies (1970)

Samples from Thalassia beds in Watering Bay contain more mud and less gravel, are finer grained and have more widely dispersed and more finely skewed grain size distributions than do comparable samples from Grand Bay. Larger waves in Grand Bay cause greater winnowing of fine sediment sizes and greater in situ organic production of coarser sediment.

If the blowouts observed in the Thalassia beds of Grand Bay migrate (Patriquin, 1973) there is a periodic reworking of the substrate to produce coarser sediments. The surface sample grain size distributions may represent only a transient population. Deposits developed below the Thalassia beds where blowouts are active, consist of gravel with interstitial sand.

and may be indistinguishable texturally from deposits of higher energy environments once evidence of grass growth is removed (Patriquin, 1973).

SCATTER PLOTS OF GRAIN SIZE DISTRIBUTION

STATISTICAL PARAMETERS

Scatter plots of the moment or graphic-statistical parameters of grain size distributions against one another have been used by many authors in an attempt to distinguish between depositional environments and to elucidate sedimentary processes.

Mason and Folk (1958) and Friedman (1961, 1967) are notable examples of studies employing scatter plots with some success to differentiate beach, river and aeolian deposits. Friedman (1967) has related the observed differences to simple process models of beaches and rivers. Beach deposits are affected mainly by waves, river deposits mainly by currents. However, submarine deposits may be affected by both waves and currents in any ratio of relative intensity. Also, in carbonate areas, sediment is produced in situ by the growth and death of organisms with calcareous skeletons. Therefore, considerably more difficulty has been experienced in differentiating submarine environments by scatter plots of grain size distribution statistical parameters (Hoskin, 1963).

Folk and Ward (1957), Folk and Robles (1964), Folk (1967) and Hoskin (1963) have found that plots of standard deviation, skewness, and kurtosis versus mean grain size often result in sinusoidal relationships. These trends, which are best developed for beach samples and poorly developed for submarine samples, have been explained (Folk and Robles,

1964) to result from the mixing of distinct grain size populations, related to different source materials (eg. skeletal materials of different organisms).

Standard deviation vs. mean grain size and standard deviations vs. skewness are plotted for samples from Jew and Grand Bays (Fig. 12) and for samples from Watering Bay (Fig. 13). The various environments from which the samples were taken are indicated by different symbols which also indicate sample localities on the index maps.

No distinct groupings and separations of samples from different environments would be evident without the symbols. Indeed grouping is somewhat obscure even with the symbols. In both areas the plot of standard deviation vs. mean grain size has the greatest resolution. This is due mainly to mean grain size. Skewness is less discriminating of environment than is mean grain size.

No sinusoidal trends are readily apparent in the plots of standard deviation vs. mean grain size. Although some trends could be forced from some of the data, their reality would be highly suspect, and they bear no relationship to what is known of the preferential grain size distributions of different skeletal materials and possible population mixing.

The patterns of the scatter plots may be explained in a very general way in terms of proximity to source and current and wave effectiveness.

Jew and Grand Bays

Samples from the fore-reef, reef front, inter-reef channel, immediate back-reef and patch reef are closest to or situated within areas of very active sediment production, and are also subjected to the strongest waves. Fore-reef sediments are also affected by strong tidal currents. Therefore samples from these areas tend to be coarse grained (Fig. 12). Except for four of the thirty samples, which are medium grained sand, their mean grain sizes fall within the very coarse and coarse grained sand size ranges. Samples from these environments also have the widest range of standard deviations of any group of samples. Samples with wide dispersions (i.e. large standard deviations) can be explained by their being collected in areas of in situ coarse sediment production. Narrowly dispersed grain size distributions of other samples are a result of strong sorting by waves and currents and a lack of coarse sediment production nearby.

Most of the samples from the back-reef unstable sand flat were collected in pairs from adjacent ripple crests and ripple troughs. Since this environment derives its sediment from the barrier reef and is not itself a very active area of sediment production, the samples tend to have a finer mean grain size and a smaller range of standard deviation values than do the samples from reef associated environments (Fig. 12). Ripple trough samples are all bimodal. Ripple crest samples are unimodal, with a mode intermediate to those of the trough samples. Therefore, these two groups of samples are not

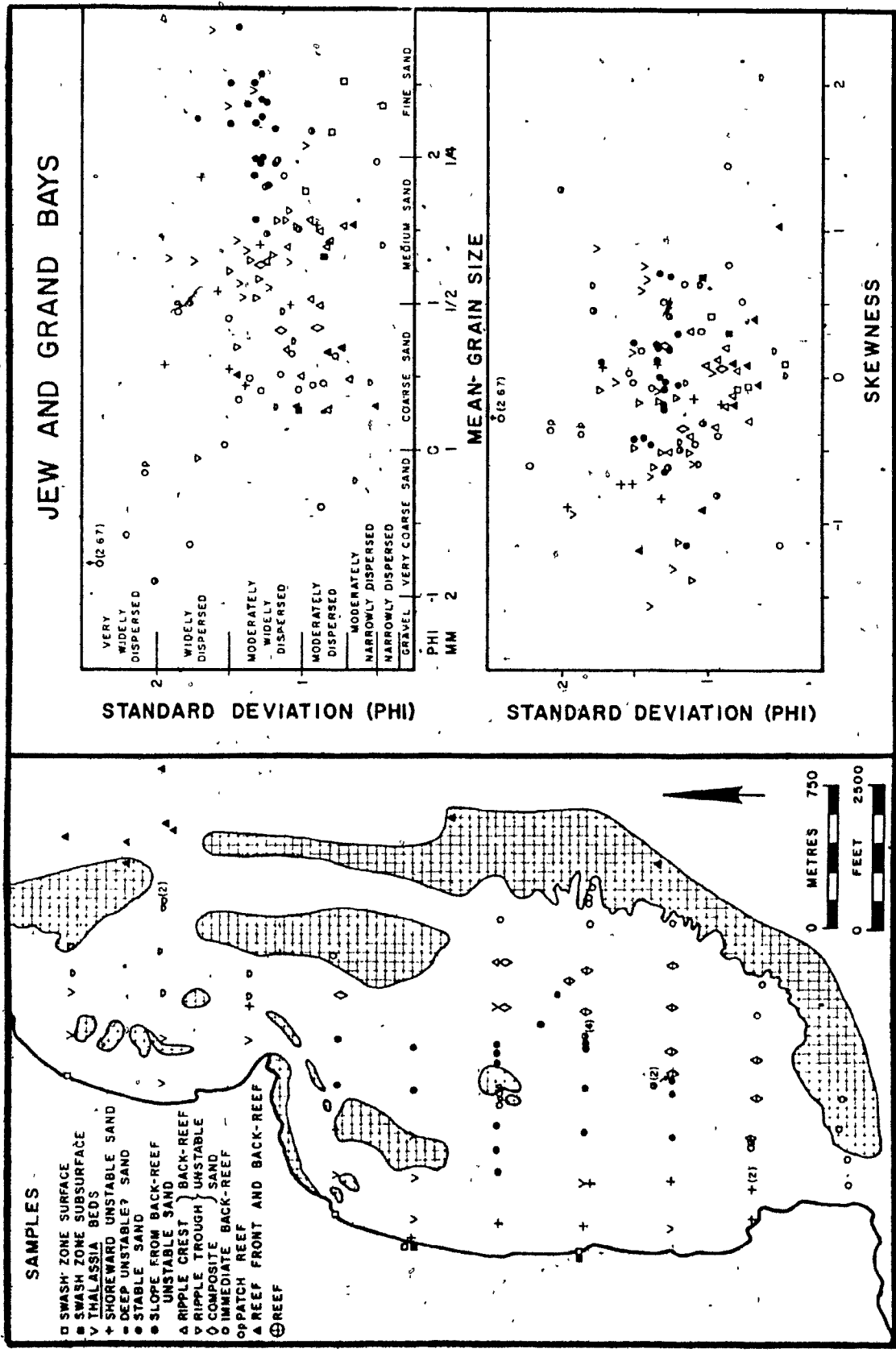


Fig. 12 Cross plots of grain size distribution statistical parameters, Jew and Grand Bays.

distinguished from one another on the basis of mean grain sizes, which are similar. They are distinguished by the wider dispersion of the grain size distributions of the trough samples. Ripple trough samples also plot separately from the ripple crest samples on the standard deviation (dispersion) vs. skewness plot. This is, in part, because the sorting power of waves forming the ripples causes the grain size distributions of the ripple crest samples to be neither preferentially coarse skewed nor preferentially fine skewed, while the dominant fine grained mode of the ripple trough samples causes the standard deviation of their grain size distributions to be coarse skewed.

The deep stable sand environment is well removed from the barrier reef and is the only bare sand area not strongly affected by the winnowing action of waves or currents. Therefore, samples from this environment tend to be fine grained and moderately widely dispersed (Fig. 12).

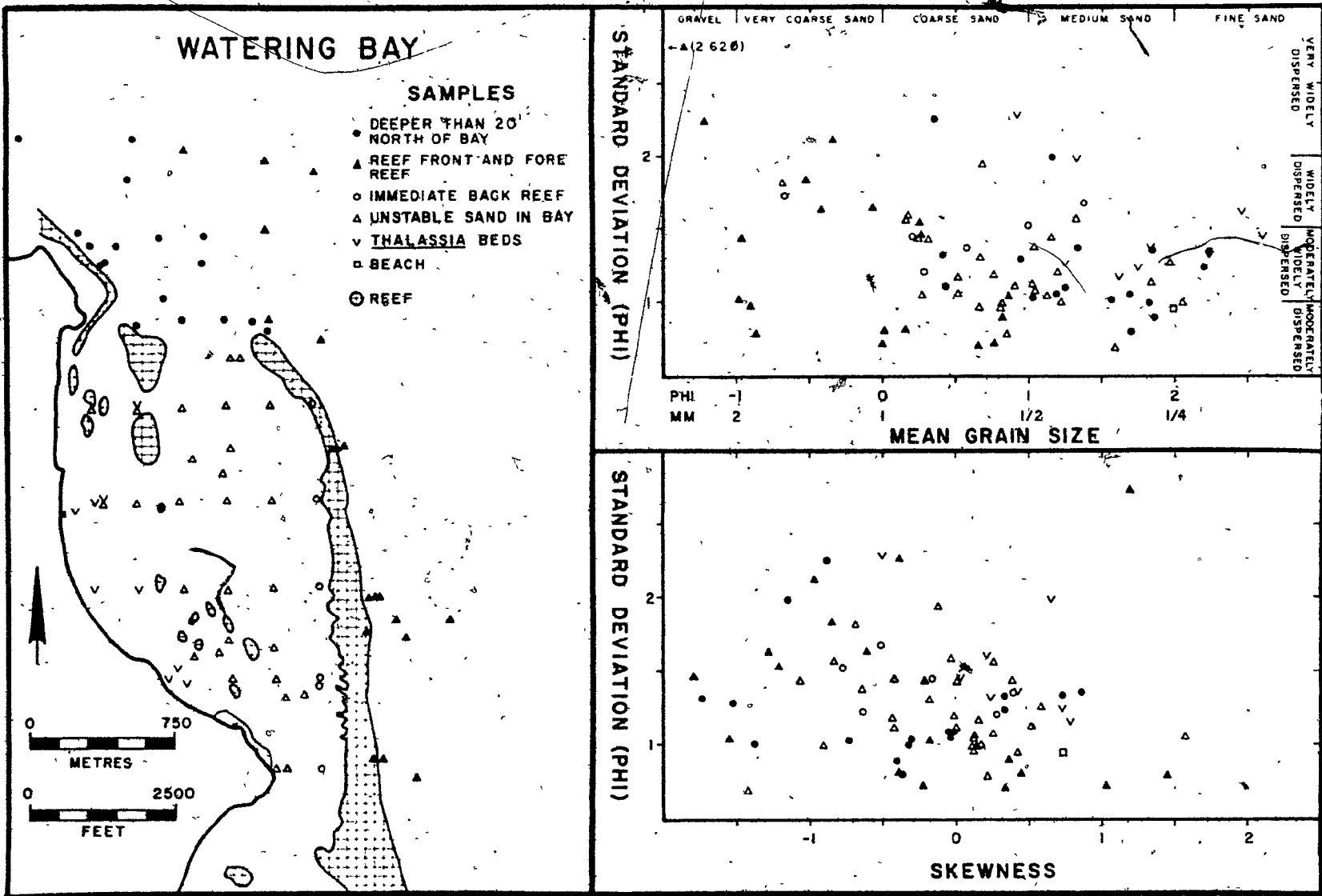
Marine grass beds in Grand Bay have a wide occurrence; from moderately quiet water areas where there is a sparse associated fauna and fine grained, widely dispersed grain size distributions are deposited, to areas of considerable agitation where an abundant associated calcareous flora and fauna is developed and coarser grained sediments (coarser fractions produced in situ) with widely dispersed grain size distributions accumulate. Thus, on the scatter plots, the field of occurrence of grass bed samples is wide and overlaps most fields of other environments (Fig. 12).

Beach samples were all collected during summer months and the surface samples are fine grained as compared to samples taken one-half to 2 inches (1 to 5 cm) below the surface. The coarser subsurface laminae probably represent winter beaches, in equilibrium with larger winter waves. All grain size distributions are narrowly to moderately dispersed and their scatter plots overlap into the fields of occurrence of back-reef unstable sand ripple crest samples and reef associated sediments (Fig. 12). The grain size distributions do not show a tendency to be either preferentially coarse skewed or fine skewed.

Watering Bay

The grain size distributions of samples from Watering Bay show a distinct trend. They become finer with a slight tendency to be more widely dispersed, moving from barrier reef environments to the unstable back-reef sand, to sand deeper than 20 feet north of the bay and to marine grass beds (Fig. 13). This progression is related to changes in proximity to sediment source and in strengths of waves and currents in each environment. The fore-reef and reef front environments are close to the sediment source and are affected by large waves and strong currents. The back-reef unstable sand environment is not an area of sediment production and is affected by weaker waves and currents than are the reef associated environments. The area north of the bay is not an area of sediment production and is the lee of the reef and back reef sediment pile with respect to the strong north flowing tidal currents. The samples from marine grass beds are.

Fig. 13 Cross plots of grain size distribution statistical parameters, Watering Bay.



all from shoreward areas which are not greatly affected by waves and currents and do not have an abundant associated calcareous flora and fauna.

CONSTITUENT GRAIN COMPOSITION

When the scatter plots and the maps of statistical parameters of grain size distributions were discussed above it was noted that ripple crest samples from the back-reef sand flat in Grand Bay consistently have unimodal coarse to medium sand size, moderately widely to moderately narrowly dispersed grain size distributions. Also the mode is consistently intermediate to the modes of corresponding bimodal ripple trough samples. Samples from the adjacent deeper stable sand environment are bimodal with a finer phi arithmetic mean grain size (fine sand) than the samples on the back-reef sand flat. The coarse mode corresponds to the mode of the ripple crest samples and the fine mode is finer than any on the sand flat.

The non-random pattern of occurrence of the grain size modes may be interpreted in one of two ways: the modes represent fundamental grain size populations controlled by the size distributions of the structural units of different organisms, or they are determined by transport and depositional processes. Control of the grain size modes by skeletal structures should be discernible by determining the grain size distributions of constituent grains.

Constituent grain compositions of each of the half phi size fractions coarser than 3.5 phi (0.088 mm) were determined for three samples from Grand Bay. Grain counts of the available

grains in thin sections of each size fraction, up to a total of 300 for each fraction, were divided into ^{eight} A classes as follows: Halimeda, corals, coralline algae, molluscs, Homotrema, echinoderms, miscellaneous, and unknowns (Appendix 2, Fig. 14).

The three samples were selected to represent the three main types of sediment grain size distributions present in Grand Bay: 138 RT is a bimodal sample from a ripple trough on the back-reef sand flat, 138 RC is a unimodal sample from a ripple crest at the same locality, 136 is a finer grained bimodal sample from the deeper stable sand environment.

Even though the grain size distributions of the two samples collected at locality 138 are dissimilar, the total constituent grain compositions are essentially the same (Fig. 14). The change in composition from location 138 to location 136 consists of an increase in the abundances of Halimeda and coral fragments and a decrease in those of coralline algae and Homotrema fragments, the abundances of the other constituents remaining the same. All of the varying constituents are supplied to the sample locations only from the barrier reef and the change in composition cannot be related to differences in supply and source. Location 136 is 625 feet (190 m) further away from the reef than location 138 and the change in composition might be considered a result of different abrasional resistances of the constituents. This might explain the decrease in abundance of Homotrema fragments away from the reef, however coralline algae, with its denser and more compact microstructure, should be more resistant to abrasion than Halimeda or coral. In the absence of abrasional resistance data this hypothesis is not indisputable.

The left side of Figure 14 consists of the grain size histograms of each of the main components in the three samples. In general the actual size distributions of the various components reflect the overall size distributions of the samples. Exceptions are the molluscan and coralline algae fragments in sample 136 and the Halimeda fragments in 138 RC, all of which have modes coarser than those of the overall distributions.

The histograms demonstrate that individual constituents do not have a strong effect on the overall grain size distributions. In order to present the data in a form which allows recognition of preferred grain size distributions of component types, histograms of grain count percent per half phi interval were constructed (centre of Fig. 13). In this way the relative proportion of a given constituent in a size fraction, independent of the abundance of that size fraction in the whole sample is obtained.

Molluscs

Molluscan fragments tend to be an important constituent in size fractions coarser than -1.5 phi (2.83 mm) relative to the other components. These sizes represent the whole or nearly whole skeletons of the molluscan infauna. In terms of absolute abundance however, mollusc fragments show a non-preferential grain size distribution or reflect the overall grain size distribution. The size distribution of a pelecypod-gastropod placer from Isla Perez, analysed by Folk and Robles (1964), had a somewhat coarser mode around -1.75 phi (3.36 mm). Conaghan

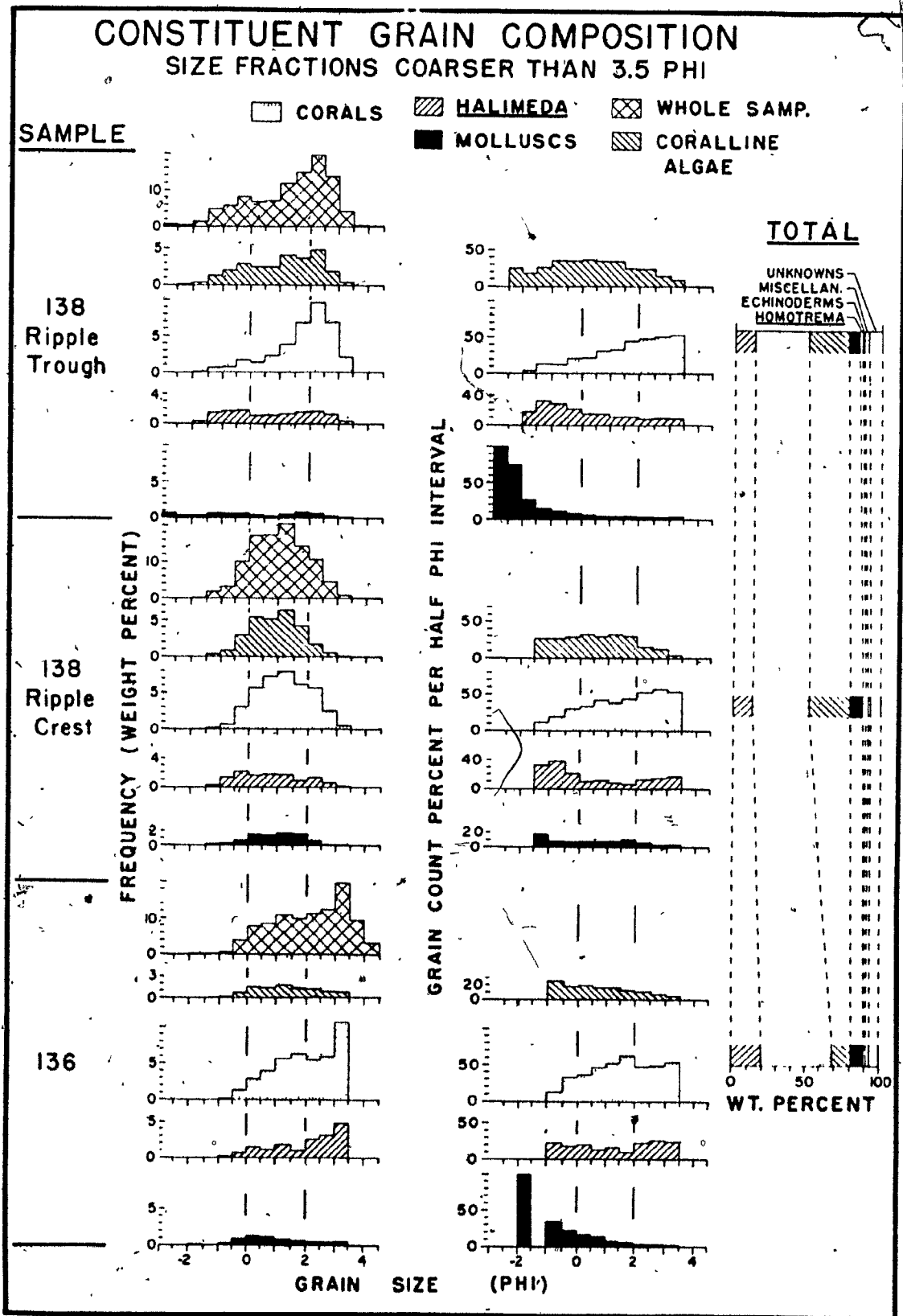


Fig. 14 Constituent grain compositions and grain size distributions of three representative samples from Grand Bay.

(1967) found that the proportion of molluscan fragments, in the various size intervals was more uniform than for most other constituents although there was a tendency for them to dominate in the size intervals coarser than 0.0 phi (1 mm) in some samples and finer than 2 phi (0.25 mm) in other samples. Samples from Mahe, analyzed by Lewis (1969), also had a higher proportion of molluscan fragments in the size intervals coarser than 0.0 phi (1 mm).

The uniform micro-structure of molluscan fragments results in their breaking down in a uniform manner so that fragments do not display preferred modes in restricted grain size ranges.

Corals

Coral fragments are most abundant in the size intervals around and finer than 2.0 phi (0.25 mm) relative to the other components. These probably represent the unit microstructures of corals, such as the 1.25 to 2.25 phi (0.5 to 0.21 mm) thick walls of Porites, noted by Folk and Robles (1964) to account for the great abundance of coral fragments around 2.0 phi (0.25 mm). Conaghan (1967) also found coral fragments to be proportionally more abundant in the size intervals finer than 2.0 phi (0.25 mm). In terms of absolute abundance however, the grain size distributions of coral fragments closely follow the overall grain size distributions.

Coralline Algae

The absolute grain size distribution of coralline algae also closely follows the overall grain size distribution.

Relative to the other components coralline algae are nearly uniformly present in all grain sizes with a possible slight preference for sizes around 0.0 phi (1.0 mm). The relative homogeneity and fineness of microstructure results in non-preferential breakdown of coralline algae in the sand size range.

Halimeda

The grain size distributions of Halimeda fragments show the greatest development of preferential breakdown independent of the overall grain size distributions. They tend to be more abundant proportionally in the grain size ranges around -1.0 phi (2.0 mm) and, to a lesser degree, finer than 2.0 phi (0.25 mm) than they do in the intermediate grain size ranges. The coarser mode is composed of whole segments or segment which have been broken in half. The finer mode consists of fragments displaying the porous texture of the surface layer or single tubes or parts of tubes from the interior. Conaghan (1967) found that Halimeda fragments tended to have a uniform distribution, with no consistent modes. Folk and Robles (1964) discussed two predominant modes at 0.5 phi and 10 phi, which they interpreted as representing broken Halimeda segments one-quarter the diameter of the whole segments and individual aragonite crystal units respectively.

Given originally slightly different size ranges, dependent upon species and growth conditions, the breakdown of Halimeda segments tends to proceed in quantum jumps. The platy, fragile whole segments tend to break across into less platy, hence

stronger fragments. This breakage continues until the resulting plates are in equilibrium with the stresses inherent in the environment, i.e. until there is insufficient leverage across the plate for the available force in the hydrodynamic environment to cause breakage. There is a lower limit to this process, probably around 1.0 phi (0.5 mm) diameter when the grain is near equi-dimensional.

Equi-dimensional Halimeda grains decrease in size mainly by abrasion rather than breakage. The resulting fragments have diameters of 2.0 phi (0.25 mm) and finer, representing the inter-tube walls and porous outer layer of the fine structure of Halimeda segments. Some grains of this size are also produced during breakage of larger plates into smaller plates.

The ultimate structural units produced by abrasion in all stages are the aragonite crystals in the 10 phi (0.98 microns) size range. Whether or not an abrasion or breakage product remains in the environment where it was produced depends on the grain transport competence of the environment. For example 10 phi dust will not remain in a beach or reef flat environment but will be removed to settle in quieter environments.

The above discussion considers only physical abrasion. Biological abrasion caused by browsing fish, holothurians and gastropods, burrowing organisms and blue green algae must also play a role in the breakdown of carbonate grains but is considered to be of lesser importance in the shallow back-reef environment studied.

SUMMARY

The main sources of bioclastic carbonate sediments east of Carriacou are barrier reefs. Patch reefs in the back-reef areas are important suppliers of sediment only in Watering Bay. Marine grass beds do not supply much sediment to adjacent bare sand environments but do produce and accumulate considerable sediment in place. The infauna of the sand environments form only a small part of the sediment. Terrestrially derived sands are important components only in beach and very nearshore environments of Watering Bay, where waves are weak and do not supply the nearshore environments with much bioclastic carbonate sediment.

Maps and scatter plots of the statistical parameters of grain size distributions are consistent with the relative intensities of waves and currents as determined by seabed surface features and general observation. Used in conjunction with one another the maps and scatter plots also allow some general interpretation of transport and depositional processes. The scatter plots by themselves do not allow separation of environments.

Samples from Thalassia beds have grain size distributions with wider dispersion and finer skewness than samples from unstable sand environments at the same water depth. Thalassia grass protects the bottom from waves and currents, allowing finer grain sizes to be deposited. Larger waves in Grand Bay than in Watering Bay cause a greater winnowing of fine grain sizes and greater in situ organic production of coarser grains.

As a result Thalassia bed samples from Watering Bay are finer grained and have more widely dispersed and finely skewed grain size distributions than do comparable samples from Grand Bay.

The grain size distributions of samples from Thalassia beds may be a transient feature of the deposits. Migration of blowouts within the grass beds (particularly in Grand Bay) would result in periodic winnowing and final deposition of sediments indistinguishable texturally from deposits of higher energy environments.

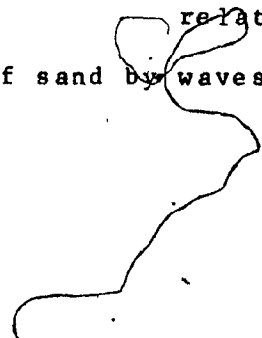
In Watering Bay long crested symmetrical ripples, indicative of wave action, are present only immediately behind the barrier reef, in the shoreward half of the bay and at the northern end of the bay. Current lineations and irregular crested, asymmetrical ripples, which are steep to the north, attest to the dominance of the north flowing tidal current over most of the bay. The currents transport all sand size material supplied by the reefs northwards. Coarse sands are deposited near the top of a slope into deeper water at the open northern end of the bay. Progressively finer (medium sand size range) sediments are deposited down the slope. Further north, the grain size of bottom sediment is again coarser as strong tidal currents from outside of the reef sweep around the northern end of the barrier reef and swing towards the west north of Carriacou. Some of the fine sand and mud produced on the reef and in the bay is deposited interstitially in the coarser sediments. However, the bulk of the finer grain sizes does not come to rest

within the study area and must be deposited in the lee of the island or in deeper water on the western side of the Antilles Ridge.

In Grand Bay there are no sea floor features indicative of current action. Waves crossing the back-reef unstable sand flat in different directions from different segments of the barrier reef produce a complex pattern of regular, long crested, symmetrical ripples. Transport and winnowing of reef sediment shoreward by waves result in decreasing mean grain sizes and increasingly coarse skewed grain size distributions across the back-reef flat. The finer grain sizes, winnowed from the back-reef flat, come to rest in the deeper stable sand environment of central Grand Bay.

The consistent pattern of occurrence of preferred modal grain sizes in ripple crest and ripple trough samples from the back-reef flat and in samples from the adjacent stable sand environment is not controlled by the breakdown of different carbonate skeletons into preferred grain sizes controlled by skeletal structural units. Only the breakdown of Halimeda appears to be strongly controlled by organic structure, but its preferred grain sizes are not related to the modes of the total sample grains size distributions.

The preferred grain size modes are related to processes of transport and deposition of sand by waves in the back-reef environment.



CHAPTER 4 - HYDRODYNAMICS OF SEDIMENT TRANSPORT

PREVIOUS WORK

In general there are two approaches followed concerning sand transport and deposition. One approach, typified by the preceding chapter, consists of treating grain size data and their derived statistical parameters by one or more analytical or plotting techniques in an effort to place them in empirically and broadly defined environmental groupings. Often an attempt is made to relate the results to processes or non-quantitative process levels such as 'winnowing action' or 'high energy'. The other approach applies hydrodynamic theory and flume studies of sand transport and deposition for which there is a considerable literature (see consolidated bibliography in Middleton, 1965; Jopling, 1966). The main geological use of most of the studies has been to interpret primary sedimentary structures in terms of flow regime.

(A few studies have attempted to apply results of theoretical and experimental work to grain size distributions of the material transported and deposited. Using an empirical transport competency curve, Inman (1949) speculated on the progressive sediment sorting effects of unidirectional flow in the Mississippi River. Brush (1965) performed flume experiments to test the basic equation describing the equilibrium suspended sediment concentration profile in steady, two-dimensional, open-channel flow and speculated on bed-load sorting due to gravitational sliding at the lee face of dunes and ripples. Jopling (1965) studied

sediment sorting and grain size distribution in suspension transport and deposited in the lee of small, flume-produced deltas and then (Jopling, 1966) applied these results in a very detailed hydrodynamic interpretation of a similar natural structure of Pleistocene age.

Before theoretical and experimental results can be applied to the geological record with any degree of confidence, they must be tested in modern natural situations where one can make in situ measurements of the process inputs as well as of the textural and sedimentary structural responses. Whether or not the responses, as preserved in the ancient record, allow adequate definition of all the parameters necessary to interpret the processes has been, and remains, a major stumbling block.

Sternberg (1967, 1968, 1971) and Kachel and Sternberg (1971) used a special remote instrument system consisting of stacked current metres and a television camera (Sternberg and Creager, 1965) to measure tidal current boundary layer conditions and to observe initiation of sediment movement and rates of ripple migration in marine channels up to 42 metres deep off northern Washington State. The results, to be discussed in Chapter V in connection with the Carriacou data, generally compared favourably with sediment transport theory and flume study results.

Dyer (1972) related variations in bed shear stresses (derived from measured tidal current velocity profiles) in the West Solent between England and the Isle of Wight to the topography of sea floor gravel waves, and suggested that these variations

can produce simultaneous deposition of sand and gravel in varying proportions.

Allen (1971) compared the areal variation of tidal current velocity and sea bottom orbital velocities of waves in the Gironde Estuary to the areal variations of bottom sample grain size parameters. He found textural parameters reflected the variations of the strengths and ratios of tidal current and wave energies as represented by velocities and these in turn were controlled by the bottom topography. He also concluded that 'hydraulic analysis and erosion curves can probably be effectively used in analyzing modern depositional environments'.

The above studies all deal with sediment transport in unidirectional flow, either in stream or tidal currents. In the study of sediment transport by oscillatory (wave) currents the experimental work by Bagnold (1946) and Manohar (1955) and the analytical work of Komar and Miller (1973, 1975) are used extensively in the following sections. Cook and Gorsline (1972) employed wave and wave current measurements and sediment traps to study sand transport by shoaling waves off several beaches in southern California.

In the present study very limited wave data were collected. However, in Watering Bay tidal current velocities were measured and sediment traps were used to sample sediment actually transported under varying conditions and at different levels near the sediment surface. As far as the author is aware, this is the only such study in a marine unidirectional flow regime.

APPLICATION OF SAND TRANSPORT EXPERIMENTS AND
THEORY TO SKELETAL CARBONATE GRAINS IN SEA WATER

Most experimental and theoretical data and results pertain to terrigenous, dominantly quartzose sands in fresh water. To apply these data and results to skeletal carbonate grains with complex structures and shapes and highly variable bulk densities (Jell et al, 1965) requires some theoretical modifications and justification. The only hydrodynamic parameter of skeletal carbonate grains for which there is sufficient data is the settling velocity.

Maiklem (1968) measured the intermediate diameters (approximating sieved sizes) and settling velocities of individual skeletal carbonate grains in sea water. The values for Halimeda, coralline algae and coral grains are replotted in Figure 15 and compared with settling velocity curves calculated by Rubey's (1933) general settling equation. The theoretical curves are for quartz spheres in fresh water at 25° C and solid aragonite and calcite spheres in sea water at 23.5° C. The settling velocities of natural grains generally plot below these curves because of lower bulk densities and/or irregular shapes. Settling velocity, controlled by shape and the difference in density of the particles and fluid medium, is the main parameter determining whether a given grain will be carried in suspension or not.

An average settling velocity curve for Carriacou skeletal sands was calculated by weighting the data 4:1 for corals and coralline algae: Halimeda (Fig. 15). The weighting of the data is based on the assumption that the three constituent grain

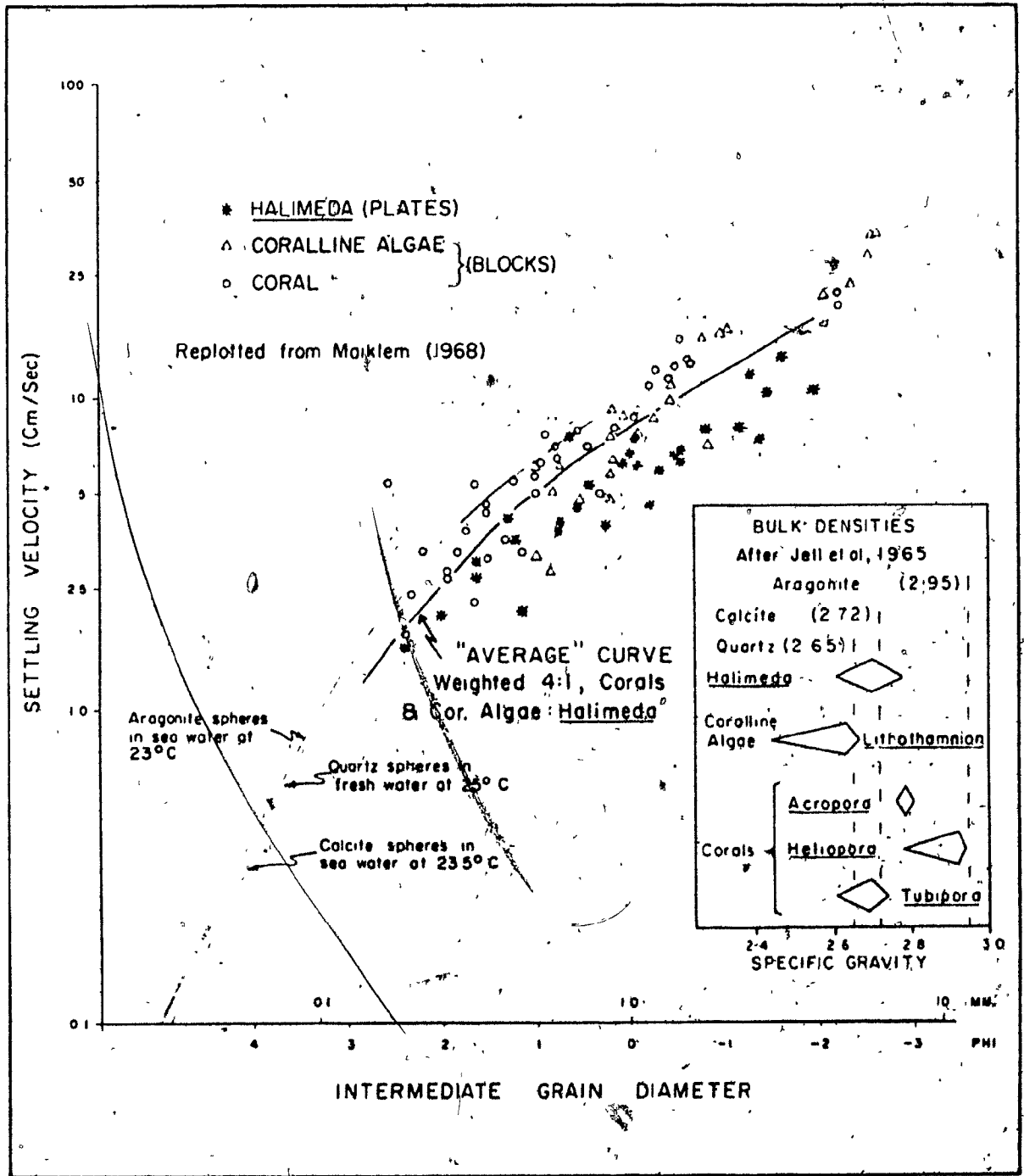


Fig. 15 Settling velocities related to grain size for skeletal carbonate grains in sea water.

analyses of samples from Grand Bay are representative of back-reef sediments east of Carriacou (61 to 68% coral and coralline algae and 12 to 21% Halimeda). Settling velocities on the average curve for skeletal carbonate grains are approximately 20% less than on the curve for quartz spheres.

From the data on bulk density of carbonate grains in Figure 15 it would appear that the average density for a mixture of skeletal types is slightly greater than for quartz (approximately 2.70 versus 2.65). An increase in bulk density of 0.05 would have the effect of increasing the settling velocity by less than 2%. Therefore, the 20% difference in settling velocity is a result mainly of shape factors.

After size, density and shape are also the main sediment grain parameters determining threshold of movement velocities and transport behavior in bed load. From the above discussion density differences can be ignored. However, the effects of shape variations in natural carbonate sediments are likely to be important but cannot be determined exactly because of the irregular and wide variation in shape. The empirical average settling velocity curve for skeletal carbonate grains (Fig. 15) will be used. This curve is approximately equivalent to that for spheres with a density of 2.2. Generally spheres are easier to dislodge and roll than are irregular shapes, which usually come to rest with their minor axes near vertical and their centres of gravity lower than those of spheres of equivalent sieve size. (approximated by intermediate diameter). Thus it may be expected that greater shear stress would be required to initiate movement of irregularly shaped carbonate grains than would be required to

initiate movement of the more equant and regularly shaped quartz grains generally used in studies on which erosion competence curves are based.

From the above, it is probable that higher current velocities are required to initiate movement of carbonate grains than equivalent size quartz grains. In the absence of a traction competence curve for carbonates, a published traction competence curve based on terrigenous (mainly quartz) grains in fresh water will be used. Bottom observations, current measurements and sediment trap results will serve as a check on the applicability of the curve to carbonate sediments in sea water. The effect of using the competence curves for quartz, which consists of velocity versus mean grain size, should be to displace the apparent representative grain size towards the coarse tail of the grain size distributions.

Unidirectional Flow

A more complete development and discussion of hydrodynamic theory as it related to sediment erosion and transport in unidirectional flow may be found in Inman (1949) and Inman (Chapter V, in Shepard, 1963). Only a brief outline of the important theoretical relationships is presented here.

Shear velocity (u_*) is defined as a measure of shear stress (τ_0) exerted by fluid flow on the bottom such that:

$$u_* = \sqrt{\tau_0 / \rho}$$

where ρ is the fluid density. For currents over a rough surface (one in which surface irregularities project through the boundary sublayer and turbulence extends to the very bottom) where velocity is related to mean average velocity (\bar{u}) at some distance z above

the bottom by the von Karman-Prandtl equation:

$$\bar{u} = \frac{u_*}{k_0} \ln \frac{z + z_0}{z_0}$$

where k_0 is the von Karman constant (approximately 0.4) and z_0 is the roughness length related to the height of the bottom roughness elements. This equation accounts for depth of flow below the measured mean average velocity and bottom roughness, both of which have a strong effect on shear stress applied to the surface below a flow of given velocity. The logarithmic von Karman-Prandtl relationship allows plotting of velocity against the logarithm of height above bottom, and straight line extrapolation to a velocity of zero to obtain an approximation of roughness length (method more fully outlined by Inman, in Shepard, 1963). The values of z_0 , \bar{u} and z may then be used to calculate shear velocity.

The von Karman-Prandtl equation may be simplified and the roughness length term removed by assuming that z_0 is small relative to two heights above bottom (z_1 and z_2) at which average velocities (U_1 and U_2) are measured.

Then:
$$u_* = k_0 \frac{U_2 - U_1}{\ln (z_2/z_1)}$$

The above equation may be used to directly calculate shear velocity.

The threshold of movement of cohesionless grains on a planar bed can be defined by the threshold shear stress or corresponding threshold shear velocity which is just sufficient

to overcome the gravitational and frictional forces holding the least firmly bedded grains in place. Inman (1949), using experimental data from White (1940), the U.S. Waterways Experimental Station, and Nevin (1946), calculated threshold shear velocities which he plotted against grain size to produce a competence curve (Fig. 16). In this figure the grain size axis has been reversed so that coarsest diameters are to the left for comparison with standard grain size histograms. These values of u_* are generally referred to as threshold criteria for initiation of grain movement, when in actual fact they are based on measurements for general sediment motion (all grain sizes on the bed in more or less continuous motion). However, Sternberg's (1971) detailed observations and data indicated that the competence curve based on u_* is applicable to terrigenous sediments in the natural marine environments. His calculated values of u_* at the times of initiation of general sediment motion on a variety of beds with different grain sizes and bedding structures correlated well with the competence curve.

The data used to construct the competence curve ^{were} based on experiments with bed materials of very limited grain size ranges, using the median diameter as the representative diameter. Sternberg (1971) used mean grain diameter for grain size distributions with phi standard deviations ranging from 0.4 phi (well sorted) to 1.97 phi (poorly sorted, approaching very poorly sorted). As reviewed by Jopling (1966), the bulk of evidence from experiments using variously sorted bed materials suggests

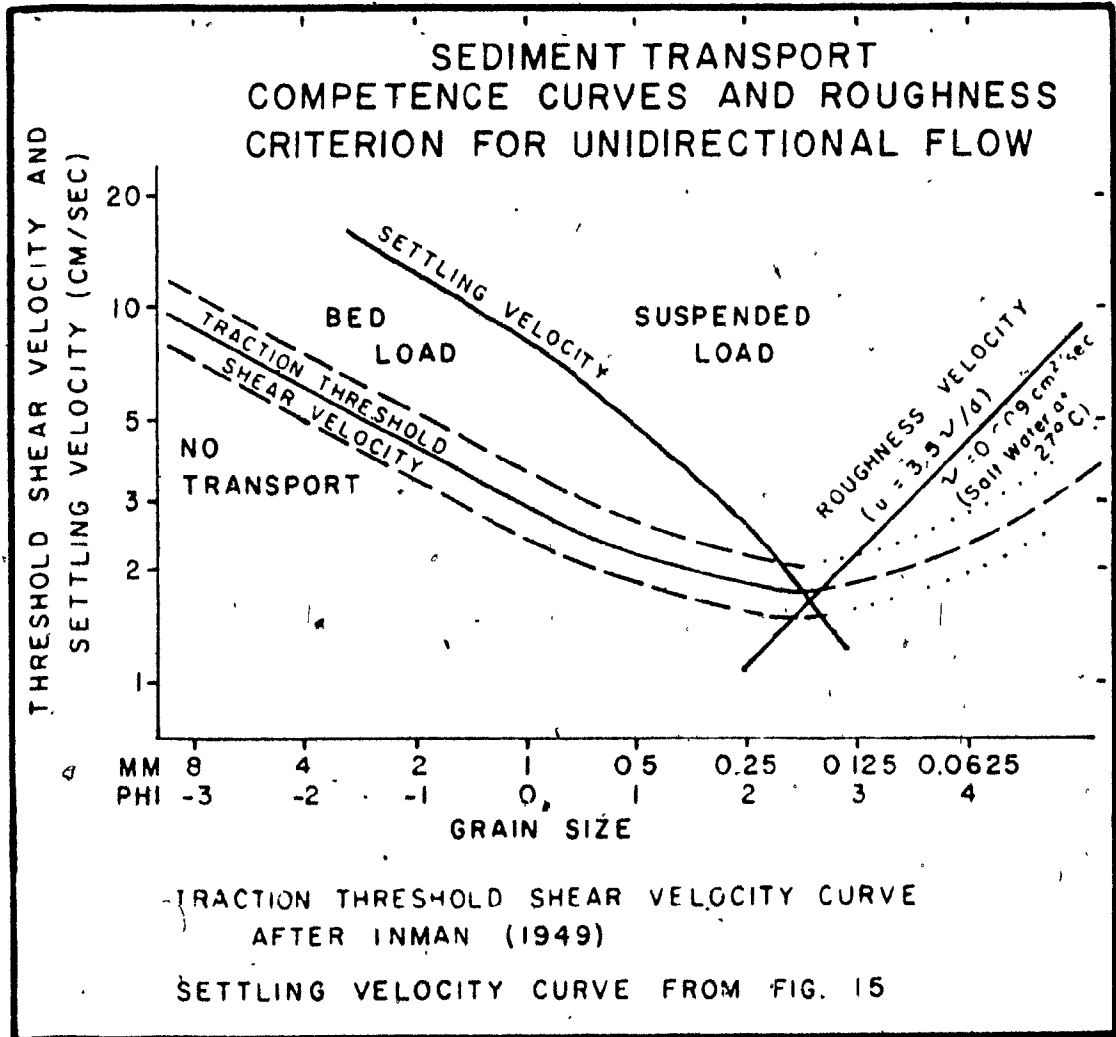


Fig. 16 Relation of grain size to settling velocity and to threshold shear velocity and roughness velocity in unidirectional flow.

that coarser particles tend to move first except where the grain size distribution of the mixture is very poorly sorted. Turbulent eddies generated by the coarser grains of moderately sorted sediment mixtures do not penetrate fully into the interstices where finer grains are partly shielded (Sundborg, 1956; as reported in Jopling, 1966). Therefore, the finer grain sizes of a moderately sorted mixture do not begin to move until after the coarser grains; and the threshold shear velocity corresponds to that of the coarser size fraction. Thus the representative grain size diameter to be used with the competence curve apparently varies from the median or mean for better sorted bed materials towards the coarse tail for more poorly sorted materials. This effect will be compounded by the apparent shift in representative grain size towards the coarse tail which results from the use of the competence curve based on quartz for skeletal carbonate grains. As discussed above, carbonate grains are expected to have higher threshold velocities than equivalent size quartz grains.

The von Karman-Prandtl equation given above for calculation of shear velocity can be used only for hydrodynamically rough surfaces. Inman (1949) stated that experiments by Nikuradse (1933), Page (1933), and White (1940) indicate that the criterion for surface roughness is a critical value of a Reynolds Number ($u_* d / \nu$, where d is bottom grain diameter and ν is the kinematic viscosity) such that if the number is greater than 3.5 the bottom is hydrodynamically rough. A curve $u_* = 3.5 \nu / d$ ($\nu = 0.009 \text{ cm}^2/\text{sec}$ for water at 27° C) is plotted on Figure 16. For plots of u_* vs

grain diameter lying above this curve, the bottom is 'rough'. From the 'roughness curve' and the competence curve (Fig. 16) it is obvious that sediment surfaces composed of sand 0.18 mm (2.5 ϕ) in diameter or coarser, and being transported by fluid flow, must be considered to be 'rough' and the von Karman-Prandtl equation for rough boundaries used.

Suspension of grains by fluid flow occurs when the grains leave the sediment surface and follow the random motion of the turbulent flow above the bed. Criteria for the onset of significant suspension were reviewed by Jopling (1966) who found that available experimental evidence indicated significant suspension of sand-sized particles should occur when shear velocity equals settling velocity. This was the criterion used by Inman (1949) on the basis of experimental work by Land and Kalinske (1933). A curve setting the average settling velocity of skeletal carbonate grains (Fig. 15) equal to shear velocity is included in Figure 16 and is an empirical suspension competence curve for the reef sediments of Carriacou.

The combination of the traction competence and suspension competence curves in Figure 16 divides the graph into three areas:

- (1) Area of no transport below both curves.
- (2) Area of bed-load or traction transport between the two curves.
- (3) Area of suspension-load transport, above the suspension competence curve.

As an example, a shear velocity of 3 cm/sec would be incapable of eroding grains coarser than $0 \text{ } \phi$ (1 mm), would transport grains between $0 \text{ } \phi$ (1 mm) and $1.81 \text{ } \phi$ (0.28 mm) in diameter as bed load, and grains finer than $1.81 \text{ } \phi$ (0.28 mm) as suspension load.

In reality the boundaries between non-transport and the two modes of transport are transitional. This transitional character is reflected by the scatter of experimental data which is enclosed in the broad band representing the traction competence curve (see Inman, 1949; Sternberg, 1971).

Oscillatory Flow

The passage of water waves produces an orbital motion of water particles in the direction of wave advance such that the particles return nearly to the same position after the passage of each wave and an oscillatory flow is set up.

Airy wave theory for sinusoidal waves of low amplitude is commonly used to describe the motion of water waves and is discussed more fully by Inman (in Shepard, 1963).

Measurements of wave period (T), water depth (h) allow calculation of an approximate wave length (L) by the equation::

$$L = T \sqrt{\frac{g}{2} \tanh \left(\frac{2\pi h}{L} \right)}$$

where g is the acceleration due to gravity. Beginning with deep water wave length on the right side of the equation a new value of L is obtained which is then re-substituted into the equation to obtain another value of L. By using this iterative process

until the value of L changes by less than a given percentage from the previous values of L, a very close approximation of the actual wave length can be calculated.

The calculated wave length and the measured parameters may then be used to calculate the theoretical maximum horizontal component of orbital velocity at the bottom:

$$u_m = \frac{\pi H}{T} \sinh \frac{2\pi h}{L}$$

where H = wave height.

When considering sediment movement by waves the maximum horizontal orbital velocity on the bottom is the obvious flow parameter to consider. However, there is no reason to assume that the threshold shear stress has a relationship to u_m similar to the relationship between shear velocity and average velocity in steady unidirectional flow.

Experiments concerning the movement of different grain size bed materials by oscillatory currents have been carried out by Bagnold (1946 and 1963), Manohar (1955) and Vincent (1958), employing oscillating beds beneath standing water to produce the currents. The data for threshold bottom velocities on quartz sand beds are replotted in Figure 17. An 'average' curve could be drawn through this data and used as a competence curve if the threshold of grain movement under oscillating currents was dependent only on orbital velocity. However, as pointed out by Bagnold (1963), movement is also dependent on acceleration and deceleration. Acceleration and deceleration is a function of not

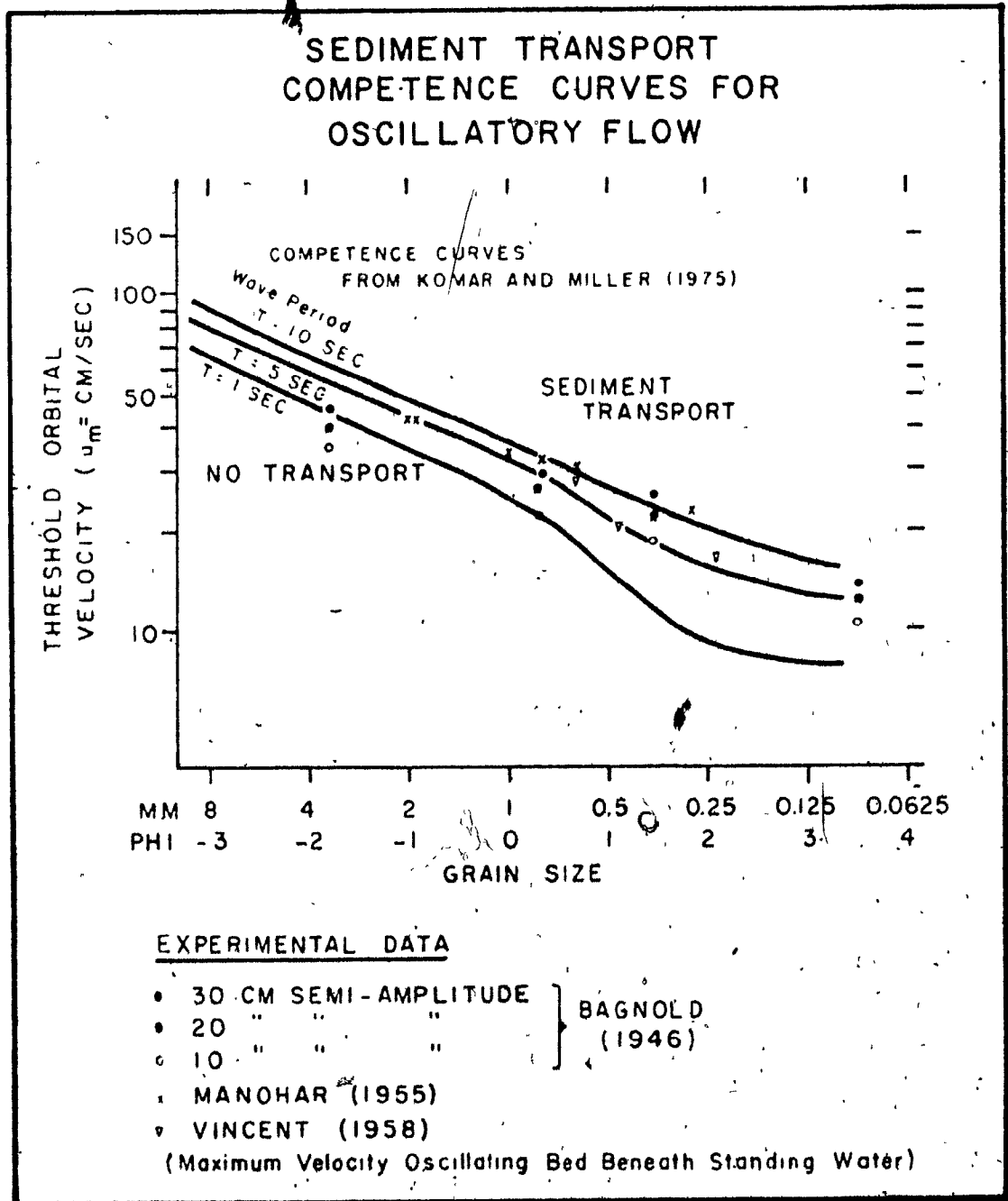


Fig. 17 Relation of grain size to threshold orbital velocity in oscillatory flow.

only velocity but wave orbital diameter and wave period also.

The work of Komar and Miller (1973 and 1975) has resolved the above problem. From published experimental data they developed empirical relationships between threshold velocity, fluid and grain density, grain diameter, orbital diameter and wave period. These relationships allow calculation and plotting of threshold of movement orbital velocities for different wave periods. The resulting competence curves for wave periods of 1, 5 and 10 seconds are replotted from Komar and Miller (1975) on Figure 17. The curves are for quartz spheres and will be used in this study for reasons given above.

The results of the above theoretical and experimental work with both unidirectional and oscillatory flow are subject to normal experimental errors and uncertainties arising from the transitional nature of sediment transport phenomena and from the approximations often necessary in developing theoretical equations. However, the results obtained by Sternberg (1968 and 1971) indicate that the theoretical and experimental results are applicable to the erosion of terrigenous sands by unidirectional flow in the marine environment.

CHAPTER 5 - SEDIMENT TRANSPORT AND DEPOSITION IN GRAND BAY

Sediment transport in Grand Bay is mainly by waves passing back from the barrier reef towards shore. At no time during field work were currents observed in the bay. However, as discussed above, the coarse grain sizes and channel off Kendeace Point at the south end of the bay indicate that strong currents may be effective in that area during strong easterly storms.

From echo sounding records made while anchored at sampling locations and from visual estimates, the most common wave period and wave heights were 4 to 5 seconds and one to two feet respectively. These are secondary waves developed in the back reef by waves breaking on the reef front. The dominant periods and heights of oceanic waves in the area are 5 to 7 seconds and 4 to 5 feet respectively (Fig. 2).

Interference patterns of refracted waves passing back from different segments of Grand Bay reef were inferred from the pattern of ripple crest orientations measured on the back-reef sand flat (Fig. 9a) and were discussed briefly in Chapter 3.

GRAIN SIZE COMPONENT POPULATIONS

It is more fruitful to discuss the Grand Bay samples in terms of their entire grain size distributions rather than in terms of abstracted statistical parameters as was done in Chapter 3. The total grain size distributions were separated into component populations. "Component population"

in this context refers to a log-normally distributed grain size population which occurs mixed with one or more other log-normal grain size distributions to make up the total sampled population. To varying degrees and by different methods Doeglass (1946), Moss (1962, 1963), Fuller (1961), Spencer (1963) and Vischer (1965, 1969) have attempted this type of analysis.

The method used here to identify and separate component populations was the method of differences described by Tanner (1959). Adjustments often had to be made by progressive estimation using both probability plots and histograms. Four widespread and distinct component populations are recognized in Grand Bay.

An example of a typical bimodal grain size distribution (sample 138 RT) and its component population is shown in Figure 18. Proportions of two major populations were estimated from the areas of the two modes on the histogram and from the point of inflection between the two major straight line segments on the probability plot.

The size distribution of population III, comprising approximately 65 percent of the total sampled population, was estimated by drawing a straight line on the probability plot, parallel to the straight line segment for sizes finer than 2 phi. This line was positioned so that its mean approximated the mode on the histogram, and it and the estimated proportions could be used to estimate the total frequency percent for sizes finer than 2 phi. The size distribution of population I was determined by

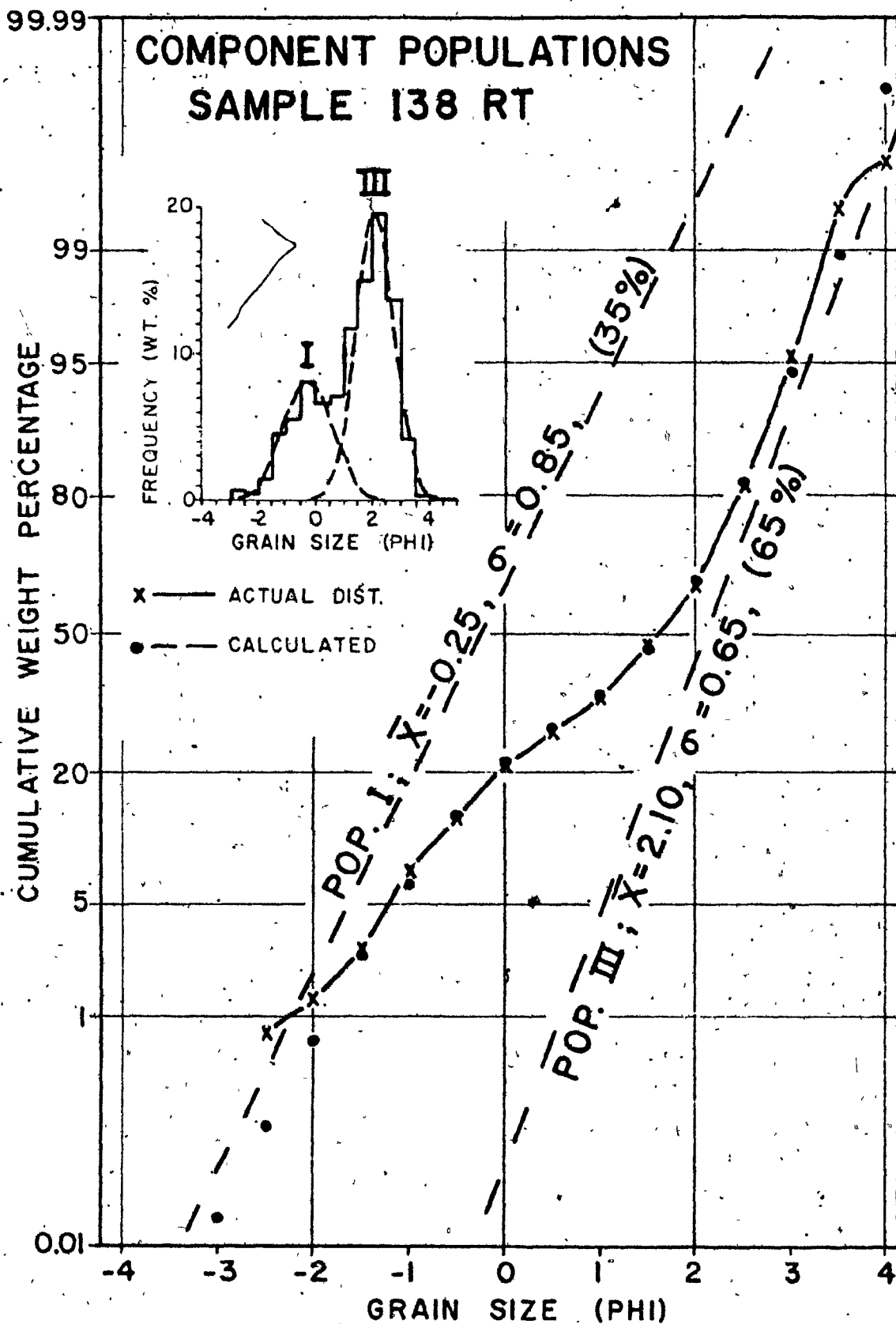


Fig. 18 Grain size component populations of sample 138RT (ripple trough), Grand Bay. R

using the estimated proportion (35%) to calculate the cumulative percentages necessary to make the final calculated total size distribution approximate the total frequency percent for sizes coarser than 0 phi. Small adjustments were made to obtain a closer agreement between the calculated and actual total distributions. The final difference between the calculated and actual whole sample histogram is greatest in the 1.5 to 2 phi interval, where the calculated whole sample weight percentage is 17.46 and the actual value is 15.08.

VARIATION IN GRAIN SIZE COMPONENT POPULATIONS FROM REEF CREST TO SHORE

Traverse 16 was the most fully sampled traverse in Grand Bay and the grain size distributions of the 20 samples were analyzed in detail by the above methods. Maximum differences between calculated and actual frequency weight percentages per half phi interval were less than 3 percent for all samples but three (differences of 3.13, 3.27 and 4.08 in samples 136, 137A, and 137B respectively). The fit of those curves could probably have been improved by adding minor component populations to the total mixture.

The variation of the component populations of the sediments from reef to shore on traverse 16 is presented in Figure 19. Nearly all of the sediment on the back-reef flat and in the lagoon is derived from the reef, approximately one mile offshore, with a relatively small amount being derived from the molluscan and echinoderm infauna of the back-reef sand.

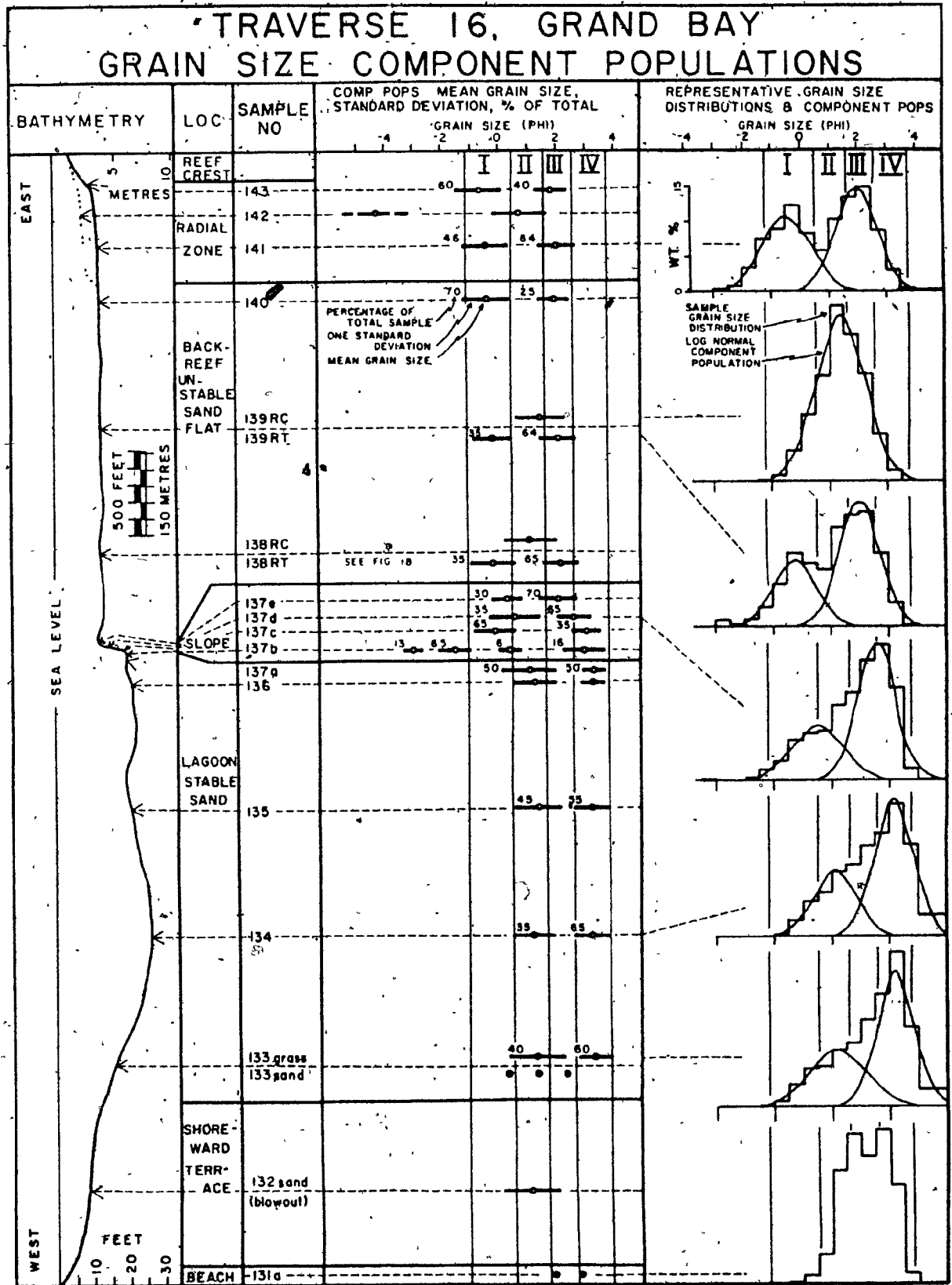


Fig. 19 Grain size component populations on traverse 16, Grand Bay.

Four main component populations are evident. (Fig. 19). These are present in different combinations and proportions to make up most of the sampled grain size populations. In order of coarseness, the main populations are as follows:

- I $\bar{x} = -0.7$ to -0.25 phi; $\sigma = 0.72$ to 0.85 phi. The coarsest representatives of this population form the predominant component (46 to 70% by weight) of the unrippled reef sands. The finer representatives constitute approximately one-third, by weight, of the ripple trough samples from the back-reef flat.
- II $\bar{x} = 1.05$ to 1.40 phi; $\sigma = 0.75$ to 0.95 phi. This population is the ripple crest population on the back-reef flat. It also forms the subordinate component (35 to 50% by weight) of the samples from the lagoon.
- III $\bar{x} = 1.80$ to 2.10 phi; $\sigma = 0.59$ to 0.70 phi. This population forms the subordinate component (25 to 54% by weight) of the reef samples and the predominant component (2/3 by weight) of the ripple trough samples from the back-reef flat.
- IV $\bar{x} = 3.15$ to 3.20 phi; $\sigma = 0.45$ to 0.66 phi. This population forms the predominant component (50 to 65% by weight) of the samples from the lagoon.

As may be seen in Figure 19 the location and relationships of these populations are consistent and distinctive. Populations I and III are not recognized in the lagoon and population IV is

restricted to the lagoon.

The mean grain sizes of the component populations of bimodal samples from the slope between the back-reef sand flat and the lagoon (samples 137b, c, d and e) do not correspond to those of the four populations listed above (Fig. 19). On the upper and middle slope the coarse component populations have a mean grain size intermediate to populations I and II and form 30 to 35 percent by weight of the total samples. At the base of the slope (sample 137c) the coarse component population is population I and forms 65 percent by weight of the total sample. The fine component population decreases in mean grain size downslope. Mean grain size decreases from similar to population III to similar to population IV.

Sample 137 b was from a linear, coarse grained deposit at the very base of the slope. The coarse size fractions are mainly large fragments and whole shells of molluscs and echinoderms. The grain size distribution is a mixture of at least four component populations, the coarsest two of which are coarser than population I. The finest component population is coarse population IV similar to that of sample 137c on the base of the slope.

In figure 20 the means and standard deviations of component populations of selected samples on traverse 16 are replotted from Figure 19 for comparison with the component populations of core samples from traverse 16 and of samples from traverses 15, 17 and 18 in Grand Bay.

Core A was taken on the back-reef flat 25 feet (7.62 m) from the edge of the slope into the stable sand environment and was 14 inches (35.6 cm) long. Grain size distribution of samples in all parts of the core display the same component populations (I and II) in approximately the same proportions as the ripple trough samples. There is no evidence of the ripple crest component population II being deposited at the site (Fig. 20).

Core B was taken part way down the slope in 13.5 feet (4.1 m) of water and was 10.5 inches (26.7 cm) long. Grain size distribution of samples from the core was essentially the same as nearby surface sample 137d (Fig. 20) with the exception of a sample from an obviously coarser layer between 5.5 and 6 inches (14 and 15.2 cm) depth. This sample had the same fine component populations III as the other samples but also had a well developed component population I rather than a fine population I or coarse population II. Also the coarse component population comprised 60 rather than 40 percent of the total sample.

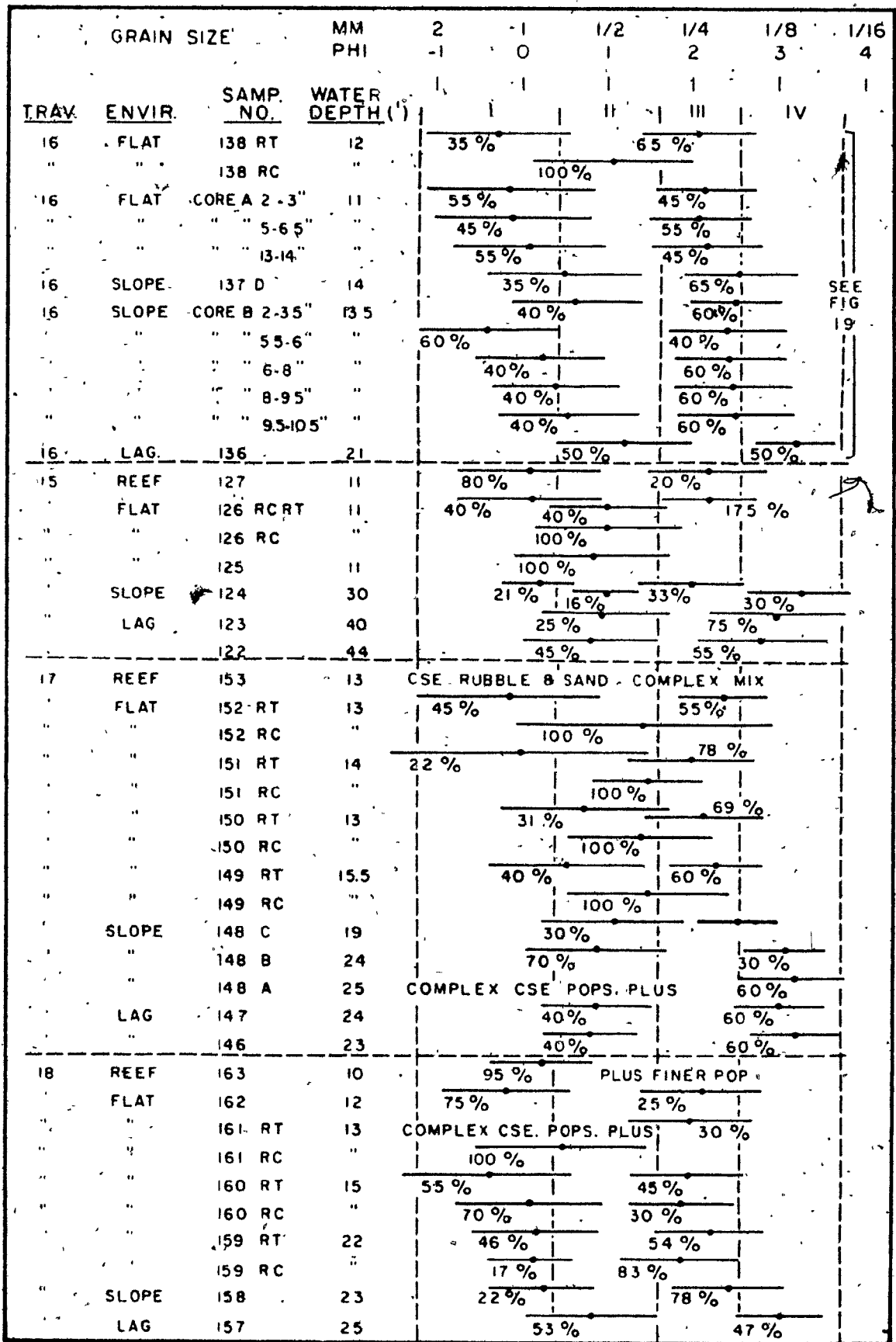
Although the component populations along the other traverses are not identical to those of traverse 16, their relationships to one another and occurrence in samples of ripple crests, ripple troughs and lagoon (stable sand environment) are similar.

On traverse 15 the reef sample is similar to those of traverse 16, composed of population I and III (Fig. 20). Only one site of rippled sand on the back-reef flat of traverse 15 was sampled. The ripple crest sample (126 RC) is identical to similar samples from traverse 16. No sample of the ripple trough was taken, however, a composite sample of ripple trough

and ripple crest can be split into three populations (I, II and III). Since the ripple crest sample was composed entirely of population II, the ripple trough must contain a bimodal grain size distribution of population I and III, the same as on traverse 16. The lagoon samples (123 and 122) are composed of grain size component populations II and IV as were similar samples on traverse 16. Only one slope sample (124) was taken on traverse 15 and it was dredged from a terrace at 30 feet depth. The grain size distribution of sample 124 appears to be a mixture of all four component populations:

Samples from traverse 17 have very similar grain size distributions to traverse 16 except for the two sets of rippled back-reef flat samples (locations 150 and 149) which have finer coarse populations in the ripple trough samples and finer ripple crest samples (Fig. 20). Note that the back-reef sand flat is 1 to 3 feet (.3 to .9 m) deeper on traverse 17 than on traverse 16. Hence for a given wave set the bottom maximum orbital velocity will be less on traverse 17 than traverse 16, accounting for the finer grain sizes.

The grain size distributions of samples from traverse 18 are similar to those from traverse 16 except for two of the three ripple crest samples (159 RC, 160 RC) which are bimodal and very similar to the ripple trough samples (Fig. 20).



SEE FIG 19

Fig. 20 Comparison of grain size component populations, traverses 15 to 18, Grand Bay. (Symbols as for Fig. 19)

INTERPRETATION

Any interpretation of the grain size data must be consistent with the observed prevailing wave and current conditions and allow for the effects of extreme, short-term conditions during storms. The bottom features and grain size distributions of Grand Bay had not been subjected to storm conditions for at least two months prior to the collection of the samples on traverse 16. Occasional disturbance by passing waves of the grains on the ripple crests during sampling suggests that they were near equilibrium with the conditions prevailing at the time (summer, 1968).

Consideration of the nature of sediment movement under wave action and the distribution of the four main populations suggests the following origins for each under prevailing wave conditions on the back-reef flat:

- Population I: Lag population
- Population II: ?Rolling)
- Population III: ?Saltating) traction populations
- Population IV: Suspended population

Population I of the reef and back-reef ripple trough samples is a coarse lag population incapable of being transported in a depth of 10 to 12 feet (3.0 to 3.7 m) by the prevailing waves. For it to be present across the back-reef flat up to one-half mile from its source on the reef indicates it must also be the storm wave traction population. From the results of core A

(Fig. 20), population I is present over the entire back-reef flat to a depth of at least 14 inches (35.6 cm). Brought to the slope off the back-reef flat during storms, this population is distributed by rolling down the steep slope under the influence of gravity. Samples at the foot of the slope (137b, 148a) contain high proportions of coarse population I (Figs. 19 and 20). Slightly higher on the slope, but still near the base (sample 137c), normal population I is abundant. Population I, mixed with population II, may comprise the coarse component populations of most slope samples, the mean grain sizes of which are intermediate to populations I and II. During extended periods of storms population I may become abundant on the slope, producing coarse grained cross beds in the back-reef sand body (sample between 5.5 and 6 inches (14 and 15.2 cm) in Core B - Fig. 20).

Population II, concentrated in the ripple crests of the back-reef flat, is the coarsest transportable material in depths of 10 to 12 feet (3 to 3.7 m) in normal weather. It is slowly brought to the slope where it is deposited. Since populations I and II are deposited at different times under different conditions, it is probable that they occur in separate laminae which were not noticed in the field and which were mixed during sampling.

During storms population II, in the ripple crests is the one most exposed to wave action, and it is rapidly moved into the lagoon (samples 134, 135, 136, 137a, 146, 147). It is also possibly distributed across the lagoon (stable sand environment)

by the storm waves.

Population III, the saltation population in water depths of 10 to 12 feet under prevailing conditions, moves rapidly across the back-reef flat to be deposited on the slope (samples 137D, Core B, 148C - Fig. 20). It is also present in the ripple troughs on the back-reef flat where it is protected by the coarser component population I.

Population IV, the suspended population in water depths of 10 to 12 feet under prevailing conditions, is the most rapidly removed population from the reef and from across the back-reef flat. It forms the main component of the lagoon sediments. The coarsest representative grain sizes settle rapidly on and near the slope where they are intimately mixed with population III (samples 137B, 137C, 137D and most of Core B - Figs. 19 and 20).

Sample 124 on traverse 15 is interesting in that it was the only sample which seemed to consist of all four of the basic component populations (see Fig. 20). This sample was dredged from a terrace at 30 feet depth on the slope into the deepest part of the lagoon. It is possible that this terrace represents the back edge of an old back-reef flat developed at a lower stand of sea level and that it has not yet been completely overridden by the back-reef flat being developed at present day sea level. The dredged sample possibly represents a mixture of the old flat surface sediments (populations I and III) and the present day lagoonal sediments (populations II and IV).

The size distributions of the grass bed and adjacent sand samples (133Th and 133S) on the slope between the shoreward

terrace and the lagoon (Fig. 19) suggest that waves act on the sediment there as they do on the back-reef flat but that the baffling effect of grass cover results in a near bottom current environment comparable to that of the deeper lagoon.

On the beach foreshore of traverse 16 the size distribution surface sample appears to be a mixture of two very close populations. These may be related to the swash and backwash of normal conditions as was postulated by Vischer (1969) for similar beach grain size distributions. One half inch (1.27 cm) beneath the surface of the foreshore the sediment grain sizes are coarser and more nearly unimodal. This material was probably deposited under storm conditions.

DISCUSSION

Are the above interpretations of the origin, transportation and depositional history of the four main component populations in Grand Bay consistent with what is known about sediment transport and wave and current conditions? To check this the means and standard deviations of the component populations of traverse 16 are replotted in Figure 21 along with the wave orbital velocity competence curves from Figure 17. Since waves in Grand Bay were observed to have periods of 4 to 5 seconds, the curve for a period of 5 seconds is emphasized in Figure 21. Interpolation between the curves for periods of 1 and 5 seconds can be made to arrive at an estimate of threshold orbital velocities for wave periods of 4 seconds.

Waves with a period of 5 seconds and having a maximum bottom orbital velocity of 27.5 cm/sec should be capable of moving populations II, III and IV, while leaving population I as a lag deposit (Fig. 21). The equivalent threshold orbital velocity for waves with a period of 4 seconds is estimated at approximately 26.5 cm/sec.

Therefore, normal waves in Grand Bay with periods of 4 to 5 seconds and heights of 1 to 2 feet (0.3 to 0.6 m) in 12 feet (3.66 m) of water (depth observed on back-reef flat on traverse 16) should have bottom orbital velocities of the order of 26.5 to 27.5 cm/sec. Waves with a period of 5 seconds and heights of 1.5 feet (0.46 m) in 12 feet (3.66 m) of water have bottom maximum orbital velocities of 30.2 cm/sec. Waves with a period of 4 seconds and a height of 1.5 feet (0.46 m) in 12 feet (3.66 m) have bottom maximum orbital velocities of 25.9 cm/sec. Therefore the interpretation of grain size population I as a lag population under normal waves in Grand Bay which transport populations II, III and IV on the back-reef flat is consistent with the orbital velocities of the observed normal waves (Fig. 21).

As a further check, the bottom orbital velocities of the normal waves in 25 feet (7.62 m) of water (depth of the lagoon on traverse 16) should not be capable of transporting or rippling grain size populations II and IV (Fig. 21). Waves with a period of 5 seconds and height of 1.5 feet (0.46 m) in 25 feet (7.62 m) of water have a bottom orbital velocity of 15.2 cm/sec (Fig. 21).

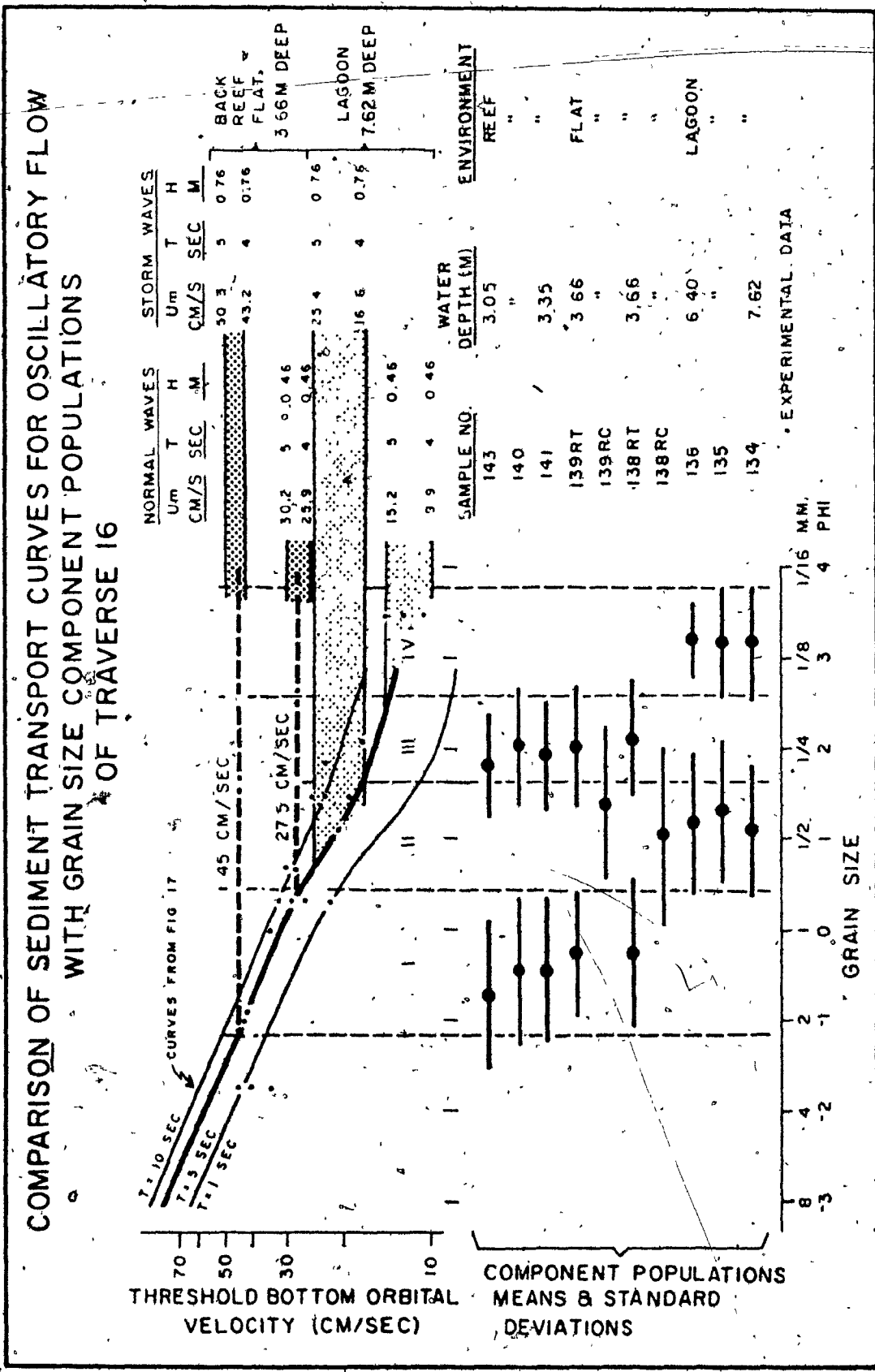


Fig. 21 Comparison of sediment transport curves for oscillatory flow with grain size component populations of traverse 16.

Waves with a period of 4 seconds and a height of 1.5 feet (0.46 m) have a bottom orbital velocity of 9.9 cm/sec. The former wave set would be capable of transporting population IV grain sizes in the lagoon. However, since grain size population IV is intimately mixed with coarser population II which cannot be moved by a bottom orbital velocity of 15.2 cm/sec, it is probable that the observed normal waves would not move any of the bottom sediment in the lagoon.

From Figure 21, bottom orbital velocities of 45.0 cm/sec would be required to move population I from the reef onto the back-reef flat. Such a level of competence was interpreted to occur during storms. No storm waves were observed in Grand Bay. However, orbital velocities of approximately 45.0 cm/sec are produced by waves with a period of 5 seconds and height of 2.5 feet (0.76 m), and by waves with a period of 4 seconds and height of 2.5 feet (0.76 m). The theoretical bottom orbital velocities of the above waves in 12 feet (3.66 m) of water are 50.3 and 43.2 cm/sec respectively (Fig. 21).

The above waves are a minimum size required to move population I onto the back-reef flat and one might expect storm waves in Grand Bay to be somewhat higher than 2.5 feet (0.76 m). A limit to the size of the waves exists however. Since population II is distributed throughout the lagoon and the bottom is not rippled, the maximum orbital velocity in 25 feet (7.62 m) of water must be very close to 27.5 cm/sec or even slightly less. Waves with a period of 5 seconds and a height of 2.5 feet (0.76 m), shown above to be capable of transporting population I on

the back-reef flat, generate a bottom maximum orbital velocity of 25.4 cm/sec in 25 feet (7.62 m) of water. They would therefore be just barely capable of transporting population II in the lagoon (Fig. 21).

The absence of grain size population III in the lagoon must be explained since one would expect this population to be transported into the lagoon during storms. Population III forms approximately 50% by weight of the ripple trough sediment on the back-reef flat and approximately 60% of the sediment on the slope into the deeper lagoon. It arrives on the slope under normal wave conditions as the fine fraction of the bed load. During storms it is probably put into suspension on the back-reef flat. Increased circulation in Grand Bay during storms would result from the increased volume of water pumped over the reef. As a result most of the sediment in suspension (population III) would be removed from the back-reef. Therefore population III is deposited on the slope during normal weather and that portion remaining on the back-reef flat is put in suspension during storms and removed from the area.

SUMMARY AND MODEL OF REEF SEDIMENT TRANSPORT AND DEPOSITION IN GRAND BAY

Sediment transport in Grand Bay is mainly by waves passing back from the barrier reef, one mile offshore. The waves cross a rippled back-reef unstable sand flat which extends halfway to shore at a fairly constant water depth about 12 feet (3.66 m). The back-reef flat ends on a 25 to 30° slope into deeper water

(20 to 40 feet - 6.10 to 12.19 m) of the central lagoon. Shoreward of the lagoon is a terrace leading to the beach. The terrace is the site of extensive Thalassia beds and most of the coarse sediment produced in this environment is probably deposited in place or transported towards the beach.

The barrier reef, back-reef flat, slope and lagoon are the main sites of sediment production, transport and deposition and were studied in most detail.

Four basic grain size component populations are present in the area. These populations are mixed in different combinations and proportions to make up most of the sampled grain size populations. In order of coarseness, the grain size characteristics and environments of occurrence of the basic component populations are as follows (Figs. 19 and 20):

I $\bar{x} = -0.7$ to -0.25 phi; $\sigma = 0.72$ to 0.85 phi.

This population forms the predominant component (45 to 95% by weight) of samples from unrippled sands within channels of the barrier reef and immediately behind the reef. Population III is the other component. Population I also constitutes 22 to 55% (by weight) of samples from ripple troughs on the back-reef sand flat. Again it is mixed with population III.

II $\bar{x} = 1.05$ to 1.40 phi; $\sigma = 0.75$ to 0.95 phi.

This population forms the unimodal grain size distribution of samples of ripple crests on the back-reef flat. It also forms the subordinate component (25 to

53% by weight) of the samples from the lagoon where it is mixed with population IV.

III $\bar{x} = 1.80$ to 2.10 phi; $\sigma = 0.59$ to 0.70 phi.

This population forms the subordinate component (20 to 54% by weight) of the reef samples and the predominant component (45 to 78% by weight) of ripple trough samples from the back-reef flat.

IV $\bar{x} = 3.15$ to 3.20 phi; $\sigma = 0.45$ to 0.66 phi.

This population forms the predominant component (47 to 75% by weight) of the samples from the lagoon.

Grain size distributions of samples from the slope between the back-reef flat and the lagoon are bimodal. The coarse component population is intermediate in grain size to populations I and II except near the base of the slope where it is coarser and similar to population I. The fine component population decreases in mean grain size downslope. Mean grain size changes from similar to population III to similar to population IV.

A 14 inch (35.6 cm) long core from the back-reef flat had component grain size populations similar to the ripple trough samples (populations I and II) to the bottom of the core. The grain size distributions of samples from a 10.5 inch (26.7 cm) long core on the slope were similar to nearby surface samples (fine populations I and III) except for a half inch (1.3 cm) thick coarse grained layer that was comprised of a normal population I and fine population III).

The sampled grain size populations of Grand Bay were in equilibrium with normal prevailing wave conditions. The grain

size component populations were interpreted in terms of lag, bed transport and suspension transport under the prevailing conditions. The interpretations are consistent with the transport competence of the observed waves and of postulated storm waves. A model of reef sediment transport and deposition in Grand Bay is presented in Figures 22 and 23.

Stage I (Fig. 22) represents the observed prevailing conditions of sediment transport in Grand Bay when waves have periods of 4 to 5 seconds and heights of 1 or 2 feet. Particles finer than 0.43 phi (0.74 mm) are transported shorewards across the back-reef sand flat. Grain size component population I is not transported under normal conditions. Component population II is transported very slowly by rolling in the bed load and is organized into ripples on the back-reef flat. Upon reaching the edge of the back-reef flat it is deposited on the slope as part of the coarse grain size component population of the slope deposits. Saltating population III is moved rapidly across the back-reef flat. Except for that part caught interstitially in the coarse population of the ripple troughs, most of population III is deposited as part of the predominant grain size component population of the slope deposits (Fig. 22).

Grain size component population IV is transported across the back-reef flat rapidly, probably in suspension. Coarser grain sizes of population IV come to rest on the slope as part of the fine grains size component population (Fig. 22). For a given wave set the maximum bottom orbital velocity decreases as the water depth increases. Therefore, progressively more and finer

portions of population IV become stable down the slope from the back-reef flat. The progressively greater proportion and fineness of population IV mixed with population III down the slope gives rise to an inverse grain size grading of the fine component of the slope deposit (Fig. 23). Most of the suspended load is deposited in the lagoon where it is recognized as population IV ($\bar{x} = 3.5$ to 3.20 phi).

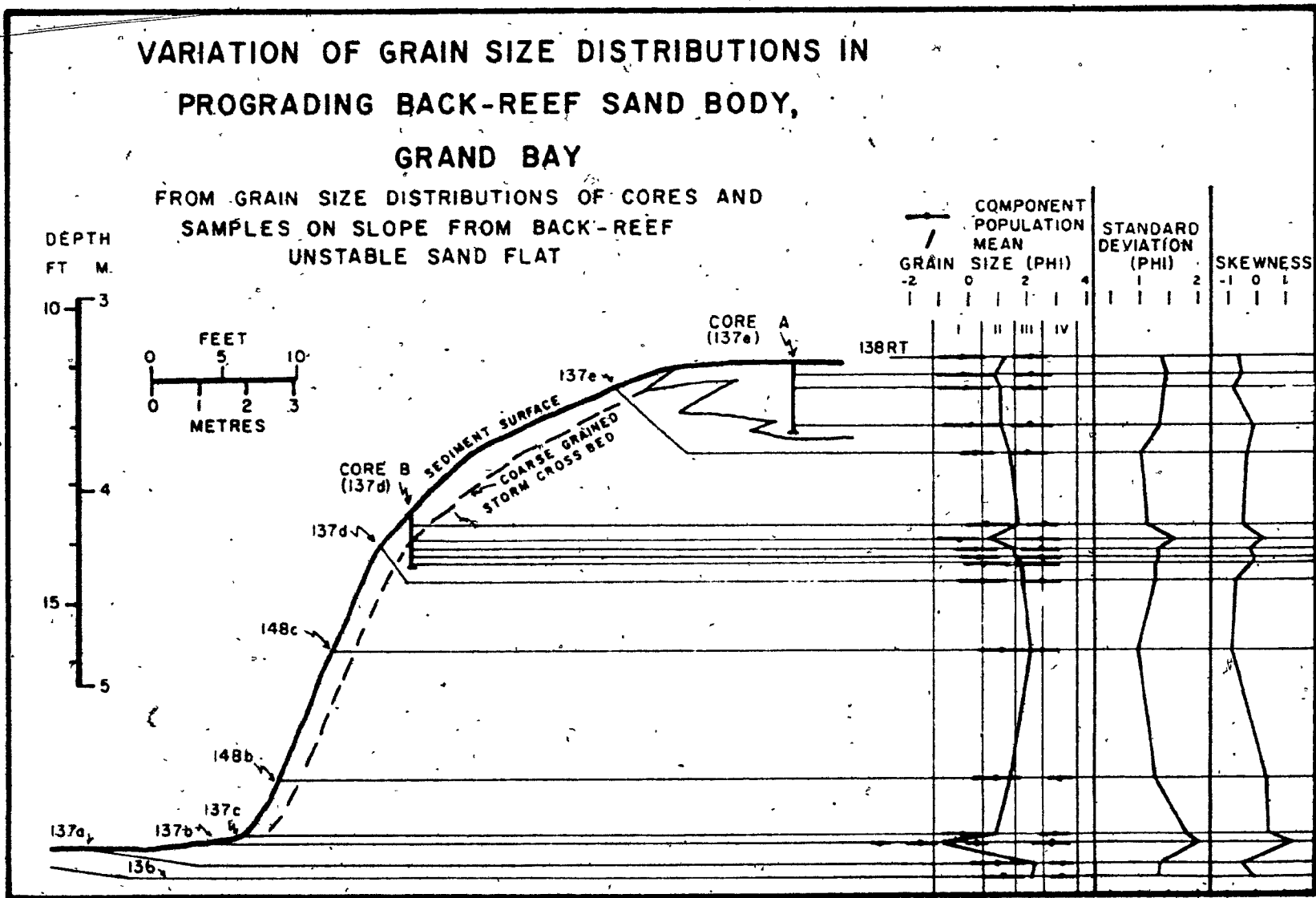
The bulk of the mud-size (finer than 4 phi) grains, which are undoubtedly produced on the reef and are not common in the bay, probably remain in suspension long enough to be removed by slow tidal and wave induced circulation to deeper water.

During storms (Stage II of Fig. 22) all available grain sizes finer than approximately -1.15 phi (2.2 mm) are transported from the reef area and across the back-reef flat. Component population I forms the coarse portion of the traction load, moving to the edge of the back-reef flat. At the top of the steep slope, which is at or near the angle of repose for finer grain sizes, the coarse grain size fractions are unstable and roll to the bottom. They form a coarse grained bottom-set deposit to the shoreward prograding back-reef sand body. If the storm were severe or long enough, sufficient population I grain sizes would be delivered to the slope to clog and form a coarse grained storm cross set in the back-reef sand body (Fig. 23).

Component population II, which makes up the normal wave ripple crests, is the most exposed grain size population on the back-reef flat during storms and is rapidly transported as the

VARIATION OF GRAIN SIZE DISTRIBUTIONS IN PROGRADING BACK-REEF SAND BODY, GRAND BAY

Fig. 23. Variation of grain size distributions in prograding back-reef sand body, Grand Bay.



finest portion of the bed load (Fig. 22). It is swept down the slope into deeper water, where the storm waves are still capable of distributing it as coarse bed load to form the coarse component population of the lagoonal deposits. One might expect the development of bed structures and laminations in the lagoonal deposits because of alternating normal and storm conditions. However, it is likely that growth of marine grasses and burrowing by various organisms during extended periods of normal weather destroy primary sedimentary structures and homogenize the upper layers of the deposit.

Component population III is probably put into suspension on the back-reef flat during a storm (Fig. 22). Its absence in the lagoonal deposits may be a result of increased circulation in Grand Bay during a storm so that the bulk of material in suspension is removed to outside of the back-reef area.

The observed water depth on the back-reef flat, established during normal weather, is not in hydrodynamic equilibrium with storm waves and scouring probably occurs during a storm. Deposition of a coarse grained (population I) top set deposit would occur during the waning stages of the storm. A return to normal conditions would re-establish the observed water depth and population III would infiltrate the coarse top-set grain size population to form the grain size distributions observed in Core A.

Alternation of normal and storm conditions in Grand Bay (Fig. 22) results in alternations of sediment transport patterns and deposition of a back-reef sand body prograding shoreward over finer grained lagoonal deposits (Fig. 23).

CHAPTER 6 - SEDIMENT TRANSPORT AND
DEPOSITION IN WATERING BAY

HYDROLOGY

Sediment transport and deposition in Watering Bay is dominated by unidirectional flow of unequal reversing tidal currents (northward flow strongest). Waves normally affect bottom only immediately behind the barrier reef and in shoreward zones. See Chapter I and Figure 2 for regional character and seasonal variation of the winds, waves and tides. More detailed information within the bay was gathered during December, 1966 and June to September 1967 (qualitative and limited quantitative observations). Since the measurements had to be fitted into a mapping, sampling and echo sounding program, the observations were infrequent and of short duration. Funds were not available for purchase of recording measurement devices which would have allowed a more complete program.

A Sonas-Rion Type V Ott current meter was used during April and May 1968. Measured current velocities are average values over three minute intervals and velocity profiles are based on successive rather than simultaneous measurements.

Water level measurements were made on a marked wooden stake driven into shallow bottom in a quiet backwater just south of the mangrove swamp at the northern end of Watering Bay. Also, when the boat was anchored for a lengthy period of current observations, some idea of tidal trends and times of high and low water

could be obtained by running the echo sounder every 15 minutes and measuring the first water bottom multiple if it was present.

Wave periods were estimated by counting the number of wave crests passing under the anchored boat during 3 to 16 minute intervals. Wave heights were estimated or, in water less than 5 feet deep immediately behind the reef, measured on a marked pole standing on bottom.

Waves

Secondary waves behind the reef in Watering Bay during two days in April 1968 had average periods of 2 to 2.5 seconds and estimated heights of 1 to 1½ feet (0.30 to 0.46 m). These waves are thought to be representative of normal conditions in Watering Bay during spring. In the winter months wave periods and heights are probably greater, following the trend for ocean swell in Figure 2.

On occasions a longer, higher wave set was observed entering Watering Bay from the north or northeast. These waves were often recognizable as far south as traverse 6, and were observed to break on the back-reef margin and on the north and west sides of Carib, a small sandy islet behind the reef (Plate II). The longer period suggests that it was ocean swell, attenuated by refraction and diffraction through and around the small islands of Pinesse, Mopion, Petit St. Vincent and Petit Martinique to the east and northeast. In the open ocean the swell is probably from an east-northeast to northeasterly direction. Waves from more northerly or southerly directions would be too dissipated by the

islands and reefs in those directions to be recognizable in Watering Bay.

The northern half of Watering Bay must be affected by long period waves to the greatest extent during the winter months when swell from the northeast is most common. From Figure 2 the most common wave period should be around six seconds. The only measured set of these waves was on April 27, 1968 when a period of 9.6 seconds and a maximum height of two or three feet (0.61 to 0.30 m) was observed at location 23 (Fig. 3).

Tides and Currents

The tidal harmonic constants listed in the Admiralty Tides Tables (1967), when used to calculate the "Formsahl" (Defant, Vol. II, p. 307, 1961), predict mixed tides with dominant diurnal components ($F = 1.86$) in Hillsborough Bay on the west coast of Carriacou, and dominant semi-diurnal components ($F = 1.02$) in Tobago Cays, nine miles to the north. Scattered observations in Watering Bay (Figs. 24 and 25) indicate that there are two high waters per day throughout the month (i.e. that the semi-diurnal components are dominant).

Figure 24 shows the relationship between predicted high and low waters in Hillsborough Bay, observed tides in Watering Bay, and measured currents in the middle of Watering Bay at the third quarter of the moon (near neap tide) and one day after the new moon (near spring tide). Limited current data for five stations two days after a full moon are compared, in Figure 25, with predicted spring tidal streams between Carriacou and Petit

TIDES AND CURRENTS, WATERING BAY

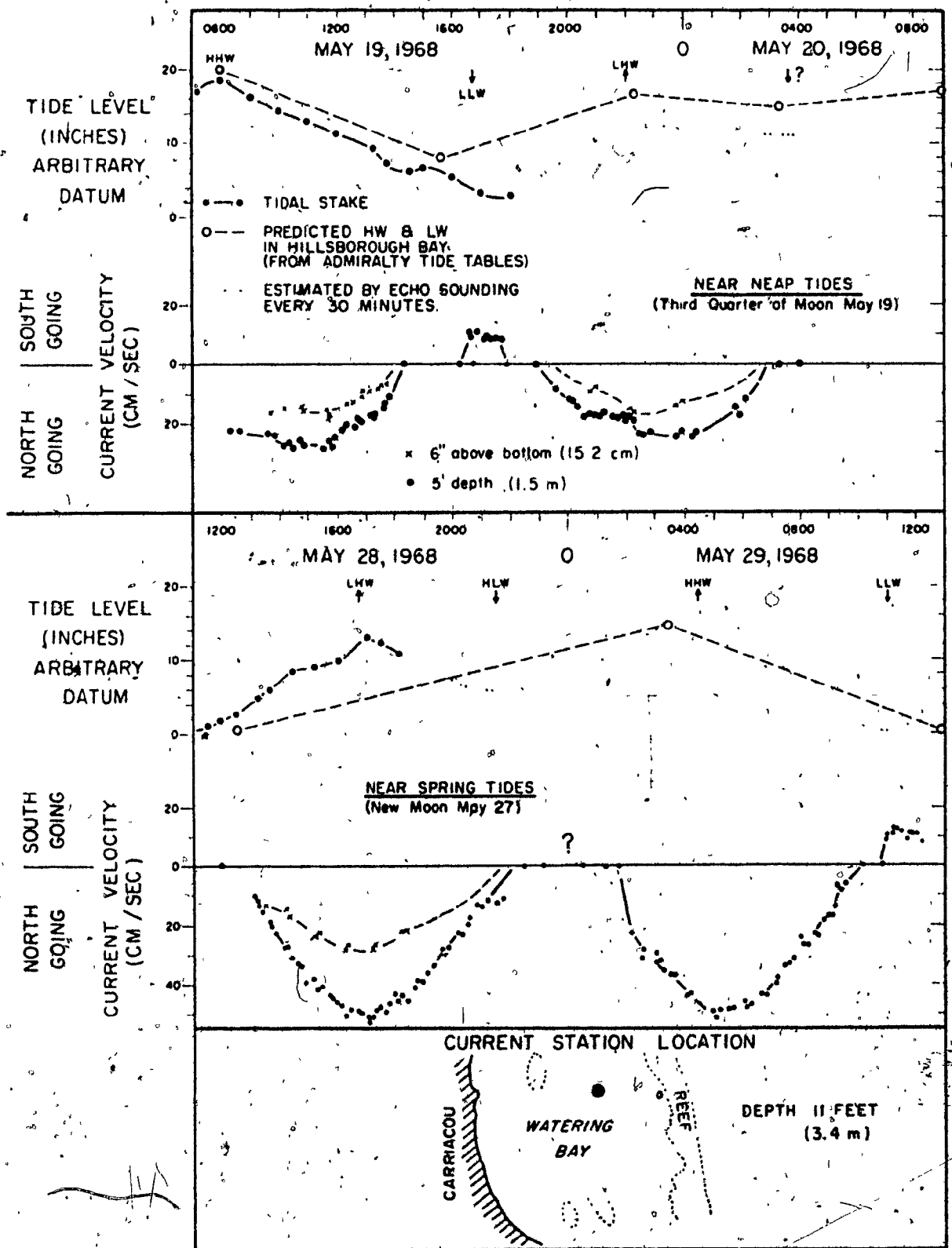
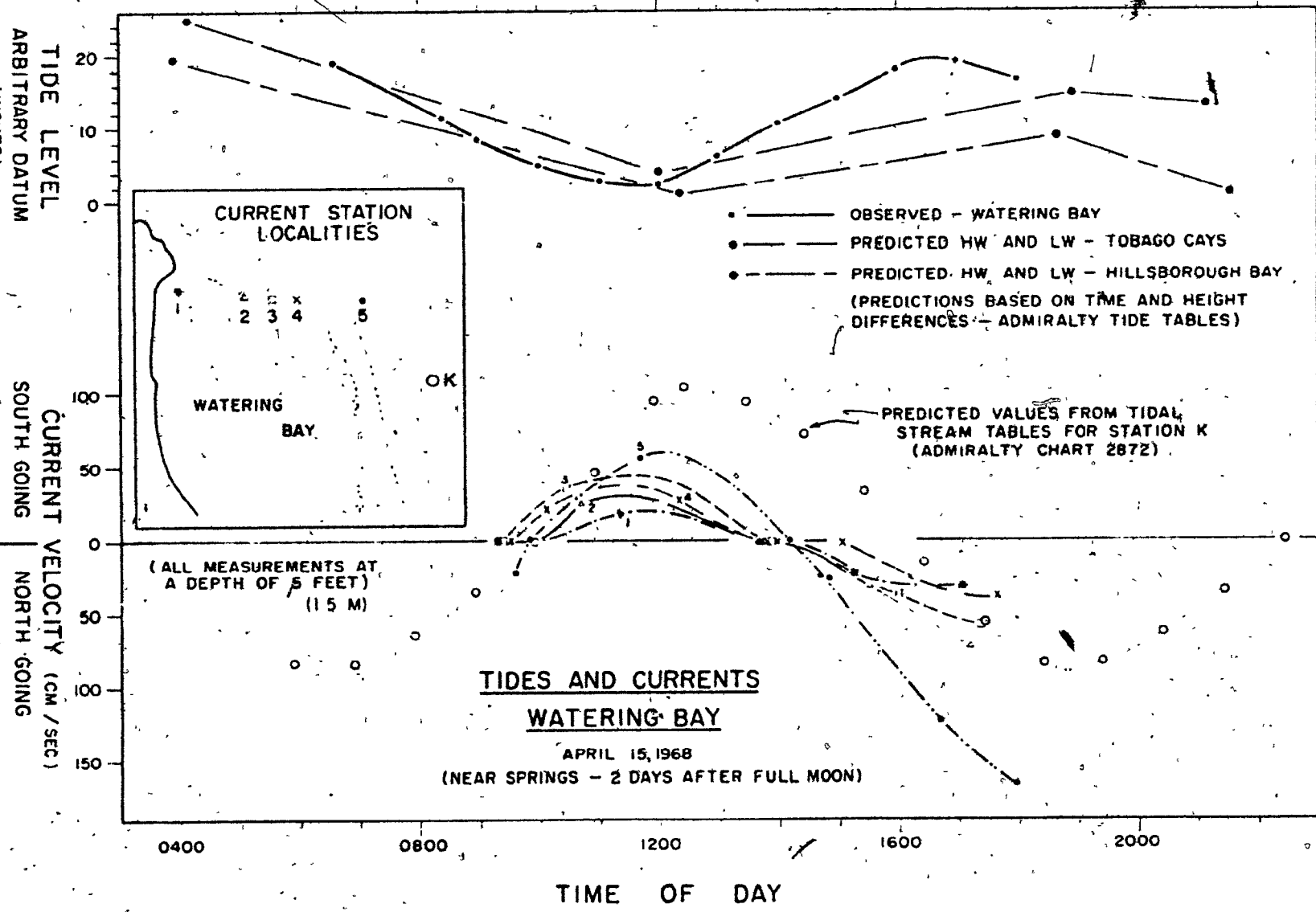


Fig. 24 Neap and spring tides and tidal currents at location 35, Watering Bay.

Fig. 25 Tidal current velocities at four stations in northern Watering Bay and one station outside reef.



Martinique (tidal stream table, Admiralty Chart 2872).

From Figures 24 and 25, the main features of the tide and current system in Watering Bay are:

- (1) Semi-diurnal tides are dominant.
- (2) The tidal range is small; the difference between spring HHW and LLW is approximately 1.5 feet (0.46 m).
- (3) Maximum current flow to the north occurs at or near high water.
- (4) Maximum current flow to the south occurs at or near low water.
- (5) Current velocities are greatest near spring tides.
- (6) Current velocities outside the reef are considerably greater than those in Watering Bay.
- (7) North flowing currents are always faster and of longer duration than south flowing currents. At times there is no flow to the south.
- (8) In Watering Bay the velocity of the north flowing current decreases from the centre towards the shore and towards the reef.
- (9) Time of slack water in Watering Bay precedes that outside the reef.
- (10) The asymmetry of current velocities indicates the presence of non-reversing north flowing currents of approximately 50 cm/sec outside the reef ($\frac{1}{2}$ to $1\frac{1}{2}$ knots, West Indian Pilot, 1955), and between 5 and 20 cm/sec in Watering Bay.

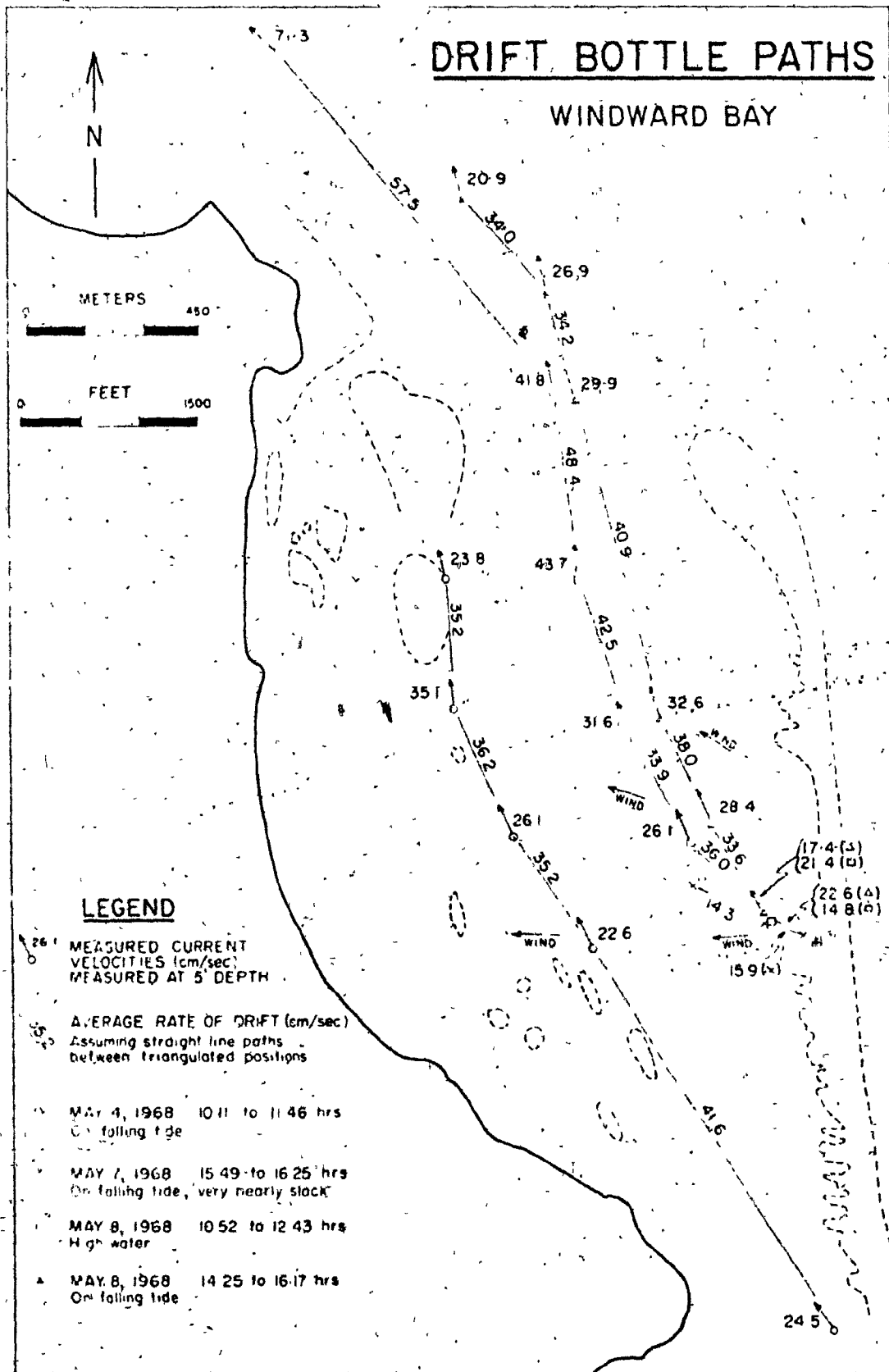


Fig. 26 Tidal current paths followed by drift bottles, released during northward flow, Watering Bay.

The north flowing currents on which the reversing tidal currents are superimposed are variable. Outside the reef and between the islands, the current is probably the regional north-westward drift. Weaker currents within Watering Bay are a result of water driven over the reef by wind and waves and flowing out the open north end. These variable currents cause variations in periodicity, relative strengths and durations of the reversing currents.

The paths followed by drift bottles, released in Watering Bay, are shown in Figure 26. During times of northerly flow, water enters the bay over the reef, accelerates gradually towards the north and passes out through the open northern end of the bay. Here it joins the strong westward flow between Carriacou Island and Union Island four miles to the north. Water also enters the bay by way of the channel between the reef and Point St. Hilaire. During times of southerly flow, most of the water leaves the bay by way of this channel. Only once was the flow over the reef observed to reverse towards the outside.

Nature of Current Flow in Watering Bay

Maximum water depth (h) in Watering Bay is slightly less than 30 feet (914 cm) and most of the bay, where transport by tidal currents is important, is greater than 5 feet (152 cm) deep. The critical value of the Reynolds Number ($R = \bar{u}h/\nu$) separating laminar from turbulent flow is 600. Using $0.008 \text{ cm}^2/\text{sec}$ for the kinematic viscosity (ν) of sea water at 25° C , the critical

values of average velocity (\bar{u}) corresponding to a Reynolds Number of 600 are 0.032 cm/sec for depths of 5 feet (152 cm) and 0.005 cm/sec for depths of 30 feet (915 cm). Tidal current velocities in Watering Bay are considerably greater than the critical velocities, and the flow is turbulent.

The critical value of the Froude Number ($F = \bar{u}/\sqrt{gh}$) separating tranquil from rapid flow is unity. At the depths given above the critical values of average flow velocity corresponding to a Froude number of unity are 386 cm/sec for depths of 5 feet (152 cm) and 946 cm/sec for depths of 30 feet (914 cm). Since tidal current velocities in Watering Bay are considerably less than the critical velocities, the flow is tranquil.

SEDIMENT TRAPS

The sediment traps employed are essentially open-ended boxes with cloth mesh bags attached to one end (Plate 7C). They were stacked on top of one another on the sea floor to sample sediment in transport at different levels.

The sediment trap design used during the summer of 1967 produced equivocal results because it had a tendency to tilt back with the current. As a result the front lip of the bottom trap was lifted from the sediment, scouring occurred beneath the trap and bed load was not adequately sampled. The results were sufficiently encouraging however, that a more stable trap was designed and used in 1968. The traps were stacked three high to sample sediment in transport at 0 to 2 inches (0-5 cm), 2 to 4

inches (5-10 cm) and 4 to 6 inches (10-15 cm) above the bottom. Trap results at 3 localities, where current velocity measurements were made will be considered in detail. Location 35 (Fig. 3) is representative of most of Watering Bay. Location 75 is in the channel between Point St. Hilaire and the reef through which much of the tidal flow passes. Location 24 is near the barrier reef at the northern end of Watering Bay and observations were made at a time when waves as well as tidal currents were having a strong influence on the bottom.

Location 35

Current Measurements

The most complete tidal current data collected during this study was at location 35 (Fig. 3) which, on the basis of bottom observations, bathymetry and central location, was selected as being representative of most of Watering Bay. Current velocity variations at this location near neap tides on May 19 and 20, 1968 and near spring tides on May 28 and 29 were presented above in Figure 24. None of the southward flowing currents represented in Figure 24 were capable of transporting sediment.

During the current measurements near neap tides on May 19, the greatest bottom shear occurred during northerly flow just after 11:30 hours, when the velocity 6 feet (183 cm) above bottom was 28.02 cm/sec and the velocity 6 inches (15 cm) above bottom was 14.30 cm/sec. From the equation

$$u_* = k_0 \frac{\bar{u}_2 - \bar{u}_1}{\ln(z_2/z_1)} \quad (\text{see page 74})$$

the corresponding shear velocity was 2.20 cm/sec. From Figure 16 this bottom shear was capable of eroding well sorted sand with a mean grain size of 0.48 mm (1.04 ϕ). Since the bottom sediment at location 35 has a mean grain size of 1.04 ϕ and is moderately to poorly sorted with a standard deviation of 1.08 ϕ , it is theoretically possible that the measured northerly flow near neap tides was just barely capable of transporting the bottom sediment for a very short time only. In fact, no sand was observed to be moving on the bottom during the current measurements of May 19.

The measured northward flowing currents on May 28 and 29 near spring tides, however, were capable of eroding and transporting the bottom sediment at location 35. They were observed to do so over a nearly planar surface with small scale current lineations on May 28.

As a general conclusion and in keeping with non-quantitative observations during the field work, net sediment transport in Watering Bay is towards the north, and it may be very seldom that the south flowing current is competent to transport bottom sand. Also, most sediment transport occurs around spring tides.

Current Velocity Profiles and Roughness Length

Eleven sets of consecutive current measurements at two depths during the afternoon of May 28 are assumed to approximate the average current profiles. A further assumption that the profiles are logarithmic allows graphical estimation of roughness lengths (Fig. 27) by the method outlined by Inman (in Shepard, 1963).

First approximation values range from 0.018 to 1.97 cm, and the profiles appear to be fairly consistent with the exception of that for the slowest currents. Ignoring the value derived from this possibly spurious profile, the roughness lengths vary from 0.78 to 1.97 cm and average 1.11 cm (-3.46 ϕ). This diameter is within the first half phi size interval coarser than the coarsest grains in the bed material.

Shear Velocities

Using a roughness length of 1.11 cm and the von Karman-Prandtl equation for rough boundaries, shear velocities were calculated for all the measured velocities and plotted on Figure 28 along with field observations.

At 13:45 hours, when there was a shear velocity of 1.7 cm/sec, no sand was observed to be moving. At 14:00 hours, when the next dive and bottom observations were made, the shear velocity was 2.7 cm/sec, and intermittant rolling of sand was noted. If the latter value is taken as threshold shear velocity, then from Figure 16, the corresponding grain size is 0.80 mm (0.31 ϕ) which is the twenty-eighth percentile of the bottom sediment grain size distribution. The theoretical threshold shear velocity, based on the mean grain size of the bottom sediment (0.47 mm (1.04 ϕ), is 2.20 cm/sec and should hold for well-sorted grain size distributions. However, the bottom sediment at location 35 is moderately to poorly sorted with a standard deviation of 1.08 ϕ , and therefore the observed displacement of the representative grain size towards the coarse tail is to be expected. From Figure 28, the

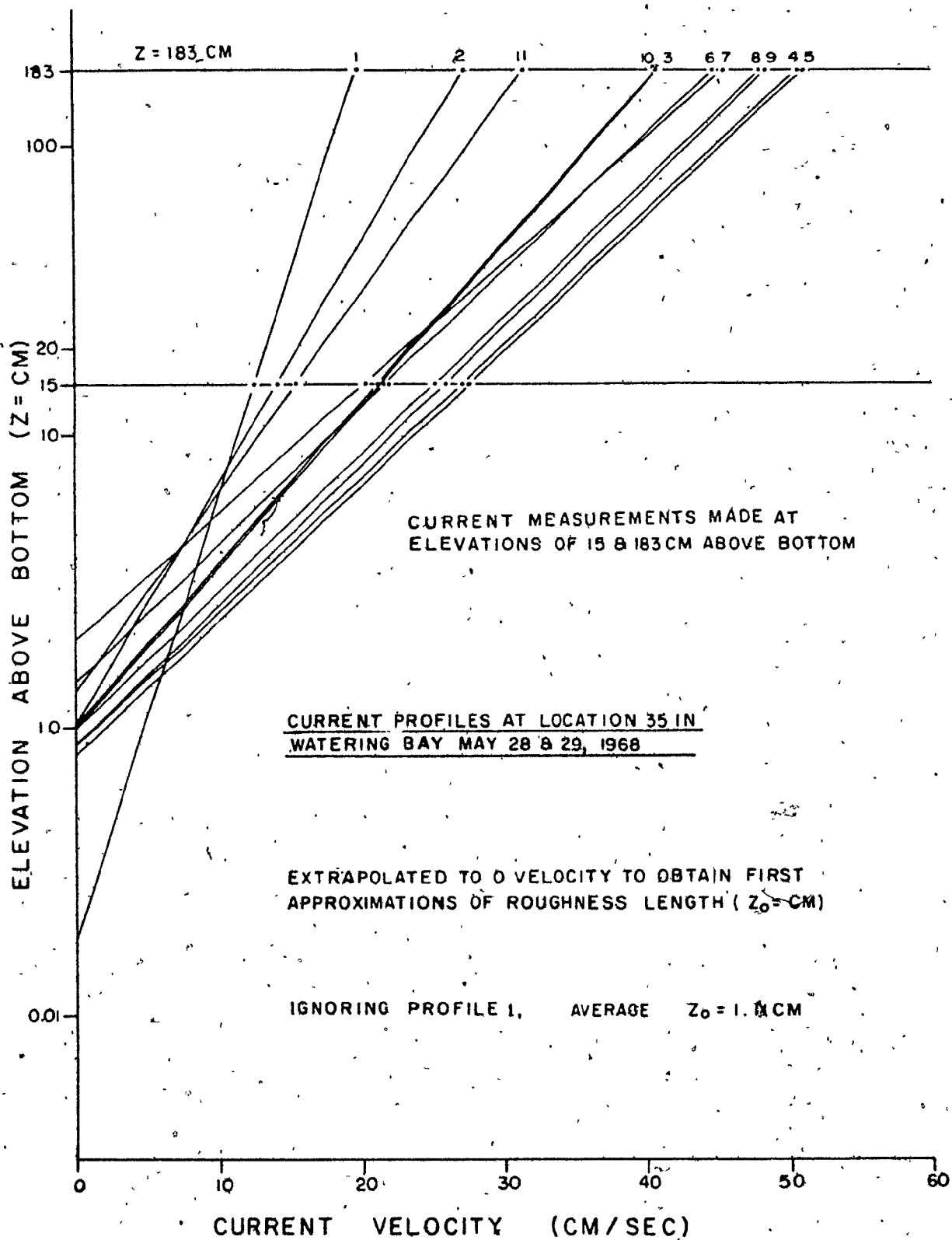


Fig. 27 First approximations of roughness length from current profiles at location 35, Watering Bay.

time during which the shear velocity was equal to or greater than the threshold shear velocity was $4.5 + 4.1 = 8.6$ hours out of every 25 hour tidal cycle near spring tides.

Theoretical Competence and Grain Size Distributions

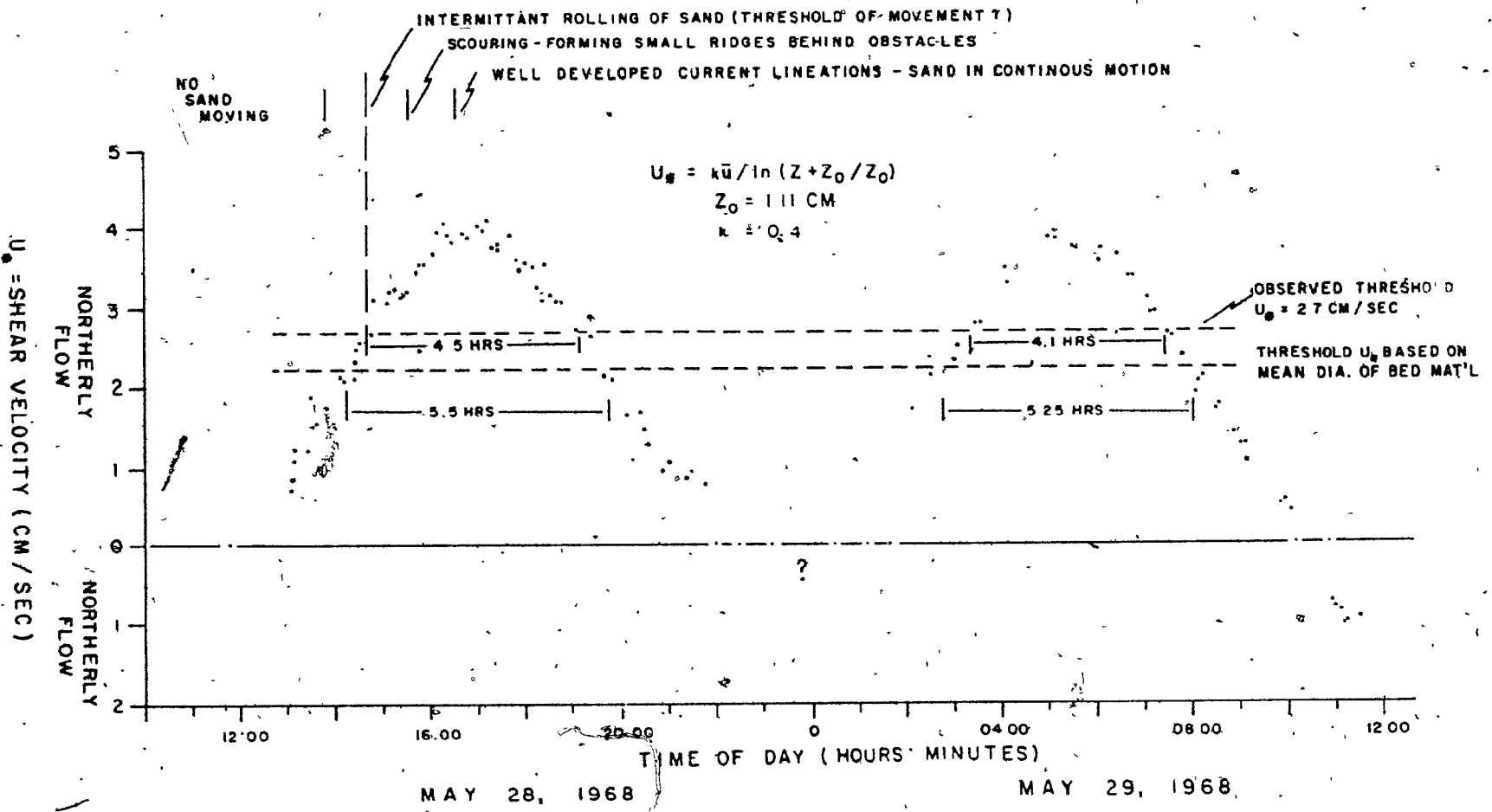
On April 14, 1968 a sediment trap assembly was emplaced at location 35 for 48 hours (nearly two full tidal cycles) during which time the currents ran northward four times. Since April 14 was near spring tides, the analysis of the currents observed on May 28 and 29 can be considered.

In Figure 29 the grain size histograms of the bed material and of the samples collected in the traps are compared to the theoretical competence curves for skeletal carbonate grains in sea water and the shear velocities calculated from the current measurements of May 28. The grain size distribution of the three trap samples are very similar, with mean grain sizes of 2.80, 2.79, and 3.08 phi, and standard deviations of 0.98, 0.92 and 1.05 phi in order of increasing height above bottom. The fineness of the bottom trap sample is unexpected until it is realized that the trap had been considerably underscoured by the time of retrieval and that the bottom lip was above the sediment surface. Therefore the bottom trap was unable to sample the traction load moving very close to the sediment surface, but sampled the suspension load.

The maximum calculated shear velocity (approx. 4 cm/sec) defines a bed load size range between 1.77 and 0.375 mm (-0.81 and 1.45 ϕ) and a suspension load size range finer than 0.375 mm.

SHEAR VELOCITIES AT LOCATION 35 WATERING BAY OVER A FULL TIDAL CYCLE NEAR SPRING TIDES

Fig. 28 Shear velocities at location 35, Watering Bay.

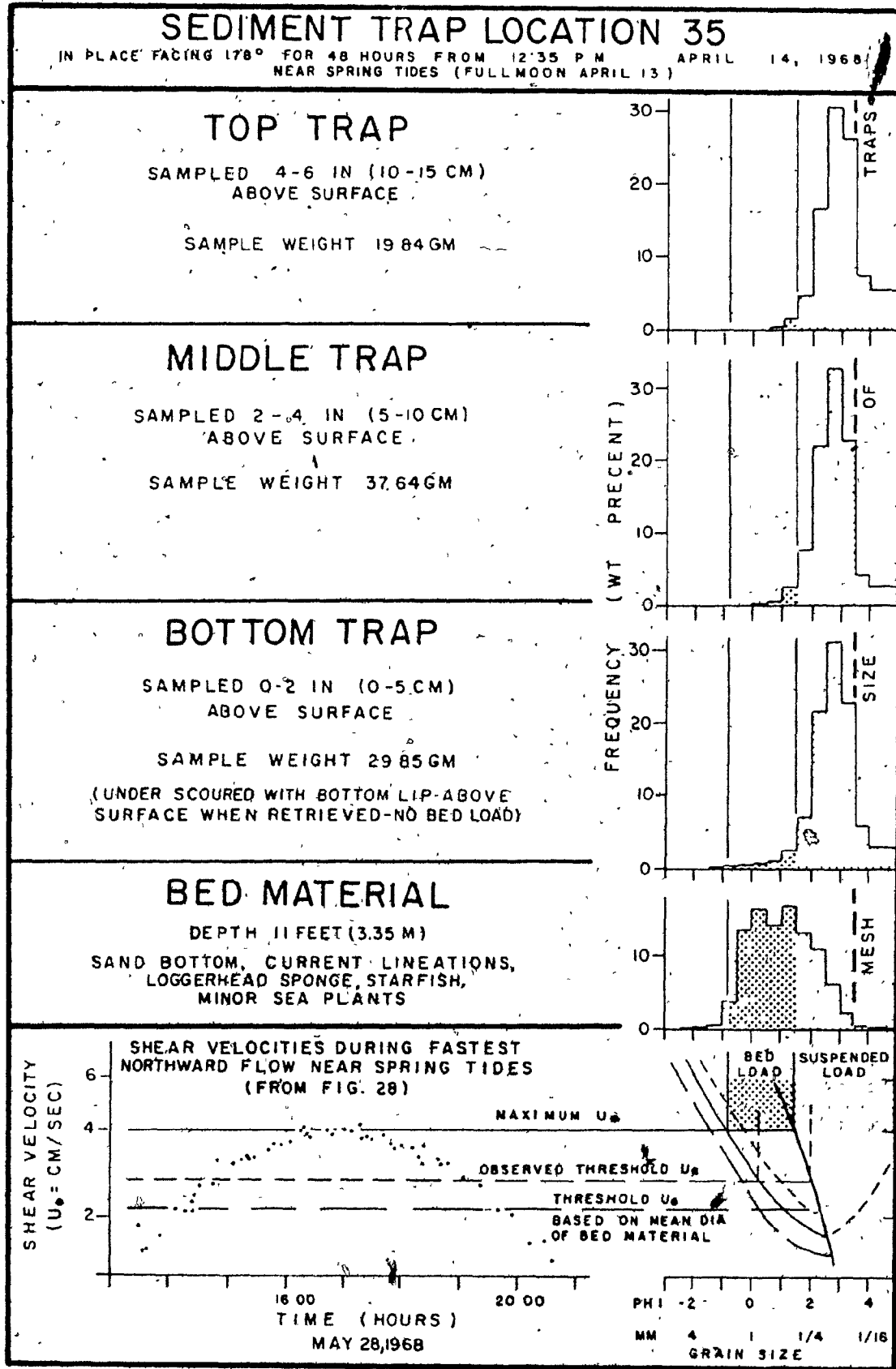


(1.45 ϕ).. The coarse grain size limit of the theoretical bed load is close to the maximum grain sizes of the bed material and corresponds to the 0.35, 0.15 and 0.12 percentiles of the trapped grain size distributions. The grain size separating bed from suspension load corresponds to the 65, 5, 3.9 and 2.3 percentiles of the grain size distributions of the bed material, bottom trap sample, middle trap sample and upper trap sample respectively.

The presence of sizes coarser than the coarsest theoretical suspended load grain size in the middle and upper traps (Figure 29) is probably a result of transitory instantaneous shear velocities which can be many times that calculated from the average velocities (Kalinske, 1943; reported in Inman, 1949).

The fine skewed (3rd moment = 0.26) nature of the bed material grain size distribution is a result of deposition of progressively fining bed load grain size distributions as the tidal currents wane and also the normal entrapment of suspended load grain sizes within the bed load.

The large amount of fine suspended load grain size collected in the middle and upper traps (37.64 and 19.84 gms respectively) would indicate that the bed material would not remain fine skewed for any length of time if it were the only source of suspended load grain sizes. It is probable that much of the suspended load material transported in Watering Bay is produced on the barrier reef, suspended by waves and swept through the bay in one tidal cycle, never coming to rest on the bottom of the bay.



In general, the data from sediment trap 35 are in agreement with sediment transport theory and experimental results, but are not completely unambiguous since the bed load was not sampled properly in the sediment trap.

Location 75

On April 10, 1968 two sediment trap assemblies were set out in the channel entering Watering Bay from the south around Point St. Hilaire. One was placed at location 75 (Fig. 3) directly off the tip of the point and facing 175° azimuth in 26 feet (7.92 m) of water. The other was placed approximately 2,200 feet (670 m) to the north-northwest and facing 140° azimuth in 18 feet (5.49 m) of water. The traps were left in place for 25 hours to sample sediment transported by the dominant north-flowing currents over a full tidal cycle.

It was thought that the results of the two traps would be similar because of the similarity of the bottom sediments at the two sites (mainly Porites rubble, algal encrusted gravel and coarse sand). The channel in which the two sites were located is probably near hydrodynamic equilibrium; all but the very coarsest material supplied to it being transported by nearly constant bottom stresses along it. The maintenance of constant shear stresses along the channel is reflected by its shallowing northward where the width between the barrier reef and the shoreward zones increases rapidly (Fig. 4). The channel must become shallower to maintain the bottom shear stresses with the decreased water flow.

On the basis of the above argument, current measurements made at the second site are related to the sediment trap data at location 75 where no current measurements were made. The sediment trap at the second site was fouled by drifting sea plants and was underscoured considerably by the time of retrieval. Therefore, the sediment collected was considered unrepresentative of the flow and no grain size analyses were made. The sediment trap at location 75, however, collected considerable sediment, and was not fouled or underscoured, and grain size analyses were made.

The channel bottom is affected only by tidal currents. Short period (2-3 sec), low (1-2 ft (30-61 cm)) waves observed in Watering Bay do not produce significant bottom oscillatory currents in water depths of the current measurement and sediment trap sites.

Current Velocity Profiles and Roughness Length

Current velocities were measured at heights of 3, 8 and 13 feet (91, 244 and 396 cm) above bottom. Measurements made consecutively at the three heights provide a close estimate of the velocity profile, which should be logarithmic in the fully turbulent flow.

Five profiles were measured and are plotted on semi-logarithmic paper in Figure 30. Best fit straight lines were drawn through the data of each profile. Deviation of each measured velocity from the line is a measure of the deviation of the profiles from log normality and are presented in table form in

Figure 30. The deviations, of which only two of the fifteen exceed 4%, indicate that the profiles are lognormal. Sternberg (1968), with much more sophisticated equipment, considered a profile to be lognormal if at least 4 of 6 velocity measurements fell within 10% of a linear relationship.

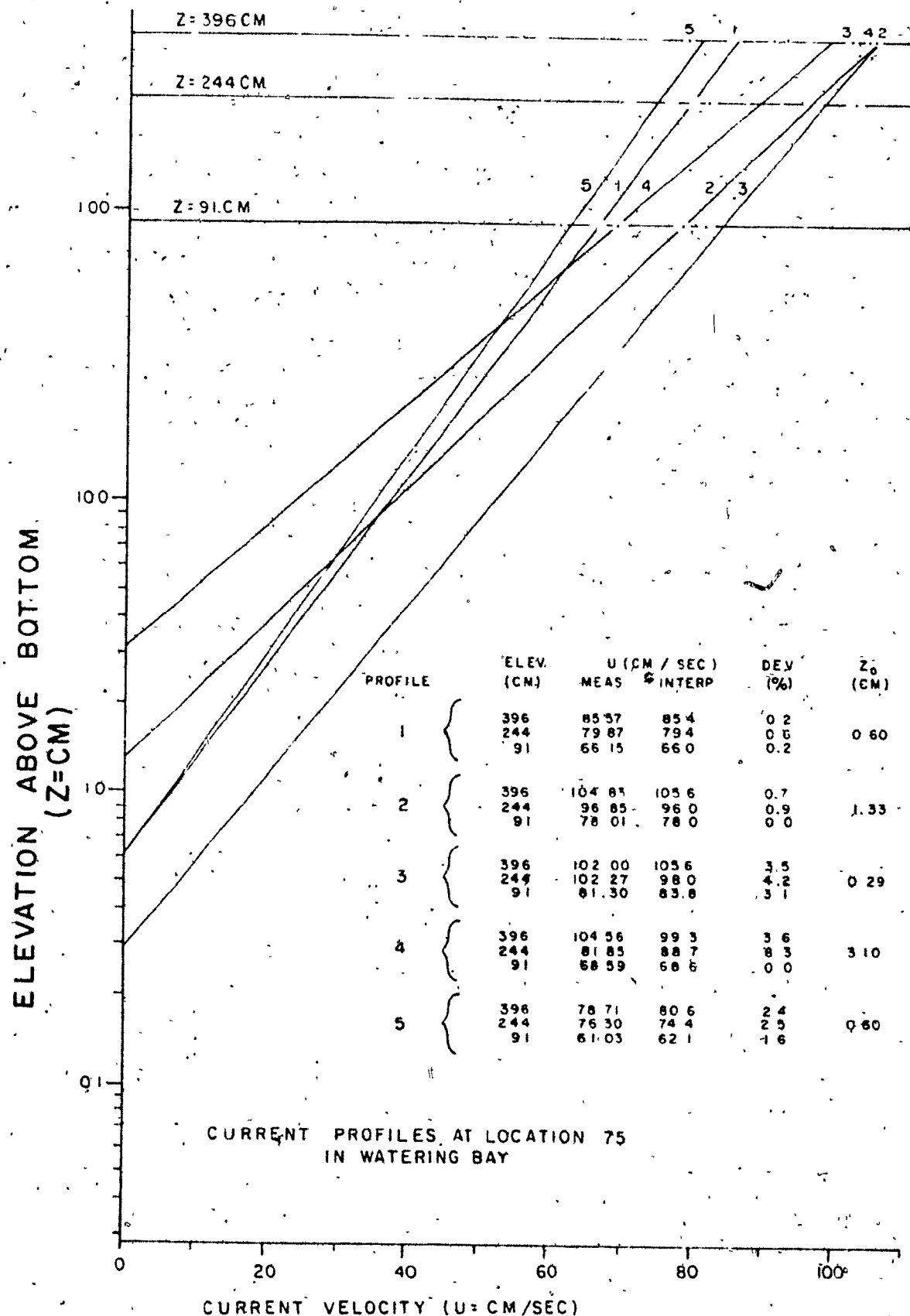
First approximations of roughness length (z_0 = height axis intercept) for each profile are also included in the table on Figure 30. The values range from 0.29 to 3.10 cm. By omitting the profile with deviations from lognormality greater than 5%, the range of values is reduced to 0.29 to 1.33 cm and the average value is 0.71 cm (-2.81 σ). This roughness length corresponds to a grain size diameter within the first half phi interval coarser than the coarsest grains in the main mode of the bed material grain size distribution.

Shear Velocities

Shear velocity values were calculated from the current measurements using the average roughness length of 0.71 cm and the von Karman-Prandtl equation for rough boundaries. The shear velocities vary from 4.98 to 7.00 cm/sec (Fig. 31).

Theoretical Competence and Grain Size Distributions

Histograms of the grain size distributions of the bottom sediment and of the trapped sediment at location 75 (Fig. 31) are compared with the theoretical competence curves for carbonate grains in sea water and the calculated shear velocities. The grain size distribution of sediment collected in the bottom trap



CURRENT PROFILES AT LOCATION 75 IN WATERING BAY

Fig. 30 First approximations of roughness length from current profiles at location 75, Watering Bay.

is similar to that of the main mode of the bed material sample and is coarser than those of the sediment collected in the middle and top traps. Based on the trapped sediment grain size distributions, the best separation of bed load and suspended load grain sizes occurs at 0.5ϕ (0.71 mm) which, from the suspension competence curve, corresponds to a 6.4 cm/sec shear velocity. This shear is capable of transporting, in traction, grain sizes up to -2.16ϕ (4.5 mm) which corresponds closely to the coarsest grain size collected in the bottom trap (in the -1.5 to -2.0ϕ size range). Also from Figure 31, the sediment trap derived shear velocity of 6.4 cm/sec is a close approximation of the maximum calculated shear velocities (6.63 to 7.00 cm/sec) occurring between 14:00 and 15:00 hours.

The grain size separating bedload from suspended load on the basis of the trapped grain size distribution and on the basis of the maximum calculated shear velocity corresponding to the 72nd and 67th percentiles of the bed material grain size distribution respectively.

Observations of bottom sediment transport were not made at location 75 as they were at location 35 and the threshold shear velocity must be estimated. The minimum threshold shear velocity, based on the median grain size of the bed material (-2.0ϕ (1.12 mm)) is approximately 3.2 cm/sec. Since the bed material at location 75 is poorly sorted with a standard deviation of 1.81ϕ , the representative grain size is expected to be coarser than the median grain size and should be at least as coarse as the twenty-eight percentile which was the representative grain

size for the moderately-sorted bed material at location 35. The threshold shear velocity, based on the twenty-eighth percentile of the bed material grain size distribution (-1.25ϕ (2.38 mm)) is 4.7 cm/sec.

Using the latter threshold shear velocity and Figure 31, it appears that the shear velocity in the channel around Point St. Hilaire is equal to or greater than the threshold shear velocity for 7.8 hours out of every 25 hour tidal cycle near spring tides as compared to 8.6 hours at location 35.

Similar to location 35, the positive (fine) skewness of the main grain size mode of the bed material at location 75 and of the sample collected in the bottom trap is probably a result of deposition of progressively fining bed load grain size distributions by waning tidal currents and the normal entrapment of suspended load grain sizes in the bed load. However, the skewness of the whole bed material grain size distribution in this case is actually negative (-0.69) because of the presence of a coarse mode.

The presence of grain sizes coarser than the coarsest theoretical suspended load grain size in the middle and upper traps (Fig. 31) is probably a result of transitory instantaneous shear velocities (Kalinske, 1943; reported in Inman, 1949). The shear velocity capable of suspending the coarsest grain sizes collected in the middle and upper traps (2ϕ (4 mm)) is approximately 16 cm/sec (Fig. 16) which is 2.3 times the maximum calculated values. From Figure 16 these transitory shear velocities are capable of moving grains up to -4.5ϕ (23 mm) in diameter. Significantly,

this is the maximum diameter of the bed material. Hence, the gravel in the coarse mode may be in very slow intermittent transport under normal conditions, and there is no need to consider it as lag material formed in situ or as material transported only under abnormal conditions.

As was found for the currents and trap data at location 35, there is generally a good correlation between sediment transport theory and experiments and the data from sediment trap 75. Also, the grain size distribution of the bed material logically reflects and relates to the hydrodynamic conditions.

Location 24

Another sediment trap and current measurement experiment was made in 14 feet (4.27 m) of water at location 24 (Fig. 3) near the northern end of Watering Bay on April 26, 1968. Three trap assemblies were emplaced consecutively, and current measurements were made at the same site throughout the day. Both waves and tidal currents had an effect on the bottom during the experiment. Observations of winds, waves, tidal current velocities and bottom features are included in Figure 32.

Winds and Waves

Winds were light and from the northeast and east-northeast throughout the day. Secondary local waves passing back from the barrier reef had periods around 2 seconds and estimated heights from 1.5 to 2.3 feet (46 to 70 cm). Calculated maximum bottom orbital velocities resulting from these waves vary from 1.9 to

8.2 cm/sec and on the basis of Figure 17 are insufficient to erode the bottom.

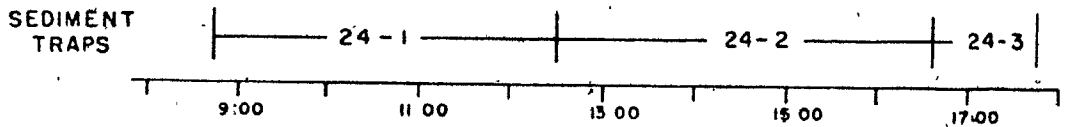
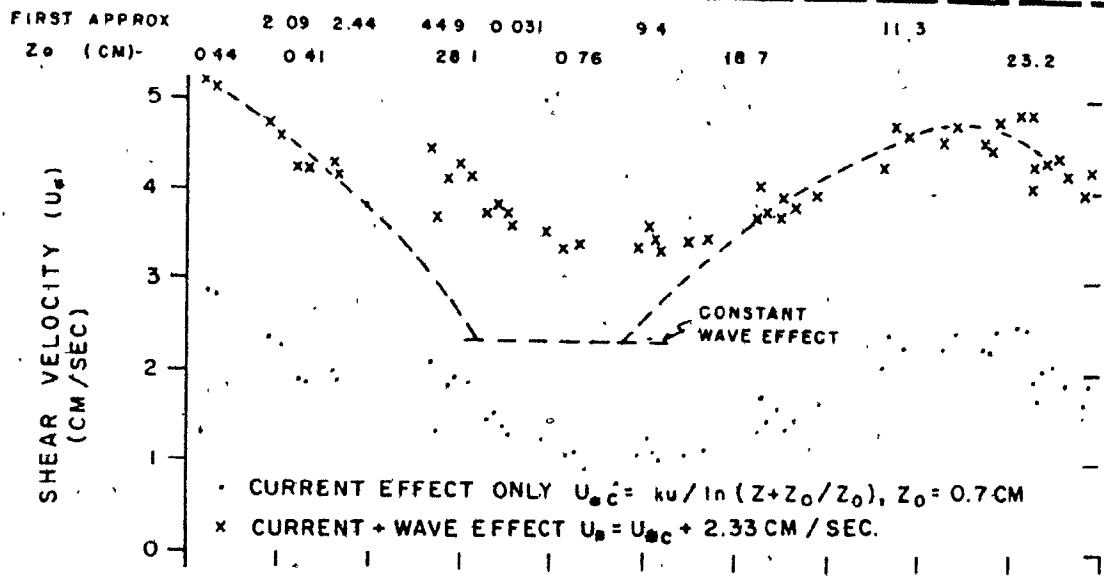
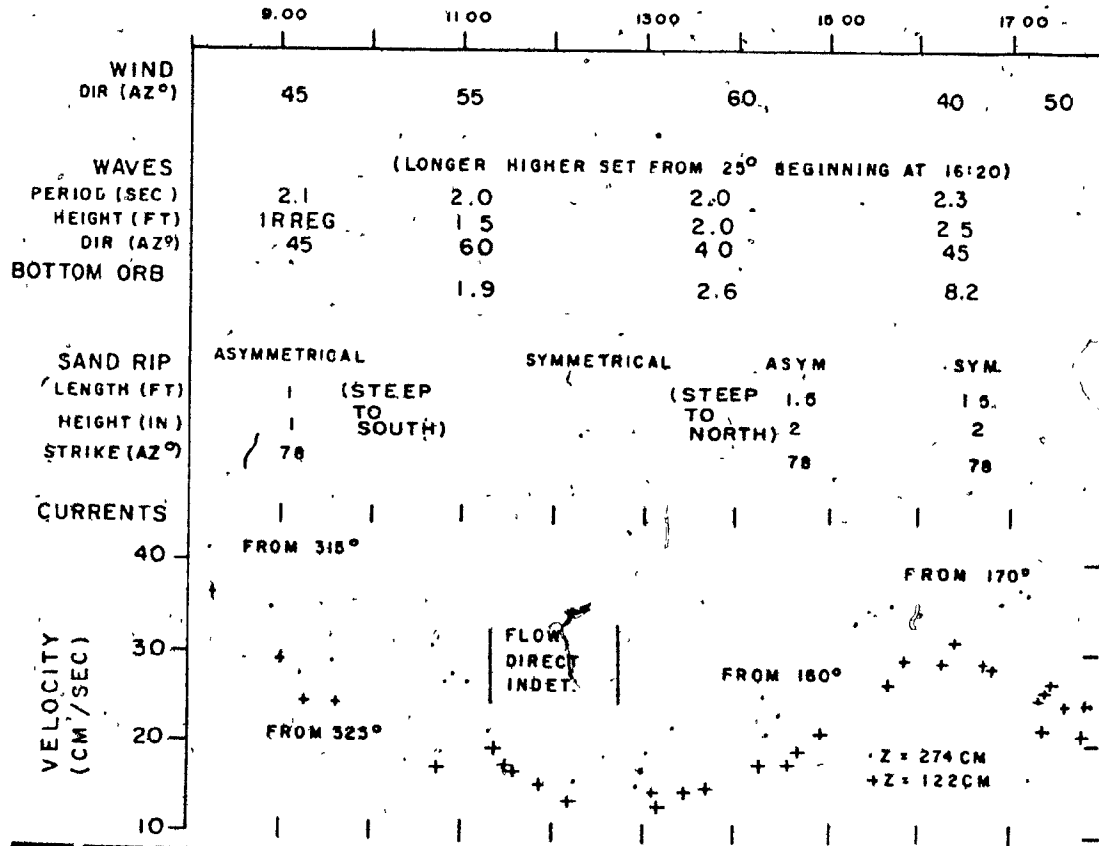
During the first wave observations of the day it was noted that there seemed to be more than one set of waves acting, but it was not possible to distinguish the character of the second set. By 16:20 hours, as noted on Figure 32, the second set became recognizable as entering the bay from a northerly direction with a longer period than the secondary set. By 16:35 hours, sand ripples on the bottom became symmetrical in spite of the north-flowing current being at its maximum rate of flow. Bottom sediment moved in an oscillatory manner, but net sediment transport was still northward.

The next day (April 27) at 11:00 hours, location 24 was revisited, and the second set of waves was clearly distinguishable as being directly from the north and having a wave period of 9.6 seconds, a wave length of approximately 200 feet (61 m) and a wave height of approximately 4 feet (1.2 m). The ease of recognition was obviously due to an increase in wave height overnight.

Since the bottom sand ripples became symmetrical when the tidal current was slack around noon April 26, the long period wave set was probably affecting the bottom at location 24 throughout the sediment trap experiment. Also the bottom orbital velocity must have been competent to move the bottom sediment. Using the mean grain size (0.85ϕ (0.55 mm)) of the moderately-sorted

WIND, WAVE, SAND RIPPLE & TIDAL CURRENT OBSERVATIONS - LOC. 24

APRIL 26, 1968 - TIME OF DAY (HR:MIN)



APRIL 26, 1968 - TIME OF DAY (HR:MIN)

Fig. 32 Wind, wave, sand ripple and tidal current observations at location 24, Watering Bay.

bed material ripple crest sample as the representative grain size and the competence curve for 10 second period waves in Figure 17, the bottom orbital velocity must have been between approximately 28 cm/sec.

Waves with a period of 10 seconds and a height of 1.19 feet (36 cm) have a bottom orbital velocity of approximately 26 cm/sec in 14 feet (4.27 m) of water. The long period and low wave height are the reason the wave set was not easily separated from the shorter period, higher secondary wave set. The wave height must have increased to around 2 feet (60cm) in order to be recognized at 16:20 hours.

For the sake of simplicity it will be assumed that the wave-induced bottom orbital velocity was constant at 28 cm/sec for the entire experiment although velocities were probably greater while trap 24-3 was in place. From Figures 16 and 17 this bottom orbital velocity is as competent to erode sediment as a shear velocity of 2.33 cm/sec in unidirectional flow. In considering the results of the experiment an increment of 2.33 cm/sec will be added to the calculated shear velocities of the tidal currents to arrive at an estimate of the total erosive and transport competence resulting from the action of both waves and currents.

Current Measurements

Observations began shortly after 8:00 hours on a waning southward flowing current (Fig. 32). Between 11:25 and 12:45

hours, the current measurements were the lowest of the day, and the current direction was indeterminate. During this time the current was probably slack and the velocity measurements resulted from the oscillatory motion of the long period waves. When tidal flow was weak the current meter was able to swing with the oscillatory currents and the velocity measurements were not due solely to tidal flow. Before 10:00 hours and after 14:00 hours, however, the tidal flow was strong enough to hold the current meter steady in one direction, and the net effect on the current measurement of the nearly equal oscillatory currents generated by the waves was near zero.

This was the only occasion when current flow to the south was observed to be as fast or faster than the northward flow and was probably a local phenomenon near the barrier reef in the northern part of the bay. The usual constant northerly flow of water pumped over the barrier reef by wind and waves was probably nullified by the long period waves entering the bay from the north and actually forming small breakers on the back of the reef as far south as traverse 6.

Current Velocity Profiles and Roughness Length

Velocity profiles were drawn on semi-logarithmic paper as straight lines between two values since there were no current measurements at a third height above bottom to serve as a check on the lognormality of the profiles. First approximations of roughness length are listed in Figure 32 immediately below the

current velocity graph. The wide range in values from 0.03 to 44.9 cm and the high average value of 11.8 cm/sec indicate that most of the profiles were not logarithmic as measured; probably because of wave action. The values derived from the current velocities measured early in the day before 10:00 hours are probably the most unaffected by wave action and indicate that the roughness length was somewhere between 0.4 and 2.4 cm.

On the basis of the results of the experiments at locations 35 and 75, the roughness length was assumed to be equivalent to a grain diameter within the first half phi grain size interval coarser than the coarsest half phi interval of the bed material, which was -2.0 to $=2.5 \phi$ (4 to 5.7 mm). A value of 7 mm ($=2.8 \phi$) was selected which is also within the range of 0.4 and 2.4 cm estimated from the velocity profiles before 10:00 hours.

Shear Velocities

Shear velocities were calculated from the current measurements using the von Karman-Prandtl equation for rough boundaries and the assumed roughness length of 0.7 cm. Values range from 2.83 to 1.03 cm/sec (Fig. 32). As discussed above, the high values before 10:00 hours and after 14:00 hours should reflect the strength of the tidal currents. However, calculated shear velocities between 10:00 and 14:00 hours are based on current measurements that are in error because of wave action.

As discussed above all shear velocity values were increased by 2.33 cm/sec in the upper shear velocity curve on Figure 32 to provide an estimate of the total erosive competence resulting

from the combination of long period waves and tidal currents. These larger shear velocities will be used when considering the sediment trap data.

Theoretical Competence and Grain Size Distributions

The intervals of time during which each of the three sediment trap assemblies were in place are indicated at the bottom of Figure 32. All traps were placed parallel with the ripples within ripple troughs and facing the current flow at the time.

In Figures 33, 34 and 35 the grain size distributions of the sediment collected in the traps are compared to the competence curves for carbonate grains in sea water and to the relevant calculated shear velocities.

The results of sediment trap 24-1, emplaced for 3 hours and 47 minutes during the waning southward current, are presented in Figure 33. The grain size separating bed load from suspended load on the basis of the trapped sediment histograms is 1.25ϕ (0.43 mm). From the suspended load competence curve (Figs. 16 and 33) a shear velocity of 4.35 cm/sec is required to suspend grains finer than 1.25ϕ (0.43 mm).

Another estimate of shear velocity is possible using the maximum grain size collected in the bottom trap. Ignoring the 0.03 percent of the sample occurring in the -1.5 to -2.0 (2.83 to 4 mm) size range the maximum grain size is -1.5ϕ (2.84 mm) which corresponds to a shear velocity of 5.2 cm/sec capable of suspending grain sizes finer than 0.9ϕ (0.53 mm).

The estimates of shear velocity (4.35 and 5.2 cm/sec) derived from the sediment trap data are of the same order as the maximum

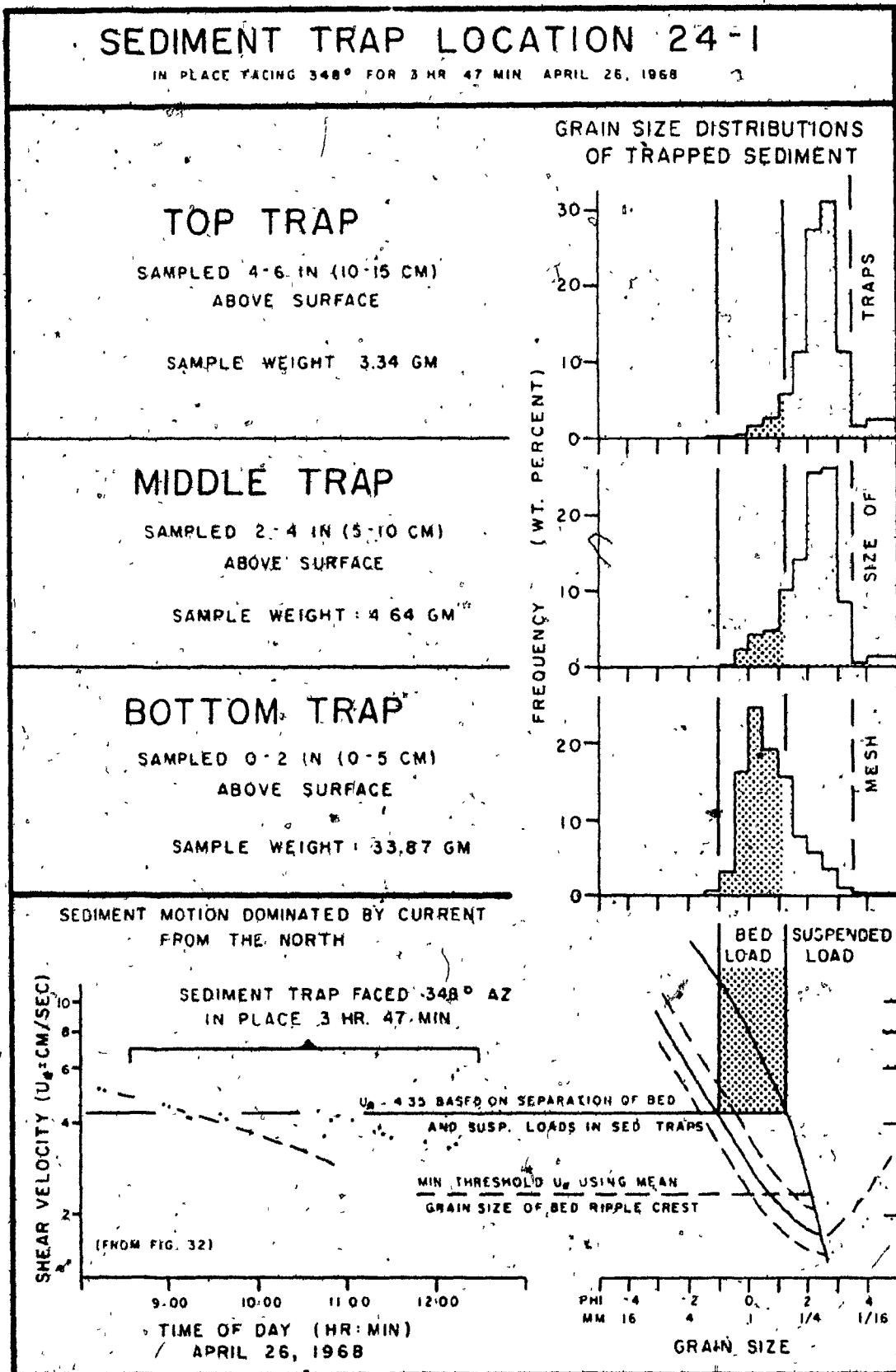


Fig. 33 Results of sediment trap 24-1 compared to transport competences of calculated shear velocities.

calculated shear velocity (4.80 cm/sec) acting while the trap was in place (Fig. 33). The maximum calculated shear velocity is capable of suspending grain sizes finer than 1.04ϕ (0.48 mm) in diameter. This upper grain size limit of the suspended load is equivalent to the 50th and 66th percentiles of the grain size distributions of the bed material ripple crest and bed material ripple trough samples respectively.

Sediment trap 24-2 was in place for 4 hours and 7 minutes facing into a waning northward flowing current. The results, in Figure 34, are similar to those of trap 24-1 and the two interpreted shear velocities are identical. The maximum calculated shear velocity of 4.74 cm/sec lies between the two interpreted shear velocities and is capable of suspending grain sizes finer than 1.08ϕ (0.47 mm) in diameter. This grain size is equivalent to the 60th and 67.5 percentiles of the grain size distribution of the bed material ripple crest and bed material ripple trough samples respectively.

Sediment trap 24-3 (Fig. 35) was in place for 1 hour and 8 minutes during which interval the northward flow decreased slightly from its maximum rate and wave action increased and became dominant.

If the waves had a 10 second period and a height of 2 feet as was likely, the bottom orbital velocity was approximately 43.8 cm/sec. From Figure 17, using the competence curve for a wave period of 10 seconds, this velocity is capable of moving grains finer than -0.56ϕ (1.45 mm). From Figure 16, shear

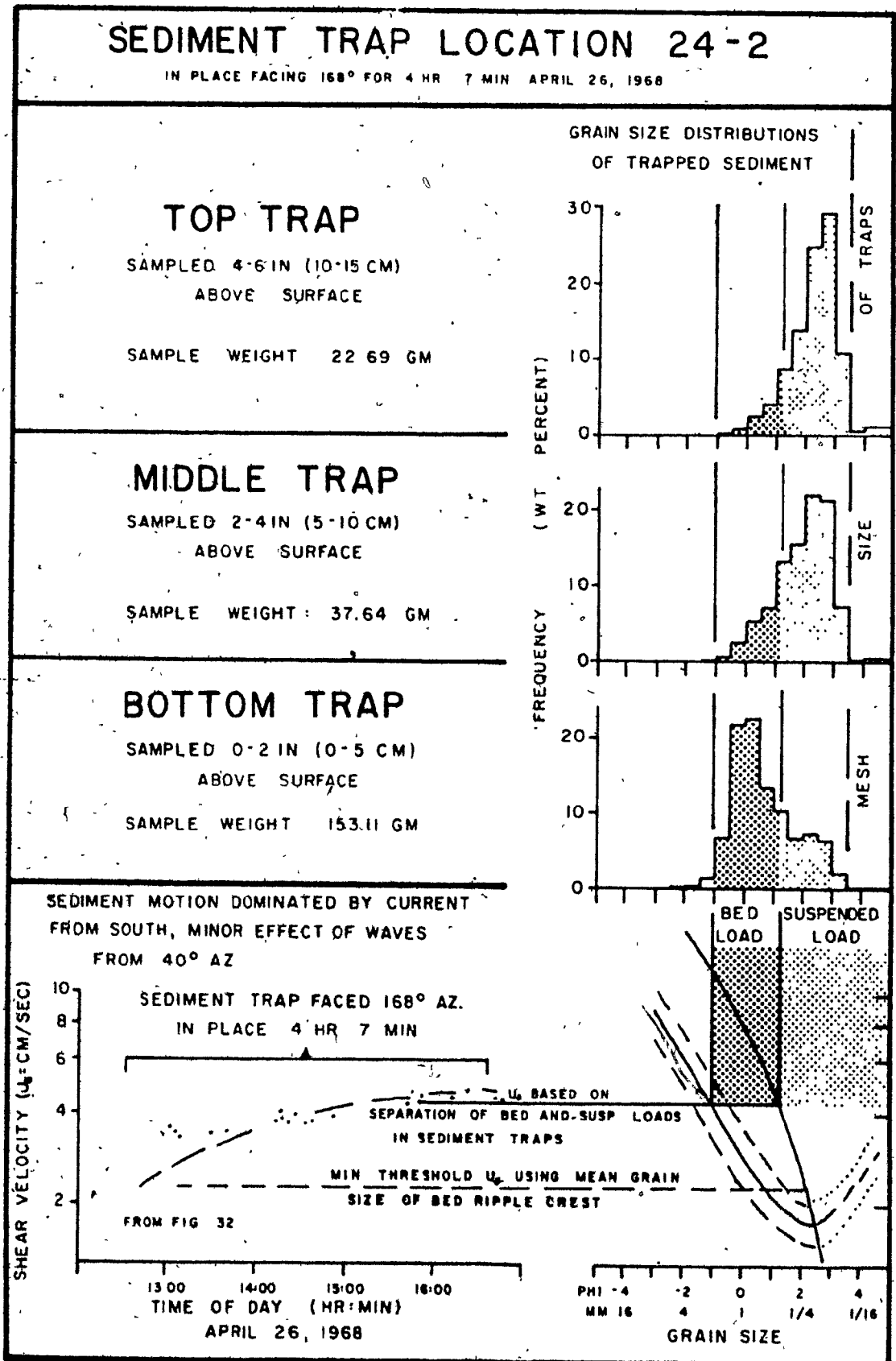


Fig. 34 Results of sediment trap 24-2 compared to transport competences of calculated shear velocities.

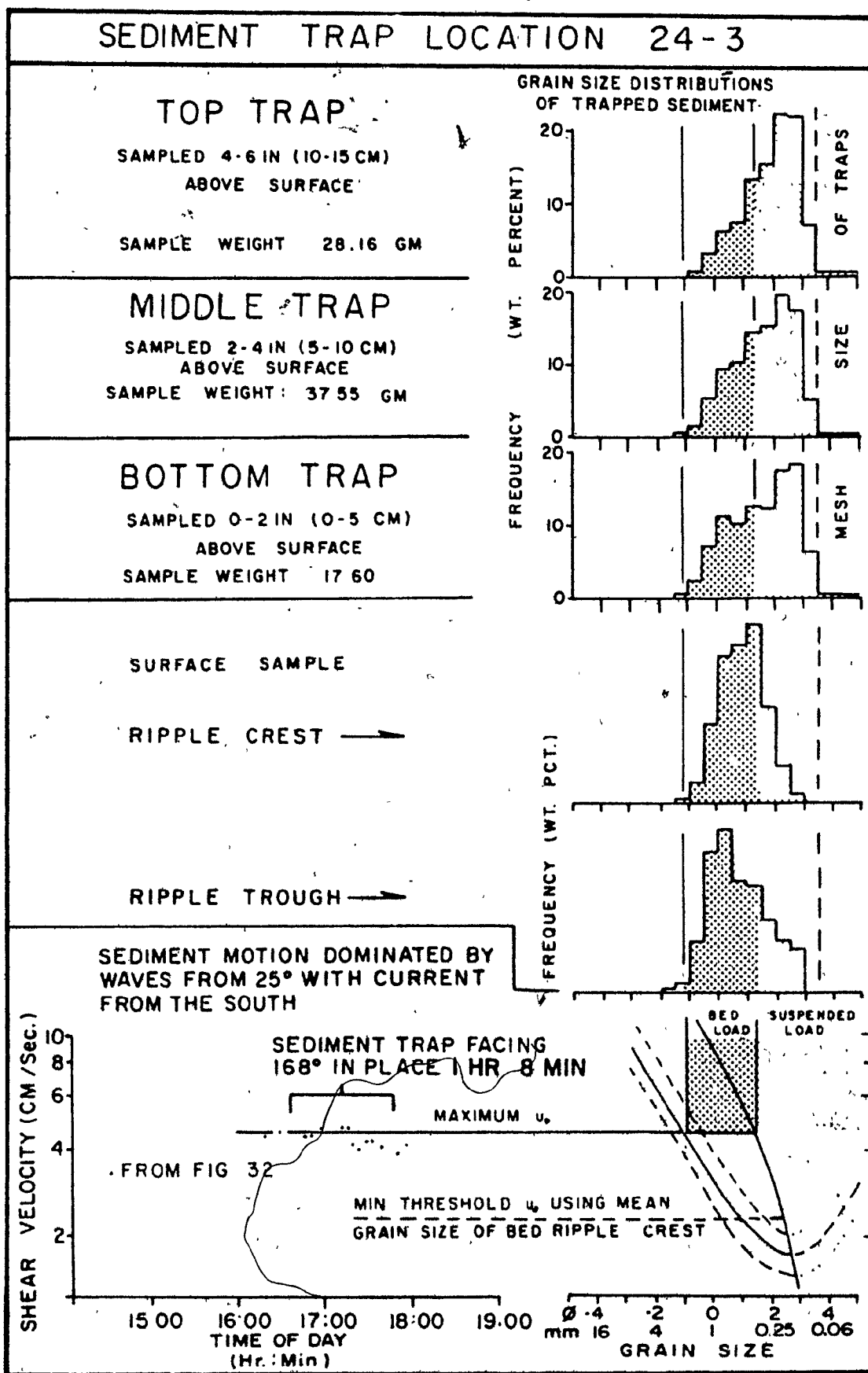


Fig. 35 Results of sediment trap 24-3 compared to transport competences of calculated shear velocities.

velocities of 3.60 cm/sec are required to move -0.56 phi (1.45 mm) size grains. The maximum shear velocity representing the sum of current and wave action would then be 6.01 cm/sec rather than 4.74 cm/sec.

However, a shear velocity of 4.74 cm/sec is already competent to move all but the very coarsest grains present in the bed material at location 24. The effect of a greater competence is to speed up the rate of transport. Another effect of the higher waves and greater competence may be observed in the increases in rate of trapping of suspended load relative to bed load (Fig. 35).

Rates of Sediment Trapping

Bleached, dry weights of samples collected in sediment traps 35, 75, 24-1, 24-2 and 24-3 are presented in Table A by half phi grain size intervals and by elevation above bottom. For a given sediment trap assembly these weights should be proportional to the concentration of sediment in transport at the sampled elevations, assuming non-interference of the traps with the flow.

The established and experimentally verified equation describing the concentration gradient of suspended sediment in equilibrium unidirectional flow is:

$$\frac{C_1}{C_a} = \frac{H - Z_1}{H - Z_a} \frac{Z_a}{Z_1} \quad W/Bk\alpha U^*$$

where C_1 is the concentration at elevation Z_1 above bottom of sediment size fraction with terminal fall velocity W , C_a is the concentration at an arbitrary reference elevation Z_a of the same

size fraction, H is total depth, B is a coefficient relating sediment diffusion coefficient to momentum diffusion coefficient, k_0 is the von Karman constant and U^* is the shear velocity (Briggs and Middleton, 1965, Brush, 1965). For a given equilibrium unidirectional flow condition the equation predicts a concentration gradient such that for each grain size fraction the concentration increases towards the bottom and finer size fractions have a more uniform distribution than coarser size fractions.

On the basis of the above, the weights of samples collected by each of the sediment trap assemblies should display the following trends:

- (1) Weights of total samples and of individual size fractions should decrease from the bottom trap to the middle trap to the top trap.
- (2) The ratio of weight of a given size fraction collected in a trap to the weight of the same size fraction in the underlying trap should increase for progressively finer grain size fractions.

It is obvious from Table A that the results do not uniformly follow the theoretical trends. In two of the five assemblies the weights of the total samples collected in the bottom traps are less than the weights of the total samples collected in the middle traps. In four of the five assemblies weights of individual size fractions collected in overlying traps are greater than the weights of the same size fractions collected in underlying traps. These inversions are greatest for the finer grain sizes and be-

TABLE A

WEIGHTS IN GRAMS OF SAMPLE COLLECTED BY EACH SEDIMENT TRAP - IN HALF PHI GRAIN SIZE INTERVALS AND IN TOTAL SAMPLE

< Sample weight in overlying trap is anomalously greater than sample weight in underlying trap.

NOTE: Trap openings 6" x 2" (15.2 x 5.0 cm)

SEDIMENT TRAP 24-1

\emptyset Mid Pt.	Bot. Trap	Mid. Trap	Top Trap
-1.75	0.01		
-1.25	0.21		<0.01
-0.75	1.12	0.01	0.01
-0.25	5.50	0.11	0.02
0.25	8.38	0.20	0.05
0.75	6.60	0.23	0.09
1.25	5.41	0.48	0.20
1.75	2.71	0.65	0.38
2.25	1.98	1.19	0.93
2.75	1.25	1.21	1.05
3.25	0.40	0.40	0.39
3.75	0.08	0.02	<0.05
Total	33.87	4.64	3.34

SEDIMENT TRAP 7-5

\emptyset Mid Pt.	Bot. Trap	Mid. Trap	Top Trap
-2.25		<0.01	
-1.75	0.70	0.10	0.06
-1.25	3.61	0.32	<0.41
-0.75	6.59	2.11	1.30
-0.25	9.10	4.00	2.50
0.25	7.39	5.68	3.89
0.75	5.39	<6.10	4.63
1.25	5.15	<7.39	6.48
1.75	2.44	<4.09	3.97
2.25	1.20	<2.05	<2.19
2.75	0.40	<0.80	<0.93
3.25	0.15	<0.39	<0.55
3.75	0.05	<0.15	<0.19
Total	42.25	33.47	27.50

SEDIMENT TRAP 24-2

\emptyset Mid Pt.	Bot. Trap	Mid. Trap	Top Trap
-2.25	0.17		
-1.75	0.43	0.01	
-1.25	2.09	0.08	
-0.75	10.37	0.29	0.10
-0.25	33.49	0.99	0.23
0.25	34.12	2.09	0.60
0.75	20.95	2.83	0.96
1.25	16.00	5.10	2.03
1.75	10.38	5.90	3.21
2.25	11.21	8.40	5.70
2.75	9.79	8.20	6.54
3.25	3.18	2.91	2.50
3.75	0.23	0.20	0.20
Total	153.11	37.64	22.69

SEDIMENT TRAP 35

\emptyset Mid Pt.	Bot. Trap	Mid. Trap	Top Trap
-1.75	0.01	<0.02	0.01
-1.25	0.07	0.03	0.01
-0.75	0.09	0.02	0.02
-0.25	0.16	0.10	0.05
0.25	0.20	0.19	0.06
0.75	0.29	<0.30	0.10
1.25	0.72	<1.01	0.30
1.75	2.10	<3.00	0.95
2.25	6.51	<8.29	3.31
2.75	9.30	<12.40	6.07
3.25	6.81	<8.65	5.20
3.75	1.78	1.55	1.51
Total	29.85	<37.64	19.84

SEDIMENT TRAP 24-3

\emptyset Mid Pt.	Bot. Trap	Mid. Trap	Top Trap
-1.75	0.01	0.01	
-1.25	0.08	<0.13	0.03
-0.75	0.40	<0.54	0.20
-0.25	1.30	<2.03	0.90
0.25	2.00	<3.61	1.75
0.75	1.80	<3.83	2.12
1.25	2.21	<5.39	3.78
1.75	2.15	<5.69	4.40
2.25	3.08	<7.30	6.23
2.75	3.21	<6.50	6.21
3.25	1.13	<1.99	<2.00
3.75	0.08	<0.17	0.15
Total	17.60	<37.55	28.16

tween bottom and middle traps. Also note that if there is an inversion in a given size fraction, other than the coarsest, the results of all finer size fractions are also inverted.

The discrepancies with theory are probably a result of the trap assemblies modifying the fluid flow. The trap assemblies may be considered as a semi-permeable barrier to the flow, the mesh of the collecting bags slowing and interfering with the flow through the traps. The streamlines of the non-random, non-turbulent component of the flow were partially deflected around and over the trap assemblies rather than being parallel to the bottom.

This introduction of a non-random upward vector to the fluid flow in front of the traps upset the random turbulence pattern on which suspended sediment transport theory is based. The grain size fractions most affected by the deviation in flow are those in suspended transport following the turbulent flow. Little or no effect should be expected on grain size fractions in bed load transport except where underscouring of the trap occurred and little or no bed load material was collected (as in sediment trap 35). Therefore, the data from the traps differentiating the grain sizes in bed load transport from those in suspended load transport remain valid but data concerning the rates of trapping or transport are suspect.

The occurrence in sediment trap 24-3 of inversion of the expected concentration gradient through virtually all collected size fractions and not just in the suspended size fractions is possibly a result of ~~list~~ developed by dominant oscillatory wave currents at the time of sampling.

For the reasons stated above, and since the results of only eleven temporally and spatially scattered sediment trap assemblies are available, no detailed analysis of variations and average sediment transport rates in Watering Bay are attempted. The results however, are presented in Table B as data to be considered in designing possible future studies: The rates of trapping, which vary from approximately 15 to 337 gm per 25 hour tidal cycle in a 6 inch cross-section from 0 to 2 inches above the bottom are minimum estimates of the rates of sediment transport by unrestricted flow. Rather than being part of a larger program, future studies should be specialized and pay more attention to the design of traps having a minimal influence on fluid flow and to a more systematic and representative sampling program with respect to variations in wind and sea states, tidal phases and seasons. They should also include observations of standing crop and sediment production rates at selected test sites on the barrier reef and patch reefs in order to compare these rates with the transport rates. On the basis of gross observations it is thought that in Watering Bay, seaward of the shoreward Thalassia beds, total sediment production and total sediment transport are equal, the bay being in hydrodynamic equilibrium.

Summary and Discussion of Sediment Trap Results

In general the grain size distributions of the samples collected by the sediment traps are significant in that they correlate with grain size ranges defined by maximum calculated shear and shear velocity-grain size competence curves. Also

TABLE B RATES OF SEDIMENT TRAPPING

Sediment Trap	Time in Place (min)	Rates (a, b, c) Between Given Elevations			
		0-2"	2-4"	3-5"	4-6"
		0-5 cm	5-10 cm	7.6-12.7cm	10-15 cm
1 24-1	227	(a) 8.95	1.23		0.88
26/4/68	(1)	(b) 13.11	1.80		1.68
1 24-2	247	(a) 37.19	9.14		5.51
	(2)	(b) 40.47	9.95		6.00
1 24-3	68	(a) 15.58	33.23		24.92
	(3)				
* 33	3000	(a) 1.65		0.64	
6/8/67	(4)	(b) 4.85		1.91	
		(c) 41.23		16.20	
* 34	3000	(a) 13.46		11.32	
6/8/67	(4)	(b) 39.61		33.29	
		(c) 336.62		282.97	
* 35	3000	(a) 0.60	0.75		0.40
14/4/68		(b) 1.76	2.22		1.17
		(c) 14.93	18.82		9.92
* 61	3000	(a) 2.62	1.87		1.28
11/4/68		(b) 7.71	5.49		3.77
		(c) 65.51	46.70		32.05
* 71	1500	(a) 4.00		4.09	
5/8/67	(5)	(b) 11.77		12.04	
		(c) 100.05		102.30	
* 72	1500	(a) 8.70		5.11	
5/8/67	(5)	(b) 25.58		15.04	
		(c) 217.47		127.81	
73	1500	(a) 3.82		1.20	
5/8/67	(5)	(b) 11.23		3.52	
		(c) 95.49		29.95	
75	1500	(a) 1.69	1.34		1.10
10/4/68		(b) 4.97	3.94		3.24
		(c) 42.26	33.47		27.50

- 1 Strong effect of long period waves from a northerly direction.
- * Traps tilted or underscoured at time of retrieval.
- (1) Only trap measuring transport towards the south.
- (2) Waxing current - full range of velocities to north.
- (3) Waning current - full range of velocities to north.
- (4) In place at same time - time period includes half hour with strong wind and whitecaps in Watering Bay.
- (5) In place at same time - no unusual conditions.
- (a) Average rate of trapping over time in place (gm/hr).
- (b) Average rate of trapping during effective transport (gm/hr).
- calculated on basis of 8.5 hours effective transport per 25 hour tidal cycle.
- (c) Amount trapped during one tidal cycle (gm/25 hr).

there appear to be fairly consistent relationships between the grain size distributions of the bed materials, hydrodynamic parameters and maximum shear velocities.

However, the sediment traps interfered with fluid flow and collected less sediment than the amount transported by unrestricted flow. Therefore sediment trapping rates cannot be used to estimate transport rates confidently.

Specific observations relating velocity and bottom shear of the tidal currents, the competence curves and grain size distributions of trapped samples and of bed samples are:

(1) Roughness lengths, extrapolated from measured current velocity profiles are of the order 0.4 to 2.4 cm. These values are equivalent to grain size diameters within the first half phi size interval coarser than the coarsest grains in the main mode of bed sample grain size distributions. A comparable range of roughness lengths (0.1 to 1.8 cm) is reported by Inman (p. 122, in Shepard, 1963) on the basis of data from several sources. No information was given concerning grain size distribution or bottom roughness elements. Sternberg (1968) calculated roughness lengths for approximately 140 measured velocity gradients in hydrodynamically rough flow over a wide variety of bottom types in tidal channels off the state of Washington. Grouping all the data, he derived a mean roughness length value of 0.07 cm and 95% confidence limits of 1.06 and 0.0006 cm. No correlation was observed between roughness lengths and the bed roughness elements or grain sizes. Mean grain sizes during Sternberg's (1968) study

varied from 4.02 to -0.12 phi and boundary roughness in the form of gravel or ripples varied from heights of 2 to 10 cm.

Sternberg's (1968) mean value of roughness length was considerably less than the values obtained in this study. However, use of his value ($Z_0 = 0.07$ cm) with the Carriacou velocity data leads to shear velocities incapable of transporting the sediments that were observed to be in transport.

(2) Calculated maximum shear velocities resulting from tidal currents near spring tides at three locations in Watering Bay varied from 2.5 to 7.0 cm/sec. Adding a correction factor for wave action at one location (24) produces a range of maximum shear velocities from 4.0 to 7.0 cm/sec.

(3) A grain size separating bed load from suspended load can be selected on the basis of the grain size distributions of sediment collected in sediment traps at different heights above bottom. Using this grain size and the shear velocity-grain size competence curves a shear velocity may be derived which corresponds closely with the measured maximum shear velocities as follows:

- (a) Sediment trap 35, measured maximum shear velocity 4.0 cm/sec versus 3.7 cm/sec from grain sizes and competence curves.
- (b) Sediment trap 75, measured maximum shear velocity 7.0 cm/sec versus 6.4 cm/sec from grain sizes and competence curves.

(c) Sediment trap 24, measured maximum shear velocities of 2.47 (current) + 2.33 (waves) = 4.80, versus 4.35 from grain sizes and competence curves.

(4) Also on the basis of the competence curves, the maximum grain sizes transportable in bed load by the above shear velocities correspond closely to the maximum grain sizes collected in the bottom traps at the sediment surface.

(5) On the basis of one observation at location 35, the representative grain size, with respect to the competence curves and threshold of movement, is the 28th percentile of the bed material grain size distribution. This is in keeping with the theory that the representative grain size should vary from the mean grain size for very well sorted bed materials towards the coarse tail for poorly sorted bed materials.

(6) The grain size boundary between bed and suspended loads (from 3 above) corresponds to a narrow range of percentiles of the bed material grain size distributions as follows:

- (a) Sediment trap 35: 65th percentile (based on suspended grain size and maximum calculated shear velocity).
- (b) Sediment trap 75: 72nd (based on suspended grain size) and 67th percentile (based on maximum shear velocity).
- (c) Sediment trap 24: 69th and 72nd (based on suspended grain size); 50th and 66th (based on maximum shear velocity); and 51st and 62nd (based on maximum grain size in bottom trap). Above pairs of percentiles are for ripple crest and ripple trough samples respectively.

The average boundary percentile is the 64th percentile.

BED MATERIAL GRAIN SIZE DISTRIBUTIONS AND
SEDIMENT TRANSPORT IN WATERING BAY

For the three sediment traps discussed in detail above, the grain size separating bed load from suspension load transport ranged from the 50th to the 72nd percentile (average 64th percentile) of the bed material grain size distributions. In order to evaluate whether this was generally true in Watering Bay, the grain size histograms of all analyzed sediment trap and corresponding bed samples are plotted in Figure 36 and the 64th percentiles of the bed sample grain size distributions indicated as the boundary between bed and suspended load.

Plotting the above grain size boundary on the competence curve for transport in suspension (Fig. 16) defines a shear velocity which allows definition, on the competence curve for transport in traction, of the maximum grain size in bed load transport. These values are also indicated in Figure 36 to define a bed load grain size range.

Of the eleven sediment traps at nine locations, only four (at locations 24 and 75) collected a sample which can be related to the bed load. These were discussed in detail above. The remaining assemblies, excepting those at locations 72 and 73, were tilted or underscoured, and sampled the suspended loads only.

On the basis of the suspended load grain size distributions (collected in the middle and top traps) and the maximum grain sizes present on the surface, the use of the 64th percentiles of the surface sample grain size distributions as the grain size

SEDIMENT TRAPS WATERING BAY

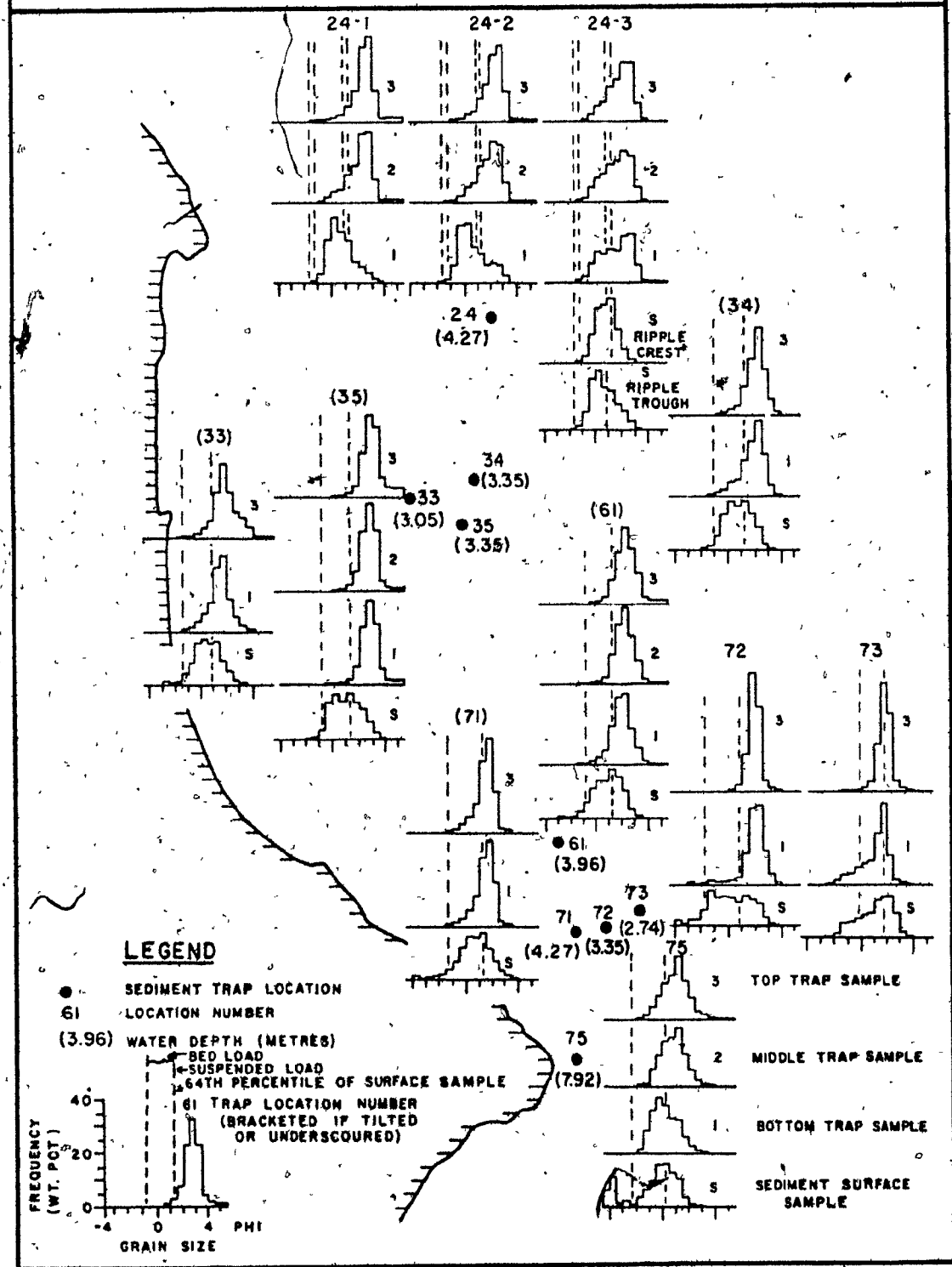


Fig. 36 Sediment trap and surface sample grain size distributions for all traps, Watering Bay.

boundary between suspended and bed load transport appears to be reasonable.

The trap assemblies at locations 72 and 73 were not tilted or underscoured. At location 72 the use of the 64th percentile as the suspended/bed load transport grain size boundary is consistent with the grain size distributions of the surface sample and of the upper trap sample. No explanation can be made as to why the bottom trap sample did not consist mainly of grain sizes in the interpreted bed load range since these grain sizes were available on the bottom. The grain size distribution of the bottom trap sample is similar to that of the upper trap sample except for a larger coarse tail.

At location 73 the 64th percentile of the bed material grain size distribution corresponds to the mode of the upper trap sample at 1.75 phi. On the basis of the trap sample grain size distributions a boundary between suspended and bed load grain sizes is selected at approximately 0.75 phi, which is the 37th percentile of the bed material grain size distribution. Location 73 was within 100 feet (30 m) of the back edge of the reef crest where the bottom was more affected by waves than by currents. The bottom was symmetrically rippled parallel to the reef crest, but weak currents and current lineations parallel to the crest were observed. The sediment trap was emplaced facing southwards into the current. The relative scarcity of bed load grain sizes compared to suspended load grain sizes in the bottom trap may be a similar effect to that observed in sediment trap assembly 24-3 where wave transport was dominant also.

Excluding the results at location 73, the use of the 64th percentiles (ranging from 0.22 to 1.42 ϕ) of bed material grain size distributions at eight widely separated locations of varying depth (10 to 26 feet) as the boundary between suspended and bedload grain sizes is consistent with the grain size distributions of sediment trap samples at those locations (Fig. 36).

On the basis of the sediment trap and current measurement results, it is suggested that in areas affected by tidal currents in Watering Bay current velocities may be derived from the grain size distribution of the bed material, the known water depth, the competence curves and the von Karmen-Prandtl equation.

The boundary between bed load and suspended load transport is derived from the 64th percentile of the bed material grain size distribution. This value is entered into the competence curve graph (Fig. 16) to derive a shear velocity (u_*) which is equivalent to the maximum shear velocity affecting the bottom during a spring tidal cycle. Roughness length (z_0) is set equal to the mid-point of the half phi grain size interval coarser than the coarsest grains in the bed material sample. These values are substituted in the von Karma-Prandtl equation:

$$\bar{u} = \frac{u_*}{0.4} \ln \left(\frac{z + z_0}{z_0} \right)$$

to obtain the mean average current velocity (\bar{u}) at any height (z) above bottom.

The above procedure was used for all samples in Watering Bay and outside the reef to give estimates of maximum current velocities during spring tides at a depth of five feet. A depth of

five feet was chosen because actual current measurements in more locations were made at that depth than at any other depth during this study and can be compared to the calculated velocities. Measured and calculated values are presented in table form in Appendix III and in map form in Figure 37.

Figure 37a is an index map of bathymetry and locations of all samples in the Watering Bay area. The sixty-fourth percentiles of their bed sample grain size distributions are mapped in Figure 37b. Not surprisingly the map pattern is similar to that for mean grain size (Fig. 10a). Coarsest values occur outside the reef, in the immediate back reef and in the channel north of Point St. Hilaire. Finest values occur in the shoreward Thalassia beds and in deeper water north of the bay.

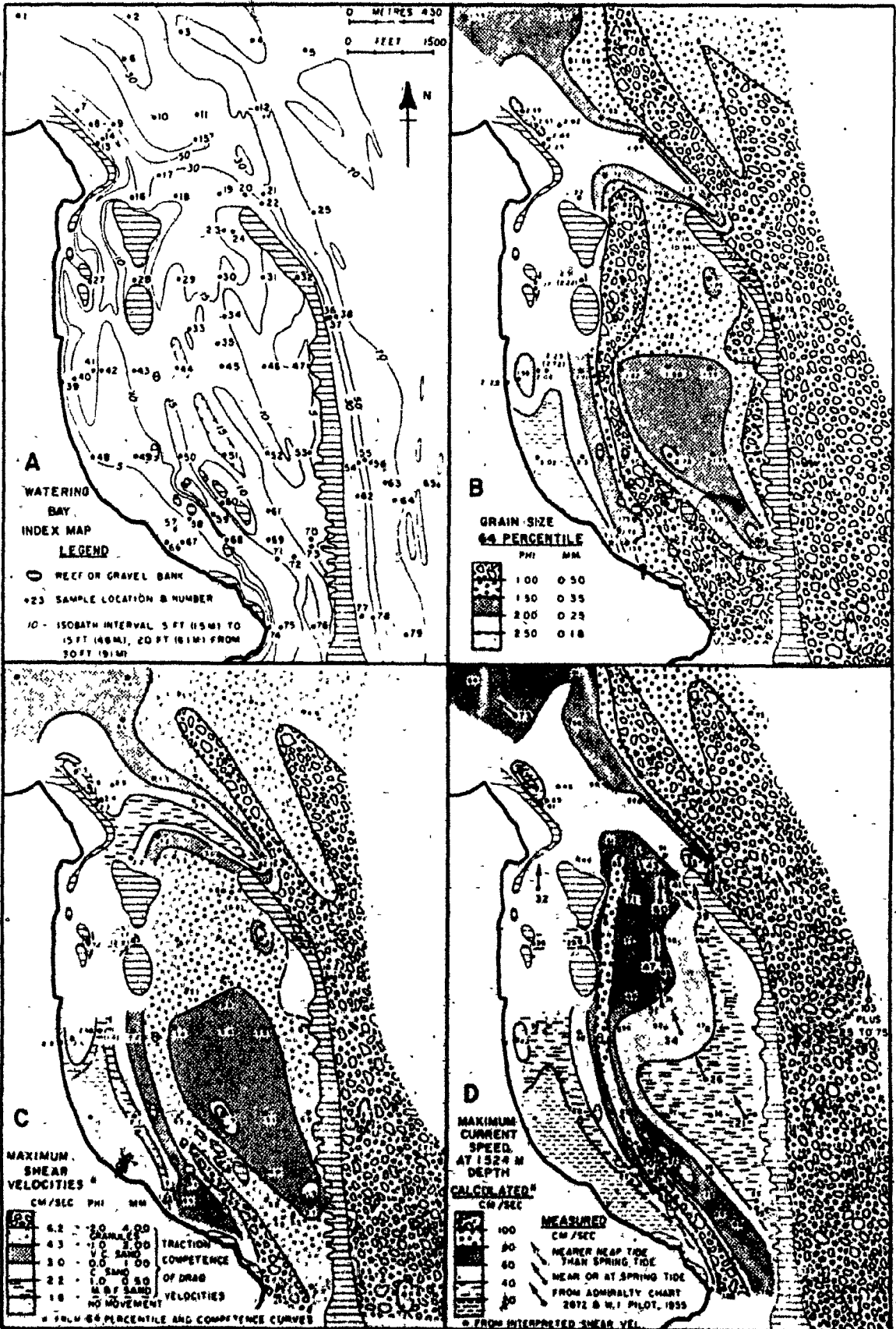
The map pattern of interpreted shear velocities in Figure 37c is similar; high shear velocities corresponding to the coarser 64th percentile values and low shear velocities corresponding to finer values.

The map pattern of calculated maximum current speeds at 5 feet depth in Figure 37d is also similar except for a decrease in values from the central bay to the back-reef. This is because, in the shallower water depths of the immediate back-reef, lower flow velocities are required to develop a given shear velocity.

Figure 37d may be used as a check on the accuracy of the method by considering volumes of flow, bathymetry and the mapped flow pattern and by comparing actual current speed measurements with those calculated at the site of the nearest bed sample.

If a given constant volume of water moves north or southwards through Watering Bay then the flow speed should increase where the east-west sectional area of the water in the bay decreases and decrease where the east-west sectional area of the water increases. Changes in the sectional area result from variations in the width and depth of the bay. The highest current speeds are mapped to the east and just north of Point St. Hilaire at the southern end of the bay, where the constriction between the barrier reef and land is greatest. The constriction is so great that the east-west sectional area has been enlarged by scouring and maintenance of a channel. In the central part of the bay, where constriction of flow is least, the velocity of flow is least. To the north the flow is again constricted between the barrier reef and the shoreward patch reefs resulting in flow speeds greater than those in the central part of the bay. The high speeds continue northward for a short distance beyond the constriction until water depth increases and velocity decreases correspondingly. At the north end of the map, flow speed increases again, joining the more rapid flow outside the reef. "Shadow zones" of low speed flow exist immediately north of the barrier reef and the shoreward patch reefs. The mapped variations in flow speed (Fig. 37d) are reasonable and expected assuming constant volume of flow through a varying cross-sectional area.

Rough estimates of average east-west sectional areas and average northward flow speeds lead to a flow rate of 1.5 to 1.8 $\times 10^3$ m^3 /sec through a given section. The volume of Watering Bay is approximately 8.8×10^6 m^3 . Therefore, during northward tidal



Page 009

flow the residence time of water in Watering Bay is 82 to 98 minutes or roughly 1.5 hours. Therefore, as stated above, it is unlikely that particles put into suspension in Watering Bay came to rest, but are flushed into deeper water within one tidal cycle.

The calculated flow velocities are interpreted to represent maximum flow velocity affecting the bottom. Therefore, they will be compared only with maximum velocities measured near or at spring tide. The eight such measurements (Fig. 37d) are listed below and compared with the calculated velocities at the nearest bed sample locations which are in comparable positions relative to channels, reef, etc.

<u>MEASURED VEL. (cm/sec)</u>	<u>NEAREST SAMPLE LOC. (Distance)</u>	<u>CALCULATED VEL. (cm/sec)</u>	<u>DIFFERENCE (cm/sec)</u>	<u>DIFFERENCE (%)</u>
32	27 (310m)	36	+4	+12.5
71	29 (260m)	77	+6	+ 8.4
60	23 (70m)	66	+6	+10.0
41	24 (0m)	73	+32	+78.0
39	31 (180m)	35	-4	-10.3
165	25 (190m)	115	-50	-30.3
51	35 (0m)	51	0	0
105	59 (40m)	107	+2	+ 1.9

The speeds interpreted and calculated from the grain size distributions of the bed samples differ from the measured speeds by +78.0% to -30.3% (average \pm 18.9%). Ignoring the speed and sample at location 24, where detailed analysis above demonstrated

a strong wave effect, and the speed and sample (25) outside the reef, the range of differences is +12.5% to -10.3% (average +7.1%).

Therefore, not only is the mapped pattern of calculated flow speeds reasonable on the basis of bathymetry and flow restriction, but the actual calculated values in Watering Bay are a close approximation of the measured flow speeds except where there is a strong wave influence. In Watering Bay the grain size distributions of bed samples may be used in conjunction with the competence curve and the von Karman-Prandtl equation to estimate the maximum shear velocity and flow speed affecting the bottom.

While the map of maximum current speeds (Fig. 37d) serves to delineate the pattern of water flow in Watering Bay, the map of shear velocities (Fig. 37c) serves to delineate sediment transport and possible depositional patterns, since shear velocity is a measure of bottom shear stress and sediment transport competence of the currents.

Not surprisingly the lowest shear velocities (1.0 cm/sec - no transport) were obtained for samples 48 and 66 in the shoreward Thalassia beds where currents were observed to be weak and Thalassia protected the bottom. However, the technique employed above to arrive at shear velocity values assumes equilibrium of the bottom sediment grain size distribution with the current flow. This is not necessarily so in an area where the currents are too weak to move any bottom sediment. In a carbonate sediment area, locally highly productive organisms such as Halimeda or gastropods may develop a bottom deposit much coarser than would be expected from the hydrodynamic regime. In particular this might be the case for sample 67 from a Thalassia bed in which currents

could have little effect on bottom. The grain size distribution of the sample however, leads to the interpretation of a current acting with a shear velocity of 3.5 cm/sec. Therefore interpreted shear velocities incapable of moving any sediment ($u_* < 1.8$ cm/sec) do indicate no sediment transport, but cannot be used to calculate a flow velocity. Also, interpreted shear velocities capable of moving fine and medium sand ($u_* = 1.8-2.2$) should be suspect unless there is corroborating sedimentary structural or other evidence of sediment transport, since they may be a result of in situ growth and breakdown of organisms.

Another problem with the shoreward Thalassia bed samples is the occurrence of 'blowouts' where storm waves have stripped away the Thalassia cover and removed finer grain sizes. The grain size distributions of the bottom sample truly reflects a hydrodynamic regime stronger than is usually associated with Thalassia beds, but it is a wave regime. Sample 57 ($u_* = 3.0$) was taken from the floor of a blowout. If blowouts migrate the entire deposit underlying a Thalassia bed may be reworked. The resulting coarse grain size distribution will not be indicative of the deposit's origin in a Thalassia bed (Patriquin, 1973).

The only other samples to indicate non-transport were samples 7 and 8 ($u_* = 1.5$ cm/sec) which were collected from a water depth of 38 feet in a trough between the northern fringing reef crest and a seaward reef ridge rising to a depth of 30 feet. These sample sites were protected from all directions and lie in a local depositional area.

In Watering Bay, just beyond the line of shoreward patch reefs, the pattern of interpreted shear velocities in Figure 37c shows a 'stream' of high sediment transport competence extending from Point St. Hilaire to the north end of the bay. Lowest shear velocity value along this trend is 5.3 cm/sec which theoretically is capable of transporting grains up to -1.8ϕ (3.3 mm) in diameter (granules). Seaward, within the main part of the bay the interpreted shear velocities are between 3.0 and 4.3 cm/sec (capable of transporting very coarse sand). In the northern part of the bay shear velocities are between 4.3 and 6.3 cm/sec (capable of transporting granules).

SUMMARY AND MODEL OF SEDIMENT TRANSPORT AND DEPOSITION IN WATERING BAY

Sediment transport and deposition in Watering Bay is dominated by unequal reversing tidal currents. Waves normally affect bottom only immediately behind the barrier reef and in shoreward shallow water areas.

Observed normal weather waves in the bay had average periods of 2 to 2.5 seconds and estimated heights of 1 to 1.5 feet (0.3 to 0.46 m). Occasionally longer, higher wave sets are observed to enter the bay from the north. These waves are probably north-easterly ocean swell which has been attenuated by small islands and banks to the northeast.

Semi-diurnal tides are dominant and the tidal range is approximately 1.5 feet (0.46 m) between high high water and low low water levels. Maximum tidal current flow to the south is at

or near low water and to the north is at or near high water. Current velocities are greatest near spring tides and least near neap tides. Within Watering Bay current velocities decrease from the centre of the bay towards the shore and towards the barrier reef. A variable non-reversing north flowing current causes the north flowing currents in the bay to be faster and of longer duration than south flowing currents. When tidal currents are weak, around neap tide, there may not be a period of flow towards the south.

During times of flow towards the north water enters the bay over the reef and through the channel off Point St. Hilaire at the south end of the bay. The flow accelerates towards the north and passes out of the bay through the open north end where it joins the strong westward flow between Carriacou Island and Union Island (4 miles north). Observed current flow in Watering Bay is turbulent (Reynolds No. > 600) and tranquil (Froude No. < 1).

Cloth mesh sediment traps, stacked above one another on the bottom; were used to sample grain size distributions of sediment in bed load and suspension transport. Current measurements, at or near three of the sediment traps, were used to calculate shear velocities. The grain size distributions of the samples collected in the sediment traps correlate well with grain size ranges defined by maximum calculated shear velocities and the shear velocity - grain size competence curves for unidirectional flow. Also there are fairly consistent relationships between the grain size distributions of surface sediment samples, hydrodynamic parameters and maximum shear velocities.

From the results of the three sediment trap experiments for which there were current measurements, and compatible with the results of six other sediment trap experiments for which there were no current measurements, the important relationships are:

- (1) Roughness lengths are equivalent to grain size diameters within the first half phi grain size interval coarser than the coarsest grains in the main grain size mode of the surface sediment samples.
- (2) Grain size boundaries between traction and suspended load transport can be defined by the grain size distributions of the trapped samples and by using the calculated maximum shear velocities and the competence curve for suspended transport. The boundaries correspond to a narrow range of percentiles of the corresponding surface sediment samples (59th to 69th percentiles; average 64th percentile).

In areas where sediment is transported by currents the 64th percentile of the grain size distribution of any surface sediment sample can be used with the competence curve for transport in suspended load (relationship 2 above) to define a maximum shear velocity. A roughness length value can be obtained equal to the mid-point of the half phi grain size interval coarser than the coarsest grains in the surface sediment sample (relationship 1 above). The values of shear velocity (u_*) and roughness length (Z_0) can be substituted in the von Karman-Prandtl equation,

$$\bar{u} = \frac{u_*}{0.4} \ln \frac{Z + Z_0}{Z_0}$$

to obtain the mean average current velocity (\bar{U}) at any height (z) above bottom. If the water depth (h) is known, the velocities at any depth ($h-z$) can be determined.

The above procedure was followed for all surface sediment samples in Watering Bay. Maps were constructed showing maximum shear velocity and maximum current velocity at 5 feet depth. Ignoring samples from areas strongly affected by waves and from Thalassia beds, the resulting map patterns of flow are consistent with what would be expected given the flow volumes and bathymetry of Watering Bay. Also, maximum velocities, calculated by the above procedure, differ from nearby measured maximum velocities by only +12.5 to -10.3%. The calculated velocities are therefore close approximations of actual velocities where the sediment surface is controlled by currents.

In the ancient record the above procedures could conceivably be used on reef associated deposits with primary sedimentary structures indicating the action of currents. Maps of paleo-shear velocity would delineate patterns of sediment transport and allow extrapolation to locate depositional areas (deeps) and source areas (reefs).

Watering Bay is essentially a sediment bypass area except in the shoreward beaches, mangroves, shoreward Thalassia beds and patch reefs. Progradation of these environments could eventually lead to filling most of the bay to sea level.

Sediment supplied by the barrier reefs to the bay are in equilibrium with the currents. The grain size distributions of the bed materials accurately reflect the sediment transported in

bed load by the currents and are not deposited except temporarily. Only a rise in relative sea level or increase in size of material supplied by the barrier reefs would result in deposition in most of Watering Bay. Then, when sufficient deposition had taken place to constrict the tidal flow and increase the tidal current shear velocities sufficiently to be competent, the equilibrium would be re-established (at the original water depths if a sea level rise occurred, and at shallower water depths if there had been an increase in grain size).

The only important site of sediment deposition in the immediate area is on the slope into deep water at the north end of the bay. The expected depositional pattern is of a slowly northward prograding sand body with increasingly fine grain sizes towards its base. This possibility is supported by the bathymetric shape of the slope which is broadly lobate northward out of the centre of the bay (Fig. 4) and by the general pattern of increasing fineness of sample grain sizes down the slope (Fig. 10A).

With the present reef configuration however, it is doubtful that sand deposition could extend much further to the north. The area is swept by strong tidal currents from outside the reef as they swing towards the west around the north end of Carriacou. If the barrier reef crest were to extend northward it would offer the protection from these currents that would be necessary for sand deposition to progress northward. This may actually be happening. The outer edge of the north end of the back-reef sand body is a coral rubble bank, with abundant growing massive corals.

mainly of various Diploria species (Fig. 5). This bank development may be the precursor of full reef development. Thus depositional prograding of sand northward beyond the edge of the reef provides a shallow environment necessary for coral boulder bank development and possibly eventual full reef development which would then provide the necessary protection for further depositional progradation to the north.

The rate limiting factor to this process is probably the rate at which the reef can be extended. Most of the sediment presently being swept from Watering Bay does not come to rest on the slope but is caught up by strong currents from outside the bay and removed from the area.

CHAPTER 7 - SUMMARY AND GENERAL MODEL OF
REEF SEDIMENT TRANSPORT AND DEPOSITION

Carriacou, W.I. ($12^{\circ}30'N.$ Lat.: $61^{\circ}26'W.$ Long.) is a small island ($13 \text{ mi}^2 - 33.7 \text{ km}^2$) on the Antilles Ridge. Bedrock consists of Upper Eocene to Pliocene volcanic tuffs and organic limestones dipping gently to the southeast. The climate is relatively dry and there are no permanent streams on the island.

Carriacou lies within the belt of constant Northeast Trade Winds. Winds and waves of late autumn and winter are mainly from the northeast while those of spring and summer are more easterly.

The area of study included the barrier coral reef and back-reef areas, extending for one-quarter to one and one-quarter miles (0.4 to 2.0 km) offshore and for approximately 4.7 miles (7.5 km) along the east coast. The back-reef area is divided into three bays. The middle bay (Jew Bay) half way up the coast is the smallest of the bays. The study concentrated on the contrasting bathymetry, environments, hydrology and sediment transport patterns of the northern (Watering) and southern (Grand) bays. No previous similar studies of this or other areas have been made.

Grand Bay is more exposed, larger, deeper and has larger waves than Watering Bay. The bottom of Watering Bay is scoured by strong, dominantly semi-diurnal, reversing tidal currents, which were not observed in Grand Bay.

In general, the flora and fauna of reef and reef associated environments are not significantly different than those described in other Caribbean reef areas. However, the above differences in size, exposure, bathymetry and hydrology cause differences in development and character of many environments in the two bays as follows:

- (1) Beaches in Grand Bay are well developed and are composed of carbonate sand transported shoreward by waves. Beaches in Watering Bay are poorly developed and are composed mainly of black, terrigenous sand transported to the shore by ephemeral streams and sheet wash during rain storms.
- (2) Shoreward Thalassia beds have a much more extensive and varied associated flora and fauna in Grand Bay than in Watering Bay.
- (3) The unstable sand substrate in Grand Bay is transported shoreward from the barrier reef into the deeper lagoon by secondary waves. That in Watering Bay is transported mainly laterally by strong tidal currents.
- (4) Nearly half of Grand Bay, between the shoreward Thalassia beds and the barrier reef, is deeper than 20 feet (6.1 m) and is floored by stable sand which is not moved by normal waves. Stable sand substrate is uncommon in Watering Bay and occurs mainly in small areas associated with the shoreward Thalassia beds behind Grand Cay.
- (5) A back-reef radial zone is well developed on the landward side of the barrier reef crest only in southern Watering Bay and in Grand Bay.

The main sources of bioclastic carbonate sediments east of Carriacou are the barrier reefs. Maps and scatter plots of the statistical parameters of grain size distributions of sediment samples are consistent with the relative intensities of waves and currents as determined by seabed surface features and direct observations. Used in conjunction with one another, the maps and scatter plots allow some general interpretations of sediment transport and deposition.

A much fuller understanding of sediment transport and deposition was obtained by considering the grain size distributions as mixtures of log normal populations represented by cumulative curves or histograms rather than by derived numbers. Use of populations allows interpretation of the complete grain size distributions as responses to processes, for which there is a considerable fund of theory and experimental data.

Sediment transport in Grand Bay is dominated by waves crossing the back-reef unstable sand flat. Increasing mean grain size and coarse skewness of grain size distributions of sediment samples across the back-reef flat away from the reef attest to the transport and progressive winnowing effects of the waves. The finer grain sizes winnowed from the flat come to rest in the deeper water stable sand environment of central Grand Bay.

To progress beyond the above interpretation it was necessary to consider the sampled grain size distributions as mixtures of basic log normal grain size distributions. Determination of the grain size distributions of different types of

organic constituents in three representative samples demonstrated that the basic populations are not a result of organic skeletal structural units controlling the grain sizes of the products of abrasion and breakage.

By comparing the basic grain size component populations with competence curves for transport by waves and the competence of the observed waves, the following model of reef sediment transport and deposition in Grand Bay was developed (see Figs. 22 and 23).

During observed normal weather conditions, waves in Grand Bay have periods of 4 to 5 seconds and heights of 1 to 2 feet (0.3 to 0.6 m). These waves are capable of transporting grain sizes finer than 0.43 phi (0.74 mm) in 12 feet (3.6 m) of water. Grain size component population I (\bar{x} = -0.7 to -0.25 phi; σ = 0.72 to 0.85 phi), occurring as the coarse mode of bimodal reef and back-reef ripple trough samples, is not transported. Component population II (\bar{x} = 1.05 to 1.40 phi; σ = 0.75 to 0.95 phi) is transported slowly by rolling and sliding and is organized into ripple crests on the back-reef sand flat. Those grains that reach the steep slope between the back-reef and the deeper water stable sand (lagoon) are deposited as part of the subordinate coarse grain size population of the bimodal slope deposits.

Population III (\bar{x} = 1.80 to 2.10 phi; σ = 0.59 to 0.70 phi) is transported rapidly across the back-reef flat as bouncing (saltating?) traction load. It is present as a transitory population in the back-reef flat ripple trough samples and as the main grain size mode of the slope deposits.

Population IV (\bar{x} = 3.15 to 3.20 phi; σ = 0.45 to 0.66 phi) is transported most rapidly across the back-reef flat, probably in suspension. The population is not recognized in bottom samples of the reef and back-reef flat environments.

Down the slope, progressively more and finer portions of population IV are mixed with population III to produce an inverse grain size grading in the fine mode of the slope deposits. Most of population IV comes to rest as the fine grain size mode of the bimodal sands of the stable sand (lagoon) environment (Figs. 22 and 23).

During storms, which were not observed, grain sizes finer than approximately -1.15 phi (2.2 mm) are transported from the reef and across the back reef flat (Fig. 22). Component population I forms the coarse grained portion of the traction load. At the top of the steep slope, which is at or near the angle of repose for finer grain sizes, the coarse grain fractions of population I roll to the bottom where they form a discontinuous bottom-set deposit of the shoreward prograding back-reef sand body (Fig. 23). Clogging of population I on the slope may occur to produce a coarse grained storm cross-set bed in the sand body. During the waning stages of a storm population I is deposited on the top of the back-reef flat where it forms the coarse grain size mode of the normal weather ripple trough samples.

Population II, in the normal wave ripple crests, is the most exposed grain size population on the back-reef flat, at the start of a storm and is rapidly transported across the back-reef flat as the finest portion of the bed load. It is

swept down the slope into deeper water where storm waves are still capable of distributing it as the coarse fraction of the traction load (Fig. 22). It forms the coarse grained component population of the bimodal lagoonal deposits. Biogenic reworking of the lagoonal deposits during non-stormy weather intimately mixes population II and IV into a homogeneous deposit.

Component population III, in the normal weather ripple troughs, is probably put into suspension on the back-reef flat during storms. Increased water circulation during storms probably removes this population from the study area. Some of population IV, originally deposited in the lagoon during normal weather may be disturbed during storms, placed in suspension, and removed from the study area. It would not be placed into suspension as high in the water column as population III on the back-reef flat, however, so much would remain in the lagoon and be redeposited after the storm.

The net result of the above model is to deposit a shoreward prograding sand body with a discontinuous, coarse grained bottom-set over homogeneous, fine grained, bimodal (populations II and IV) lagoonal deposits (Fig. 23). The grain size distributions of the sands in the main body are bimodal (populations I to II plus III to IV). The grain sizes of the modes decreases downwards within the sand body. The mean grain size of whole sample grain size distributions increases downwards however, because of the increasing proportion of the coarse mode. The sand body is capped by a coarse grained, bimodal (populations I and III) top-set deposit, the thickness of

which depends of the difference in scouring abilities of normal weather and storm waves.

Sediment transport in Watering Bay is dominated by unequal, reversing tidal currents of which the northward flow is the strongest. Sand sized sediment, supplied by the barrier reefs, is moved into the bay by waves and transported northward by the tidal currents. Waves during normal weather have little or no effect on the bottom sediments over most of the bay.

Grain size distributions of samples collected in cloth mesh sediment traps at the sediment surface and at various heights above bottom correlate well with traction and suspended load grain size ranges defined by maximum shear velocity calculated from current measurements and plotted on transport competence curves (shear velocity vs. grain size).

From the sediment trap results it was found that the grain size distributions of bottom sediment samples in equilibrium with the currents could be used to define the grain size boundary between traction and suspended load and the roughness length. Using the boundary and the transport competence curves, the maximum shear velocity acting on the bottom was defined. The shear velocity and roughness length values were used, with water depths, in the von Karman-Prandtl equation to calculate current velocities at 5 feet (1.52 m) depth. These calculated velocities were approximately the same ($\pm 12.5\%$) as measured maximum velocities at nearby locations.

Maps of maximum shear velocity and current velocity, the

results of the sediment traps and current measurements, and maps of grain size distribution statistical parameters were all used to develop a model of reef sediment transport and deposition in Watering Bay. The only sites of sediment deposition in Watering Bay are the beaches, mangroves, shoreward Thalassia beds and patch reefs which could conceivably eventually lead to filling most of the bay to sea level.

The unstable sand environments are sediment bypass areas, in equilibrium with the currents. The grain size distributions of the bed materials accurately reflect the sediment transported by the currents, and are not deposited except temporarily, when the currents are slack or weak.

Significant deposition in Watering Bay would occur only if there were a rise in relative sea level or an increase in the grain sizes supplied by the reef. Deposition would continue until tidal flow was constricted sufficiently that shear velocities were competent to transport all sediment supplied by the reef. The new equilibrium surface so established would be at original water depths if a sea level rise had occurred and at shallower depths if an increase in grain size had occurred.

Much of the sediment swept from the bay at present is deposited on the slope into deeper water at the northern end of the bay to form a slowly northward prograding sand body. Continued progradation northward is dependent on extension of the barrier reef to protect the deposit from strong tidal currents sweeping around the north end of the reef.

An unknown, but probably major, portion of the sand swept from the bay continues to be transported outside of the study area by the currents from outside of the reef.

GENERAL MODEL

The above models for reef sediment transport and deposition in Grand and Watering Bays were developed on the basis of present day sedimentary patterns and processes. Implicit in the models is an unchanging sediment supply and constant relative sea level. Continuity of sediment supply from the reef might be expected barring major ecologic and/or evolutionary changes. However, it is obvious from the geologic record that a long term sea level still stand is an unusual occurrence. Therefore a discussion of the models is incomplete without considering at least the time and sea level factors and the possible relationship of the Grand Bay model to the Watering Bay model.

The two models may be at different stages rather than just different types of back-reef sedimentation. Given a constant sea level, one can imagine the progradational filling of the back-reef according to the Grand Bay model to the point that the cross-sectional area of water above the deposits is small relative to the area of the deposit (i.e. small in terms of the volume of water that must flow through the cross-sectional area to allow for tidal exchange over the area of the deposit and for the pumping of water by waves over the reef). At this stage significant currents would be set up

and the Watering Bay model would come into effect. This is model #1 illustrated in Figure 38. Its essential characteristics are a continual increase in the areal extent of the reef and reef derived sediments and a continual supplying of reef detritus into the adjoining basin. The rate of areal increase is dependent upon the productivity of the reef and the depth of water in the adjoining basin. Over-steepening of slopes and sudden, catastrophic collapse to send debris flows out into the basin should be a common feature of the model.

A modification of the first model (Stage 3 of Fig. 38) would result if the reef were in front of a land mass, as in Watering Bay. In this case, depositional prograding of the shoreward environments would cap the sequence with a mixed pattern of coral patch reef, coral rubble, beach, and fine grained organic-rich mangrove swamp and Thalassia bed facies extending to the intertidal level. The thickness of these facies would represent the equilibrium depth of the back-reef sediment bypass environment (Watering Bay model). Eventually the reduction in area of the back-reef would decrease the tidal exchange and the rates of current flow.

The end result would be a wide, low coastal plain with mangrove swamps behind a narrow, very shallow, very coarse grained back-reef flat, and what would then be essentially a fringing reef. All of the sand size and finer grains produced on the reef would be transported into the basin in front of the reef.

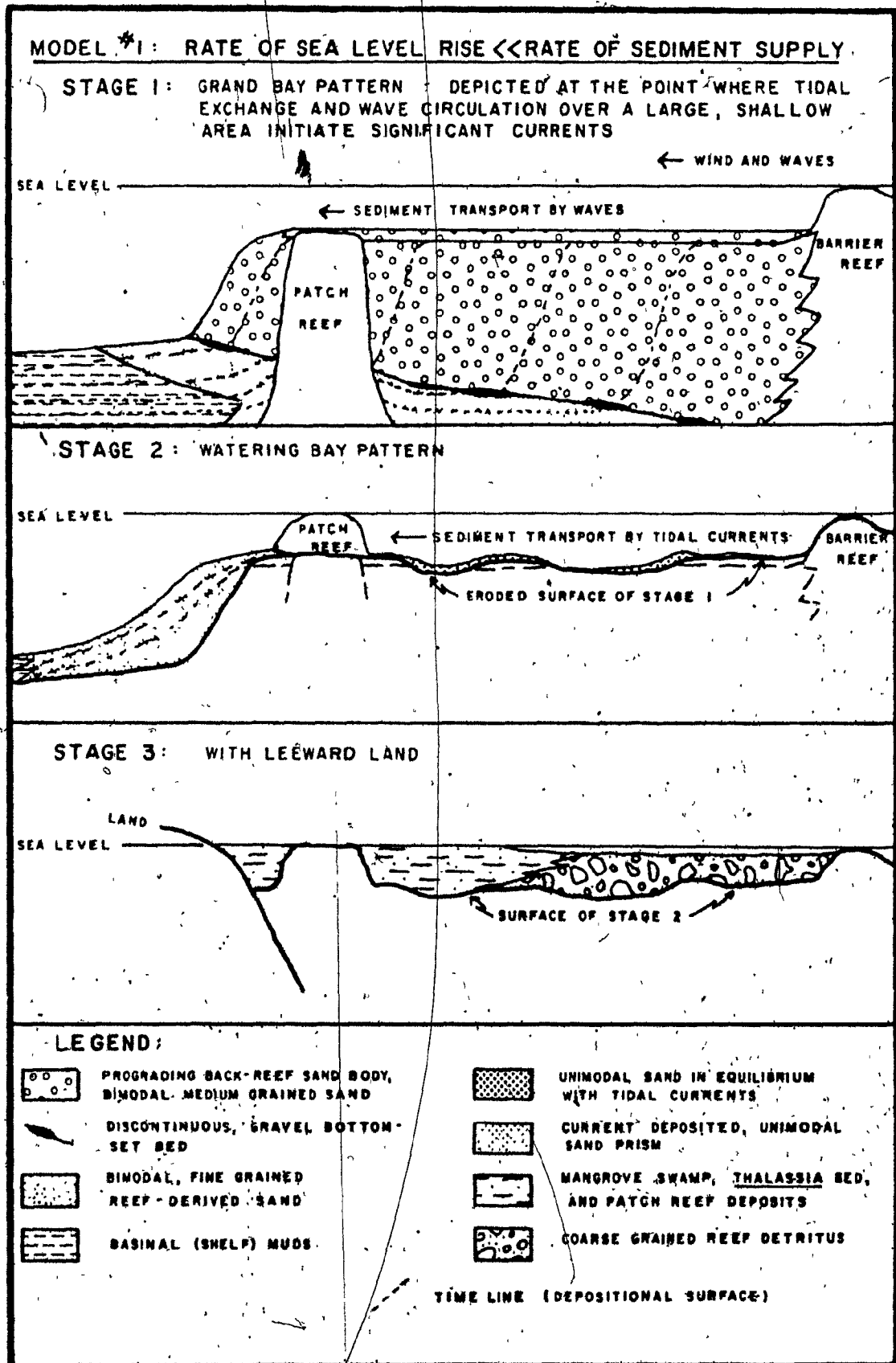


Fig. 38 General models of back-reef sedimentation, with constant sea level

The second model to be considered is one in which the rate of sea level rise is subequal to the rate of sediment supply. There are two possibilities, depending on whether the Grand Bay or the Watering Bay model is in effect when the rate of sea level rise becomes subequal to the rate of sediment supply (A and B respectively in Fig. 39).

The Grand Bay model (Fig. 39A) would result in the Grand Bay type cross bedded back-reef sand body being capped by a sequence of laminar bedded to massive, bimodal grain sized, storm reworked sands, interbedded with wave ripple cross - laminated, unimodal grain sized sands. Cross laminated beds would have sharp contacts with underlying storm reworked beds and scoured and eroded upper contacts with overlying storm deposits. The model is one of slow growth in areal extent of the reef and reef associated sediments. Also, less reef derived detritus is supplied to the adjacent basin than in model #1.

Beginning with the Watering Bay model (Fig. 39B) the result would be very similar to model #2A, except the sediments deposited in the back-reef would consist of sands reflecting the unidirectional transport regime, with lensitic bedding and evidence of cut and fill. Units with current ripple cross laminae would be common, as would lensitic coarse rubble deposits representing the occasional washing in of coarse reef debris during storms. Small patch reefs and lenses of Porites debris would also be common.

Model #3 (Fig. 39C) involves a rate of sea level rise much greater than the rate of sediment supply. In this

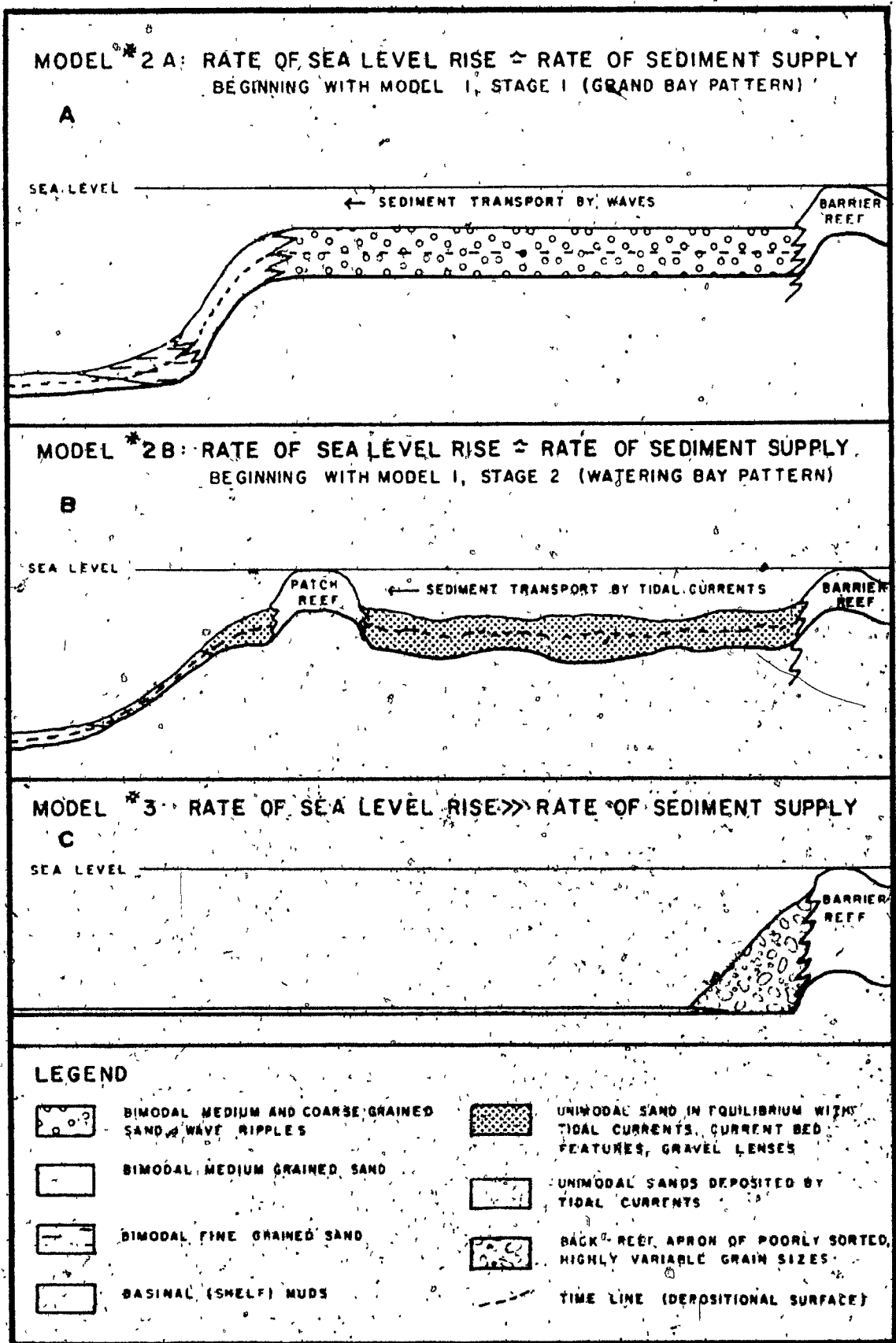


Fig. 39 General models of back-reef sedimentation
 A&B - rate of sea level rise subequal to rate of sediment supply
 C - rate of sea level rise much greater than rate of sediment supply

case the reef derived detritus does not extend far into the adjacent basin, all of it staying in the vicinity of the reef to form a steeply dipping wedge, or apron, of sediment.

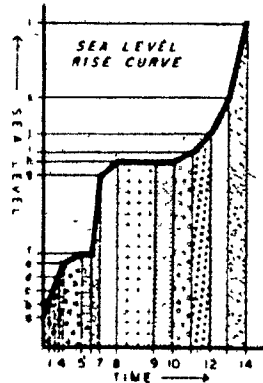
In the discussion of the above models several characteristics and processes of carbonate sediment production and deposition have been ignored because this study has dealt mainly with back-reef sedimentation in an area with only organic carbonate clasts. Processes on the reef, such as rate of sediment supply, cementation and organic abrasion in particular may be important factors affecting the present day northward extension of the Watering Bay barrier reef.

Another factor not considered is the effect of friction over a large shallow area to reduce tidal exchange and current strength. The enlargement of the back-reef area could lead to quiet water conditions and deposition of carbonate muds. Around the margins of the back-reef area, waves and tidal currents would still be active. Oolite shoals would be developed in the agitated, nutrient-poor, possibly supersaturated waters at the margins of a large carbonate bank area similar to the present day Bahamas Bank behind Andros Island. The area at which the Bahamas Bank model would come into effect would depend mainly on the tidal range and the strength of prevailing winds and waves. If tidal range was small and winds and waves were weak it is possible that the Bahamas Bank model, rather than the Watering Bay model, would succeed the Grand Bay model. The Bahamas Bank model will not be considered further here.

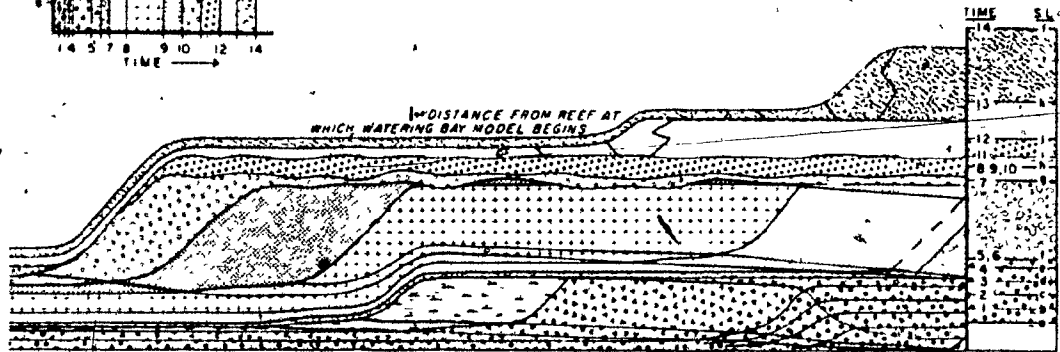
The stratigraphic and sedimentologic sequences that would result from the operation of the Grand Bay and Watering Bay models during intermittent and variable rates of sea level rise are illustrated in cross section in Figure 40. The assumptions and simplifications used in constructing the figure are as follows:

1. The reef is developed near the outer edge of a uniformly subsiding shelf sea without the influence of coarse grained terrestrial sediments.
2. Wind, wave and tidal conditions are constant. The direction of winds and waves is landward and normal to the shelf edge.
3. There is no inorganic production of carbonate except for cementation inherent in the production and maintenance of a reef framework.
4. All sediment is considered to be derived from the reef, although recent studies by Neumann and Land (1975) have demonstrated that important sources and a high rate of sediment production can exist in back-reef quiet water environments.
5. In a given unit of time a constant thickness of basinal sediment and constant volume (area in cross section) of reef framework and/or reef derived sediment are deposited.
6. Only detritus shed into the back-reef is considered. Fore-reef processes and the supply of reef sediment to the reef slope are ignored.
7. The reef grows vertically and no consideration is given to lateral expansion, contraction or migration.

STRATIGRAPHIC SEQUENCE FROM GIVEN SEA LEVEL RISE CURVE AND CARRIACOU BASED MODELS OF BACK-REEF SEDIMENTATION



TIME BOUNDED GENETIC UNITS



LITHOLOGIC UNITS

- | | | | |
|--|---|--|--|
| | BARRIER REEF CORE
(CORAL-ALGAL ROCK) | | BIMODAL FINE GRAINED SAND
(LAGOON-GRAND BAY) |
| | BACK-REEF COARSE GRAINED APRON
(NOT OBSERVED) | | UNIMODAL COARSE-MEDIUM GRAINED SAND
(BED LOAD-WATERING BAY) |
| | BIMODAL COARSE GRAINED SAND
(RIPPLE TROUGH-GRAND BAY) | | UNIMODAL SAND-COARSENING UPWARDS
(SLOPE-NORTH END WATERING BAY) |
| | BIMODAL MEDIUM GRAINED SAND
(SLOPE-GRAND BAY-DISCONTINUOUS GRAVEL BED AT BASE) | | BASINAL MUDDS |

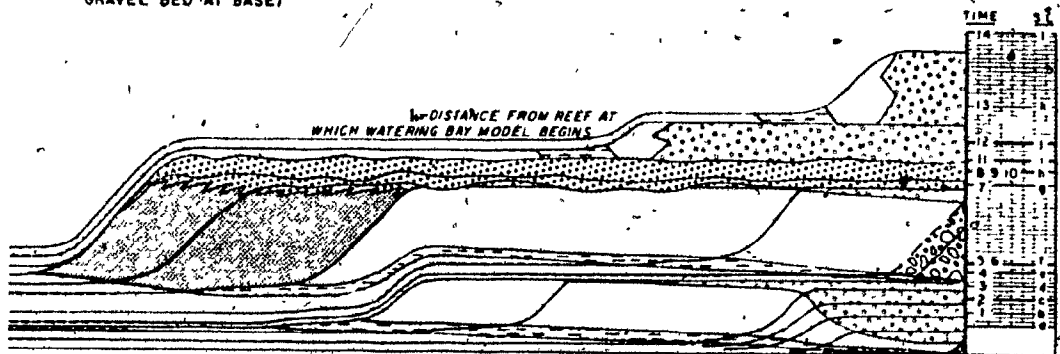


Fig. 40 Sequence of back-reef sedimentation for a given sea level rise curve.

8. Before sediment can be derived from the reef it must be at sea level.
9. No consideration is given to possible lowering of relative sea level, an occurrence which has been demonstrated to be common and important in many ancient reefs. Therefore, the effects of subaerial diagenesis and island formation on water flow patterns and reef development are ignored.
10. There is a water depth above which back-reef sediments cannot be deposited and which represents the equilibrium surface for the grain sizes of the sediment and the wind, wave and current conditions.
11. When the back-reef sediment pile reaches a given distance from the reef, strong tidal currents are developed to facilitate water exchange in a shallow, wide water column. Thus the Watering Bay model replaces the Grand Bay model of back-reef sedimentation.

The sea level rise curve (Fig. 40) was designed to investigate the effects on back-reef sedimentation of several different patterns of sea level rise. From time 0 to 5 the rate of sea level rise is moderate and decreasing. A short period (time 5 to 6) of sea level still stand separates the first sea level rise from a rise which initially outstrips the rate of sediment production and then decreases to a prolonged still stand from time 8 to 10. The still stand is followed by a gradually accelerating rate of sea level rise to complete the modeling sequence.

The sequence begins at time 0 and sea level "a", with the reef at sea level and no back-reef sediment deposited.

From time 0 to 4 there is a constant rate of sea level rise from level a to e. This rise has been broken into four equal time stages to demonstrate the difference between facies and time boundaries. In the early part of time 0 to 1, back-reef sediment is deposited as an apron (model 3) until it reaches the equilibrium depth (assumption 10) and deposition according to the Grand Bay model begins. At the given rate of sea level rise, the back-reef sand body does not prograde rapidly, much of the carbonate production being required to keep the reef at sea level and the top of the back reef flat at the equilibrium depth (model 2A). Most of the back-reef sediment is deposited as horizontally bedded, bimodal, coarse grained sands similar to the back-reef ripple trough samples of Grand Bay. Preservation of wave produced ripples with unimodal, well sorted grain sizes is possible.

From time 4 to 5, the rate of sea level rise is decreased. Less material is required by the reef and back-reef sand flat to keep pace with the rise. The dominant deposits are bimodal, medium grained sands of the slope. The sand body progrades rapidly away from the reef.

During the subsequent sea level still stand (time 5 to 6) the reef and back-reef flat are sediment bypass areas, all carbonate production being deposited on the slope. Progradation of the back-reef sand body away from the reef is at a maximum (model 1A).

The requirements of the reef keeping pace with the very rapid sea level rise from time 6 to 7 do not leave sufficient

sediment for the back-reef deposits to maintain an equilibrium surface. As a result, a sediment apron (model 3) is deposited adjacent to the reef and, if bottom currents allow, basinal muds transgress over the previous equilibrium surface.

From time 7 to 8 the rate of sea level rise is decreased so as not to exceed sediment supply. Initially deposition of a sediment apron continues until the equilibrium depth is reached and the Grand Bay model of deposition established.

The subsequent sea level still stand from time 8 to 10 allows the back-reef sand body to prograde rapidly away from the reef (model 1A). The Watering Bay model of back-reef sand body deposition takes effect at time 9. Channels are cut in the back-reef equilibrium surface and dunes established. All sediment bypasses the reef and back-reef flat to be deposited on the slope. The deposit consists of sand with unimodal grain size distributions similar to those at the north end of Watering Bay.

The following low rate of sea level rise from time 10 to 11 produces a continuation of the Watering Bay model of deposition with some aggradation on top of the back-reef sand body to maintain the equilibrium surface (model 2B). The top set deposits are irregularly bedded with abundant scour and fill features and abundant current ripple and dune cross-laminae. Grain size distributions of the sands are similar to those of samples from Watering Bay.

The increase in rate of sea level rise from time 11 to

12 causes an increase in the rate of aggradation of the top set deposits, and does not leave sufficient volumes of sediment for significant deposition on the slope.

Increasing rates of sea level rise, from time 12 to 13, and from time 13 to 14, lead to reduction in the area of the back-reef sand body and transgression of basinal muds over previous deposits. Since the increases in rates of sea level rise are abrupt and step-like, the resulting deposits are step-like. A gently curving sea level rise curve would result in a sedimentary wedge, thinning away from the reef, and capping the sequence.

Elements of the above or similar sequences may be recognizable in the ancient sedimentary record allowing interpretation in terms of the Grand Bay and Watering Bay sedimentary models. Allowances would have to be made for periods of sub-aerial exposure and early and late diagenetic effects. It should be possible to derive sea level rise curves for the ancient sequences and then analyse elements for details of the transport and depositional processes. If the degree of diagenesis allows, grain size distributions plus estimates of water depths should allow estimates to be made of current velocities and patterns and possible combinations of wave periods and heights.

Tests of the above procedure would be best carried out initially on young and hence organically similar sequences, such as the Pleistocene reef terraces of Barbados, W.I.

CONCLUSIONS

1. Cumulative curves, histograms, and the concept of mixtures of log normal populations provide a much more complete representation of bottom sample grain size distributions than do derived statistical parameters. They are also more easily and completely related to transport and depositional processes.
2. In Grand Bay there are strikingly consistent and systematic differences in the grain size distributions of bottom samples from different environments.
3. Basic grain size component populations and the pattern of their occurrence in Grand Bay are consistent with the transport competence of observed waves and do not reflect structural units of different organic skeletons.
4. Alternation of normal and storm conditions in Grand Bay results in transport and deposition of reef derived sediment as a shoreward prograding, cross bedded body of bimodal, medium grained sand. The top of the sand body is a ripple marked, non-depositional surface at approximately 12 feet (3.6 m) water depth. The depth represents an equilibrium between grain sizes supplied from the reef and the transport competence of the waves. The base of the sand body is a discontinuous bed of dominantly molluscan gravel overlying bimodal, fine grained lagoonal sand at 20 to 30 feet (6.1 to 9.1 m) water depth.
5. In Watering Bay sediment transport and deposition in the back reef is controlled by semi-diurnal, reversing tidal currents.
6. Net sediment transport is towards the north, parallel to the reef. The south flowing current is very seldom competent to transport sediment.

7. Tidal current velocities, observations of sediment transport, and grain size distributions of sediment in transport are consistent with published transport competence curves (threshold shear velocity and settling velocity versus grain size).

8. Grain size distributions of bottom sediment samples from Watering Bay reflect the maximum shear velocities attained during peak northward tidal flow. The 64th percentile of a bottom sediment grain size distribution may be used as an estimate of the boundary between bed and suspended load, and plotted on the suspension transport competence curve to estimate the maximum shear velocity. An estimate of maximum flow velocity at any water depth may then be calculated using the von Karman-Prandtl equation for flow above a rough boundary.

9. The floor of Watering Bay is a non-depositional surface across which tidal currents sweep all reef sediment supplied to it. The sediment is either deposited on a slope into deeper water at the northern end of the bay or removed from the immediate area by strong tidal currents from outside the reef. Since there is no or limited deposition in the current swept deeper water areas outside Watering Bay, there is little or no interfingering of back-reef with deeper water sediment.

10. Northward progradation of the back-reef sands in Watering Bay is dependent on the northward extension of the barrier reef to protect the sand from the external strong tidal currents.

11. The patterns of sediment transport and deposition in Grand and Watering Bays appear to represent different stages in a continuum from which a model of back-reef sedimentation may be derived. At a constant sea level, partial filling of the back-

reef according to the Grand Bay pattern could reach a stage where significant tidal currents would be necessary to facilitate water exchange over a shallow, wide, back-reef flat. The development of tidal currents would mark the establishment of the Watering Bay pattern of back-reef sedimentation.

12. The Grand and Watering Bay patterns of back-reef sediment transport and deposition, with their distinctive sand body geometries and grain size distributions, were used with a varying sea level rise curve to model a hypothetical, realistic back-reef sedimentary sequence. Elements of that or similar sequences may be recognizable in the ancient stratigraphic record.

REFERENCES

- Allen, G.P., 1971, Relationship between grain size parameter distribution and current patterns in the Gironde Estuary (France): Jour. Sedimentary Petrology, v. 41, p. 74-88.
- Anonymous, 1948, Monthly meteorological charts of the Atlantic Ocean: Air Ministry, Meteorological Office, Marine Branch, M.O. 483.
- Anonymous, 1959, Climatological and oceanographic atlas for mariners, vol. I: U.S. Office of Climatology and Division of Oceanography.
- Anonymous, 1967, Admiralty tide tables, vol. II, Atlantic and Indian Oceans: Hydrographer of the Navy, London.
- Bagnold, R.A., 1946, Motion of waves in shallow water, interaction between waves and sand bottom: Proc. Roy. Soc. London, Series A, v. 187, p. 1-15.
- , 1963, Mechanics of marine sedimentation, in Hill, M.N., ed., The sea, vol. 3, The earth beneath the sea: John Wiley and Sons Inc., p. 507-528.
- Bathurst, R.G.C., 1971, Carbonate sediments and their diagenesis: Developments in Sedimentology 12, Elsevier, Amsterdam.
- B-1995 L 1 and Middleton G.V., 1965 Hydromechanical Principles of Sediment Structure Formation in Middleton G.V. ed. Primary Sedimentary Structures, Soc Econ Pal & Min Sp Pub 12, 5-16*
- Brush, L.M. Jr., 1965, Sediment sorting in alluvial channels: in Middleton, G.V., ed., Primary sedimentary structures and their hydrodynamic interpretation: Soc. Econ. Paleontologists and Mineralogists, Spec. Pub. No. 12, p. 25-33.
- Conaghan, P.J., 1967, Marine geology of the southern tropical shelf, Queensland: unpublished PhD thesis, Univ. of Queensland, Australia.
- Cook, D.O. and Gorsline, D.S., 1972, Field observations of sand transport by shoaling waves: Marine Geology, v. 13, p. 31-35.
- Davies, G.R., 1970, Carbonate bank sedimentation, Eastern Shark Bay, Western Australia: in Logan, B.W. et al, Carbonate sedimentation and environments, Shark Bay, Western Australia: Am. Assoc. Petroleum Geologists, Memoir 13, p. 85-168.
- Defant, A., 1961, Physical oceanography: v. II, Pergamon Press, New York.

Doeglass, D.J., 1946, Interpretation of the results of mechanical analysis: Jour. Sedimentary Petrology, v. 16, p. 19-40.

Dyer, K.R., 1972, Bed shear stresses and the sedimentation of sandy gravels: Marine Geology, v. 13, p. M31-M36.

Fage, A., 1933, Fluid flow in rough pipes: Rep. Memo. Aero. Res. Comm., London, No. 1585; as reported in Inman (1949).

Folk, R.L., 1967, Carbonate sediments of Isla Mujeres, Quintana Roo, Mexico and vicinity: New Orleans Geological Soc., Guidebook 1967, Annual Meeting, 2nd Edition, p. 100-121.

-----, 1968, Petrology of sedimentary rocks: Hemphills, Austin, Texas, 170 p.

-----, Andrews, P.B., and Lewis, D.W., 1970, Detrital sedimentary rock classification and nomenclature for use in New Zealand: N.Z. Jour. Geology Geophysics, v. 13, p. 937-968.

----- and Ward, W.C., 1957, Brazos River bar: A study in the significance of grain size parameters: Jour. Sedimentary Petrology, v. 27, p. 3-26.

----- and Robles, R., 1964, Carbonate sands of Isla Perez; Alacran Reef Complex, Yucatan: Jour. Geology, v. 72, p. 255-292.

Friedman, G.M., 1961, Distinction between dune, beach and river sands from their textural characteristics: Jour. Sedimentary Petrology, v. 31, p. 514-529.

-----, 1967, Dynamic processes and statistical parameters compared for size frequency distributions of beach and river sands: Jour. Sedimentary Petrology, v. 37, p. 327-354.

Fuller, A.O., 1961, Size distribution characteristics of shallow marine sands from the Cape of Good Hope, South Africa: Jour. Sedimentary Petrology, v. 31, p. 256-261.

Ginsburg, R.N., and Lowenstam, H.A., 1958, The influence of marine bottom communities on the depositional environments of sediments: Jour. Geology, v. 66, p. 310-318.

Goreau, T.F., and Hartman, W.D., 1963, Boring sponges as controlling factors in the formation and maintenance of coral reefs: in Mechanisms of hard tissue destruction: Amer. Assoc. for the Advancement of Science, Pub. No. 75; p. 25-54.

Harms, J.C., 1969, Hydraulic significance of some sand ripples: Geol. Soc. America Bull., v. 80. p.363-396.

Hoskins, C.M., 1963, Recent carbonate sedimentation on Alacran Reef, Yucatan, Mexico: Washington, Nat. Acad. Sci.-Nat. Res. Council, Pub. 1089, 160 p.

Inman, D.L., 1949, Sorting of sediments in the light of fluid mechanics: Jour. Sedimentary Petrology, v. 19, p. 51-70.

-----, 1963, Chapt. III, Ocean waves and associated currents; Chapt. V, Sediments-physical properties and mechanics of sedimentation: in Shepard, F.P., Submarine geology: 2nd edition, Harper and Row, New York, 557p.

Jell, J.S., Maxwell, W.G.H., and McKellar, R.G., 1965, The significance of the larger foraminifera in the Heron Island Reef sediments: Jour. Paleontology, v. 39, p.273-279.

Jopling, A.V., 1965, Laboratory study of the distribution of grain sizes in cross-bedded deposits: in Middleton, G.M., ed., Primary sedimentary structures and their hydrodynamic interpretation: Soc. Econ. Paleontologists and Mineralogists, Spec. Pub. No. 12, p. 53-65.

-----, 1966, Some principles and techniques used in reconstructing the hydraulic parameters of a paleo-flow regime: Jour. Sedimentary Petrology, v. 36, p. 5-49.

Kachel, N.B., and Sørenberg, R.W., 1971, Transport of bed load as ripples during an ebb current: Marine Geology, v. 10, p. 229-244.

Kalinske, A.A., 1943, Turbulence and the transport of sand and silt by wind: Annals New York Acad. Sci., v. XLIV, p. 4-54; as reported in Inman, 1949.

Kay, Frances, 1966, This is Grenada: Caribbean Printers Ltd., Trinidad, W.I.

Komar, P.D. and Miller, M.C., 1973, The threshold of sediment movement under oscillatory water waves: Jour. Sedimentary Petrology, v. 43, p.1101-1110.

----- and ----- 1975, Reply: On the comparison between the threshold of sediment motion under waves and unidirectional currents with a discussion of the practical evaluation of the threshold: Jour. Sedimentary Petrology, v. 45, p. 362-367.

- Kranck, Kate, 1968, Carriacou shore Party: in Marlowe, J.I., Atlantic Oceanographic Laboratory, Bedford Institute, cruise report No. 209, C.S.S. Hudson, Jan. 24-Mar. 22, 1968, April 2-11, 1968: Dept. Energy, Mines and Resources, Marine Sciences Branch, p.16-18.
- Lewis MS, 1968, The morphology of the fringing reefs along the east coast of Male, Seyelles*
- Maiklem, W.R., 1968, Some hydraulic properties of bioclastic carbonate grains: Sedimentology, v. 10, p. 101-109.
- Manohar, Madhav, 1955, Mechanics of bottom sediment movement due to wave action: U.S. Army Corps of Engineers, Beach Erosion Board, Tech. Memo. No. 75, 121 p.
- Martin-Kaye, P.H., 1958, The geology of Carriacou: Bull. Amer. Paleont., v. 38, p. 395-405.
- Mason, C.C., and Folk, R.L., 1958, Differentiation of beach, dune, and aeolian flat environments by size analysis: Jour. Sedimentary Petrology, v. 28, p. 211-226.
- Middleton, G.V., ed., 1965, Primary sedimentary structures and their hydrodynamic interpretation: Soc. Econ. Paleontologists and Mineralogists, Spec. Pub. 12, 265 p.
- Milliman, J.D., 1974, Marine Carbonates: Springer-Verlag, New York, 375 p.
- Moss, A.J., 1962, The physical nature of common sandy and pebbly deposits, Part I: Amer. Jour. Science, v. 260, p. 337-373.
- , 1963, The physical nature of common sandy and pebbly deposits, Part II: Amer. Jour. Science, v. 261, p. 297-343.
- Neumann, A.C., and Land, L.S., 1975, Lime mud deposition and calcareous algae in the bight of Abaco, Bahamas: a Budget: Jour. Sedimentary Petrology, v. 45, p. 763-786.
- Nevin, Chas., 1946, Competency of moving water to transport debris: Bull. Geol. Soc. Amer., v. 57, p. 651-674.
- Nikuradse, J., 1933, Stromungsgesetze in rauhen rohren: Forschungsheft 361, Vereines Deutscher Ingenieure: as reported in Inman (1949).
- Ogilvie, W., 1968, Wind data for Pearls Airport, Grenada, W.I., for the years 1963-1967 inclusive: personal written communication.

- Patriquin, D.G., 1973, Erosional structures in seagrass beds at Barbados and Carriacou, southern Caribbean: Copy of type-written manuscript, 52 p.
- Rubey, W.W., 1933, Settling velocities of gravel, sand and silt particles: Amer. Jour. Science, v. 25, p. 325-338.
- Scóffin, T.P., 1970, The trapping and binding of subtidal carbonate sediments by marine vegetation in Bimini Lagoon, Bahamas: Jour. Sedimentary Petrology, v. 40, p. 249-273.
- Spencer, D.W., 1963, The interpretation of grain size distribution curves of clastic sediments, Jour. Sedimentary Petrology, v. 33, p. 180-190.
- Sternberg, R.W., 1967, Measurements of sediment movement and ripple migration in a shallow marine environment: Marine Geology, v. 5, p. 195-205.
- , 1968, Friction factors in tidal channels with differing bed roughness: Marine Geology, v. 6, p. 243-261.
- , 1971, Measurements of incipient motion of sediment particles in the marine environment: Marine Geology, v. 10, p. 113-119.
- , and Creager, J.S., 1965, An instrument system to measure boundary-layer conditions at the sea floor: Marine Geology, v. 3, p. 475-482.
- Sundborg, F.A., 1956, The river Klaralven, a study of fluvial processes: Geograf, Ann., v. 38, 127-316. as reported in Jopling (1966).
- Swinchatt, J.P., 1965, Significance of constituent composition, texture, and skeletal breakdown in some Recent carbonate sediments: Jour. Sedimentary Petrology, v. 35, p. 71-90.
- Tanner, W.F., 1959, Sample components by the method of differences: Jour. Sedimentary Petrology, v. 29, p. 408-411.
- Trechmann, C.T., 1935, The geology and fossils of Carriacou, West Indies: Geol. Mag., v. 72, p. 529-555.
- Vincent, G.E., 1958, Contribution to the study of sediment transport on a horizontal bed due to wave action: in Proc. 6th Conf. Coastal Engineering, Council on Wave Research, The Engineering Foundation, Univ. Calif., Richmond, Calif., p. 326-355.

Vischer, G.S., 1965, Fluvial processes as interpreted from ancient and recent fluvial deposits: in Middleton, G.V. (ed.), Primary sedimentary structures and their hydrodynamic interpretation: Soc. Econ. Paleontologists and Mineralogists, Spec. Pub. 12, p. 116-132.

-----, 1969, Grain size distribution and depositional processes: Jour. Sedimentary Petrology, v. 39, p. 1074-1106.

White, C.M., 1940, The equilibrium of grains on the bed of a stream: Proc. Royal Soc. London, Series A, v.174, p.322-338.

PLATE 1:
AERIAL PHOTOGRAPH - EASTERN COAST AND NORTHERN CARRIACOU.

The study area includes the back-reef and near fore-reef environments east of the island. The lagoonal bays, from north to south, are Watering Bay, Jew Bay, and Grand Bay.

Wave action on the reef front is least intense along the northern half of the Watering Bay barrier reef, which is protected from oceanic waves by the banks and islands to the east (Islands of Fota and Little Tobago to the right on the photograph. The larger island of Petit Martinique is just to the east).

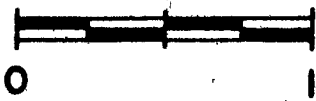
12° 32' N

61° 27' W

CARRIACOU,

W. I.

Scale



miles

PLATE 2
AERIAL PHOTOGRAPH - WATERING BAY.

The back-reef environments and sediment transport are controlled by north-south reversing tidal currents. These are reflected by the lineation of the marine grass and macroscopic algae beds in the main lagoon. The dominance of the northward flow is demonstrated by the sediment lobes leading from the back edge of the barrier reef and by the grass bed "tails" north of banks and patch reefs.

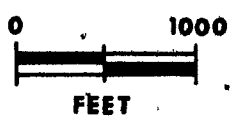
The northern end of the bay is open between the barrier reef and the fringing reef around the mangrove swamp. Grand Cay (the largest patch reef east of Carriacou) and the coral and gravel bank to the north of it cause some constriction of the currents. The greatest constriction occurs between the barrier reef and Pt. St. Hilaire, where a 26 feet (8 m) deep channel is present. Water depths over most of the bay are between 10 and 15 feet (3 and 4.6 m). The effect of the tidal currents diminishes shorewards, where marine grass banks with a dense growth of Thalassia are developed.

Carib is a sand cay built of coarse, reef derived sand, and undergoes a yearly cycle of buildup and destruction related to seasonal variations in the directions and strengths of waves.

A well-developed trickle zone, consisting of coral and algal ridges and sand and gravel channels, is present only behind the southern half of the barrier reef because the northern half is protected from waves by banks and islands to the east (Plate 1).

Windward village was the operational base for this study.

MANGROVE



GRAND CAY

WINDWARD

CARIB

PT. ST. HILAIRE

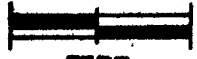
PLATE 3:
AERIAL PHOTOGRAPH _ SOUTHWEST GRAND BAY.

The back-reef environments and sediment transport are controlled by waves, which are larger than those in Watering Bay. No tidal currents were observed.

Sand, derived from the barrier reef, is transported shorewards across the 12 feet (3.7 m) deep back-reef sand flat and deposited on the slope to the main lagoon floor at 20 to 43 (6 to 13 m) depth. Fine sand to silt size material is deposited in the lagoon.

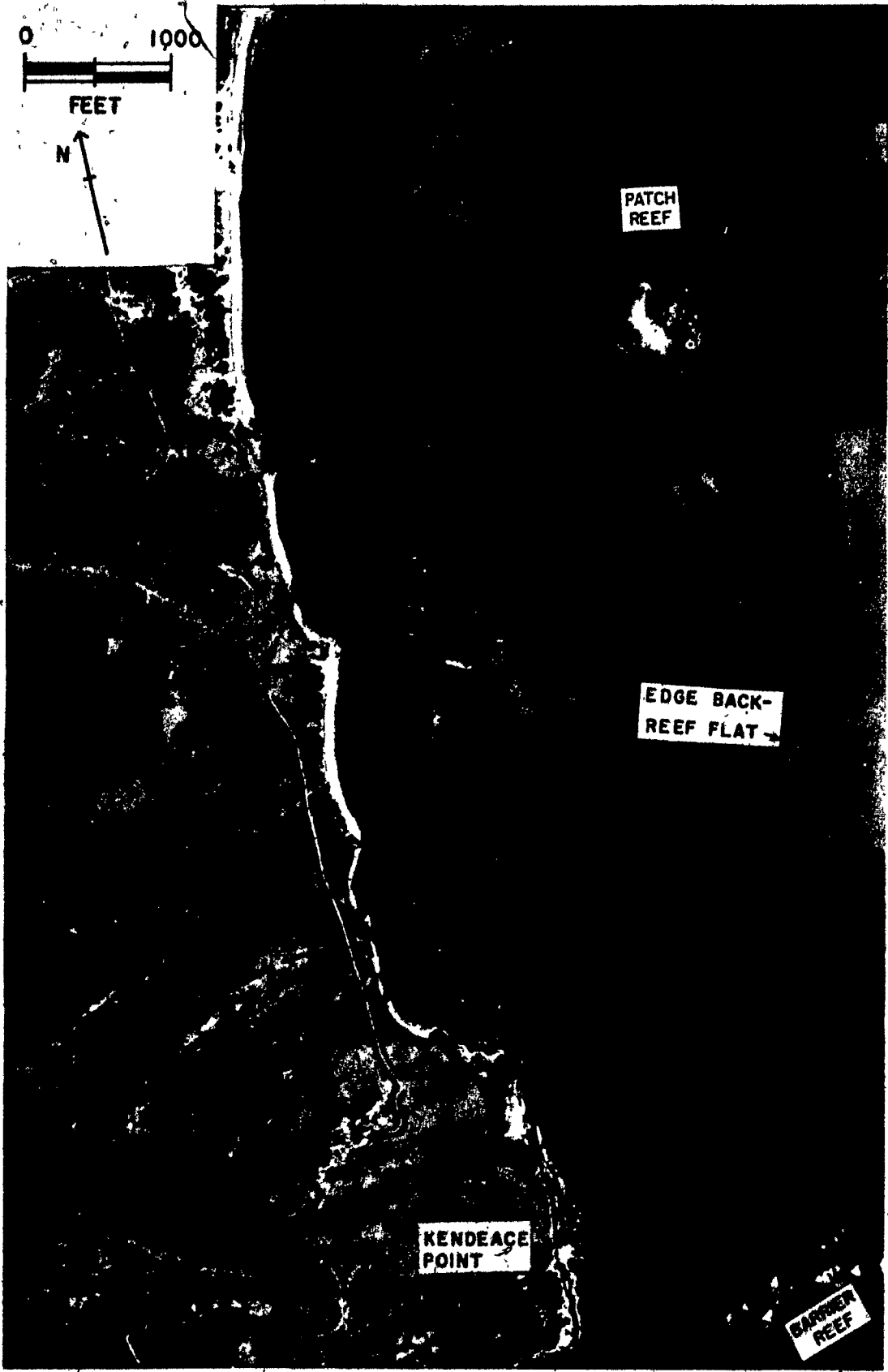
The 30 feet (9 m) deep terrace and re-entrant on the back-reef flat seaward of the patch reef to the north may be an old back-reef sand flat surface, which is being transgressed and covered by the present day back-reef flat.

0 1000



FEET

N



PATCH REEF

EDGE BACK-REEF FLAT

KENDEACE POINT

BARNER REEF

PLATE 4:
REEF SLOPE AND FORE-REEF ENVIRONMENTS, WATERING BAY, TRAVERSE
SIX.

A and B:

Reef slope surface at approximately 40 feet (12.2 m) depth and 50 feet (15.2 m) depth respectively. Note platy Diploria, Montastrea, and abundant Gorgonians.

C and D:

Base of reef slope and start of fore-reef environments at 60 to 65 feet (18.3-19.8 m) depth.

(Photographs courtesy of R. Boulanger, Atlantic Oceanographic Laboratory, Bedford Institute, Dartmouth, Nova Scotia)

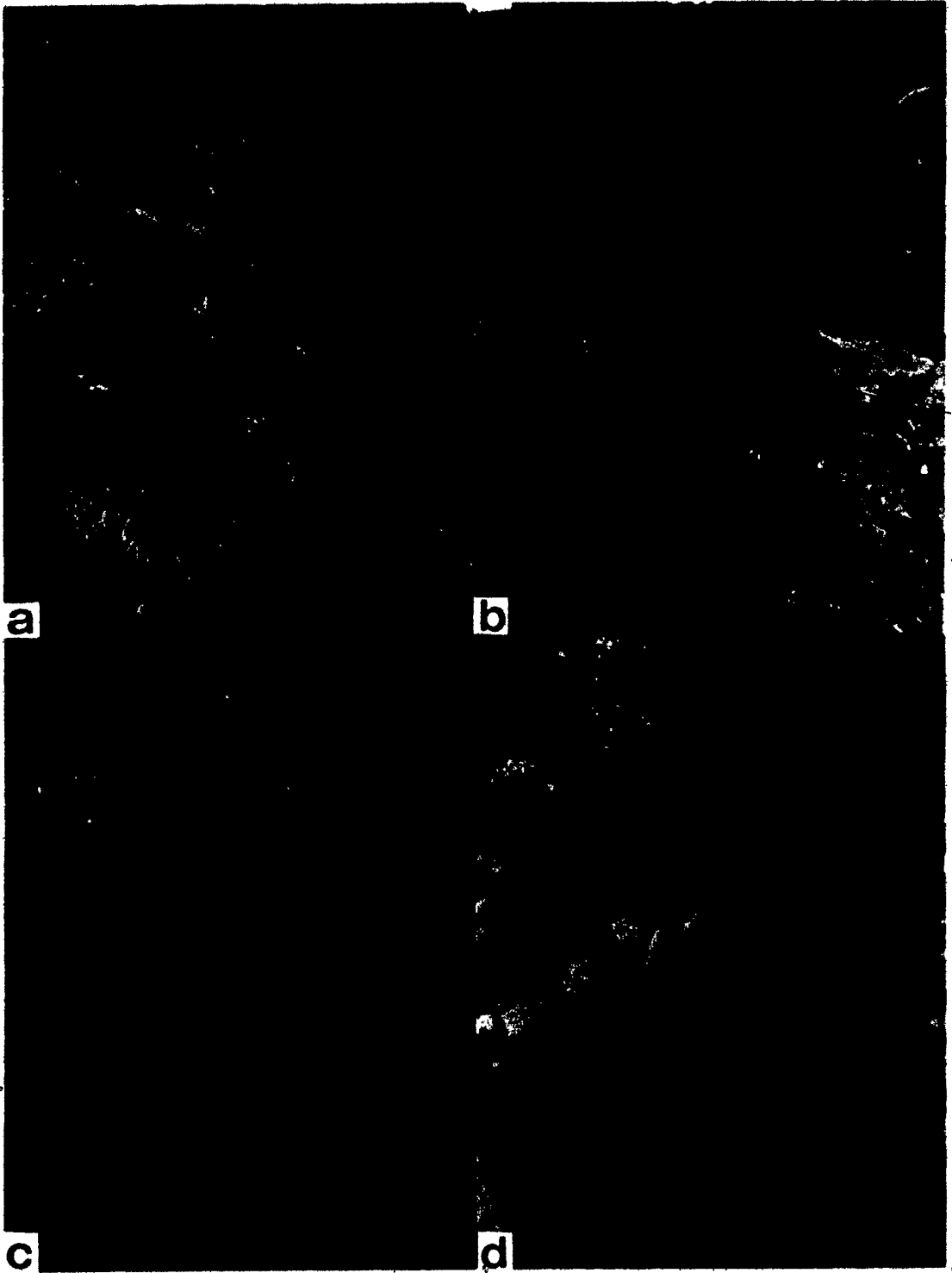


PLATE 5:

UPPER REEF SLOPE AND REEF CREST ENVIRONMENTS, WATERING BAY BARRIER REEF.

A: Front of reef crest between traverses 5 and 6 in water depth of 7 feet (2.1 m). Red algal coated coral rock is encrusted with the bladed growth form of the hydrozoan Millepora. Most of the coral rock appears to have been formed originally by Montastrea annularis of which a remnant knob is seen towards the top of the photograph. Weakly oriented to unoriented growths of Acropora palmata (right foreground and background of photograph) are scattered throughout this environment to a depth of approximately 10 feet (3 m).

B: Reef slope near base of a cliff between traverses 5 and 6 in 25 (7.6 m) water depth. Coral rock with living Montastrea annularis and a delicately branched growth form of Millepora. Abundant gorgonians and sponges.

C: Reef crest immediately behind front ridge of red algal encrusted coral rock. Between traverses 5 and 6 in 2 feet (0.6 m) water depth. Unoriented growth form of Acropora palmata to the right in the photograph. Porites porites and Porites astreoides are the other abundant corals. Stick is marked in inch (2.54 cm) and foot (0.3m) intervals.

D: Boulder flat on lagoonward half of reef crest on approximately traverse 9: Depth 2 feet (0.6 m). Red algae encrusted boulders, derived mainly from Acropora palmata, average 4 to 6 inches (10 to 15 cm) across. Large boulder in centre has sent out a small branch of living Acropora palmata. Abundant calcareous green algae Halimeda opuntia (foreground of photograph).

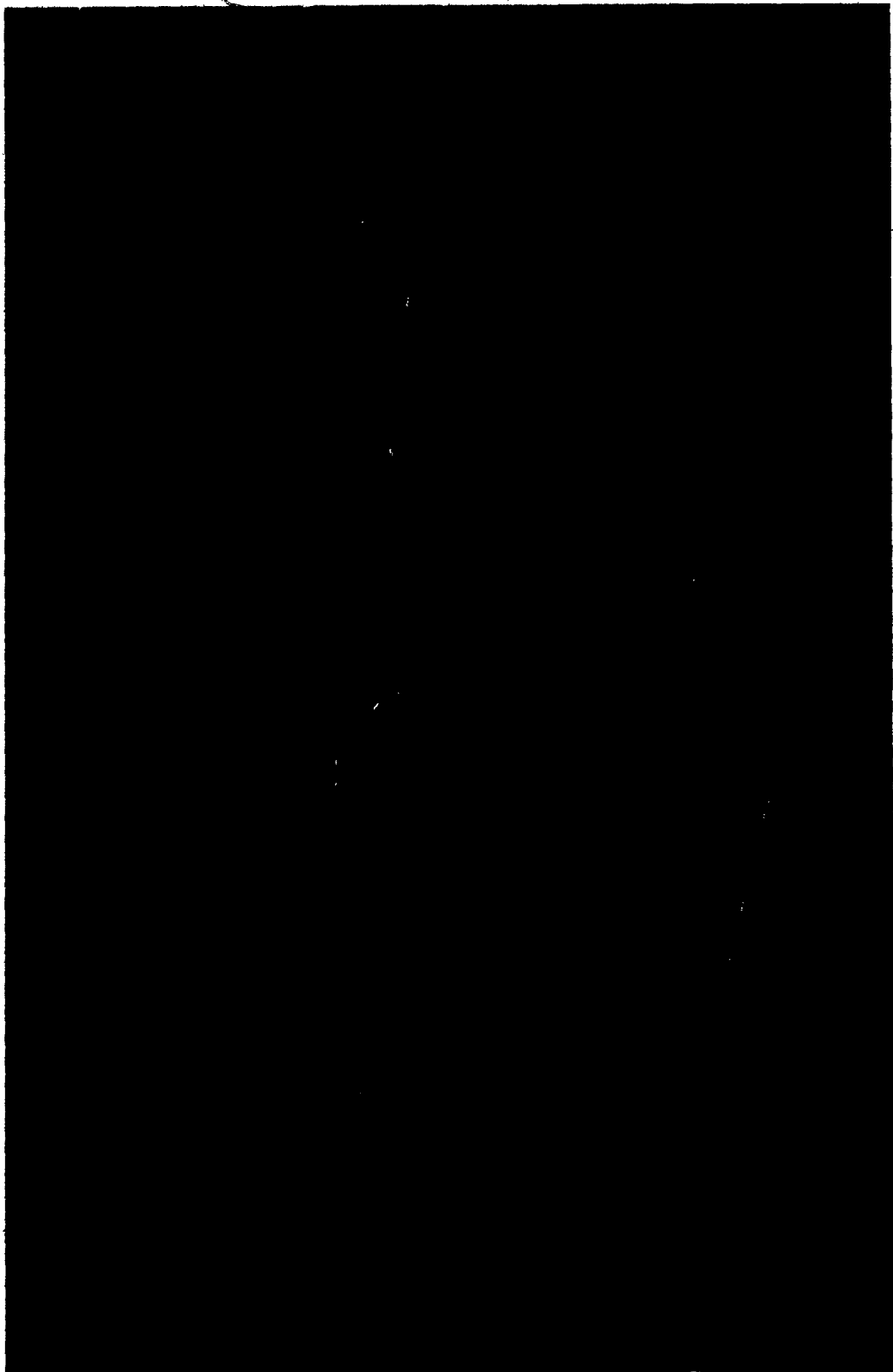


PLATE 6:
BACK EDGE OF REEF CREST:

A: Near lagoonward margin of boulder flat on reef crest in Watering Bay. Depth 2.5 feet (0.76 m). Red algal encrusted coral rubble (Porites porites and Acropora palmata) with interstitial sand. Abundant macroscopic green algae (?Cladophora).

B: Abrupt lagoonward edge of reef crest on traverse 18 in Grand Bay. Depth to sand 11 feet (3.4 m). Algal encrusted coral rock originally Montastrea annularis which is still growing near the top. Accessory corals are mainly Diploria.

C: Near lagoonward edge of reef crest in trickle zone between traverses 8 and 9 in Watering Bay. Ridge composed of Acropora palmata. Overturned A. palmata at 0.5 feet (1.5 m) depth in coral gravel and coarse sand floored channel.

D: Unstable sand behind reef crest boulder flat just north of traverse 6 in Watering Bay. Depth 2 feet (0.6 m). Symmetrical, rounded, wave ripples are parallel to the reef crest which is to the left of the photograph. Pole is marked in 1 inch (2.54 cm) intervals.

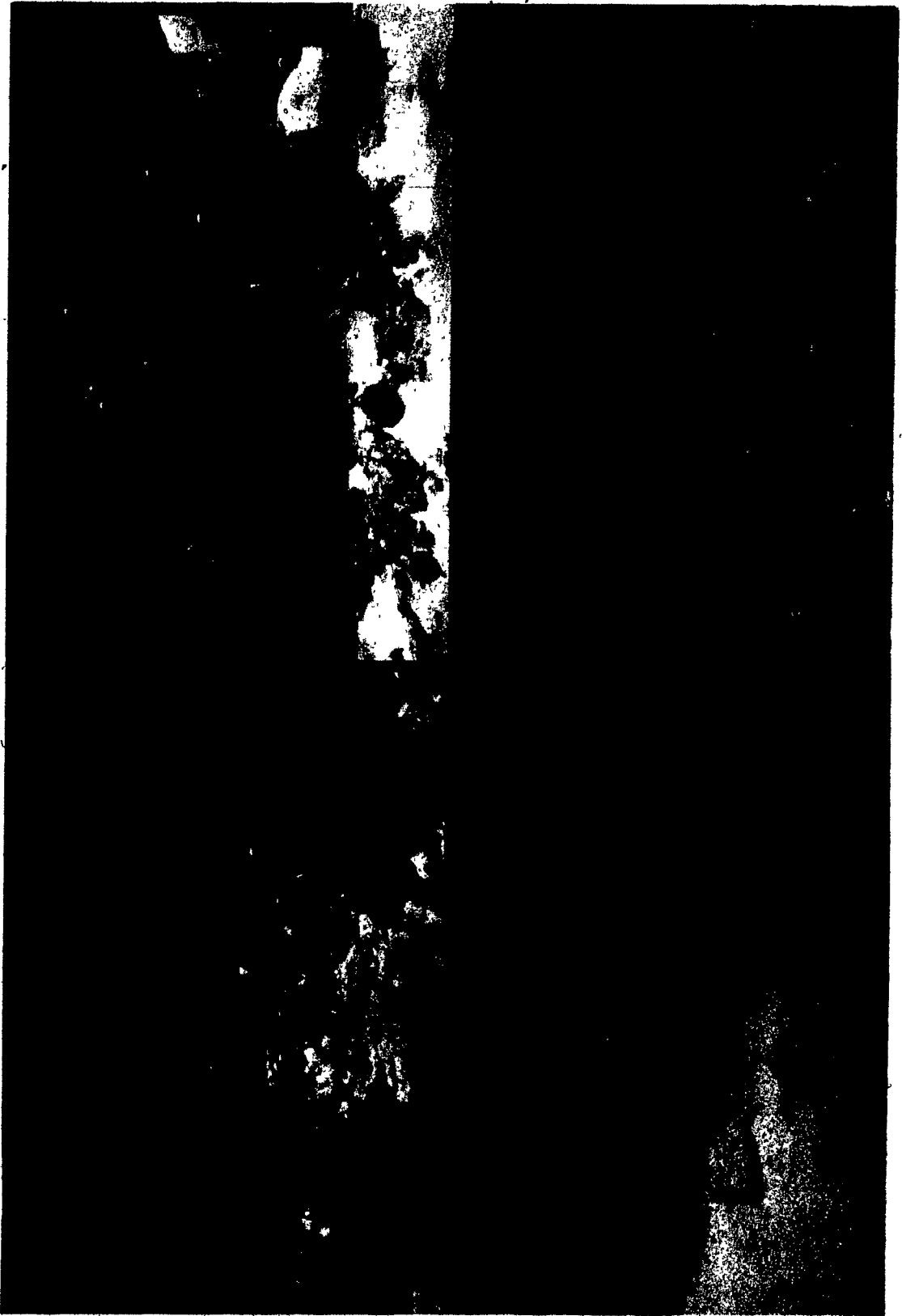


PLATE 7:
WATERING BAY LAGOON ENVIRONMENTS.

A: Unstable sand environment with Porites rubble, sea plants and crescentic, irregular, current ripples. Depth approximately 10 feet (3 m).

B: Loggerhead sponge in approximately 15 feet (4.6 m) water depth in north-central Watering Bay. Unstable sand environment.

C: Sediment trap assembly in place in unstable sand environment in central Watering Bay. Water depth 11 feet (3.4 m). Current is from the right in the photograph. Note cloth mesh bags billowing to the left of the sediment trap boxes which are stacked 6 inches (15.2 cm) high.

D: Shoreward Thalassia bed in approximately 5 feet (1.52 m) water depth on traverse 8.

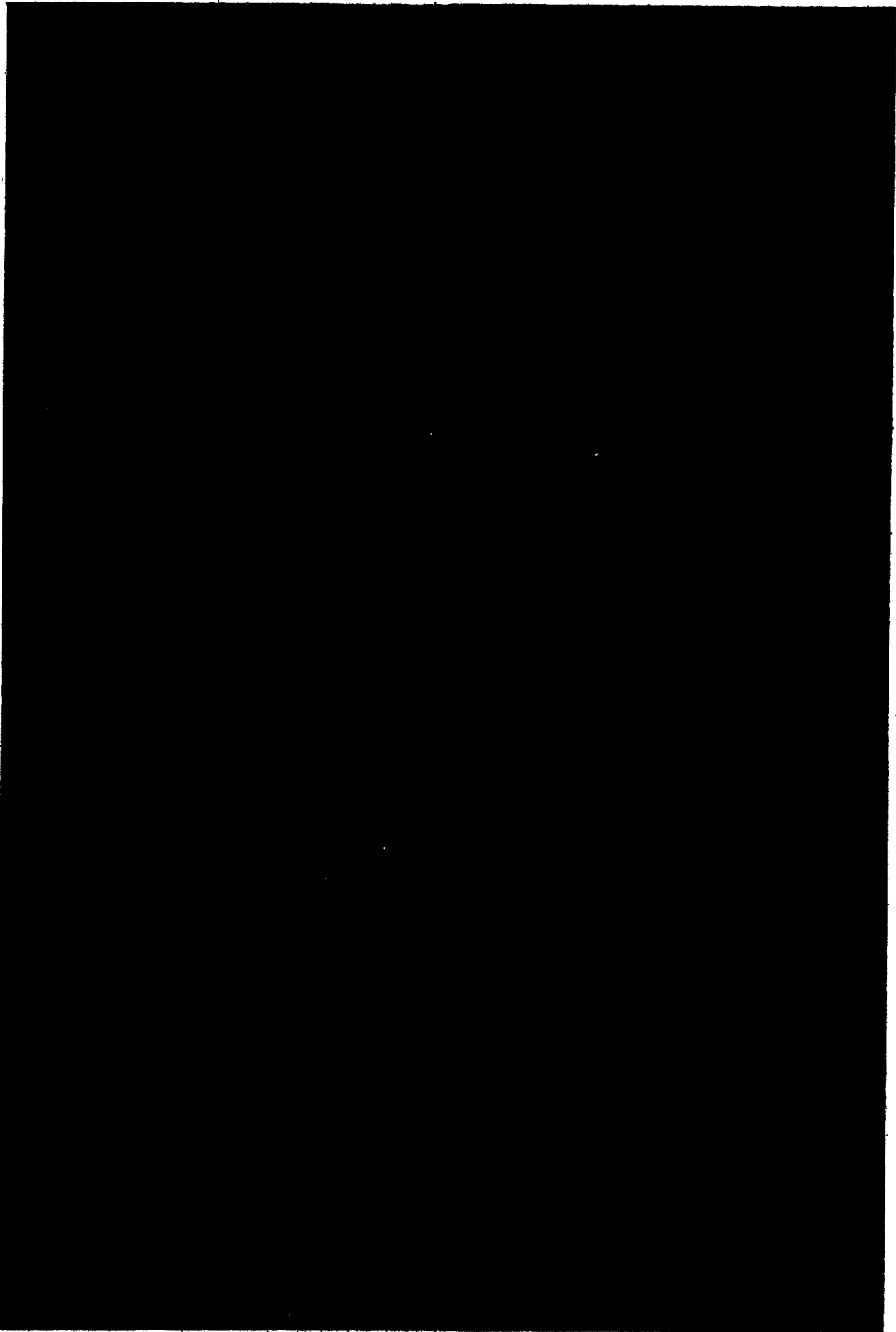


PLATE 8:
WATERING BAY LAGOON AND PATCH REEF ENVIRONMENTS.

A and B:

North end of Grand Cay patch reef at 3 feet (1 m) water depth. Thick finger coral is Porites porites. Thin finger coral in lower right of A is Porites divaricata. Lumpy coral head in centre of A is Porites astreoides. Spiny sea urchin to top of B is Diadema antillarum. Abundant calcareous green algae Halimeda opuntia is visible amongst the corals in both A and B.

C: Stable, burrowed sand adjacent to shoreward Thalassia bed shoreward of Grand Cay. Water depth 10 feet (3 m). Abundant Cladophora associated with Thalassia.

D: Shoreward Thalassia bed near traverse 8 in 6 feet (1.8 m) water depth. Small clump of Porites porites top centre of photograph - approximately 6 inches (15.2 cm) high.

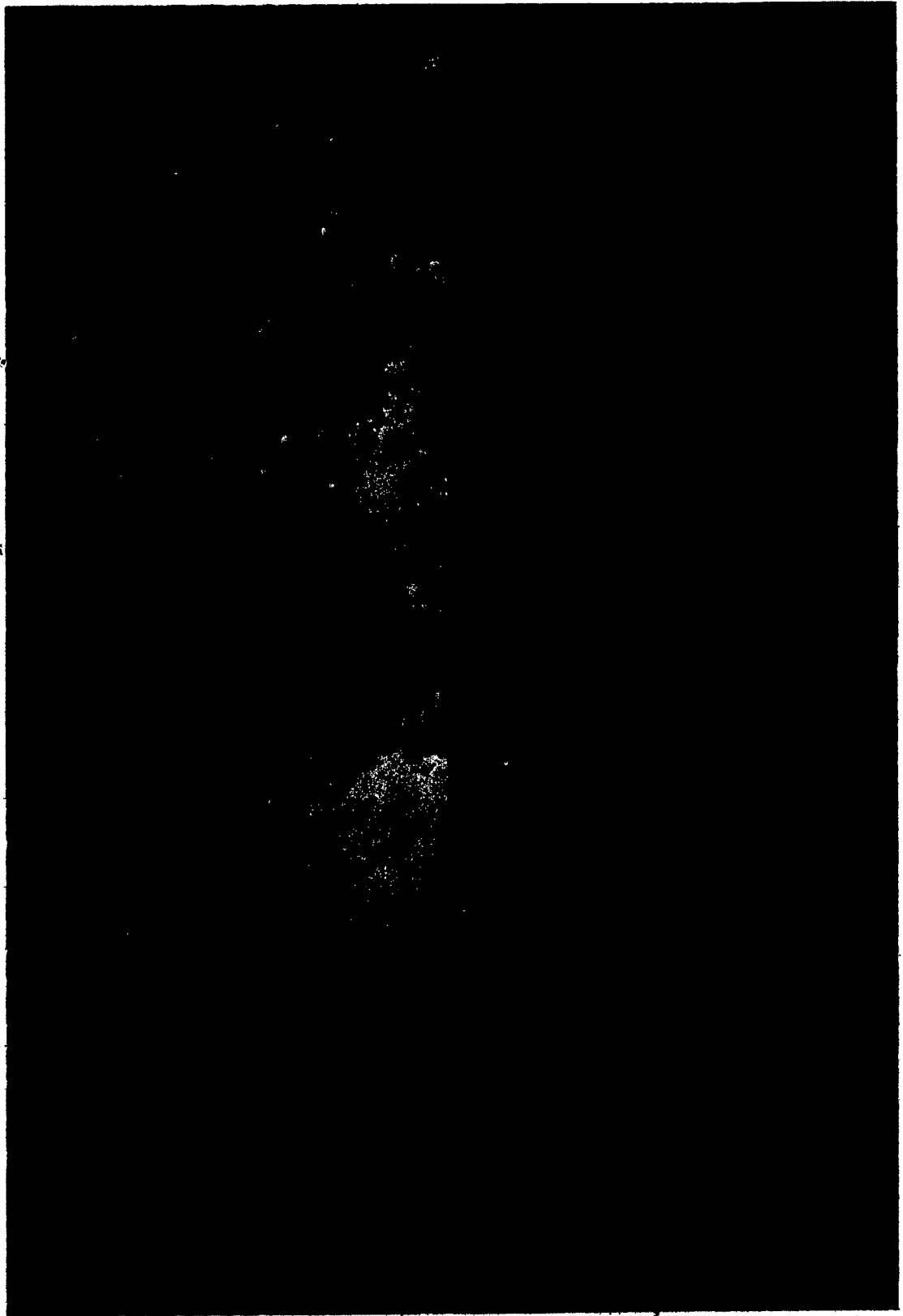


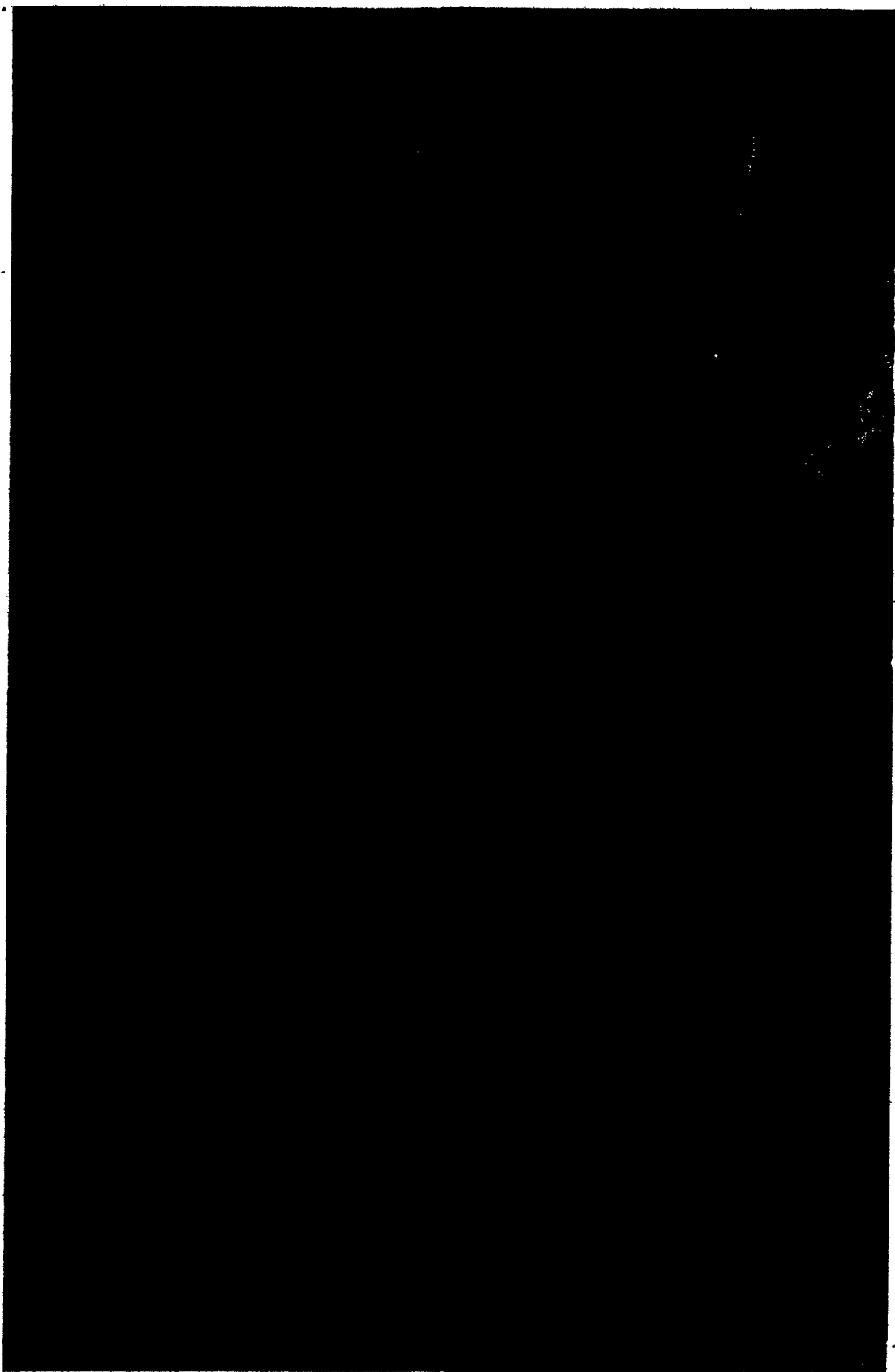
PLATE 9:
GRAND BAY LAGOON ENVIRONMENTS.

A: Back-reef unstable sand flat at 12 feet (3.7 m) water depth. Regular wave ripples are 1 foot (0.3 m) crest to crest and 4 inches (10 cm) high. Looking towards reef.

B: Slope from back-reef unstable sand flat to stable sand of deeper lagoon.

C and D:

Stable sand environment of the deeper lagoon on traverses 17 and 16 respectively. Water depths 21 to 24 feet (6.4 to 7.3 m). Grasses are Diplanthera and Solerpa. Abundant calcareous green algae: Udotea, Penicillus and Halimeda.



APPENDIX 1

GRAIN SIZE ANALYSIS

Wet samples, which had been stored in the field in bottles with a few drops of formalin, were split by quartering on a glass plate until a representative sample weighing approximately 50 gm had been obtained. The sample was then treated with bleach (sodium hypochlorite) to break down and remove organic matter. Wet sieving through a U.S.S. 230 mesh (62.5μ) sieve washed the sample and separated grain sizes finer than 4 phi, which were recovered by washing through a Millipore vacuum filter.

The sample coarser than 4 phi (62.5μ) was dried and sieved into half-phi size intervals on a Tyler Ro-Tap machine. The pan fraction, passing through the U.S.S. 230 mesh sieve, was added to the wet sieved and filtered fraction.

The grain size fractions were then weighed. A simple computer program was devised to transform the weight and size data into individual and cumulative weight percentages; to calculate the phi arithmetic mean, standard deviation, skewness and kurtosis (moment measures given by Friedman, 1967); to calculate the percentages of gravel, sand and mud; and to classify according to Folk's (1968) textural classification.

In the following table a sample identification code is used. The first number (1 to 167) identifies the location of the sample (Chapt. 1, Fig. 3). An "S" and a number following the location number signifies a sample taken from below the sediment surface and gives the depth in cm. "TH" signifies a sample from a Thalassia bed. "ST" signifies a sediment trap

sample ("STA"-sediment surface sample, "STB"-trap sample between 0 and 2" (0 and 5 cm) above surface, "STC"-trap sample between 2 and 4" (5 and 10 cm) above surface, "STD"-trap sample between 4 and 6" (10 and 15 cm) above surface, "STE"-trap sample between 3 and 5" (7.6 and 12.7 cm) above surface). "RT" denotes a ripple trough sample and "RC" a ripple crest sample. "a", "b", "c", etc. following the location number signify samples taken in close proximity to one another. Differences are usually in water depth on a slope or in elevation on a beach.

SAMPLE	WATER DEPTH (M)	%	%	%	MOMENT MEASURES			
					GRAV.	SAND	MUD	MEAN $\bar{\phi}$
1	18.3	3.09	96.68	0.22	1.03	1.03	-0.73	4.96
2S3	10.7	1.86	94.37	3.77	1.34	1.37	0.87	4.37
3	20.4	22.94	76.72	0.34	-0.33	2.12	-0.96	2.73
4	17.4	0.34	99.32	0.34	0.76	0.73	1.04	8.51
5	23.8	1.82	97.81	0.37	0.82	0.90	0.36	5.03
6	7.6	6.05	93.51	0.44	0.95	1.29	-1.52	7.62
7	11.6	0.20	93.52	6.28	2.23	1.34	0.34	3.50
8	11.6	0.16	95.24	4.60	2.20	1.23	0.33	3.77
9	15.2	1.46	98.32	0.22	1.57	1.01	-1.38	8.44
10	11.9	21.71	77.94	0.35	0.36	2.25	-0.88	2.50
11	10.7	8.09	91.58	0.34	0.42	1.32	-1.74	7.59
12	19.8	3.31	96.38	0.31	0.86	1.04	-1.55	10.64
13	9.1	0.18	99.30	0.53	1.69	1.04	-0.30	3.06
14	10.7	11.22	86.90	1.88	1.17	1.99	-1.15	4.62
15	14.9	0.41	99.30	0.29	1.70	0.80	-0.36	4.79
16	9.4	0.00	94.68	5.32	1.85	1.35	0.73	3.73
17	8.5	0.52	99.33	0.15	1.19	1.05	-0.03	2.30
18	6.4	7.79	92.07	0.13	0.44	1.10	-0.05	3.65
19	6.4	0.85	98.91	0.24	1.25	1.10	-0.01	2.49
20	6.4	0.13	99.46	0.41	1.83	0.99	-0.32	3.01
21	13.1	75.57	23.54	0.89	-2.62	2.75	1.20	2.86
22	8.5	0.43	99.04	0.53	1.86	0.89	-0.40	4.67
23	4.9	1.38	98.51	0.10	0.82	0.99	0.11	3.13
24STARC	4.6	0.64	99.25	0.10	0.85	0.79	0.22	3.82
24START	"	1.78	98.13	0.10	0.66	0.96	0.43	3.04
24ST-1B	"	0.65	98.70	0.65	0.79	0.98	1.12	5.60
24ST-1C	"	0.00	96.98	3.02	2.17	1.03	0.33	5.05
24ST-1D	"	0.30	94.91	4.79	2.48	1.00	0.57	6.19
24ST-2B	"	1.76	97.79	0.46	0.72	1.13	0.81	3.64
24ST-2C	"	0.24	98.06	1.70	1.96	1.04	0.06	4.37
24ST-2D	"	0.00	97.27	2.73	2.29	0.96	0.30	5.53
24ST-3B	"	0.51	98.64	0.85	1.60	1.17	-0.05	2.84

SAMPLE	WATER DEPTH (M)	% GRAV.	% SAND	% MUD	MOMENT MEASURES			
					MEAN Ø	STND. DEV. Ø	SKEW.	KURT.
24ST-3C	4.6	0.37	98.67	0.96	1.67	1.09	-0.01	3.38
24ST-3D	"	0.11	98.51	1.39	1.93	1.02	-0.01	4.08
25	22.3	1.91	97.85	0.24	0.66	0.72	0.34	8.47
26	11.9	0.09	99.75	0.16	0.84	0.62	0.89	7.78
27	2.1	6.03	91.69	2.28	1.16	1.44	-0.39	3.32
28	2.1	0.70	98.75	0.55	2.06	1.00	-0.91	4.53
28TH	"	0.52	97.13	2.35	1.75	1.22	0.32	3.60
29	3.4	10.63	88.96	0.42	0.25	1.44	-1.06	5.39
30	3.4	4.64	95.02	0.34	0.76	1.19	-0.43	5.06
31	2.1	0.61	99.21	0.18	1.59	0.70	-1.42	11.30
32	0.6	31.39	68.29	0.31	-0.67	1.73	-0.63	3.12
33STA	3.4	8.06	91.42	0.52	0.52	1.17	0.16	4.42
33STB	"	1.31	98.31	0.38	1.44	0.93	-0.10	4.67
33STE	"	1.14	97.35	1.51	1.88	1.05	0.17	4.88
34STA	3.4	2.40	97.45	0.15	0.82	0.97	0.12	3.22
34STB	"	0.52	99.39	0.09	1.81	0.91	-0.74	3.78
34STE	"	0.21	99.43	0.35	2.04	0.08	-0.49	5.16
35STA	3.4	1.18	98.48	0.34	1.04	1.08	0.26	3.24
35STB	"	0.27	93.67	6.06	2.80	0.98	0.41	6.15
35STC	"	0.13	94.10	5.77	2.79	0.92	0.82	6.32
35STD	"	0.10	88.56	11.34	3.08	1.05	0.80	4.60
36	1.2	45.68	54.32	0.00	-0.98	1.03	-0.17	3.31
37	3.0	46.25	53.75	0.00	-0.90	0.98	0.14	3.15
38	18.3	51.00	48.98	0.02	-0.97	1.44	-0.21	3.02
39	0.0	0.01	98.57	1.41	1.99	0.95	0.73	4.21
40	3.0	0.27	97.07	2.66	1.62	1.16	0.79	4.65
41	3.0	19.08	76.95	3.97	0.93	2.29	-0.50	2.83
42	2.4	0.00	97.48	2.52	1.84	1.13	0.51	4.21
42TH	"	0.47	93.96	5.57	2.23	1.33	0.22	3.44
43	3.4	2.97	96.13	0.90	1.20	1.20	-0.01	3.80
44	4.0	0.10	99.76	0.14	1.22	1.00	0.17	2.39
45	3.7	0.88	98.79	0.33	1.13	1.04	0.11	3.02
46	3.0	3.74	96.14	0.12	1.02	1.12	-0.42	2.98
47	1.5	11.97	87.35	0.68	0.58	1.36	0.40	3.21
48	1.8	0.74	87.21	12.05	2.46	1.61	0.21	2.64
49	2.1	0.43	95.53	4.03	1.84	1.36	0.43	3.39
50	5.2	16.40	82.71	0.89	0.32	1.43	0.01	3.94
51	4.6	0.15	95.34	4.51	1.97	1.27	0.59	3.91
52	2.1	7.12	92.27	0.61	1.04	1.38	-0.64	4.19
53	1.5	17.00	82.65	0.35	0.21	1.45	-0.16	3.59
54	10.1	6.56	93.16	0.28	0.16	0.82	0.45	7.99
55	13.7	9.27	90.52	0.21	0.27	1.47	-1.80	6.82
56	17.7	40.27	59.50	0.23	-1.21	2.26	-0.39	1.77
57	1.2	9.78	79.95	10.27	1.33	1.99	0.66	2.66
58	1.5	24.13	73.11	2.76	0.69	1.95	-0.12	2.78
59	5.2	7.08	91.63	1.29	0.27	1.06	1.57	9.09
60	2.7	6.72	90.00	3.28	1.33	1.56	0.26	3.10
61STA	4.0	3.77	95.79	0.44	0.91	1.11	0.00	3.83
61STB	"	0.38	97.91	1.72	1.98	0.93	0.32	6.40
61STC	"	0.24	96.78	2.98	2.24	0.93	0.83	6.48
61STD	"	0.11	95.24	4.65	2.39	0.99	1.01	5.93

SAMPLE	WATER			MOMENT MEASURES				
	DEPTH (M)	% GRAV.	% SAND	% MUD	MEAN Ø	STND. DEV. Ø	SKEW.	KURT.
62	4.0	8.89	90.98	0.13	0.01	0.82	-0.38	7.24
63	20.1	15.34	84.24	0.42	-0.06	1.64	-1.28	4.78
64	19.8	26.27	73.53	0.20	-0.52	1.84	-0.85	2.72
65	23.5	23.49	75.85	0.66	-0.42	1.63	-0.61	3.79
66	6.1	0.67	89.31	10.02	2.60	1.45	0.03	3.30
67	9.1	1.57	96.49	1.94	1.25	1.26	0.73	3.96
68	5.2	17.69	81.96	0.35	0.16	1.56	-0.84	3.75
69	4.0	16.78	82.74	0.48	0.24	1.45	-0.42	3.74
70	2.7	10.91	88.17	0.92	1.38	1.67	-0.51	2.50
71STA	4.3	8.61	90.58	0.81	0.67	1.31	-0.18	4.80
71STB	"	1.24	98.74	0.02	1.37	0.79	-0.92	4.60
71STE	"	0.76	99.20	0.04	1.40	0.73	-0.88	4.71
72STA	3.0	26.00	73.45	0.56	0.17	1.59	-0.03	2.91
72STB	"	4.07	95.77	0.16	1.78	1.07	-1.99	9.07
72STE	"	0.20	99.72	0.08	1.85	0.53	-0.48	8.82
73STA	2.4	10.61	88.77	0.62	1.00	1.52	-0.77	4.06
73STB	"	6.38	93.46	0.16	1.08	1.11	-0.72	3.50
73STE	"	0.34	99.56	0.10	1.79	0.62	-0.59	7.50
74	1.5	7.25	92.34	0.41	0.52	1.07	0.13	4.32
75STA	7.9	31.11	68.76	0.13	-0.68	1.81	-0.69	2.57
75STB	"	10.20	89.59	0.21	0.20	1.01	0.67	4.08
75STC	"	1.28	97.88	0.84	0.88	1.03	0.78	5.44
75STD	"	1.71	96.84	1.45	1.07	1.11	0.82	5.43
76	2.1	13.30	86.28	0.42	0.28	1.20	0.28	4.04
77	3.0	43.03	56.74	0.22	-0.86	0.80	1.45	12.65
78	9.1	8.45	91.45	0.10	0.00	0.73	-0.22	6.99
79	19.2	16.50	83.38	0.12	0.26	1.54	-1.21	4.09
80	0.0	0.03	99.57	0.40	1.76	0.98	0.41	2.70
81	2.7	3.42	94.87	1.70	1.03	1.42	0.66	3.13
82	8.5	0.19	91.57	8.24	2.33	1.52	0.17	2.70
83	13.7	0.03	98.69	1.28	1.52	1.05	0.63	4.28
84	2.7	39.86	59.86	0.26	-0.79	2.67	-0.29	1.68
85	18.3	2.30	97.52	0.18	0.69	0.74	0.08	6.41
86	3.4	5.50	91.07	3.43	1.13	1.44	0.75	4.28
87	3.4	4.38	94.46	1.16	1.27	1.09	-0.59	7.57
88	8.8	5.60	93.98	0.42	0.94	1.15	-0.03	3.13
89	10.1	7.65	91.93	0.42	0.28	1.19	-0.44	7.08
90	19.2	0.07	99.82	0.11	1.39	0.47	0.01	11.84
91a	15.2	8.31	91.45	0.24	-0.23	0.65	2.05	18.46
91b	18.3	1.36	98.58	0.07	0.46	0.55	0.18	8.84
92	5.2	1.76	98.14	0.10	0.47	0.69	0.40	5.99
93	15.2	0.13	99.66	0.21	1.53	0.67	-0.05	5.94
94	18.3	9.04	90.76	0.21	0.28	1.03	-0.91	6.44
95	18.3	2.70	97.18	0.12	0.67	0.83	-0.19	4.50
96	24.4	10.90	88.81	0.29	0.51	1.46	-1.19	4.97
97	3.4	4.42	95.04	0.54	1.10	1.24	-1.31	7.61
98	4.9	11.06	88.45	0.49	0.44	1.40	-0.68	4.86
99	8.5	39.74	58.70	1.56	-0.66	1.79	0.62	4.44
100	7.6	7.91	92.00	0.09	0.73	1.06	-0.59	3.95
101	0.0	0.00	99.93	0.07	2.34	0.47	0.09	4.49
102	4.3	0.00	98.89	1.11	2.07	0.98	0.03	3.68

SAMPLE	WATER DEPTH (M)	% GRAV.	% SAND	% MUD	MOMENT MEASURES			
					MEAN Ø	STND. DEV. Ø	SKEW.	KURT.
103	3.4	11.63	88.00	0.37	0.55	1.52	-0.73	3.89
104	6.7	4.12	95.13	0.75	1.87	1.14	-1.15	5.26
105	11.0	0.02	97.87	2.11	1.94	1.20	0.30	3.17
106	5.8	3.03	95.53	1.44	1.26	1.30	0.21	3.97
107	3.0	0.11	99.82	0.07	1.96	0.51	-1.15	10.06
108a	+1.2	0.00	99.38	0.62	1.73	0.92	0.20	3.80
108b	+1.5	0.00	99.84	0.16	2.06	0.69	-0.17	3.91
108c	+0.9	0.00	99.91	0.09	2.30	0.54	-0.16	4.35
108ds1	+0.9	0.00	99.90	0.10	1.75	0.71	0.42	3.72
108e	0.0	0.00	99.23	0.77	2.52	0.73	-0.73	4.83
108fs5	0.0	0.13	99.83	0.03	1.32	0.87	0.30	3.00
108g	0.3	2.80	96.79	0.40	1.27	1.35	0.09	2.21
109	4.3	0.67	82.27	17.06	2.86	1.64	-0.04	2.54
110	2.7	9.45	86.61	3.94	1.30	1.93	-0.94	4.92
111	4.6	4.31	88.10	7.59	1.28	1.76	0.88	3.19
112	12.2	0.03	96.63	3.35	1.80	1.25	0.69	3.81
113	11.6	0.56	89.43	10.01	2.88	1.44	-0.42	3.52
114	3.0	5.47	94.45	0.09	0.44	0.93	-0.40	5.27
115	3.4	0.86	99.03	0.11	0.29	0.52	1.03	14.44
116	3.4	3.58	91.15	5.28	1.86	1.72	0.07	2.32
117	6.7	1.74	88.27	9.99	2.25	1.73	-0.10	2.39
118	8.2	0.06	96.66	3.28	1.57	1.33	0.71	3.60
119	9.4	0.04	93.15	6.80	2.22	1.50	0.23	2.65
120	3.7	16.75	81.82	1.42	0.93	1.87	-0.40	2.74
121	2.7	29.59	69.33	1.08	-0.16	2.09	-0.37	2.83
122	13.4	0.00	97.04	2.96	1.98	1.33	0.20	2.84
123	12.2	0.11	94.61	5.92	2.56	1.29	-0.03	3.08
124	9.1	0.03	97.61	2.36	1.87	1.35	0.22	2.63
125	3.7	2.08	97.84	0.08	0.83	0.91	0.06	3.20
125A	"	7.19	92.71	0.10	1.35	1.39	-1.57	5.47
126RC	3.4	0.73	99.16	0.11	0.99	0.88	0.20	3.45
126RCRT	"	6.83	93.06	0.12	0.81	1.17	-0.35	3.22
127	3.4	5.81	93.92	0.27	0.51	1.16	0.63	3.46
128	7.0	0.14	97.07	2.80	2.27	1.29	-0.22	2.92
129	4.9	1.86	97.34	0.08	1.99	1.29	-0.65	3.15
130RC	3.4	1.61	98.36	0.03	1.38	1.11	-0.41	2.34
130RT	"	5.62	94.23	0.15	1.03	1.33	-0.17	2.11
131a	0.0	0.00	99.84	0.16	2.16	0.80	-0.08	2.78
131bs13	"	8.30	91.67	0.03	0.28	1.04	0.68	3.83
132	2.7	3.34	96.32	0.35	0.99	1.09	-0.15	4.51
133	4.9	1.96	97.62	0.42	1.40	1.31	-0.83	5.61
133TH	"	0.25	94.41	5.34	2.45	1.35	-0.10	3.10
134	7.6	0.03	93.56	6.41	2.50	1.34	0.10	2.99
135	6.4	0.05	99.55	4.40	2.37	1.26	0.19	3.05
136	6.4	0.05	96.70	3.24	2.22	1.33	0.00	2.64
137a	5.8	0.84	96.34	2.83	2.35	1.38	-0.42	2.95
137b	"	66.39	31.82	1.78	-0.91	2.02	1.28	3.95
137c	"	9.90	87.43	2.68	0.99	1.78	0.45	2.30
137d	4.3	2.37	97.23	0.41	0.79	1.26	-0.62	3.05
137ds7	4.1	0.92	98.61	0.48	1.81	1.13	-0.45	3.02

SAMPLE	WATER DEPTH (M)	% GRAV.	% SAND	% MUD	MOMENT MEASURES			
					MEAN Ø	STND. DEV. Ø	SKEW.	KURT.
137dS15	4.1	12.95	86.35	0.71	0.76	1.59	0.26	2.14
137dS18	"	1.82	97.33	0.86	1.59	1.29	-0.21	2.61
137dS22	"	1.37	96.93	1.70	1.66	1.32	-0.01	2.93
137dS25	"	1.17	96.61	2.22	1.87	1.28	-0.08	3.35
137e	3.4	0.88	98.95	0.16	1.50	1.03	-0.31	2.79
137eS6	"	10.55	89.23	0.21	0.88	1.49	-0.47	2.79
137eS13	"	8.94	90.77	0.29	1.05	1.47	-0.72	3.33
137eS34	"	6.03	93.01	0.96	1.04	1.39	-0.02	3.02
138RC	3.7	0.95	98.97	0.08	1.02	0.94	0.11	2.82
138RT	"	7.50	92.29	0.21	1.28	1.37	-0.62	2.78
139RC	3.7	0.26	99.67	0.07	1.38	0.84	-0.12	3.12
139RT	"	5.65	94.22	0.13	1.16	1.31	0.51	2.85
140	3.7	24.43	75.37	0.20	0.03	1.54	0.02	2.64
141	3.4	12.55	86.65	0.08	0.89	1.51	-0.04	2.43
142	2.1	29.97	69.84	0.19	-0.59	2.22	-0.61	2.04
143	2.4	20.81	78.75	0.44	0.34	1.45	0.18	2.44
144	2.4	3.93	91.32	4.75	1.42	1.45	0.58	4.80
145	5.2	12.59	87.09	0.32	1.08	1.59	-0.73	3.06
146	7.3	0.11	96.42	3.47	2.38	1.29	-0.08	2.75
147	7.3	0.00	98.21	1.79	2.18	1.20	-0.05	2.74
148a	7.6	2.14	91.23	6.63	2.50	1.50	-0.43	3.43
148b	7.3	0.96	97.80	1.24	1.47	1.26	0.41	2.98
148c	5.8	0.34	99.31	0.35	2.16	0.94	-0.81	4.13
149RC	4.7	0.28	99.66	0.06	1.49	0.89	-0.20	2.78
149RT	"	1.67	98.12	0.21	1.57	1.13	-0.51	2.77
150RC	4.0	0.15	99.73	0.11	1.42	0.82	0.05	3.14
150RT	"	1.89	98.00	0.11	1.63	1.10	-1.39	6.79
151RC	4.3	0.27	99.65	0.08	1.53	0.73	-0.30	5.28
151RT	"	4.18	95.74	0.08	1.56	1.19	-1.13	4.54
152RC	4.0	4.78	94.89	0.32	1.28	1.26	-0.51	3.23
152RT	"	9.34	90.32	0.34	1.21	1.50	-0.49	2.45
153	4.0	6.03	93.47	0.50	0.40	1.04	0.32	6.44
154	2.7	7.86	91.86	0.28	0.26	0.83	0.09	7.44
155	2.4	19.85	79.48	0.66	0.58	1.96	-0.90	3.07
156RC	5.8	0.16	99.75	0.09	1.40	0.83	-0.11	3.18
156RT	"	0.17	99.69	0.14	1.54	0.92	-0.19	3.00
157	7.9	0.54	98.32	1.14	1.95	1.30	-0.18	2.43
158	7.0	1.01	98.02	0.96	1.97	1.18	-0.50	3.29
159RC	6.7	0.42	99.40	0.17	1.57	0.95	-0.34	3.17
159RT	"	2.06	97.67	0.27	1.32	1.22	-0.14	2.32
160RC	4.6	4.40	95.35	0.24	0.68	1.11	0.31	3.03
160RT	"	14.29	85.47	0.24	0.70	1.46	-0.18	2.35
161RC	4.3	6.23	93.69	0.08	0.50	1.01	0.08	3.57
161RT	"	33.68	66.20	0.12	-0.07	1.74	-0.09	2.07
162	4.0	11.94	87.68	0.38	0.40	1.30	0.51	3.15
163	3.0	3.48	96.20	0.32	0.45	0.87	0.77	6.59
164	5.2	5.80	94.12	0.08	0.65	1.08	-0.46	4.39
165	5.2	25.07	74.55	0.38	-0.40	0.88	1.45	10.53
166	1.5	1.97	97.67	0.36	0.63	0.78	0.51	7.72
167	1.5	22.78	76.66	0.56	0.48	1.38	-0.08	2.60

APPENDIX 2

CONSTITUENT GRAIN COMPOSITION ANALYSIS

The grain size fractions coarser than 3.5 ϕ (0.088 mm) in three representative samples from Grand Bay were analyzed for skeletal constituents. The three samples were 138RT, 138RC and 136. The former two samples were ripple trough and ripple crest samples from the unstable sand flat and the latter sample was from the deeper water of the stable sand environment. The distance between location 138 and 136 was 625 feet (190 m). A total of 35 sub-samples (sieved grain size fractions) were analyzed.

The constituents of the coarser size fractions were usually recognizable under a binocular microscope. To identify the constituents of the finer size fractions it was necessary to mount the grains in epoxy and grind them down so they would be identifiable under a light transmitting microscope. Grain counts of the available grains in each size fraction, up to a total of 300 grains for each fraction, were divided into ^{eight} classes as follows: Halimeda, corals, coralline algae, molluscs, Homotrema, echinoderms, miscellaneous (eg. crab fragments, foraminifera), and unknowns.

Grain counts were normalized to percentages of each size fraction. Each grain count percentage was then multiplied by the weight percentage of the size fraction in the whole, original sample. The result was an estimate of the abundance of the given constituent in the given grain size fraction as a percentage of the whole sample.

SAMPLE 138RQ - CONSTITUENT COMPOSITION

GRAIN SIZE (PHI) FRACTION	Hal.	Co ² .	Cor. Alg.	Mol.	Hom.	Ech.	Mis.	Unk.
<u>-2.0 to -1.5</u>	(Wt. % = 0.08)							
Grain Count							1	
Pct. of Frac.							100	
Pct. of Whole								
<u>-1.5 to -1.0</u>	(Wt. % = 0.88)							
Grain Count	11	4	9	6	1		3	
Pct. of Frac.	32.4	11.8	26.5	17.6	2.9		8.8	
Pct. of Whole	0.29	0.10	0.23	0.15	0.03		0.08	
<u>-1.0 to +0.5</u>	(Wt. % = 3.19)							
Grain Count	52	25	35	12	5	1	1	2
Pct. of Frac.	29.1	18.8	26.3	9.0	3.8	0.8	0.7	1.5
Pct. of Whole	1.25	0.60	0.84	0.29	0.12	0.03	0.02	0.05
<u>-0.5 to 0.0</u>	(Wt. % = 10.04)							
Grain Count	62	90	88	23	10	3	2	22
Pct. of Frac.	20.7	30.0	29.3	7.7	3.3	1.0	0.7	7.3
Pct. of Whole	2.08	3.01	2.94	0.77	0.33	0.10	0.07	0.73
<u>0.0 to 0.5</u>	(Wt. % = 17.28)							
Grain Count	30	100	94	26	12	5	5	28
Pct. of Frac.	10.0	33.3	31.3	8.7	4.0	1.7	1.7	9.3
Pct. of Whole	1.73	5.75	5.41	1.50	0.69	0.29	0.29	1.61
<u>0.5 to 1.0</u>	(Wt. % = 17.46)							
Grain Count	31	124	88	24	6	1	6	20
Pct. of Frac.	10.3	41.3	29.4	8.0	2.0	0.3	2.0	6.7
Pct. of Whole	1.80	7.21	5.13	1.40	0.35	0.05	0.35	1.17
<u>1.0 to 1.5</u>	(Wt. % = 20.47)							
Grain Count	26	116	93	26	9	7	6	17
Pct. of Frac.	8.7	38.7	31.0	8.7	3.0	2.3	2.0	5.6
Pct. of Whole	1.78	7.92	6.35	1.78	0.61	0.47	0.41	1.15
<u>1.5 to 2.0</u>	(Wt. % = 14.27)							
Grain Count	20	134	89	32	0	3	4	18
Pct. of Frac.	6.7	42.7	29.6	10.7	0	1.0	1.3	6.0
Pct. of Whole	0.96	6.09	4.22	1.53	0	0.14	0.19	0.86
<u>2.0 to 2.5</u>	(Wt. % = 10.79)							
Grain Count	39	160	47	19	1	2	3	29
Pct. of Frac.	13.0	53.3	15.7	6.3	0.3	0.7	1.0	9.7
Pct. of Whole	1.40	5.75	1.69	0.68	0.03	0.08	0.11	1.05
<u>2.5 to 3.0</u>	(Wt. % = 4.51)							
Grain Count	47	171	36	8	0	1	4	33
Pct. of Frac.	15.6	57.0	12.0	2.7	0	0.3	1.4	11.0
Pct. of Whole	0.70	2.57	0.54	0.12	0	0.01	0.06	0.50
<u>3.0 to 3.5</u>	(Wt. % = 0.88)							
Grain Count	52	160	11	10	0	5	2	60
Pct. of Frac.	11.3	53.3	3.7	3.3	0	1.7	0.7	20.0
Pct. of Whole	0.45	0.47	0.03	0.03	0	0.01	0.01	0.18

SAMPLE 138RT - CONSTITUENT COMPOSITION

GRAIN SIZE (PHI) FRACTION	Hal.	Cor.	Cor. Alg.	Mol.	Hom.	Ech.	Mis.	Unk.
<u>-3.0 to -2.5</u>	(Wt. % = 0.78)							
Grain Count				4				
Pct. of Frac.				100				
Pct. of Whole				0.78				
<u>-2.5 to -2.0</u>	(Wt. % = 0.54)							
Grain Count			1	3				
Pct. of Frac.			25.0	75.0				
Pct. of Whole			0.13	0.41				
<u>-2.0 to -1.5</u>	(Wt. % = 2.47)							
Grain Count	4	1	4	6	4	0	3	0
Pct. of Frac.	18.2	4.6	18.2	27.3	18.2	0	13.6	0
Pct. of Whole	0.27	0.07	0.27	0.40	0.27	0	0.19	0
<u>-1.5 to -1.0</u>	(Wt. % = 4.71)							
Grain Count	43	19	35	20	14	0	2	
Pct. of Frac.	32.3	14.3	26.3	15.0	10.5	0	1.50	
Pct. of Whole	1.52	0.67	1.24	0.71	0.50	0	0.07	
<u>-1.0 to -0.5</u>	(Wt. % = 5.60)							
Grain Count	111	46	133	44	27	0	11	0
Pct. of Frac.	29.8	12.4	35.75	11.82	7.3	0	3.0	0
Pct. of Whole	1.67	0.69	2.00	0.66	0.41	0	0.17	0
<u>-0.5 to 0.0</u>	(Wt. % = 8.14)							
Grain Count	63	62	107	26	9	2	14	17
Pct. of Frac.	21.0	20.6	35.6	8.7	3.0	0.7	4.7	5.7
Pct. of Whole	1.71	1.68	2.90	0.71	0.24	0.06	0.38	0.46
<u>0.0 to 0.5</u>	(Wt. % = 6.72)							
Grain Count	47	64	108	21	11	4	18	27
Pct. of Frac.	15.7	21.3	36.0	7.0	3.7	1.7	6.0	9.0
Pct. of Whole	1.05	1.43	2.42	0.47	0.25	0.11	0.40	0.60
<u>0.5 to 1.0</u>	(Wt. % = 7.12)							
Grain Count	44	95	105	14	7	5	9	21
Pct. of Frac.	14.7	31.7	35.0	4.6	2.3	1.7	3.0	7.0
Pct. of Whole	1.05	2.26	2.49	0.33	0.16	0.12	0.21	0.50
<u>1.0 to 1.5</u>	(Wt. % = 11.81)							
Grain Count	33	101	104	13	6	4	14	25
Pct. of Frac.	11.0	33.0	34.7	4.4	2.0	1.3	4.6	8.3
Pct. of Whole	1.3	3.90	4.10	0.52	0.24	0.15	0.54	0.98
<u>1.5 to 2.0</u>	(Wt. % = 15.08)							
Grain Count	32	137	74	16	3	3	10	25
Pct. of Frac.	10.7	45.7	24.7	5.3	1.0	1.0	3.3	8.3
Pct. of Whole	1.61	6.89	3.72	0.80	0.15	0.15	0.50	1.25
<u>2.0 to 2.5</u>	(Wt. % = 19.60)							
Grain Count	25	147	74	11	4	2	8	29
Pct. of Frac.	8.3	49.0	24.6	3.7	1.3	0.7	2.7	9.7
Pct. of Whole	1.63	9.60	4.82	0.73	0.25	0.14	0.53	1.90
<u>2.5 to 3.0</u>	(Wt. % = 13.77)							
Grain Count	29	151	43	7	1	2	6	61
Pct. of Frac.	9.7	50.3	14.3	2.4	0.3	0.7	2.0	20.3
Pct. of Whole	1.34	6.93	1.97	0.33	0.04	0.10	0.28	2.80
<u>3.0 to 3.5</u>	(Wt. % = 4.15)							
Grain Count	28	158	29	11	0	3	4	67
Pct. of Frac.	9.3	52.7	9.7	3.7	0	1.0	1.3	22.3
Pct. of Whole	0.39	2.19	0.40	0.15	0	0.04	0.05	0.93

SAMPLE 136 - CONSTITUENT COMPOSITION

GRAIN SIZE (PHI) FRACTION	Hal.	Cor.	Cor. Alg.	Mol.	Hom.	Ech.	Mis.	Unk.
<u>-2.0 to -1.5</u>	(Wt. % = 0.03)							
Grain Count				1				
Pct. of Frac.				100				
Pct. of Whole				0.03				
<u>-1.5 to -1.0</u>	(Wt. % = 0.03)							
Grain Count							1	
Pct. of Frac.							100	
Pct. of Whole							0.03	
<u>-1.0 to -0.5</u>	(Wt. % = 0.62)							
Grain Count	12	7	14	19	1	0	1	0
Pct. of Frac.	22.2	13.0	25.9	35.2	1.90	0	1.90	0
Pct. of Whole	0.14	0.08	0.16	0.22	0.01	0	0.01	0
<u>-0.5 to 0.0</u>	(Wt. % = 3.94)							
Grain Count	55	100	56	71	0	3	8	7
Pct. of Frac.	18.3	33.3	18.7	23.7	0	1.0	2.7	2.3
Pct. of Whole	0.72	1.31	0.74	0.93	0	0.04	0.11	0.09
<u>0.0 to 0.5</u>	(Wt. % = 7.86)							
Grain Count	60	112	60	50	1	2	6	9
Pct. of Frac.	20.0	37.3	20.0	16.7	0.3	0.7	2.0	3.0
Pct. of Whole	1.57	2.93	1.57	1.31	0.02	0.06	0.16	0.24
<u>0.5 to 1.0</u>	(Wt. % = 8.48)							
Grain Count	40	140	51	43	0	2	7	17
Pct. of Frac.	13.3	46.7	17.0	14.3	0	0.7	2.3	5.7
Pct. of Whole	1.13	3.96	1.44	1.21	0	0.06	0.20	0.48
<u>1.0 to 1.5</u>	(Wt. % = 11.02)							
Grain Count	51	156	51	23	0	1	5	13
Pct. of Frac.	17.0	52.0	17.0	7.7	0	0.3	1.7	4.3
Pct. of Whole	1.87	5.73	1.87	0.85	0	0.03	0.19	0.47
<u>1.5 to 2.0</u>	(Wt. % = 9.97)							
Grain Count	30	190	40	19	0	5	6	10
Pct. of Frac.	10.0	63.3	13.4	6.3	0	1.7	2.0	3.3
Pct. of Whole	1.00	6.31	1.34	0.63	0	0.17	0.20	0.33
<u>2.0 to 2.5</u>	(Wt. % = 11.38)							
Grain Count	68	145	33	13	0	3	9	29
Pct. of Frac.	22.7	48.3	11.0	4.3	0	1.0	3.0	9.7
Pct. of Whole	2.58	5.50	1.25	0.49	0	0.11	0.34	1.10
<u>2.5 to 3.0</u>	(Wt. % = 12.19)							
Grain Count	78	147	24	12	0	5	4	30
Pct. of Frac.	26.0	49.0	8.0	4.0	0	1.7	1.3	10.0
Pct. of Whole	3.17	5.97	0.98	0.49	0	0.21	0.16	1.22
<u>3.0 to 3.5</u>	(Wt. % = 19.75)							
Grain Count	72	162	14	8	0	4	3	37
Pct. of Frac.	24.0	54.0	4.7	2.7	0	1.3	1.0	12.3
Pct. of Whole	4.74	10.67	0.93	0.53	0	0.26	0.20	2.43

APPENDIX 3

WATERING BAY - CURRENT VELOCITIES

AT FIVE FEET (1.52 M)

Detailed analysis of sediment trap and tidal current data (Chapt. 6) demonstrated that in Watering Bay the 64th percentile of the bottom sediment grain size distribution is a close approximation of the grain size boundary between bed and suspended load transport. This boundary reflects the competence of the maximum current velocities. The 64th percentile may therefore be used to obtain an approximation of the maximum shear velocity (u_*) from a transport competence curve (Fig. 16). It was also found that the mid-point of the half phi grain size interval coarser than the coarsest interval in the bottom sediment grain size distribution is an approximation of roughness length (z_0). From the above, and knowing the water depth, the maximum current velocity at any given depth can be calculated from the von Karman-Prandtl equation for unidirectional flow over a hydrodynamically rough boundary:

$$\bar{u} = \frac{u_*}{k_0} \ln \frac{z+z_0}{z_0}$$

Where \bar{u} is the average current velocity at a height z above bottom, and k_0 is the von Karman constant (0.4). The above procedure was followed for all bottom sediment samples from Watering Bay to obtain current velocity values at a depth of 5 feet (1.52 m). The results are presented in Figure 37 and the following table.

The following code is used in the table: RC = ripple crest sample, RT = ripple trough sample, Thal. = Thalassia bed sample, NBLM = no bed load movement, ST5 = shallower than 5 feet (1.52 m).

SAMP. NO.	64th PERCENTILE	SHEAR VEL. u_* (cm/sec)	ROUGH LENGTH z_0 (cm)	WATER DEPTH -5' (1.52m) z (cm)	VELOCITY AT \bar{u} (cm/sec)
1	1.53	3.6	1.36	1,676	64
2	1.60	3.4	0.68	914	61
3	0.77	5.7	1.36	1,981	104
4	1.01	5.0	0.34	1,585	106
5	1.15	4.6	0.68	2,225	93
6	1.39	4.0	0.68	610	68
7	2.69	1.5	0.34	1,006	NBLM
8	2.63	1.5	0.48	1,006	NBLM
9	2.02	2.5	0.96	1,372	45
10	1.65	3.3	0.68	1,036	60
11	0.90	5.3	0.48	884	100
12	1.19	4.5	0.68	2,134	91
13	2.25	2.1	0.34	762	41
14	2.09	2.4	0.68	853	43
15	2.04	2.5	0.48	1,341	50
16	2.22	2.2	0.24	762	44
17	1.72	3.2	0.34	701	61
18	0.89	5.3	0.96	488	83
19	1.78	3.0	0.48	457	51
20	2.37	1.9	0.34	518	35
21	-3.54				
22	2.23	2.1	0.48	701	38
23	1.19	4.5	0.96	335	66
24RC	1.14	4.6	0.48	274	73
24RT	0.96	5.2	0.68	274	78
25	0.92	5.3	0.34	2,073	115
26	1.02	5.0	0.48	1,067	96
27	1.71	3.2	0.68	61	36
28	2.51	1.7	0.48	61	25
28Thal.	2.22	2.2	0.48	61	27
29	0.77	5.7	0.68	152	77
30	1.18	4.5	0.96	183	59
31	1.85	2.9	0.48	61	35
32	0.19	7.4	1.36		ST5
33	0.97	5.1	0.68	152	69
34	1.20	4.5	0.68	183	63
35	1.42	3.9	0.96	183	51
36	-0.58	10.2	1.36		ST5
37	-0.51	10.0	1.36	152	118
38	-0.44	9.7	1.36	1,676	173
39	2.20	2.2	0.34		ST5
40	1.98	2.6	0.34	152	40
41	2.08	2.4	0.68	152	32
42	2.23	2.1	0.24	91	31
42Thal.	2.72	1.4	0.48	91	NBLM
43	1.71	3.2	0.48	183	48
44	1.62	3.4	0.34	244	56
45	1.60	3.4	0.48	213	52
46	1.58	3.5	0.68	152	47
47	1.03	4.9	0.68		ST5
48	3.02	1.0	0.48	30	NBLM
49	2.31	2.0	0.48	46	23

SAMP. NO.	64th PERCENTILE	SHEAR VEL. u_s (cm/sec)	ROUGH LENGTH z_o (cm)	WATER DEPTH -5' (1.52m) z (cm)	VELOCITY AT 5' (1.52 m) \bar{u} (cm/sec)
50	0.90	5.3	0.68	366	83
51	2.33	2.0	0.68	305	31
52	1.75	3.1	0.96	61	32
53	0.69	5.9	1.36		ST5
54	0.40	6.8	0.68	853	121
55	0.84	5.5	0.96	1,219	98
56	0.20	7.4	1.94	1,615	124
57	1.78	3.0			ST5
58	1.73	3.1	0.96	30	27
59	0.45	6.6	0.68	457	107
60	1.99	2.6	0.68	91	32
61	1.38	4.0	0.96	244	55
62	0.31	7.0	0.68	244	103
63	0.61	6.2	0.68	1,859	123
64	0.48	6.5	0.96	1,829	123
65	0.28	7.1	0.96	2,195	137
66	3.08				ST5
67	1.58	3.5	0.48		ST5
68	0.91	5.3	0.68	366	83
69	0.89	5.3	0.96	244	73
70	2.40	1.9	0.96	222	23
71	1.16	4.6	1.36	244	60
72	0.92	5.3	1.36	252	63
73	1.76	3.1	0.96	91	35
74	0.52	6.4	0.68		ST5
75	0.22	7.3	0.68	640	125